University College London

Institute of Neurology

Detecting and tracking early neurodegeneration in familial Alzheimer's disease

A thesis submitted for the degree

of Doctor of Philosophy

Philip S.J. Weston

For Emma and Evie

Declaration of authorship and originality

I, Philip S.J. Weston, confirm that the work presented in this thesis is my own. Where information has been derived from other sources, I confirm that this has been indicated in the thesis.

Philip S.J. Weston

Acknowledgements

Above all I would like to thank the FAD family members who so kindly donated their time and energy to participate in research. Without their effort and dedication none of the studies reported in this thesis would have been possible.

I am grateful to the Medical Research Council for funding my Clinical Research Training Fellowship, and to the National Institute of Health Research, which provided valuable funds for other aspects of the study.

My primary supervisor, Nick Fox, has been a constant source of support, inspiration, and motivation. I am grateful to Nick for entrusting me with such a valuable cohort of special individuals, and for allowing me to oversee the conduct of the studies presented here. I also thank my secondary supervisor Jon Schott for providing additional useful advice and support throughout.

Finally I would like to thank my co-workers, collaborators and colleagues. On the two imaging projects: Manja Lehman, Natalie Ryan, Marc Modat, Ivor Simpson, Nico Toussaint, and Seb Ourselin. On the serum neurofilament light project: Henrik Zetterberg, Kaj Blennow, Simon Mead, and Ron Druyeh. On the accelerated long-term forgetting study: Adam Zeman, Chris Butler, Yuying Liang, Seb Crutch, and Susie Henley. I also thank Kirsty Macpherson for undertaking the majority of the neuropsychological testing, and to Jenny Nicholas and Tess Poole provided invaluable statistical support. I am also grateful to Martin Rossor, who was always available to offer guidance relating numerous aspects of the research. I lastly thank Chris Lane, Camilla Clark, Tom Parker, Cat Slattery, Ross Paterson, Alex Faulkes and Phil Fletcher, for being a constant source of friendship, support, and amusement.

Abstract

Alzheimer's disease (AD) is recognized to have a long presymptomatic period, with initial deposition of extracellular amyloid and intracellular tau, followed by downstream neurodegeneration and cognitive decline. There is great interest in testing potential disease-modifying treatments for AD prior to the onset of symptoms, when minimal neuronal loss has occurred. To facilitate this, robust and sensitive methods are needed to identify at-risk individuals, stage their disease, and track progression.

Familial Alzheimer's disease (FAD) shares many features, clinically, radiologically, and neurophysiologically, with the more common sporadic form of disease. Carriers of autosomal dominantly inherited mutations in the presenilin 1, presenilin 2, and amyloid precursor protein genes have relatively predictable ages at symptom onset, based on family history. Study of FAD mutation carriers therefore provides the opportunity for the prospective study of asymptomatic individuals with known underlying AD pathology prior to the onset of clinical disease.

The studies presented herein aim to improve the identification and characterization of early FAD neurodegenerative change and its earliest downstream cognitive effects. A multimodal approach is taken, with both presymptomatic and mildly symptomatic individuals included. Chapter one provides an introduction to AD and methods for measuring early neurodegeneration. Chapter two then outlines the general methodological approach across the different studies. Chapters three and four present results of magnetic resonance imaging studies of macrostructural (cortical thickness) and microstructural (diffusion-weighted imaging) cortical change. Chapter five reports results for a new blood-based biomarker of neurodegeneration – serum neurofilament-light. Chapter six investigates a novel approach to presymptomatic cognitive testing –

assessing accelerated long-term forgetting. In all studies, significant differences between mutation carriers and non-carrier controls are detectable during the presymptomatic period. The thesis draws together these different approaches and discusses how they advance our understanding of the neurobiology of AD and their potential utility in both clinical assessment and presymptomatic therapeutic trials.

Table of Contents

List of tables

List of figures

Abbreviations

AAO	Age at onset
AD	Alzheimer's disease
AD-D	Alzheimer's disease dementia
ALF	Accelerated long-term forgetting
AMIPB	Adult Memory and Information Processing Battery
ANOVA	Analysis of variance
ApoE	Apolipoprotein E
APP	Amyloid precursor protein
AR	At risk
ARIA	Amyloid-related imaging abnormalities
AUC	Area under the curve
Aβ	Amyloid β
BACE	β site of APP cleavage enzyme
BSI	Boundary shift integral
CAA	Cerebral amyloid angiopathy
CBD	Corticobasal degeneration
CBS	Corticobasal syndrome
CDR	Clinical dementia rating scale
CI	Confidence interval
CSF	Cerebrospinal fluid
CT	Computed tomography
CTF	C-terminal fragment
CTh	Cortical thickness
DIAN	Dominantly inherited Alzheimer's Network
DLB	Dementia with Lewy bodies
DRC	Dementia Research Centre
DTI	Diffusion tensor imaging
DWI	Diffusion-weighted imaging
EDTA	ethylenediaminetetraacetic acid
ELISA	Enzyme-linked immunosorbent assay
EMQ	Everyday memory questionnaire
EPI	Echo planar imaging
EPS	Early presymptomatic
EYO	Estimated years to onset
FA	Fractional anisotropy

FAD	Familial Alzheimer's disease
FDG	Fluorodeoxyglucose
FLAIR	fluid attenuated inversion recovery
FTD	Frontotemporal dementia
GM	Grey matter
GWAS	Genome-wide association study
HADS	Hospital Anxiety and Depression Scale
IBA1	Ionized calcium binding adaptor molecule 1
IPD	Idiopathic Parkinson's disease
LPA	Logopenic aphasia
LPS	Late presymptomatic
MCI	Mild cognitive impairment
MD	Mean diffusivity
MMSE	Mini mental state examination
MNI	Montreal Neurological Institute
MP-RAGE	Magnetization-prepared rapid gradient-echo
MRI	Magnetic resonance imaging
MSA	Multisystem atrophy
MTL	Medial temporal lobe
NART	National Adult Reading Test
NC	Normal control
NCT	Nicastrin
NfH	Neurofilament heavy
NfL	Neurofilament light
NfM	Neurofilament medium
NFT	Neurofibrally tangle
NMDAR	N-methyl-D-aspartate receptor
NMR	Nuclear magnetic resonance
NTF	N-terminal fragment
OR	Odds ratio
PAL	Paired associate learning
PCA	Posterior cortical atrophy
PCC	Posterior cingulate cortex
PEN	Presenilin enhancer
PET	Positron emission tomography
PiB	Pittsburgh compound B
PLD	Phospholipase D
PMC	Presymptomatic mutation carriers

PSEN	Presenilin
PSP	Progressive supranuclear palsy
RMT	Recognition Memory Test
ROC	Receiver operator curve
ROI	Region of interest
ROS	Reactive oxygen species
SMC	Symptomatic mutation carriers
SOB	Sum of boxes
SUVR	Standardized uptake value ratio
SVM	Support vector machine
TIV	Total intracranial volume
UCL	University College London
VBM	Voxel-based morphometry
VOSP	Visual Object and Space Perception battery
WASI	Wechsler Abbreviated Scale of Intelligence

1 Introduction

1.1 Alzheimer's disease

1.1.1 A brief history

The first case of what we now refer to as Alzheimer's disease (AD) was reported in 1907 by the German psychiatrist and neuropathologist Aloysius 'Alois' Alzheimer. Alzheimer reported post-mortem findings in a 56-year-old woman whom he had first seen in 1901. In life the patient, Auguste Deter, had suffered from young onset dementia with multiple cognitive deficits including reduced episodic memory, disorientation, expressive aphasia, impaired comprehension, and unpredictable behaviour. In addition to marked cerebral atrophy, neuropathological examination revealed two distinct histopathological features: extracellular plaques of dystrophic neurites and intracellular neurofibrillary tangles (NFTs). Emil Kraepelin (1856-1926), the head of Alzheimer's department, later ensured that the illness gained its familiar eponym: 'Alzheimersche krankheit' (Alzheimer's disease).

For over half a century thereafter the term 'Alzheimer's disease' was used exclusively to describe the rare forms of young onset or "presenile" dementia in which the characteristic neuropathological changes of plaques and tangles were evident. However in 1968 a relationship was found between the amount of neuritic plaques in the brains of elderly individuals and the risk of dementia, thereby implying that the neuropathology of presenile and senile forms of degenerative dementia were not significantly different (Blessed et al., 1968). This seminal observation also challenged the then accepted idea that late onset cognitive decline was simply a consequence of ageing. Furthermore, it was a crucial step in defining a pathological disease entity that has come to dominate the study of dementia ever since.

1.1.2 The size of the problem

Over 100 years after Alzheimer's original publication, AD is now recognized to impose an enormous human and economic burden on society. AD accounts for over 50% of all dementia cases, with dementia now the largest cause of death in females in the UK and the second biggest cause in males (www.ons.gov). Meta-analyses have reported a prevalence of 1% in the 60-65 year old age group, doubling every 4-6 years thereafter to reach over 30% by 90-95 (Hofman et al., 1991, Ritchie and Kildea, 1995, Jorm et al., 1987). In 2005, over 24 million people worldwide were estimated to have a diagnosis of dementia, with this figure expected to treble by 2040 (Ferri et al., 2005). The primary reason for the increasing prevalence of dementia, including AD, is the ageing population, with age known to be the biggest risk factor for developing disease. However, whilst deaths from other diseases where age is a prominent risk factor, such as ischaemic heart disease and stroke, are decreasing, AD-deaths continue to rise (Association, 2015). Recent studies suggest that age-specific incidence may be falling slightly in some developed economies, partially, but only partially, mitigating the increasing prevalence due to an ever-older population (Matthews et al., 2016).

As a result of the above, dementia is now recognized as a major global public health issue. In 2009 the UK government published the UK's first National Dementia Strategy, which outlined a plan to facilitate earlier diagnosis and more effective services for those with AD and other forms of dementia (Helath, 2009).

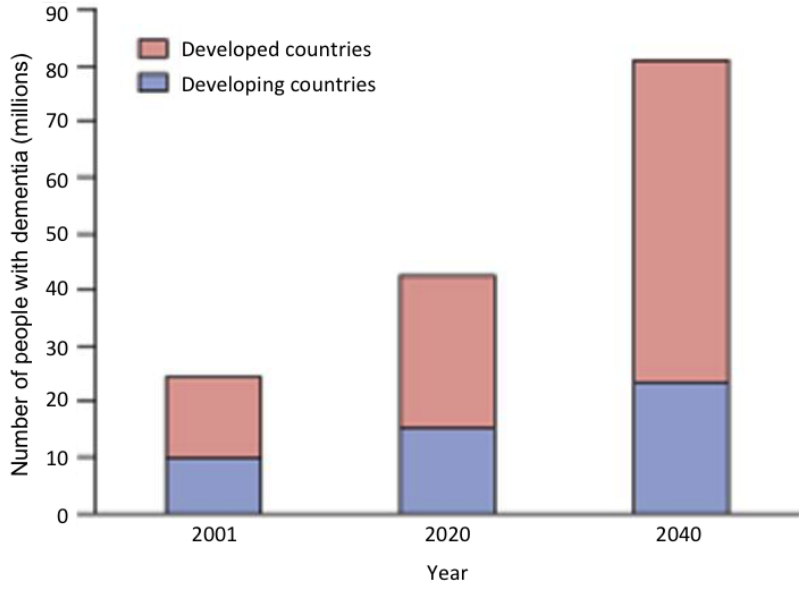

Figure 1-1. Estimated number of cases of dementia in the coming decades (reproduced from Ferri et al., 2005)

The annual global cost of dementia in 2009 was estimated at being over US$400 billion, an increase of 34% compared to just four years earlier, with over 70% of the costs occurring in Europe and North America (Wimo et al., 2010). UK costs have been estimated at £26 billion/year (Society, 2014). This cost is likely to continue to rise with increasing prevalence.

1.1.3 Clinical features

From a clinical perspective, AD is characterized by gradually progressive, inexorable, cognitive decline involving multiple cognitive domains over time. It is a clinically heterogeneous condition, with the diagnosis of AD referring to the presumed underlying pathology rather than a specific clinical syndrome. Common features across almost all cases include an insidious onset, with slow unrelenting progression thereafter, and prominent impairment of cerebral cortical function more so than subcortical regions. Estimates of the average time from diagnosis to death have varied from three to eight years (figure 1-2) (Brodaty et al., 2012, Larson et al., 2004, Wolfson et al., 2001), likely reflecting a significant variability in time from onset of symptoms to

diagnosis. In the majority of cases, termed *typical* AD (Dubois et al., 2014), the first symptom is of progressive loss of episodic memory (i.e. memory for recent events), indicating medial temporal cortical dysfunction. Initially, the clinical syndrome often affects only this one cognitive domain, and has minimal impact on day-to-day functioning – so-called amnestic mild cognitive impairment (MCI) (Gauthier et al., 2006). MCI is not however specific to AD, with only a minority of cases progressing to AD dementia (Mitchell and Shiri-Feshki, 2009), meaning the term has limited diagnostic value. For those who do have underlying AD, as the disease progresses other brain regions, including frontal, lateral temporal and parieto-occipital cortex become involved, with widespread impairment and significant functional decline inevitably resulting. It is this multi-domain cognitive impairment with co-existing functional dependency that defines the term *dementia.* Historically a definitive diagnosis of AD required histopathological confirmation of AD pathology (plaques and tangles) in an individual who had had dementia in life (McKhann et al., 1984).

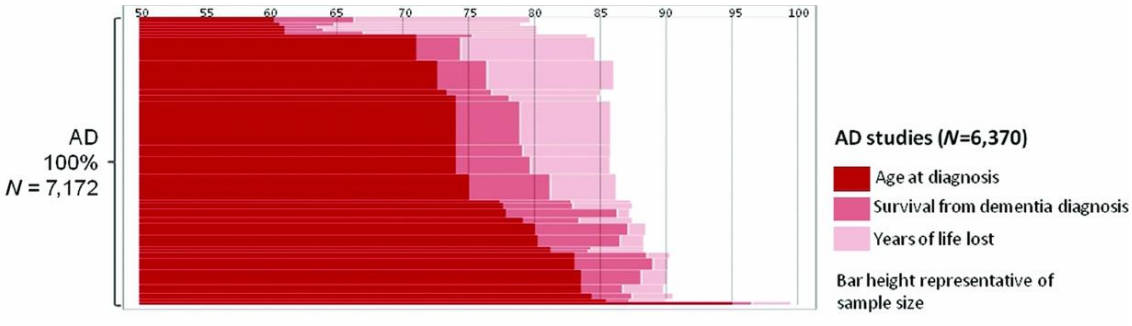

Figure 1-2. Results of a systematic review of survival times in AD (reproduced from Brodaty et al., 2012)

Average number of years from diagnosis to death, and estimated years of life lost are shown for different ages at diagnosis.

Whilst most cases of AD begin with amnestic symptoms, in recent years there has been increasing recognition of so-called atypical AD syndromes, where loss of episodic memory is not the leading feature (Dubois et al., 2014). These include:

- posterior cortical atrophy (PCA), the commonest of the atypical variants, characterized by early visuoperceptual and visuospatial dysfunction, indicating early prominent parieto-occipital involvement (Crutch et al., 2012).
- logopenic aphasia (LPA), charaterised by word-finding pauses and impaired sentence repetition, indicating posterior temporal dysfunction (Gorno-Tempini et al., 2008).
- behavioural/dysexecutive variant, characterized by early frontal lobe dysfunction (Ossenkoppele et al., 2015).

The reason that the same pathological entity may effect different cortical regions in different individuals – the so-called paradox of syndromic diversity – is not well understood (Warren et al., 2012). However, the fact that, as disease progresses, these clinically diverse syndromes tend to converge to each involve the same combination of domains, has added strength to the theory that AD affects a common distributed network of multiple vulnerable brain regions (Warren et al., 2013).

In addition to the cognitive features of AD, neuropsychiatric symptoms are also relatively common, including depression, anxiety, and agitation (Mega et al., 1996). Depression in particular can be an early presenting feature of clinical disease, sometimes preceding cognitive decline (Ownby et al., 2006).

1.1.4 Neuropathological features

1.1.4.1 The pathological hallmarks of AD

Alzheimer described the presence of extracellular plaques of dystrophic neurites, intracellular NFTs, and cortical atrophy, which remain the pathological hallmarks of AD to this day. However, it was not until the 1980s that it was possible to identify the core constituent of plaques as being the protein amyloid (Masters et al., 1985). It was at around the same time that the main constituent of NFTs was identified as being a hyperphosphorylated form of microtubule-associated protein tau (Wood et al., 1986).

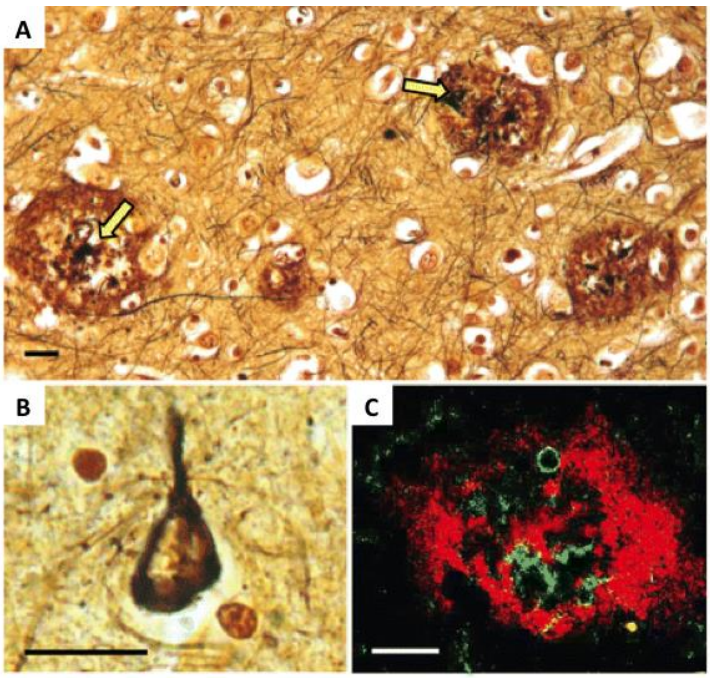

Figure 1-3. The pathological hallmarks of AD (reproduced from O'Brien and Wong, 2011)

*Brain sections from a patient with dementia are stained with silver, revealing **(A)** neuritic plaques and **(B)** an NFT. The plaques in panel **A** consist of an amorphous reddish protein (Aβ) with dystrophic neurites (yellow arrows, dark black material). In **C** an Aβ plaque stained with an anti-Aβ antibody (red) shows infiltrating microglia stained with an IBA1 antibody (green). Each line is 40 microns. Aβ=amyloid β; NFT=neurofibrally tangle; IBAI=Ionized calcium binding adaptor molecule 1.*

1.1.4.2 Amyloid β

The classic senile plaque of AD is a complex lesion containing several abnormal elements, including a central core of amyloid fibrils surrounded by a rim of dystrophic neurites, activated microglia, and fibrillary astrocytes (Selkoe, 1991). Amyloid is a generic term used to describe a group of chemically heterogeneous proteins found in a variety of different diseases and tissues, and is defined by a β-pleated sheet structure. The amyloid fibrils in AD plaques are composed of the amyloid β (Aβ) peptide, a 39-43 amino acid residue peptide produced by cleavage from a larger amyloid precursor protein (APP). APP is a transmembrane protein expressed at high levels in the brain and metabolized in a complex fashion (Bayer et al., 1999, O'Brien and Wong, 2011). Enzymes recognized to cleave APP include α-secretase, β-secretase and γ-secretase (figure 1-3). α-secretase is considered to be part of the non-amyloidogenic pathway in APP processing. It precludes Aβ formation as it cleaves within the segment of APP that would otherwise give rise to Aβ. Alternatively, APP may undergo sequential cleavage by β- and γ-secretase. Extracellular cleavage by β-secretase generates a soluble extracellular fragment, and is followed by the cleavage of APP within its trans-membrane domain by γ-secretase. An unusual property of γ-secretase is that it cleaves APP sequentially typically generating peptides from 39–43 amino acids in length: the family of Aβ peptides (figure 1-4).

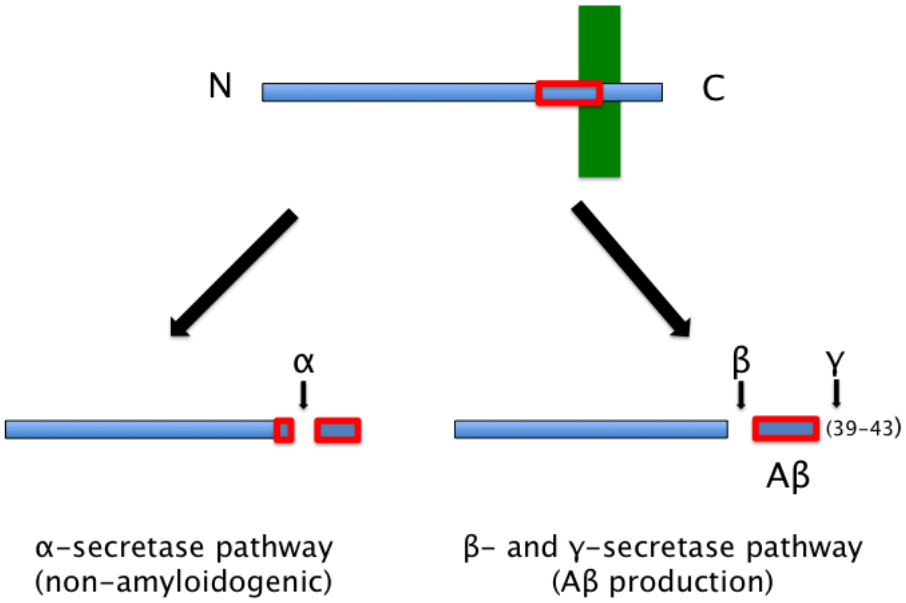

Figure 1-4. Cleavage of APP to produce Aβ

APP is cleaved first by either α-secretase (non-amyloidogenic pathway) or β-secretase followed by γ-secretase, which produces Aβ. γ-secretase cleaves APP in the trans-membrane domain, to produce an Aβ polypeptide that is typically between 39 and 43 amino acids in length. Aβ= amyloid β.

The Aβ peptide is present in unaffected individuals and may have a normal physiological role. In AD however, an imbalance develops between Aβ production and Aβ clearance. Aβ can assemble itself into a variety of structures ranging from soluble monomers and oligomers to the large insoluble fibrils that form aggregates and are deposited extracellularly as amyloid plaques in the neuropil and in cerebral blood vessels. It is now understood that these various amyloid pools comprising different Aβ species exist in dynamic equilibrium in the AD brain. Whilst it was the fibrillar plaque form that was first described in AD, evidence suggests that soluble oligomers, whether intra- or extracellular, may be the most neurotoxic species, (McLean et al., 1999), and are associated with clinical impairment (Lesne et al., 2006, Tomic et al., 2009). Conversely, whilst plaque burden can discriminate AD from healthy aging, it has little

correlation with disease severity or pattern of cognitive deficits (McLean et al., 1999).

Several potential mechanisms for Aβ oligomer toxicity have been proposed. Binding to specific excitatory post-synaptic sites has been demonstrated, causing impairment of synaptic plasticity in hippocampal neurons (Lambert et al., 1998), thus providing a plausible mechanism for impairment of memory formation. Extracellular Aβ oligomers bind to the cell membrane, leading to functional disruption of a number of receptors, including the N-methyl-D-aspartate receptor (NMDAR) (Snyder et al., 2005), resulting in synaptic dysfunction and neurodegeneration. Aβ oligomers have been found to disrupt neuronal calcium homeostasis such that cytosolic calcium is increased, resulting in cellular dysfunction and/or apoptosis. This may occur via an increase in membrane permeability, with the formation of aberrant membrane channels being responsible (Pollard et al., 1995). Increased intracellular calcium also contributes to the formation of reactive oxygen species (ROS), mitochondrial dysfunction and oxidative stress (Schubert et al., 1995). Furthermore, Aβ oligomers potentiate increased synaptic levels of the excitatory neurotransmitter glutamate, by way of both potentiating release and inhibiting uptake, resulting in excito-neurotoxicity (Harris et al., 1996, Fernandez-Tome et al., 2004). However, the neurotoxic nature of oligomeric Aβ, and the interactions between different Aβ pools remain unclear.

Of the different potential Aβ peptides (i.e. $A\beta_{39}$ to $A\beta_{43}$), the major species in Aβ production are $A\beta_{40}$ and $A\beta_{42}$, with $A\beta_{40}$ being the most abundant at a ratio of approximately 10:1 (De Strooper, 2010). It is however $A\beta_{42}$ that is thought to be the more neurotoxic, being predominant in neuritic plaques of AD patients and showing a higher *in vitro* propensity to aggregate and form amyloid fibrils.

In addition to soluble amyloid species and cortical neuritic plaque formation, Aβ is also deposited in vascular structures – known as cerebral amyloid angiopathy (CAA). CAA

is characterised by the gradual deposition of Aβ in the media and adventitia of small leptomeningeal and cortical vessels (Vinters, 1987). CAA has been found, independent of cortical plaque deposition, to be associated with both sub-cortical white matter and cortical grey matter degeneration (Gurol et al., 2013, Fotiadis et al., 2016).

1.1.4.3 Hyperphosphorylated tau

Tau, the predominant constituent of NFTs, is a protein expressed in all axons of the central nervous system. Its primary role is thought to promote assembly and stability of mictrotubules (Cleveland et al., 1977), which provide cytoskeletal stability and facilitation of intracellular transport. There are six known isoforms of tau, ranging from 352 to 441 amino acids in length. Three tau isoforms have three microtubule binding domains and three have four such domains, and are therefore termed 'three repeat tau' and 'four repeat tau' respectively (Goedert et al., 1989). In AD, tau is arranged in to paired helical filaments, containing all six known isoforms (Goedert and Jakes, 1990, Ihara et al., 1986). The most common post-translational modifications of tau are phosphorylation and glycosylation (Buee et al., 2000). The phosphorylation of tau is key to the pathophysiology of AD, with hyperphosphorylation inhibiting the stabilization of microtubules. All tau species present within the paired helical filaments of NFTs are hyperphosphorylated. In addition to AD, accumulation of three or four repeat tau forms the pathological basis for a number of other neurodegenerative diseases including corticobasal degeneration (CBD), progressive supranuclear palsy (PSP), and a significant proportion of frototemporal dementia (FTD) (Iqbal et al., 2005).

Tau pathology demonstrates a relatively consistent anatomical pattern of progression in all AD patients (Braak and Braak, 1991). Pathology typically first appears in the entorhinal cortex (stages I-II), before appearing in the limbic cortex (stages III-IV) and then the neocortex (stages V-VI) (figure 1-5). It has subsequently been found that the

anatomical distribution of cortical tau pathology is much more closely associated with both cortical atrophy and the severity and pattern of cognitive impairment, than amyloid is (Arriagada et al., 1992, Bierer et al., 1995, Whitwell et al., 2008, Gomez-Isla et al., 1997).

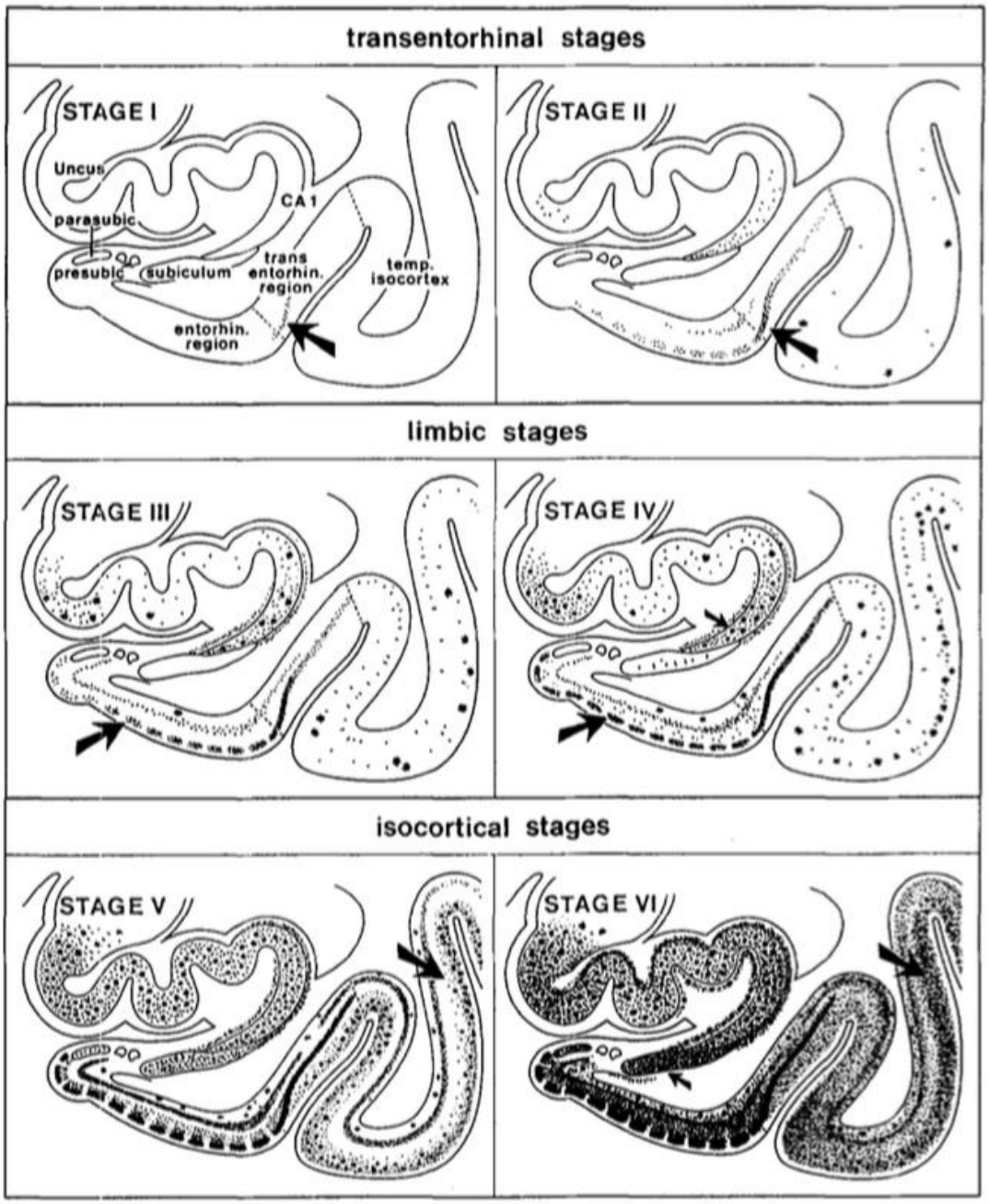

Figure 1-5. Braak staging of tau pathology in AD (reproduced from (Braak and Braak, 1995)

1.1.4.4 What comes first? – The amyloid hypothesis

Following the identification of the principal pathological proteins involved in AD, there has been much discussion over the relative contributions of amyloid and tau to clinical disease, and the temporal ordering of when they appear. In 1991, Hardy and Allsop proposed that it was the presence of excessive extracellular amyloid, due to APP mis-metabolism causing an imbalance between amyloid production and clearance, that is the primary initiating factor in the pathological cascade of AD (Hardy and Allsop, 1991, Hardy and Higgins, 1992). The authors proposed that the pathological sequence is likely to be: 1) Aβ deposition, followed by 2) tau phosphorylation and NFT formation, and 3) neuronal death. The model postulates that tau pathology is a downstream process to the initial deposition of Aβ. The so-called amyloid cascade hypothesis has been the basis for a large proportion of AD research in the intervening decades.

The order of pathological events proposed by the amyloid cascade hypothesis has not however gone unchallenged. The universality of tau pathology in AD and the poor correlation between fibrillar amyloid deposition and clinical status (Giannakopoulos et al., 2003, Arriagada et al., 1992) provides support for AD being considered a form of primary 'tauopathy'. Some critics of the amyloid cascade hypothesis have gone further, asserting that, rather than being an initiating factor, amyloid deposition is actually a downstream protective response to neuronal insult (Lee et al., 2007), with some postulating that novel anti-amyloid therapies will be ineffective or possibly even harmful (Smith et al., 2002).

An important body of evidence supports the primacy of Aβ in the AD pathological cascade. This includes genetic support from the discovery of autosomal dominant familial AD (FAD) genetic mutations known to increase Aβ production or alter the

amyloidogenecity of the peptides produced (Goate et al., 1991, Sherrington et al., 1995), discussed in detail in section 1-3. Further support comes from recent cohort studies assessing progressive molecular and neurodegenerative changes in-vivo (Bateman et al., 2012, Villemagne et al., 2013), discussed in detail in section 1-4.

1.1.4.5 Neurodegeneration – neuronal loss

Although the defining histopathological hallmarks of AD are Aβ plaques and NFTs, it is the loss of neurons seen on histopathological examination that is thought to link most closely to clinical decline.

Whilst neurodegeneration in AD is widespread, particularly in later disease, not all brain areas are affected equally (Brun and Englund, 1981, Warren et al., 2013). Neurodegeneration in AD appears to affect most prominently the cortical grey matter. The cerebral cortex is usually arranged in to six distinct microscopic layers, or laminae, but as AD progresses, there is initial blurring and subsequent derangement of the normal cytoarchitecture, with associated reduction in neuronal numbers and cortical thickness. However some cortical regions have been found to be affected more than others, with medial temporal regions, the posterior cingulate cortex and superior parietal regions particularly vulnerable. Conversely, other regions, including the sensorimotor, calcarine and anterior cingulate cortex show relative sparing until the very late stages of disease.

1.1.4.6 Neuroinflammation

An additional observation made on histopathological assessment has been changes in the numbers of non-neuronal glial cells, and in particular an increase in the number of microglia – the primary immune cell of the central nervous system (Brun and Englund, 1981). This has led, following further work, to a growing recognition of an additional

pathological process in AD – neuroinflammation – occurring either shortly before or in parallel to neurodegeneration (Rubio-Perez and Morillas-Ruiz, 2012, Heneka et al., 2015). It is thought that Aβ binds to pattern recognition receptors on microglia and astrocytes, and triggers an innate immune response characterised by release of inflammatory mediators, which contribute to disease progression and severity. Whilst not the focus of this thesis, there is now great interest in better understanding the role of neuroinflammation in AD, and how it interplays with the other pathological processes discussed above.

1.1.4.7 Vascular pathology

As discussed in section 1.1.4.2, AD is known, at least in a proportion of cases, to involve the deposition of Aβ in the walls of cerebral vessels. However, over the last two decades there has been increasing recognition of a more generalized and widespread involvement of vascular pathology in AD (de la Torre, 2002). Not only does CAA potentially play a more influential role than perhaps previously thought, but AD patients (at least those with late onset sporadic disease) have also been found to have a greater number of arteriosclerotic vascular lesions than one would expect to see in the general population (Thal et al., 2003). A further large study found that the co-existance of both AD molecular pathology and vascular pathology have a potential synergistic effect with regards to the overall impact on cognition and daily functioning, implying that some form of interaction may be present between the two (Tyas et al., 2007). Indeed, the function and well-being of neurons and glial cells have been found to be inextricably linked to that of the cerebrovascular cells of the vessels that supply them, with these cellular elements together forming a functional domain termed the "neurovascular unit" (Iadecola, 2004). Further support for the role that vascular mechanisms may play in AD pathogensis is provided by the finding of a number of shared environmental risk factors, discussed further in section 1.1.6.

1.1.5 Genetic risk factors in sporadic AD

The vast majority (>99%) of AD is described as being “sporadic”, in that it is not genetically inherited in a Mendelial fashion, and in most cases the main aetiological mechanisms are not well understood. However, the development of seemingly sporadic AD is significantly influenced by genetic factors. Twin studies suggest there is a higher concordance of AD in monozygotic twins than in dizygotic twins (Raiha et al., 1996, Bergem and Lannfelt, 1997). Genetic variation may play a crucial role in determining the risk of late-onset AD. The discovery of a number of genetic polymorphisms that can increase one’s risk of developing late-onset AD has further strengthened this argument.

By far the most important genetic risk factor for developing sporadic AD is Apolipoprotein E (ApoE) 4 (Corder et al., 1993). The expression of ApoE and its receptor are important in regulating lipid transport and metabolism in the brain. Individuals may have various combinations of ApoE alleles 2, 3 and 4 on chromosome 19, with the alleles differing from each other at two amino acid residues (112 and 158). Frequencies in the general population of the different ApoE alleles – 2, 3 and 4 – are 8.4%, 77.9% and 13.7% respectively (Liu et al., 2013). ApoE4 homozygosity confers the greatest risk of developing AD (odds ratio (OR) compared to the general population = 14.9), whilst ApoE2 homzygosity confers the least risk (OR = 0.6) (Farrer et al., 1997). ApoE has an important role in Aβ metabolism, affecting clearance, aggregation and deposition in an isoform-dependent manner, with ApoE4 carriers having significantly more Aβ deposition than non-carriers. ApoE4 also contributes to AD pathogenesis by Aβ-independent mechanisms that involve synaptic plasticity, cholesterol homeostasis, neurovascular functions, and neuroinflammation. Carriers of

APOE4 have been found to not only have an increased risk of developing AD, but also on average have a significantly younger age at symptom onset (table 1-1) and a more rapid symptomatic decline (Liu et al., 2013, Pietrzak et al., 2015).

Genetic carrier status	APOE4 non-carrier	APOE4 heterozygous	APOE4 homozygous
AD frequency (%)	20	47	91
Mean age at symptom onset	84	76	68

Table 1-1. The effect of APOE4 on AD frequency (lifetime risk) and age at onset (Liu et al., 2013)

Genome-wide association studies (GWASs) have identified nine putative novel candidate genes associated with late-onset sporadic AD (Harold et al., 2009, Lambert et al., 2009, Naj et al., 2011, Seshadri et al., 2010). Further study has shown the function of these genes to implicate a number of different pathways, including Aβ aggregation and clearance, phosphorylation of tau, lipid metabolism, neuroinflammation, and neuronal cell cycle control and apoptosis (Kim et al., 2014). However, compared to ApoE4, the odds ratios associated with each individual polymorphism identified from AD GWASs are small, typically <1.5. The genetics of autosomal dominantly inherited FAD are discussed in section 3.

1.1.6 Environmental risk factors in AD

Environmental risk factors for the development of AD remain relatively poorly understood. By far the biggest risk factor for sporadic AD is age (Hofman et al., 1991, Ritchie and Kildea, 1995, Jorm et al., 1987). A recent systematic evaluation of previous meta-analyses, which included 28 separate studies, found only two (non-genetic) risk

factors other than age with strong evidence of an association with AD. The first of these was a history of late life depression (Diniz et al., 2013). However, given that depressive symptoms are recognized to be a possible early feature of AD (Ownby et al., 2006), it can be difficult to disentangle whether a diagnosis of depression is actually a risk factor for later development of AD or is itself a manifestation of disease.

The other factor with convincing evidence of an association with sporadic AD is type 2 diabetes (Gudala et al., 2013); a condition more commonly associated with vascular causes of cognitive impairment rather than neurodegenerative ones. The possibility that vascular dysfunction more generally may contribute to AD risk is suggested by the finding (from the same systematic evaluation) of possible associations between AD and a number of other vascular factors, including level of physical activity, mid-life body mass index, previous stroke, alcohol intake, and long-term prescription of statins or aspirin (Anstey et al., 2011, Meng et al., 2014, Zhou et al., 2015, Anstey et al., 2009, Richardson et al., 2013, Wang et al., 2015). However, the current evidence for these latter associations remains weak at best.

There is emerging evidence of an association between AD and previous traumatic brain injury (Perry et al., 2016). Again though, further work is needed to clarify the nature of any association. There is evidence to suggest that previous educational attainment is inversely related to risk of later AD (Meng and D'Arcy, 2012), with those who have a higher intellectual baseline said to have greater “cognitive reserve”, making them less susceptible to the negative cognitive effects of AD pathology (Stern, 2012).

1.1.7 Treatment

1.1.7.1 Current therapies

Therapeutics options for AD are currently very limited, with no treatment yet proven to modify the underlying pathophysiological process. Currently licensed AD treatments are targeted at improving clinical symptoms, with four currently available in the UK: donepezil, galantamine, rivastigmine and memantine.

Donepezil, galantamine, and rivastigmine have a similar mechanism of action, each inhibiting acetylcholinesterase, in order to increase synaptic availability of the neurotransmittor acetylcholine (Rogers et al., 1998, Tariot et al., 2000, Cummings, 2000, Apostolova et al., 2011). The theoretical basis for these agents came from work in the early 1980s, which found a significant reduction of cholinergic neurons in the basal forebrains of AD patients, leading to reduced cortical availability of acetylcholine (Whitehouse et al., 1982, Coyle et al., 1983, Bartus et al., 1982, Rossor, 1983). Donepezil and galantamine are selective inhibitors of acetylcholinesterase, with galantamine also acting as an allosteric ligand at nicotinic acetylcholine receptors to increase presynaptic acetylcholine release and postsynaptic neurotransmission (Scott and Goa, 2000). In addition to the inhibition of acetylcholinesterase, rivastigmine also inhibits butyrylcholinesterase, which accounts for about 10% of the total cholinesterase in normal human brains. All the cholinesterase inhibitors are approximately equal when it comes to efficacy and tolerability. However, the overall beneficial effect is modest (e.g. 1.3 points on the MMSE for donepezil after six months), and any reports of improvement in quality of life have been inconsistent. A study of donepezil over a longer follow-up period reported disappointing results, with long-term benefits found to be below prespecified thresholds (Courtney et al., 2004).

Memantine, the only other currently licensed AD symptomatic medication, is an NMDA glutamate receptor antagonist. Its postulated mode of action is to protect neurons from the excitotoxic effects of an excess of extracellular glutamate, which can build up in the presence of on-going neurodegeneration. The patient group initially shown to benefit from memantine was those in the advanced clinical stages of AD (Winblad and Poritis, 1999, Reisberg et al., 2003). However, as with cholinesterase inhibitors, although benefits were statistically significant the treatment effects were small, with no effect on the underlying disease process. More recently, studies have assessed the benefit of adding memantine in patients already taking cholinesterase inhibitors, who have moderate to severe AD, however results appear to be inconsistent in terms of whether this provides additional benefit (Howard et al., 2012, Porsteinsson et al., 2008).

1.1.7.2 Putative disease modifying therapies

Whilst currently licensed AD medications have been shown to confer some, albeit relatively modest, symptomatic benefit, they do not modify the underlying neurodegenerative process. Over the past decade, there has been increasing interest in developing medications that will modify the underlying pathophysiological process of AD, with much of the work to date being guided by the amyloid cascade hypothesis (Hardy and Allsop, 1991) (see section 1.1.4.3). As such, efforts to develop disease-modifying therapies have largely centred on reducing Aβ production and/or increasing Aβ clearance (figure 1-6). When it comes to modulating production of Aβ, a number of strategies are potentially available, which come from our knowledge of the process of proteolytic cleavage of APP to produce Aβ (see section 1.1.4.1). These would include inhibition of β- or γ-secretase to reduce Aβ production, or stimulation of α-secretase to enhance the so-called non-amyloidogenic pathway.

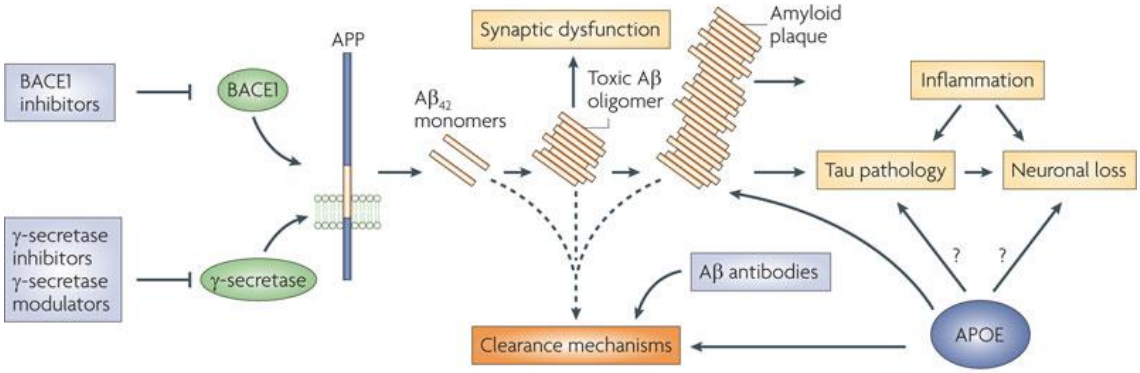

Figure 1-6. The amyloid cascade and major therapeutic approaches (from Citron, 2010)

BACE= β site of APP cleavage enzyme; APP=amyloid precursor protein; Aβ=amyloid β; ApoE=apolipoprotein E

γ-secretase inhibition was one of the first strategies to be attempted, and proved effective in mouse models (Dovey et al., 2001). However, attempts to transfer this success in to a clinically beneficial effect in human trials have thus far been unsuccessful (Doody et al., 2013). The complex structure of γ-secretase has made obtaining a detailed understanding of the active site difficult, although understanding of its regulation, assembly, and specificity does continue to improve (Chavez-Gutierrez et al., 2012). γ-secretase inhibitor development has been compounded further by the fact that the enzyme has been found to act on multiple substrates other than APP (Parks and Curtis, 2007). In particular, γ-secretase has a crucial role in interacting with the Notch receptor (De Strooper et al., 1999), which has a number of key roles (Varnum-Finney et al., 1998). Ideally therefore, strategies are required to reduce $A\beta_{42}$ production without suppressing Notch cleavage. Agents aiming to address this problem have been trialed, but were not found to produces significant clinical benefit, with a recent study actually showing an adverse effect on cognition and neurodegeneration (Green et al., 2009, Doody et al., 2015).

The second main strategy for reducing production of Aβ has been to inhibit the enzyme β-secretase, which has been identified as the transmembrane protease "β site of APP cleavage enzyme" or BACE1 (Vassar et al., 1999), and like γ-secretase is involved in the cleavage of APP to produce Aβ. A BACE1 knockout mouse model has shown to have significantly reduced Aβ, and importantly without any evidence of additional mechanism-based side effects (Ohno et al., 2004). This lack of side effects, as much perhaps as the potential therapeutic benefits, has led to many to consider BACE1 inhibition as the best therapeutic target for reduction of Aβ production. Over the past decade, substantial research efforts have been directed toward the development of BACE1 inhibitors for use in human clinical trials. Studies have shown certain candidate BACE1 inhibitors to reduce $A\beta_{40}$ and $A\beta_{42}$ in the cerebrospinal fluid (CSF) of healthy individuals, as well as also in AD patients (Kennedy et al., 2016, May et al., 2015), although evidence of improved clinical outcomes is still awaited. A recent study in mice also showed a beneficial effect in reducing CSF tau (thought to lie downstream to Aβ), which is encouraging. A number of BACE1 inhibitors are currently undergoing phase II and/or phase III human trials.

A third option for reducing Aβ production would be to stimulate the α-secretase (i.e. non-amyloidogenic) pathway, as this would theoretically lead to a reduction in the amount of APP substrate available for Aβ production, with in-vitro study showing this to be the case (Fahrenholz and Postina, 2006). However, much more APP enters the α-secretase pathway than the β/γ-secretase pathway, so the desired reduction in Aβ would require a marked change in the metabolism of both APP and various other α-secretase substrates. This therapeutic pathway has therefore not been pursued to the same extent as those discussed above.

Rather than inhibiting Aβ production, an alternative approach is to aim to increase clearance of Aβ from the brain. Over the past few years, Aβ immunotherapy has become one of the therapeutic areas of greatest interest. Both active and passive immunization strategies have been tried. Despite positive results in animal models (Schenk et al., 1999, Morgan et al., 2000), the first phase II trial using active immunization, by which the Aβ peptide is injected to stimulate antibody production, was halted due to the occurrence of meningo-encephalitis in a proportion of participants (Senior, 2002, Gilman et al., 2005, Fox et al., 2005).

Passive immunotherapies, using monoclonal antibodies, have faired better from a side-effect point of view. However, these agents are also not without potential risk, with imaging changes consistent with both vasogenic oedema and microhaemorrhage found in association with a number of agents (Salloway et al., 2009, Ostrowitzki et al., 2012, Doody et al., 2014). These changes, termed amyloid-related imaging abnormalities (ARIA) (Sperling et al., 2011c), are dose-dependent and are thought to be related to Aβ clearance from vessel walls.

Despite the problems posed by ARIA, a number of agents have reached phase III trials. The first two major phase III trials to report assessed the agents bapineuzemab and solaneuzemab respectively in mild-to-moderate AD (Salloway et al., 2014, Doody et al., 2014). Bapneuzemab had been found in preclinical studies to bind to fibrillar, and soluble oligomeric/monomeric forms of Aβ, whilst solaneuzemab selectively binds to soluble Aβ only. Whilst both agents demonstrated an effect on certain in-vivo measures of Aβ physiology, neither was able to produce significant clinical benefit. A more recent study, although only in phase IB, did offer cause for optimism. This study treated individuals with either prodromal (i.e. amnestic MCI) or mild AD with the agent aducanumab, which targets fibrillar Aβ (Sevigny et al., 2016). The study found

significant reduction in the rate of clinical decline compared to placebo, as well as increased amyloid clearance, with the drug now undergoing phase II trials.

Overall, whilst results of anti-amyloid trials have shown some promise, and particularly in animal studies would appear to confirm the amyloid cascade hypothesis, results have thus far generally been disappointing. This has led some to consider other therapeutic targets, with a number of authors suggesting anti-tau treatments should be the focus (Giacobini and Gold, 2013, Boutajangout et al., 2011b). Tau pathology has been shown to correlate more closely than amyloid with clinical status (Arriagada et al., 1992, Brier et al., 2016), and preclinical studies have shown functional benefit of passive tau immunization (Boutajangout et al., 2011a). However in a recent phase III study, an agent that aimed to inhibit tau aggregation was shown to have no beneficial effect on clinical outcome (Gauthier et al., 2016). A further area of increasing interest in AD is anti-inflammatory medication, to target the inflammatory component of the AD pathological cascade (Rubio-Perez and Morillas-Ruiz, 2012). However, to date, anti-inflammatory drug trials in AD have been unsuccessful (Group, 2015, Wilcock et al., 2008).

An emerging theory in recent years as to the reason for failure of disease modifying treatment trials in AD is that, rather than choosing the wrong therapeutic target, it may be that the choice of target (i.e. amyloid in most cases) is correct but we are targeting it too late in the disease process (Sperling et al., 2011b). All published trials to date have focused on individuals with clinical symptoms of decline, which would signify that significant neuronal loss has already occurred. It may be therefore that targeting the disease earlier, possibly before the onset of clinical decline will produce better long-term clinical outcomes, and studies have now been set up with this in mind (Sperling et al., 2014, Mills et al., 2013). The concept of a presymptomatic phase to Alzheimer's disease, with the pathological cascade beginning years before the onset of symptoms,

and the need for robust methods to detect and track disease during this period, are discussed in detail in the following sections.

1.2 The presymptomatic phase of Alzheimer's disease

1.2.1 Theoretical models of presymptomatic disease

There has been growing evidence over the last couple of decades that the pathological process underlying AD begins several years before the onset of clinical symptoms (Bateman et al., 2012, Villemagne et al., 2013), with presymptomatic AD pathology found to be relatively common in cognitively normal elderly individuals (Vos et al., 2013). AD is therefore now considered as a continuum of progressive pathophysiological changes, which includes both symptomatic and presymptomatic disease stages (Dubois et al., 2016). The presymptomatic stage is also sometimes referred to as the "preclinical" stage, with the two terms seemingly used interchangeably, albeit with there being a subtle difference between them: "presymptomatic" implies no subjective experience of decline noticed by the patient, whilst preclinical implies an individual without any objective signs of clinical impairment on assessment.

In keeping with the amyloid cascade hypothesis (Hardy and Allsop, 1991, Hardy and Higgins, 1992), a number of theoretical models have been proposed, which attempt to outline the temporal sequence of biological changes that occur, both before and after the onset of symptomatic disease. The most prominent model of sequential AD-related changes was proposed by Jack and colleagues in 2010 (Jack et al., 2010) (figure 1-7).

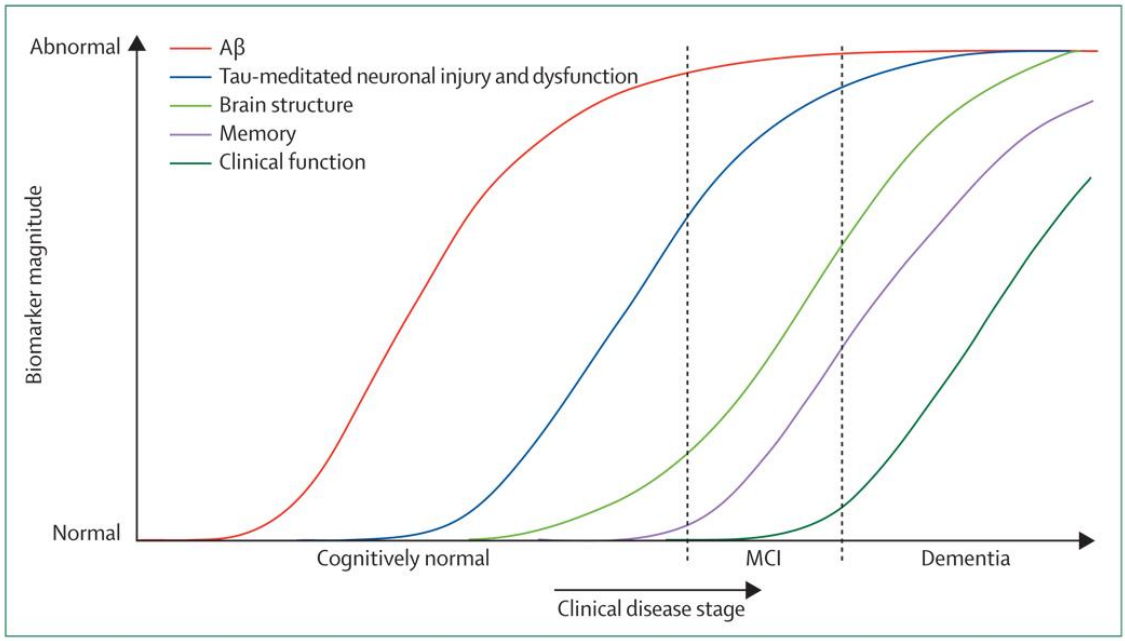

Figure 1-7 Dynamic biological changes of the Alzheimer's pathological cascade (reproduced from Jack et al., 2010).

There has been increasing research interest in better understanding and defining the presymptomatic phase of AD, with recognition that effective disease-modifying therapies may have maximum benefit if given as early as possible, when minimal neuronal loss has occurred (Sperling et al., 2011b). A 'self-perpetuating' aspect to neurodegeneration that is difficult to slow once established, may account, at least in part, for trial failures in individuals who had already reached the symptomatic phase of disease. In 2011, a framework was proposed by The National Institute on Aging and the Alzheimer Association (NIA/AA) for staging individuals who enter presymptomatic AD research studies (Sperling et al., 2011a). This framework divides presymptomatic AD in to three separate stages as outlined below:

- stage 1 – presymptomatic amyloidosis
- stage 2 – amyloidosis and neurodegeneration

- stage 3 – amyloidosis, neurodegeneration and subtle cognitive decline

1.2.2 The need for biomarkers of presymptomatic AD

In order to operationalize the above, or any similar framework, and carry out effective trials of novel therapies in presymptomatic AD, sensitive and robust measures are needed to identify those individuals at risk, to stage their disease, and to track disease progression. As these individuals, by definition, have not yet reached the clinical phase of the illness, it is not feasible to use clinical outcome measures (e.g. symptom progression or decline on conventional cognitive tests) to gauge disease stage and/or progression, and hence surrogate measures of disease biology – or biomarkers – are required. A biomarker is defined as a biological characteristic that is objectively measured and evaluated as an indicator of normal biological or pathological processes, or a response to a therapeutic intervention (Biomarkers Definitions Working, 2001). Desirable characteristics of an AD biomarker, as defined by the Working Group on molecular and biochemical markers of Alzheimer's disease (Disease", 1998), are outlined below:

1. able to detect a fundamental feature of Alzheimer's neuropathology
2. validated in neuropathologically confirmed AD cases
3. precise (able to detect AD early in its course and distinguish it from other dementias)
4. reliable
5. non-invasive
6. simple to perform
7. inexpensive

This need for accessible and reliable biomarkers of early disease change has prompted a huge effort in recent years by the AD research community to develop more effective AD biomarkers. The principal biomarkers of underlying AD pathology that are currently used to detect early disease changes are listed below, and are discussed in more detail in section 1.4:

- amyloidosis – CSF $A\beta_{42}$ and/or amyloid positron emission tomography (PET)
- tau pathology – CSF total tau, CSF phosphorylated tau, and/or tau PET
- neurodegeneration – structural magnetic resonance imaging (MRI) and/or fluorodeoxyglucose (FDG) PET (and possibly CSF total tau)

In 2013, an updated version of the Jack model was published, which focused more on outlining measurable biomarker changes for each step in the pathological cascade, as opposed to simply stating the underlying biological processes (figure 1-8)(Jack et al., 2013). This updated model also states that it may be possible for tau pathology to be present in the entorhinal cortex (Braak stage I) prior to the deposition of Aβ, but it is only once Aβ is present that the spread of tau beyond the medial temporal lobe is triggered. A further modification to the model was the recognition that, whilst the temporal ordering of presymptomatic changes is relatively consistent, the timing of clinical onset can be variable, presumably due to genetic and other modifying factors (e.g. cognitive reserve).

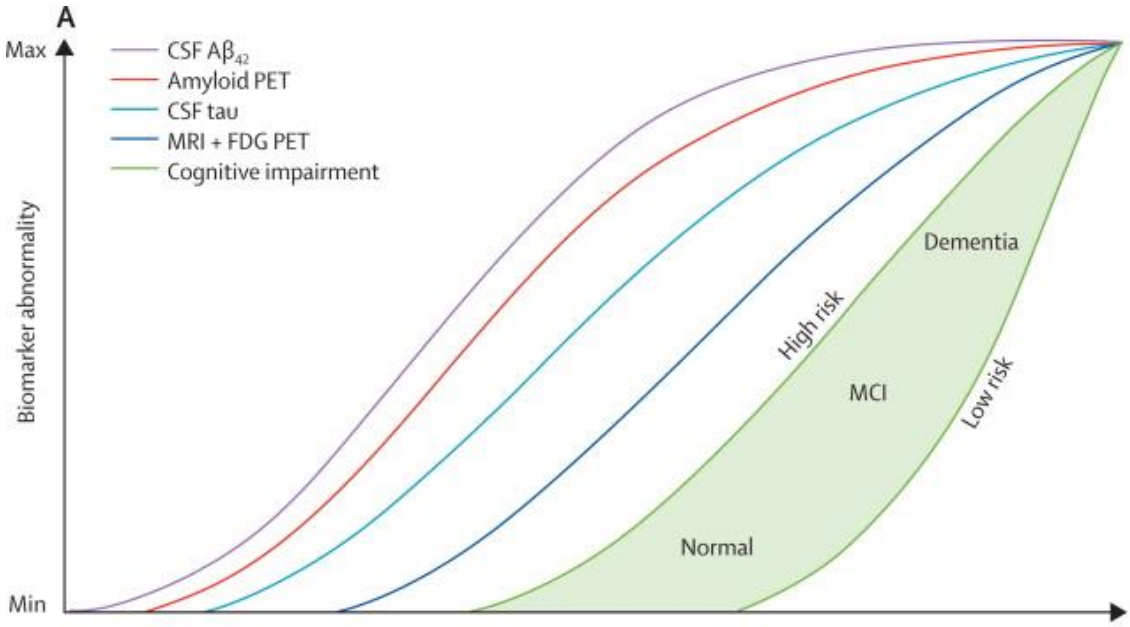

Figure 1-8. An updated model of the pathological cascade of AD, (reproduced from Jack et al., 2013)

The above model focuses more on measurable biomarker changes than the underlying biological processes.

More recently, some have suggested the initial "amyloidosis + neurodegeneration" framework proposed by Sperling et al. be updated to incorporate an additional category for evidence of the presence or absence of tau pathology (Jack et al., 2016a).

1.2.3 The limitations of studying presymptomatic sporadic AD

Despite the growing availability of AD biomarkers, issues remain when trying to recruit asymptomatic individuals to studies of presymptomatic AD. Firstly, no biomarker is 100% sensitive and specific, meaning that is impossible to be certain at the point of recruitment whether or not an individual definitely has presymptomatic AD based on biomarkers alone. Secondly, whilst it may be possible to predict with relatively high accuracy who does and doesn't have presymptomatic AD, it is currently impossible to know, for presymptomatic sporadic AD, how far an individual is from symptom onset at

a given time point. One potential solution to both of the above issues is to study individuals with presymptomatic FAD, rather than the commoner sporadic AD. FAD, and its utility in AD research are discussed in detail in the following section.

1.3 Familial Alzheimer's disease

1.3.1 The genetic inheritance of FAD

The vast majority of AD is sporadic, with no clear pattern of autosomal dominant inheritance within families. Affected individuals often have no family history and usually have symptom onset relatively late in life, with prevalence increasing with age in an exponential fashion. However, it was observed as early as the 1930s that in some cases dementia due to AD can occur at a much earlier age and may cluster within families. In 1991, a genetic linkage study of a family originating from Nottingham, in whom young onset AD was highly prevalent, led to the discovery of the first FAD pathogenic mutation in the *APP* gene on chromosome 21 (Goate et al., 1991). This was followed by the identification of pathogenic mutations in two other genes: the presenilin 1 (*PSEN1*) gene on chromosome 14 and the presenilin 2 (*PSEN2*) gene on chromosome 1 (Sherrington et al., 1995, Levy-Lahad et al., 1995). Over 200 autosomal dominantly inherited genetic mutations have now been described across *APP*, *PSEN1* and *PSEN2,* all demonstrating 100% penetrance (Ryan and Rossor, 2010). Although rare, accounting for less than 1% of all known AD cases, the study of FAD mutation carriers has proven invaluable in advancing our understanding of AD, both in terms of presymptomatic and symptomatic disease. Mutations in all three of the recognized FAD genes are known to result in increased production and/or deposition of Aβ, with either an increase in both $A\beta_{40}$ and $A\beta_{42}$, or an alteration in their ratio to produce a relative increase in the more amyloidogenic $A\beta_{42}$. (Scheuner et al., 1996). However, the mechanisms through which these mutations achieve these changes in Aβ can be complex and variable.

1.3.2 The amyloid precursor protein gene

The first FAD mutation to be identified was the V717I missense mutation in the *APP* gene – the so-called London mutation – which causes AD by producing a relative increase in longer Aβ moieties such as $A\beta_{42}$ (Goate et al., 1991). APP is a transmembrane protein whose exact function has yet to be fully determined, although it is thought to play a role in neural plasticity and regulation of synapse formation. Thirty-two separate pathogenic *APP* mutations have now been described to date (figure 1.9.), with *APP* mutations accounting for about 20% of all FAD (Tang et al., 2016). As discussed in section 1.1.4.2., APP can be enzymatically cleaved along one of two parallel pathways.

Cleavage by α-secretase is part of the so-called non-amyloidogenic pathway, whilst sequential cleavage of β- and γ-secretase results in Aβ formation (figures 1-4 and 1-9). Extracellular cleavage by β-secretase leads to generation of a soluble extracellular fragment and is followed by cleavage within the transmembrane domain by γ-secretase. Cleavage by γ-secretase can result in a protein of variable length, with by far the most common two being $A\beta_{40}$ and $A\beta_{42}$. The majority of pathogenic *APP* mutations lie within or close by either the β-secretase or γ-secretase cleavage sites.

In addition to point mutations, it has also now been shown that *APP* copy number variation can give rise to FAD, with a number of APP duplication cases now reported (Rovelet-Lecrux et al., 2006). This finding is also consistent with the frequent occurrence of young onset AD in individuals who have Down's syndrome, in whom an extra copy of chromosome 21 is present.

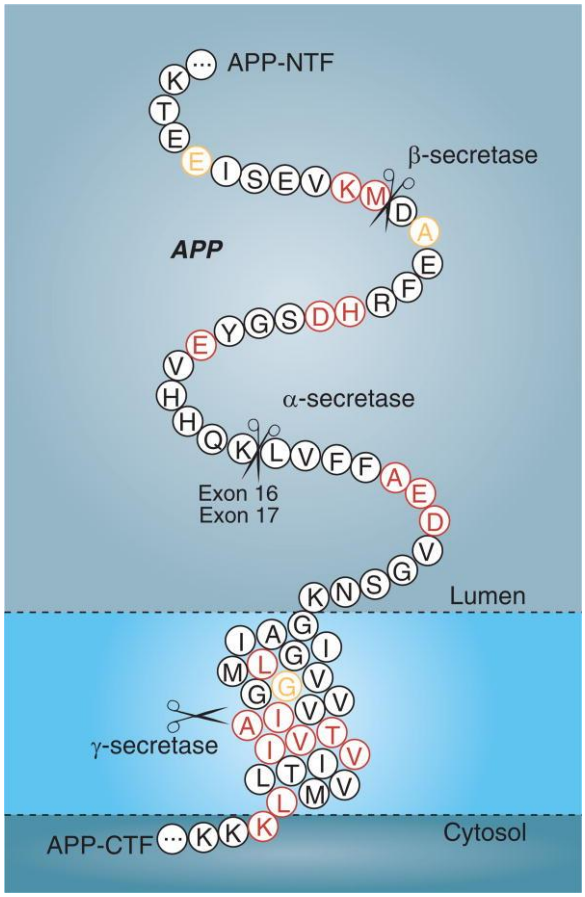

Figure 1-9. APP linked mutations (reproduced from Ryan and Rossor, 2010)

FAD mutations are in red while non-pathogenic mutations are in orange. APP=amyloid precursor protein; CTF=C-terminal fragment; NTF=N-terminal fragment.

1.3.3 The presenilin genes

The *PSEN1* gene has 13 exons, although only exons 3-12 code the PSEN1 protein, which comprises eight transmembrane domains. The PSEN1 protein forms part of the γ-secretase complex that is responsible for the transmembrane cleavage of APP to form Aβ (De Strooper et al., 1998). *PSEN1* mutations are thought to account for 70-80% of all FAD. Over 180 pathogenic *PSEN1* missense mutations have been reported, with the majority located in areas thought to lie close to PSEN1's transmembrane domains (figure 1-10). Both missense mutations and deletions have been reported.

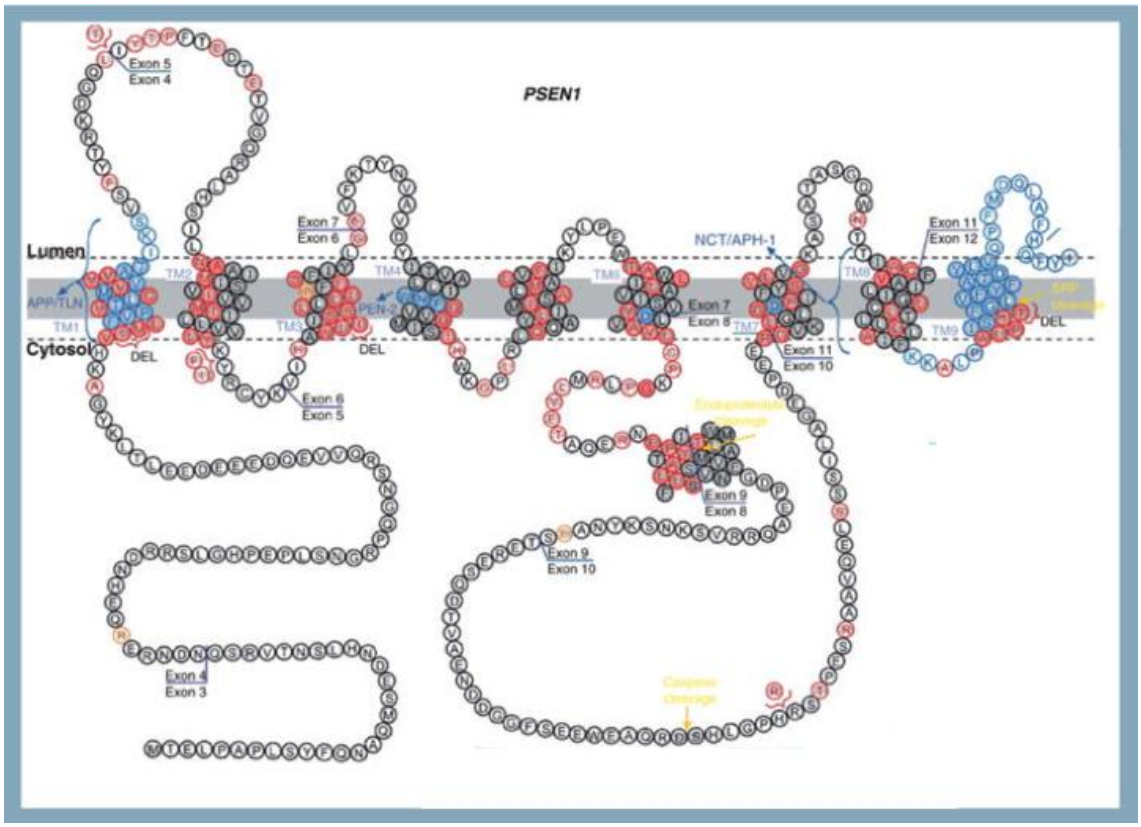

Figure 1-10. PSEN1-linked FAD mutations (reproduced from Ryan and Rossor, 2010)

FAD mutations are in red while non-pathogenic mutations are in orange. Interaction domains with APP/TLN or NCT/APH-1/PEN-2 are marked in blue. APP=amyloid precursor protein; CTF= C-terminal fragment; NTF=N-terminal fragment; PEN=Presenilin enhancer; PLD=Phospholipase D; PSEN=Presenilin; NCT=Nicastrin.

Like PSEN1, PSEN2 also forms an important part of the γ–secretase complex. Pathogenic mutations in *PSEN2* are less common than both *APP* and *PSEN1* mutations, accounting for no more than 5% of total FAD cases.

1.3.4 Clinical features

The key clinical feature that tends to differ between sporadic AD and FAD is the age at symptom onset. On average, *PSEN1* mutations produce the youngest age at onset (AAO), with mean AAO±SD = 43.3±8.6 (Shea et al., 2016). *APP* mutations tend to have an AAO of 47.6±7.1, with *PSEN2* 58.1±9.5 years. Disease duration is largely similar for FAD and sporadic AD, with *PSEN1* carriers generally having between 4.8 and 6.8 years from onset to death. This is slightly longer for *APP* and *PSEN2*. (Holmes, 2002).

Whilst the ages of the individuals who suffer from FAD and sporadic AD tend to differ significantly, when it comes to clinical phenotype the two are similar. Just like sporadic AD, FAD typically presents with the insidious onset of episodic memory problems, with atypical AD syndromes such as PCA or LPA being rare. A recent analysis of all cases seen at the UCL Dementia Research Centre over a period of more than 28 years found 84% of *PSEN1* cases and 97% of *APP* cases to have amnestic presentations (Ryan et al., 2016). Other non-amnestic features often do develop over time, and include visuoperceptual dysfunction, language impairment and behavioural change (Tang et al., 2016, Ryan et al., 2016). The relative frequency of these atypical cognitive features across the different genes is not entirely clear, and does appear to vary between different studies. Depression can also be a prominent feature in a proportion of cases (Shea et al., 2016).

Additional non-cognitive neurological features are seen in a proportion of FAD cases, and increase in frequency as the clinical disease progresses. Potential additional neurological features include myoclonus, seizures, spasticity, and, less commonly, extrapyramidal and cerebellar signs (Ryan et al., 2016). However, the frequency of these additional neurological features in FAD compared to sporadic AD is not certain,

with evidence emerging that they may not be as common as previously thought (Tang et al., 2016). A summary of the clinical features of FAD across the three known genes, from Tang et al., is shown in figure 1-11.

1.3.5 Genotype-phenotype interactions

Whilst the majority of FAD cases present with a typical AD syndrome, a significant amount of the phenotypic variability that does exist can be explained by differences in the underlying mutation, both between the different genes and within the same gene (Ryan et al., 2016), with genotype-phenotype variations helping to inform our understanding of AD's pathophysiology. For example, in PSEN1 mutations alone, 72% of the variance in AAO has been found to be explained by mutation, with mutations located before codon 200 tending to have an earlier AAO.

Clinical symptoms and signs are also influenced by mutation. For example, *PSEN1* mutations after codon 200, which have later ages at onset, are more likely to have more atypical cognitive presentations and pyramidal signs. While pyramidal signs such as spasticity are known to occur in a proportion of *PSEN1* cases, they are almost unheard of in *APP* mutations (Ryan et al., 2016, Tang et al., 2016). This has led to the suggestion that *PSEN1* mutations may cause spasticity via γ-secretase interacting with an alternative substrate to APP.

When compared to *PSEN1*, *APP* mutations can often have a prolonged, relatively isolated amnestic phase, which may last several years prior to the onset of non-amnestic cognitive features. This phenotypic difference is also reflected radiologically, with some APP mutations showing very little atrophy beyond the medial temporal lobe even several years after onset (Scahill et al., 2013).

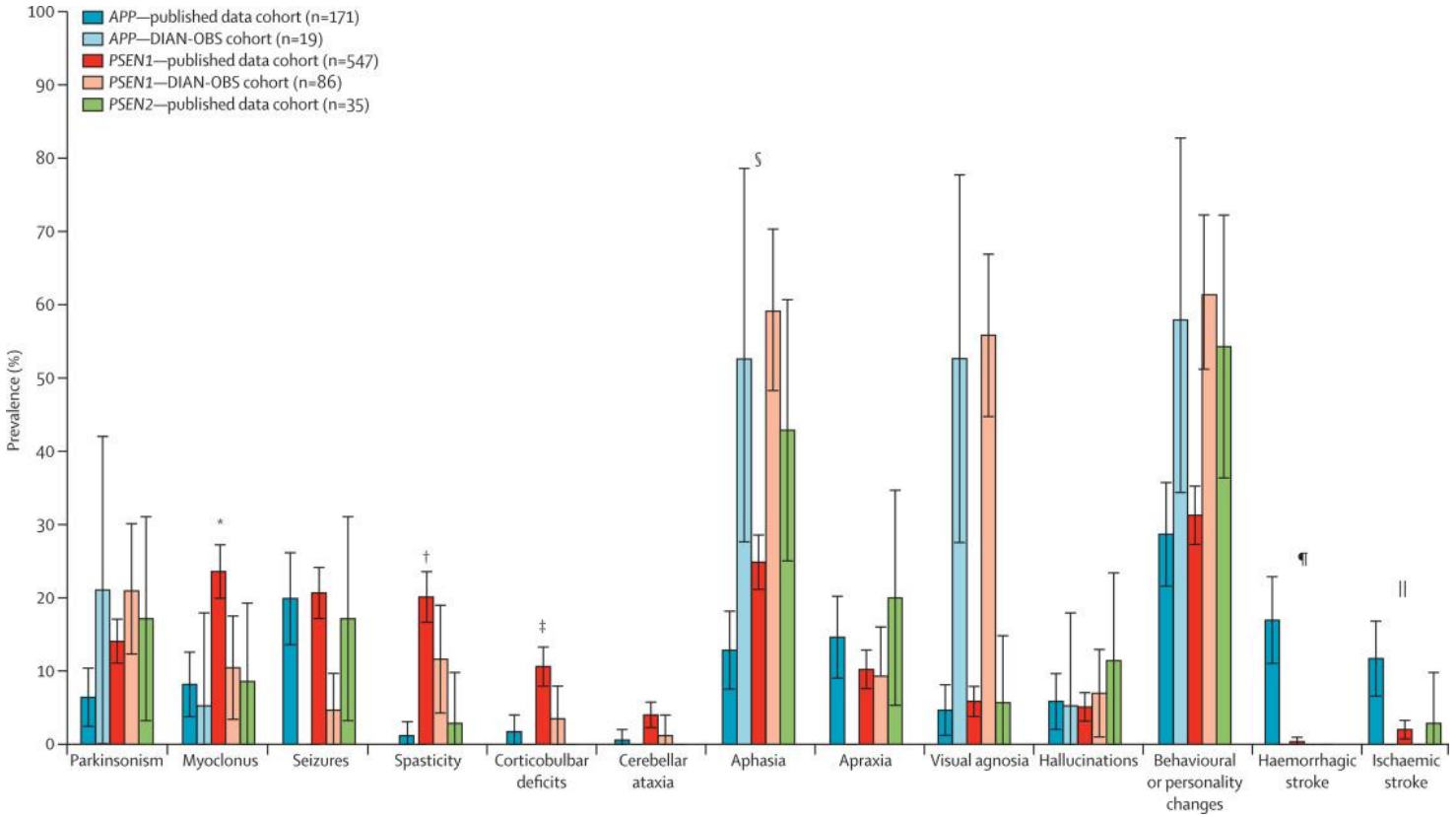

Figure 1-11. A Summary of the prevalence of non-amnestic features in FAD (reproduced from Tang et al., 2016)

Frequencies from both the large multicenter Dominantly Inherited Alzheimer's Disease Network (DIAN) are shown, in addition to frequencies from a literature search of the published FAD literature. For PSEN2, only frequencies from the published literature are shown, due to their being few PSEN2 cases in DIAN.

The majority of APP mutations occur at the cleavage sites of γ- and β-secretase. However a number of rare pathogenic mutations at the α-secretase site, including the A692G Flemish mutation E693Q Dutch mutation, and E693G Artic mutation, have been found to have quite a different clinical phenotype (Hendriks et al., 1992, Levy et al., 1990, Nilsberth et al., 2001), Carriers of these mutations have frequent cerebral haemorrhages, due to underlying cerebral amyloid angiopathy, resulting in frequent stroke-like episodes. The specific mechanistic reason for this phenotypic difference remains uncertain.

1.3.6 Predicting age at onset

All known FAD mutations are inherited in an autosomal dominant fashion and demonstrate 100% penetrance. Therefore, any child of a mutation carrier will be at 50% risk of inheriting the mutation, and if they do inherit the mutation they will be almost certain to develop clinical disease (assuming that they do not die of another cause prior to symptom onset). Furthermore, as well as being able to predict who will and will not develop symptomatic disease, it is also possible to predict with relatively high accuracy at what age an individual mutation carrier will develop symptoms (Mullan et al., 1993, Ryman et al., 2014). This predictability of age at onset (AAO) at the individual level is one of the features that makes FAD an attractive model for the research of presymptomatic disease, as it means it is possible to predict, at a given time point, how many years from symptom onset an individual is; usually referred to as “estimated years to symptom onset” (EYO). Prospectively calculating EYO is not possible in sporadic disease, for which following each individual longitudinally, often over many years, to the point they develop symptoms is the only way of knowing the AAO with any accuracy.

A number of methods have been used to predict AAO in FAD mutation carriers, including estimating based on the parental AAO, estimating based on the mean AAO for the individual's family, and estimating based on the mean AAO for the specific mutation (Ryman et al., 2014). A systematic review and meta-analysis of over 3,000 individuals with FAD found all three of these methods for predicting AAO to produce estimates that show highly significant correlations with the actual years to onset. Given generational and regional differences in clinically diagnosing AD, it is generally more reliable to define "onset" as the development of the first symptom of progressive cognitive decline, rather than the time of formal diagnosis. Historically, parental AAO has been the most commonly used method. Using a family mean AAO can be problematic, as reliable clinical information for all individuals within an extended family is often unavailable. Generally, the parental age at symptom onset is determined through interviewing other family members and asking them when they first noticed a change. This retrospective way of ascertaining AAO has been found to produce similar estimates to using the information that had been obtained contemporaneously in the clinical notes at the time of original assessment (Doody et al., 2004).

However, whilst the ability to predict EYO is useful, it inevitably has a degree of error. Within certain families AAO has been found to show significant fluctuation, with the underlying reason uncertain. Both genetic and environmental factors have been proposed as possible modifying factors, but nothing has yet been proven to have a significant effect. Interestingly, whilst APOE carrier status is known to significantly influence AAO in sporadic disease (Liu et al., 2013), it remains uncertain whether it has same effect in FAD. A number of studies have suggested that APOE genotype does influence AAO in FAD (Mann et al., 2001, Wijsman et al., 2005), but the systematic review by Ryman and colleagues found no significant association (Ryman et al., 2014).

1.3.7 Genetic support for the amyloid cascade hypothesis

The information gained from studying the genetics of FAD has been central to the progress that has been made over the last 25 years in understanding the sequence of pathophysiological changes underlying AD. It was the discovery of the *APP* V717I mutation in 1991 (Goate et al., 1991) that first provided evidence that Aβ deposition is not only an end result of AD, but that an initial alteration in Aβ physiology is sufficient to cause disease. It was shortly after this initial genetic discovery that the amyloid cascade hypothesis was proposed (Hardy and Higgins, 1992, Hardy and Selkoe, 2002), with subsequent identification of mutations in *PSEN1* and *PSEN2* providing further support.

More recently the Decode study on APP identified a mutation (A673T) that protects against late onset sporadic Alzheimer's disease and cognitive decline in elderly individuals (Jonsson et al., 2012). This mutation is adjacent to APP's β-secretase cleavage site, and results in an approximately 40% reduction in the formation of amyloidogenic peptides in vitro. The protective effect of the A673T substitution against sporadic AD provides further evidence of principle for the amyloid cascade hypothesis, and would support the idea that reducing the β-cleavage of APP may protect against the development of AD. Moreover, the finding that alteration of a gene known to be heavily implicated in the development of FAD can also mediate risk of sporadic AD, provides strong support that the two share a common pathophysiology.

1.3.8 The utility of FAD in the research of presymptomatic disease

The study of FAD has been useful in a number of different ways. However, perhaps its greatest utility, at least in terms of clinical research, is in helping improve understanding of the presymptomatic phase of disease. Unlike in presymptomatic sporadic AD, the ability to identify FAD mutations by a simple blood test enables

researchers to know who will and will not go on to develop symptomatic disease long before the onset of clinical symptoms. Also unlike sporadic AD, it is possible in FAD carriers to be certain of the underlying pathology in life, without requiring post-mortem confirmation. Furthermore, as the AAO is relatively predictable (see section 1.3.6.), it is usually possible to estimate how far away from symptom onset an individual is at a given point in time. Also, as presymptomatic FAD mutation carriers are usually relatively young, they tend to have far less comorbidity than older individuals, which means it is possible to assess the direct pathological consequences of AD without having to account for other co-existing pathologies. Although, as discussed previously, the presence of vascular changes in older people with sporadic AD, may well, at least in a proportion of individuals, be a direct consequence of AD itself, rather than a separate co-exisitng, process, and so should not necessarily be considered as a confound in such cases. Overall however, carriers of FAD mutations provide a valuable opportunity for prospective longitudinal study of asymptomatic individuals prior to the onset of clinical disease (Bateman et al., 2011).

1.4 Evidence of presymptomatic changes in familial and sporadic AD

1.4.1 The need for markers of early disease

As discussed in earlier sections, potential new disease-modifying treatments for AD are likely to be most effective if given as early as possible, prior to significant irreversible neuronal loss (Sperling et al., 2011b). To carry out such trials prior to the onset of symptomatic decline it is important to understand the timing and sequence of early measurable AD changes, and in parallel develop sensitive and reliable methods, or biomarkers, for detecting and tracking the underlying disease process *in-vivo*. Such measures of disease activity aim to detect changes between AD and controls (i.e. healthy aging) either in severity of disease at a single time point (cross-sectional) or in the rate/intensity of disease progression across multiple time points (longitudinal). Generally a new measure of disease will first be assessed cross-sectionally to assess its ability to separate disease and controls, before then potentially being used longitudinally (figure 1-12).

A large amount of research in recent years has focused on identifying and improving methods of detecting and tracking presymptomatic disease. Due to the advantages outlined in section 1.3.8, a significant proportion of presymptomatic research to date has been performed in FAD rather than sporadic disease. This work provided both an initial basis for the theoretical models outlined in section 1.2, and then also provided additional evidence to support or refute these models, thus allowing ongoing modifications.

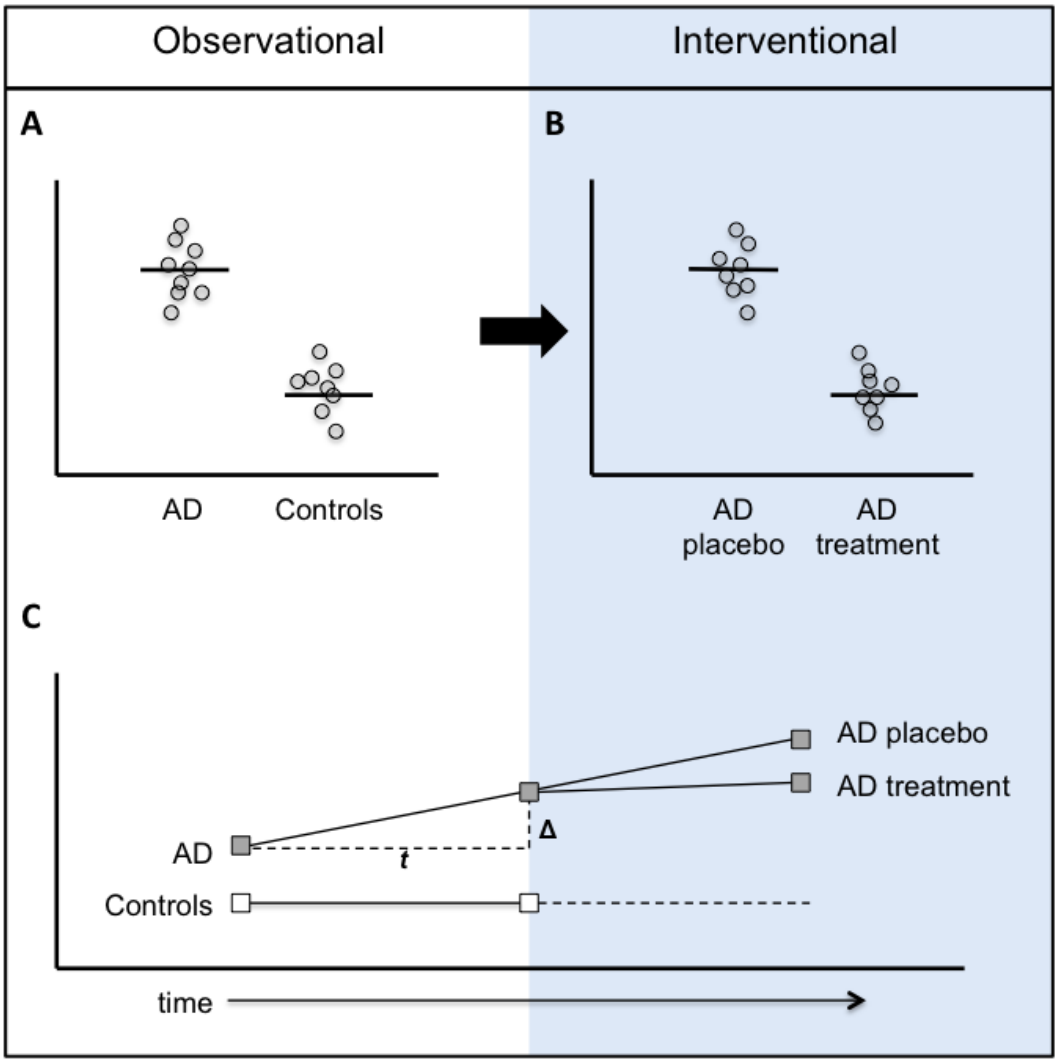

Figure 1-12. Outline of the evaluation of utility of potential biomarkers for AD

AD biomarker candidates, whatever the specific modality, would ideally demonstrate a significant difference between disease and controls at a single cross-sectional time point ***(A),*** *which is particularly useful in identifying those who carry disease pathology and/or are at greatest risk of experiencing progressive cognitive decline. If used in a clinical trial* ***(B)****, following a period of treatment, such a marker may have utility as a trial end-point, ideally demonstrating a difference between those with AD on treatment and those with AD on placebo. Biomarkers may also be used longitudinally* ***(C)*** *to track rate of disease progression (Δ/t), either within groups or within individuals.*

Modalities used for detecting and tracking early AD pathology vary greatly: from expensive neuroimaging methods, to more invasive tests such as CSF measurement, to direct assessment of subtle cognitive change. Each of the numerous assessment methods now available have their own strengths and weaknesses. These markers of early AD change can be broadly divided in to two categories: 1) those that aim to assess early molecular pathology (i.e. Aβ and/or phosphorylated tau), and 2) those that aim to assess the effects of downstream neurodegeneration. The main benefit in measuring the molecular pathology, and particularly Aβ, is that the pathology is specific to AD. This is not the case for neurodegeneration, which occurs in a number of other diseases, although it may be that certain aspects of neurodegeneration in AD (e.g. the neuroanatomical distribution) allow discrimination from other neurodegenerative diseases.

The focus of this thesis is on detecting and tracking early AD-related neurodegeneration. FAD is a particularly good model for researching AD-related neurodegeneration, without necessarily also having to measure molecular pathology, as unlike people who are thought to have sporadic AD, in confirmed FAD mutation carriers the molecular pathology is already known with certainty. Therefore, even without trying to confirm the presence of Aβ pathology, in a relatively young person who carries an FAD mutation, and is otherwise healthy, one can be relatively certain that any neurodegenerative change observed will be a result of AD pathology.

In the following sections, a number of currently available methods for detecting and tracking presymptomatic AD changes in-vivo will be described. After briefly summarizing current methods for assessing molecular pathology (section 1.4.2.), the main focus will be on methods for assessing neurodegeneration, or its downstream cognitive effects. For each method, after first describing the methodological approach,

the results of studies to detect presymptomatic change in both FAD and sporadic AD will be discussed, prior to then comparing findings from the two disease sub-types.

1.4.2 Measuring AD molecular pathology

1.4.2.1 Amyloid β

An early in-vivo measure of Aβ molecular pathology shown to discriminate AD dementia from controls was measurement of $A\beta_{42}$ in CSF using an enzyme-linked immunosorbent assay (ELISA) method (Hulstaert et al., 1999, Lewczuk et al., 2004). $A\beta_{42}$ is consistently lower in individuals with AD compared to controls, but with no significant difference found for $A\beta_{40}$. It appears that equilibrium is disrupted, possibly via the inhibition of soluble Aβ transport between brain and CSF by insoluble plaques and/or increased clearance of Aβ into plaques. Over the last decade, the evidence supporting the clinical use of $A\beta_{42}$ to help diagnose individuals presenting with cognitive impairment has continued to grow. The diagnostic utility of this marker is increased further if combined with CSF total tau, which increases in AD, to calculate a tau/$A\beta_{42}$ ratio, with studies suggesting that a cut-off somewhere between 0.5 and 1 (dependent on the assay used) provides relatively good diagnostic value (Hulstaert et al., 1999, Lewczuk et al., 2004, Duits et al., 2014, Weston et al., 2015). Studies of FAD mutation carriers have shown that alterations in CSF $A\beta_{42}$ begin many years, possibly over two decades, before the onset of symptomatic disease, and may be the earliest presymptomatic AD biomarker change (Bateman et al., 2012, Thordardottir et al., 2015).

The development of amyloid tracers for use with PET was a major step forward, in that it provided a relatively non-invasive method of assessing fibrillar Aβ pathology (Klunk et al., 2004). As amyloid PET provides visualization of Aβ, it allows assessment of the anatomical distribution of amyloid in addition to simply quantifying it. The first

radioligand to be licensed was the C^{11} Pittsburgh compound B (PiB). The short half-life of C^{11}, meaning it has to be produced on-site, initially limited the widespread use of amyloid PET, but this issue has been somewhat resolved with the more recent development of three F^{18}-labelled compounds, which decay less quickly (Clark et al., 2011, Vandenberghe et al., 2010, Barthel et al., 2011). Amyloid PET has shown presymptomatic Aβ deposition in FAD mutation carriers, although not quite as early as for CSF measurements (Bateman et al., 2012, Knight et al., 2011b, Fleisher et al., 2012) (figure 1-13). This discrepancy probably relates to differences in the sensitivity of the methods. Both CSF and PET measures of Aβ are included as "in-vivo evidence of Alzheimer's pathology" in the most recently published AD diagnostic criteria (Dubois et al., 2014). However, in the clinical setting, if an individual has already undergone CSF sampling for neurodegenerative markers (which is significantly less expensive than PET) it is only in a minority of cases that amyloid PET is likely to add additional diagnostic value (Weston et al., 2016).

When comparing the timing of presymptomatic CSF and PET Aβ changes in FAD to the timing of changes in sporadic AD, the two appear to be similar (Bateman et al., 2012, Villemagne et al., 2013, Fagan et al., 2007), with alterations in CSF Aβ being the earliest measurable biomarker change for both. The anatomical distribution of Aβ, as measured by amyloid PET, has however been shown to differ somewhat, with some FAD mutations showing relatively more deposition in thalamus and basal ganglia and sporadic AD showing relatively more in frontotemporal cortex (Knight et al., 2011a, Klunk et al., 2007).

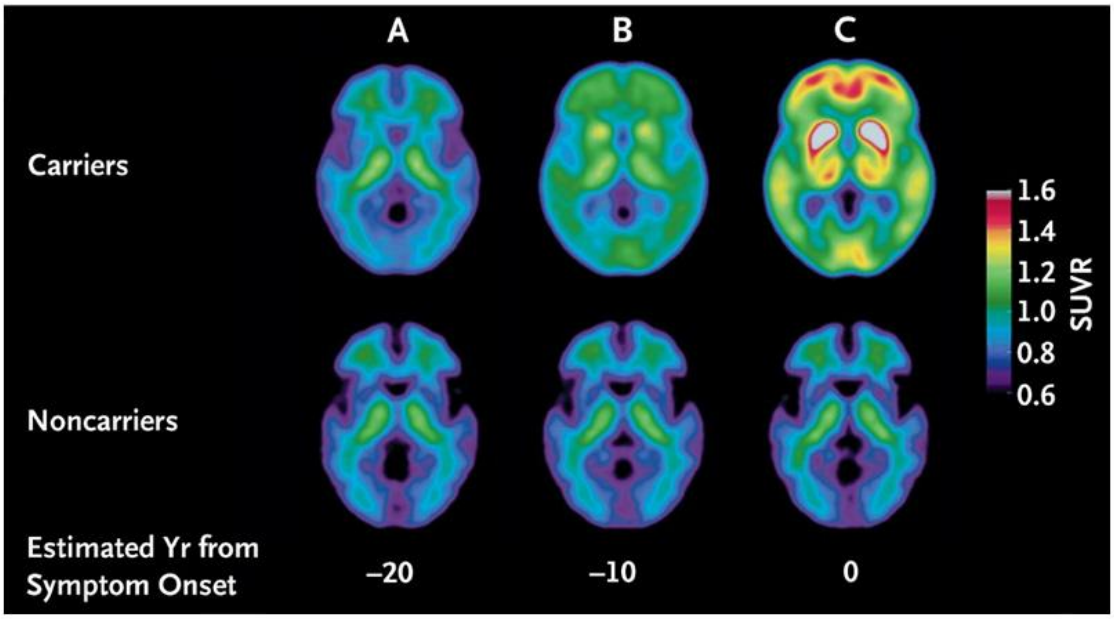

Figure 1-13. Comparison of fibrillar amyloid deposition, as measured by PiB PET, between FAD mutation carriers and non-carriers (reproduced from Bateman et al., 2012)

SUVR=standardized uptake value ratio.

Whilst providing high molecular specificity for AD, Aβ, whether measured by CSF or PET, has been shown to plateau relatively early in the overall disease course with little if any ongoing progression as someone approaches the last few years prior to symptom onset, in both familial and sporadic disease (Fleisher et al., 2012, Villemagne et al., 2013). Measurement of Aβ may therefore be of limited value when it comes to tracking disease progression, or assessing the effect of treatment on neurodegeneration, unless done in the setting of very early presymptomatic disease.

A further potential method of measuring Aβ, which would provide far greater convenience if it were possible, is to measure it in the blood, in either plasma or serum. Methods of doing this have been explored in recent years. However, studies attempting to measure blood levels of Aβ have so far produced conflicting results, with no strong

overall evidence of a difference between AD and controls (Olsson et al., 2016, Lista et al., 2015).

1.4.2.2 Tau

Both total tau and phosphorylated tau can be reliably measured in CSF, with CSF total tau and phosphotau both being used in the clinical investigation of individuals with cognitive impairment (Hulstaert et al., 1999, Lewczuk et al., 2004, Duits et al., 2014). When used in isolation, phosphotau has been found to have significantly more specificity for AD than total tau; however total tau can be very useful diagnostically when measured in combination with $A\beta_{42}$ to calculate the tau/$A\beta_{42}$ ratio. Both total tau and phosphotau have been found to rise presymptomatically in FAD, although with detectable elevation occurring significantly later than the rise in β amyloid (Bateman et al., 2012, Thordardottir et al., 2015).

Until recently CSF sampling had been the only method to measure tau in-vivo. However, a number of tau PET ligands have recently been developed (Villemagne and Okamura, 2014, Okamura et al., 2014), allowing visualization of tau protein in-vivo. Initial published findings in symptomatic sporadic AD look promising, with the anatomical distribution of tau closely mirroring the underlying clinical phenotype (Brier et al., 2016, Ossenkoppele et al., 2016). The utility of this imaging method in detecting and tracking presymptomatic change has yet to be established, with no results yet available in FAD mutation carriers.

Unlike Aβ, it appears that tau can now be reliably measured in serum, using a recently developed assay (Zetterberg et al., 2013). The assay is sensitive to all isoforms of tau, giving a measurement of total tau. However, currently blood levels of tau are only able to discriminate AD from controls when individuals have reached the dementia stage of

the illness, and there remains a large overlap between AD groups and control groups (Mattsson et al., 2016, Olsson et al., 2016). The limited sensitivity of this assay prevents it having any utility at earlier (i.e. MCI or presymptomatic) disease stages.

1.4.3 Measuring neurodegeneration with structural MRI

1.4.3.1 The basic principles of MRI

Whilst markers of molecular pathology, and particularly amyloid, are useful with regards to their molecular specificity, Aβ alone is not sufficient to cause symptomatic AD (Jack et al., 2016b). Downstream markers of neuronal loss are therefore vital in helping identify those who are at greatest risk of developing cognitive decline in the near future and in tracking disease progression. Unlike Aβ load, both the rate and severity of neurodegeneration in AD have been found to be closely linked to an individual's clinical status (Gomez-Isla et al., 1997, Fox et al., 1996, Jack et al., 2005, Ridha et al., 2006).

The most validated and currently used modality for measuring AD-related neurodegeneration *in-vivo* is MRI. The phenomenon of nuclear magnetic resonance (NMR) was first identified in the 1940s, and began to be developed as a medical imaging tool in the 1970s (Hinshaw et al., 1977, Grannell and Mansfield, 1975). All protons and neutrons (the components of atomic nuclei) possess angular momentum. This is often referred to as spin. In NMR imaging (now usually referred to simply as MRI) it is this nuclear spin and accompanying magnetic moment that is of interest. Hydrogen (^{1}H) is by far the most commonly used element, due to its abundance in the human body and propensity to give a strong MRI signal.

In the normal environment, a sample of ^{1}H nuclei, which are essentially single protons, and their accompanying magnetic moments, will be randomly orientated. However if

these nuclei are then placed in an external magnetic field (B_0), they will each orientate themselves in accordance with one of two possible energy levels. Those in the lower energy state each align their axis of spin (and hence magnetic moment) parallel to the externally applied field, whilst those in the higher energy state align their spin anti-parallel (i.e. at 180˚) to it. At physiological temperatures there is a small imbalance in the number of nuclei that occupy these two states, and equilibrium is reached with the majority being at the lower energy level. If an alternating magnetic field B_1 is then applied perpendicular to the static B_0, the nuclei start to precess in phase with the applied signal, and hence with each other.

As the brief B_1 pulse is then removed and the absorbed energy dissipates – released as electromagnetic (radio frequency) radiation – the signal decays exponentially, until the original equilibrium is restored. This release of energy, known as relaxation, involves two separate processes: recovery of the longitudinal signal (T_1 relaxation) and recovery of the transverse signal (T_2 relaxation). The relative ^1H content, and thus the T_1 and T_2 relaxation times, differ between different tissues (e.g. cerebral grey matter and cerebral white matter), producing a contrast between different tissues on the resulting image. When it comes to measuring macrostructural whole brain and regional brain volumes, it is images weighted to detect the T_1 signal that are generally most useful.

In order for an MRI image to be produced the received signal must be spatially resolved. Spatial resolution is achieved by applying a spatially varying (although only very slightly) external B_0 field, through the use of gradient coils. The coils cause subtle linear field gradients to occur in B_0 in all three orthogonal spatial planes; hence the value of B_0 will vary slightly for each point in three-dimensional space.

The ability to examine the brain's structure in vivo represented a major advance in the diagnosis of neurodegenerative diseases, including AD. For some time, neuroimaging, whether it be MRI or lower resolution computed tomography (CT), was primarily used in dementia to exclude lesions amenable to surgery, such as tumours and haematomas. However, with the progressive development of more sensitive and precise image acquisition and analysis techniques, MRI is now able to detect and track primary neurodegenerative pathology, and so is useful in both staging of disease and differentiating between different likely underlying pathologies. On most current 3-Tesla scanners, structural T_1-weighted imaging is able to provide spatial resolution of around $1mm^3$ or less. The results from studies that have used structural MRI in AD to assess atrophy in a number of different ways will be discussed in the following sections.

1.4.3.2 Measurement of hippocampal volume

In AD, pathological studies have identified both neurofibrally tangle deposition and neuronal loss to disproportionately affect the medial temporal lobe (Braak and Braak, 1991, Arriagada et al., 1992, Brun and Englund, 1981, Hyman et al., 1984, West et al., 1994). This is also consistent with the medial temporal lobe, and particularly the hippocampal formation, playing an important role in episodic memory function, which is known to be the principally affected cognitive domain in most patients. In the 1990s, the use of manual measurement of hippocampal volume on T_1-weighted structural MRI scans to aid diagnosis of AD was investigated. It was found that hippocampal volume measurement could discriminate patients with sporadic AD dementia from controls (Jack et al., 1992, Scheltens et al., 1992, Jack et al., 1997). In individuals with MCI affecting a single domain, who do not yet meet criteria for AD-dementia, hippocampal volume at baseline has been found to be predictive of who will and will not go on to receive a clinical diagnosis of AD (Jack et al., 1999). However, subsequent studies have suggested that the predictive value of such measures, particularly when applied

as a single cross-sectional measure at the level of the individual, may be limited prior to the onset of dementia (Van Petten, 2004, Jack et al., 2005).

The study of FAD mutation carriers allowed hippocampal volume measurement in presymptomatic disease to be assessed, with significant differences detectable at two to three years before the onset of symptoms (Fox et al., 1996). A further study showed that assessing the longitudinal rate of atrophy within the hippocampus across multiple scans allows earlier detection of significant volume loss in mutation carriers (compared to controls), at approximately 5.5 years pre-onset, than assessing cross-sectional volume only (Ridha et al., 2006). The same study also found that hippocampal atrophy rate was more sensitive than measuring whole brain atrophy rate. Moreover, not only does hippocampal volume measurement appear more sensitive than whole brain volume to presymptomatic changes in FAD, it is also more disease-specific, as the hippocampus appears to be more selectively vulnerable to FAD pathology than it is to other neurodegenerative proteinopathies.

More recently, similar results to those found in presymptomatic FAD have been found in asymptomatic individuals who are found later to develop sporadic AD, with the hippocampus showing some for the earliest changes (Tondelli et al., 2012, Villemagne et al., 2013). However, not all studies have found a benefit in measuring longitudinal atrophy rates compared to doing a single scan alone (Laakso et al., 2000).

In addition to its use in research, hippocampal measurement has found wide clinical utility in the investigation of individuals with progressive cognitive decline. A validated visual rating scale was published to provide additional assistance in the clinical setting (Scheltens et al., 1995).

1.4.3.3 Measurement of whole brain and ventricular volume

Whilst perhaps not as sensitive or specific as measurement of the hippocampus, measurement of whole brain and ventricular volumes on MRI are also used relatively widely in AD research, and in some cases may provide complementary information to hippocampal volume (Jack et al., 2005). Assessing longitudinal rate of whole brain atrophy in presymptomatic FAD showed there to be a significant difference compared to controls at about 3.5 years pre-onset (Ridha et al., 2006).

As well as being able to parcellate and measure different specific cerebral structures manually, a number of semi-automated methodologies for both measuring cross-sectional volumes and tracking longitudinal within-subject change across scans have been developed (Freeborough et al., 1997, Freeborough and Fox, 1997).

1.4.3.4 Voxel based morphometry

Voxel-based morphometry (VBM) is a whole brain unbiased voxel-wise method of assessing regional grey matter volume differences between two groups of individuals (Ashburner and Friston, 2000). It differs from the above region of interest (ROI) methods, in that the entire cerebral grey matter volume is assessed in an unbiased manner. After initial preprocessing steps, which include grey matter segmentation, normalization, and spatial smoothing, voxel-wise parametric statistical tests are used to compare the smoothed grey matter images from the two groups. VBM has been used in a number of studies in AD (Testa et al., 2004, Mak et al., 2011). VBM has shown the hippocampal formation to undergo the most significant regional volume loss in symptomatic sporadic AD, with other regions identified as undergoing significant change including the insular/perisylvian cortex, frontal cortex, other medial temporal structures, the posterior cingulate cortex and adjacent precuneus, the temperoparietal association cortex, and the caudate nucleus (Frisoni et al., 2002, Baron et al., 2001).

In a relatively large VBM study of FAD mutation carriers, those mutation carriers who were mildly symptomatic (clinical dementia rating scale (CDR) <0.5) were found to have significant volume loss compared to non-carriers in the temporal lobe, precuneus, and cingulate gyrus, as well as also in two subcortical grey matter structures: the thalamus and putamen (Cash et al., 2013). In presymptomatic mutation carriers, Cash et al. did not find any grey matter structures where volume loss was significant after correction for multiple voxel-wise testing.

1.4.3.5 Measurement of cortical thickness

Histopathological and imaging studies have shown AD to be a disease with prominent early neocortical involvement, both in terms of molecular pathology and neuronal loss (Wang et al., 2009, Braak and Braak, 1998, Grignon et al., 1998, Brun and Englund, 1981), with the extent of cortical changes being a key predictor of clinical decline (Walhovd et al., 2010, Arriagada et al., 1992). Advances in neuroimaging acquisition and analysis techniques over the last two decades have led to the development of techniques for high quality measures of cortical thickness, with the most widely used and validated software being a package called FreeSurfer (Dale et al., 1999, Fischl and Dale, 2000). The software constructs an estimate of the cortical grey/white matter boundary by classifying all white matter voxels in an MRI volume. The surface of the connected white matter voxels is then refined to obtain sub-voxel accuracy in the representation of the grey/white boundary, and subsequently deformed outward to find the pial surface. Thickness is measured across the entire cortical mantle at a large number of different vertices, with each white matter vertex related to a grey matter equivalent. Cortical thickness is defined as the shortest distance between these linked vertices. Sub-voxel accuracy is achieved through interpolation, using information about the intensity of each voxel, the nature of surrounding voxels, and the ability to assume

that the radius of surface curvature and thickness of tissue to be measured exceed the size of the voxels themselves. FreeSurfer is able to separate the cortex in to a number of different cortical regions to allow comparison of mean cortical thickness between different brain areas. This process of cortical thickness measurement has been shown to have high inter-scan reliability (Han et al., 2006, Dickerson et al., 2008).

In symptomatic sporadic AD, thinning of the cortex has been identified. Compared to VBM, which tends to be disproportionately sensitive to medial temporal atrophy, it has been suggested that cortical thickness measurement gives a more reliable representation of regional atrophy across the whole brain (Diaz-de-Grenu et al., 2014). Cortical thickness has also been found to produce more reliable measures of within subject longitudinal change than longitudinal VBM (Clarkson et al., 2011).

Whilst neurodegeneration in itself is not specific to AD, the observed variation in the degree of cortical thinning across different cortical regions on MRI has proven useful in discriminating AD from other neurodegenerative diseases such as frontotemporal dementia (FTD) or dementia with Ley bodies (DLB) (Blanc et al., 2015, Du et al., 2007). Moreover, cortical thickness patterns differ between different clinical sub-types of AD, such as typical AD and PCA (Lehmann et al., 2011). In 2008, Dickerson et al. described a specific combination of different cortical regions consistently found to undergo significant cortical thinning is sporadic Alzheimer's disease (Dickerson et al., 2009). An exploratory map of cortical thinning in mild AD was used to define regions of interest that were applied in a hypothesis-driven fashion to separate participant cohorts. The combination of regions identified was termed the "cortical signature" of AD. Nine vulnerable cortical regions were included in the cortical signature, as listed below (see also figure 1-14):

- medial temporal cortex

- inferior temporal gyrus
- temporal pole
- superior frontal gyrus
- inferior frontal sulcus
- angular gyrus
- supramarginal gyrus
- superior parietal lobule
- precuneus

The predominant regions of the cerebral cortex that make up this AD cortical signature are medial/anterior temporal, medial/lateral parietal, and frontal regions. The cortical signature would appear to reflect known regional vulnerability to AD neuropathology from previous histopathological studies (Braak and Braak, 1991, Grignon et al., 1998, Brun and Englund, 1981). Cortical thinning within these regions was closely associated with symptom severity. As well as comparing AD patients and healthy controls, with significant differences found, the signature regions were also assessed in amyloid positive asymptomatic individuals, but with only one of the nine regions (temporal pole), showing significant thinning. Following this initial publication, a number of other studies assessed the application of this cortical signature in different sporadic AD groups. Findings have included that cortical thinning within the cortical signature is detectable in those with extremely mild AD symptoms, and may even be a risk factor for later development of clinical AD in asymptomatic individuals (Bakkour et al., 2009, Dickerson et al., 2011). There was also found to be a trend towards an association between cortical signature thinning and CSF $A\beta_{42}$ (Dickerson et al., 2012).

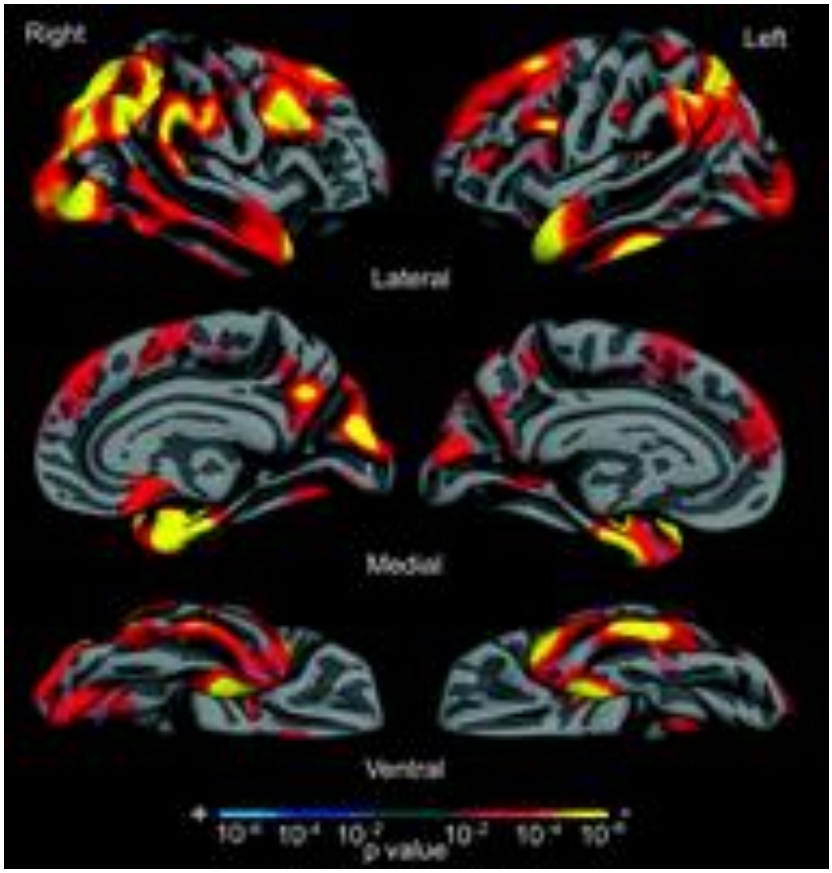

Figure 1-14. The cortical signature of sporadic AD (reproduced from Dickerson et al., 2009)

A Freesurfer map of cortical thinning across the hemispheres in symptomatic sporadic AD compared to controls.

A further study measured the thickness across the sporadic AD cortical signature regions in a group of presymptomatic *PSEN1* E280A mutation carriers, with a mean EYO of six years (Quiroz et al., 2013). Significant presymptomatic thinning was identified in three of nine cortical regions. The presymptomatic cortical changes seen, assessed cross-sectionally only (i.e. at a single time point), were happening slightly earlier in the presymptomatic phase of FAD than previously observed hippocampal volume changes (Fox et al., 1996, Ridha et al., 2006). However, as only cortical regions from the predefined cortical signature for sporadic AD were measured, it

remains uncertain how comparable the thinning patterns across the cerebral cortex are between sporadic and familial disease. Another study of FAD mutation carriers, from the large DIAN cohort, which performed an unbiased analysis across the whole cortex, found evidence of thinning 5 years prior to predicted symptom onset (Benzinger et al., 2013). The most extensive thinning occurred in the precuneus, with thinning also evident in entorhinal, lateral temporal, and lateral parietal cortices, which is similar to the pattern seen in sporadic disease (although with apparently less frontal involvement). It is currently unclear whether the association between cortical signature thickness and cognition is present prior to the onset of symptoms. Furthermore, whilst assessing longitudinal rates of atrophy is potentially more sensitive than a single cross-sectional measurement when using volumetric measures, it is unclear whether the same is true for cortical thickness.

One further interesting finding from presymptomatic FAD cortical thickness studies, not found in the studies mentioned above, is of a transient increase in cortical thickness during the presymptomatic phase prior to progressive thinning (Fortea et al., 2010, Sala-Llonch et al., 2015, Pegueroles et al., 2017). The authors of these studies, all from the same group, suggested the initial presymptomatic increase in cortical thickness may relate to either an early neuroinflammatory component or the accumulation of extracelluar amyloid. However, further replication of this finding, possibly with additional in-vitro study of the underlying mechanism, is required.

1.4.4 Measuring neurodegeneration with diffusion-weighted MRI

1.4.4.1 The principles of diffusion-weighted imaging

During the process of acquiring an image, water molecules within the various tissue types will be constantly moving via the process of diffusion (so-called Brownian

motion). This means that between the beginning and end of a single MRI acquisition any water molecules will have undergone a degree of displacement, usually in the order of micrometres. The amount of displacement able to occur is significantly influenced by any physical barriers present, including cell membranes, macromolecules and intracellular organelles. Such barriers will vary depending on the structural integrity of the cell, which in turn can be influenced by a number of potential pathological factors. Water molecule diffusion patterns can therefore reveal details relating to tissue microstructure and potential pathological processes.

Diffusion-weighted imaging (DWI), first described in the 1980s (Taylor and Bushell, 1985), is an MRI modality that uses the random motion of water molecules to generate contrast on images, with the intensity of each image voxel reflecting the rate of water diffusion at that location. Instead of a homogeneous magnetic field, as used for T_1- and T_2-weighted images, the homogeneity is varied linearly by a pulsed field gradient. Since precession of atomic nuclei is proportional to the magnet strength, the introduction of a field gradient causes protons to begin to spin at different rates, resulting in dispersion of the phase and signal loss. Another gradient pulse is applied in the same magnitude but with opposite direction to refocus or rephase the spins. The refocusing will not be perfect for protons that have moved during the time interval between the pulses, and so the signal measured by the MRI receiver coil is reduced. The degree of reduction, or distortion, in the MRI signal, which is dependent on the degree of diffusion, provides information on tissue microstructure, including neuronal integrity. The amount of diffusion-weighting applied to an image acquisition can be quantified by the *B*-value, which is a product of the following three factors:

1. the strength of the gradient pulse.
2. the duration for which the gradient is applied.

3. the time between application of the initial gradient pulse and the opposing gradient pulse.

The degree of signal distortion depends on both the *B*-value and the direction in which the gradient is applied. The gradient pulses are applied multiple times throughout an image acquisition protocol in multiple different directions (the minimum required being six), to build up an overall impression of the water diffusion in three-dimensional space.

During neurodegeneration, the breakdown of microstructural barriers, such as myelin, cell membranes and intracellular organelles, which would normally restrict the Brownian motion of water molecules, results in a measureable difference in the diffusion of water molecules, detectable on DWI. Whilst conventional T_1-weighted imaging is effective at assessing tissue macrostructure in AD, it is not able to visualize change at the microscopic level. DWI now provides the opportunity to measure AD-related microstructural change, which may lie upstream from macrostructural atrophy.

1.4.4.2 White matter diffusion tensor imaging in Alzheimer's disease

The initial focus of diffusion-weighted MRI in neurodegeneration research, was on the study of white matter tract integrity, using the diffusion tensor model (Ulug et al., 1999). Diffusion tensor imaging (DTI) models each voxel as a tensor (shaped as an ellipsoid), which has both a rate of diffusion and a preferred direction of diffusion (described in terms of three-dimensional space). The properties of each voxel of a single DTI image are usually calculated by vector mathematics. DTI research into white matter tract integrity in AD commonly uses the metric of fractional anisotropy (FA), which describes the directional coherence of diffusion along fibres.

Patients with a clinical diagnosis of sporadic AD have been found to have reduced FA in the corpus callosum, cingulum, and frontal, parietal and temporal white matter compared to controls (Bozzali et al., 2002b, Head et al., 2004, Stahl et al., 2007, Zhang et al., 2007). The regions most frequently found to have reduced FA are temporal and parietal. However, the specific anatomical distribution of white matter microstructural change in AD-dementia in these studies varies quite significantly, with findings in MCI even less consistent.

In FAD mutation carriers, white matter damage as measured by DTI has been reported in frontal sub-cortical white matter and the columns of the fornix in both the early symptomatic and presymptomatic disease stages (Ringman et al., 2007). This apparent early frontal damage, with less change seen posteriorly, would appear to be the converse to what is most commonly found in symptomatic sporadic disease. Mutation carriers with more severe clinical impairment have been found to have much more widespread abnormalities in white matter DTI measures (Ryan et al., 2013).

1.4.4.3 The potential benefits of measuring diffusion in cortical grey matter

While studying the breakdown of white matter structural connectivity has helped broaden our understanding of AD, the specific mechanisms underlying white matter damage remain unclear (Ringman et al., 2007, Bozzali et al., 2002b, Takahashi et al., 2002). One suggestion has been that white matter changes are the result of Wallerian degeneration; a downstream consequence following the earlier loss of cortical neurons (Bozzali et al., 2002b). Also, from a histopathological standpoint, AD is primarily a cortical disease, particularly in the early stages (Braak and Braak, 1998). Grey matter changes have also been shown to correlate more closely with clinical abnormalities than white matter changes (Walhovd et al., 2009), and have a closer link to clinical symptoms than amyloid deposition (Josephs et al., 2008, Villemagne et al., 2013). The

application of DWI to the detection of microscopic grey matter abnormalities, particularly in the cortex, may therefore be a potentially powerful tool in identifying the earliest AD changes (Figure 1-16).

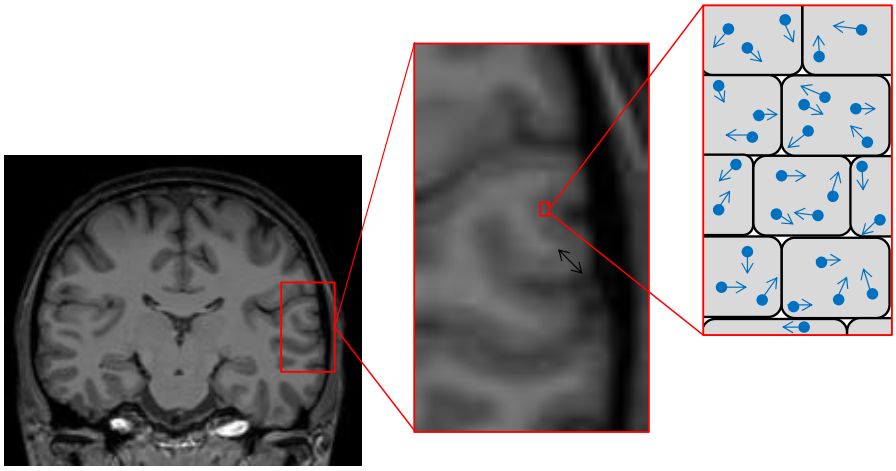

Figure 1-15. From ROI volumetry, to cortical thickness, to cortical diffusivity (reproduced from Weston et al., 2015)

Coronal view of a T1-weighted MRI of the brain (left image); magnified area of cortex, with the black arrow indicating the cortical thickness (centre); on the right is a schematic representation of a magnified region of cortex, with water molecules diffusing within the cells, dependent on the integrity of the cell structure.

A growing body of literature is emerging that describes the use of DWI to detect microscopic grey matter changes in a number of neurodegenerative disorders. Indeed in one such condition – Creutzfeldt-Jakob disease (CJD) – detection of diffusivity changes in grey matter has now become the gold standard in clinical diagnostic practice (Demaerel et al., 1999, Zerr et al., 2009). Alzheimer's disease is a less rapidly progressive condition than CJD, and CJD has marked spongiform changes that likely influence diffusivity, and so diffusivity changes in AD might not be as marked.

However, the use of diffusion MRI for the detection of grey matter abnormalities has shown promise in less rapidly progressive conditions such as multiple sclerosis, where it was used to demonstrate the existence of cortical grey matter damage (Bozzali et al., 2002a).

More recently diffusion-weighted imaging of grey matter in AD has been successfully used in a number of different studies. The majority of studies have used the metric of mean diffusivity (MD), which assesses the average degree of diffusion in all directions, as opposed to quantifying directionality. It has been argued that, compared to FA, MD lends itself better to the assessment of cortical and subcortical grey matter, where net diffusion is essentially isotropic and so may not be expected to conform to any one specific direction (Chiapponi et al., 2013). As cellular microstructure breaks down and there are fewer obstacles to diffusion, molecules are able to diffuse more freely and MD is generally expected to increase (Le Bihan, 2003).

1.4.4.4 Measuring hippocampal diffusivity

Early studies of grey matter diffusion assessed MD in the hippocampi of patients with amnestic mild cognitive impairment (MCI), and compared the imaging results of those who did and did not go on to progress to clinical AD (Muller et al., 2005, Kantarci et al., 2005). In these studies, which contained 18 (Muller et al.) and 24 (Kantarci et al.) amnestic MCI patients, hippocampi were segmented manually, with care taken to ensure that none of the surrounding CSF was included. The studies found that those who did progress to AD-dementia had significantly higher hippocampal MD at baseline than those who did not. Also, compared to macroscopic volume measurements, MD was a more sensitive predictor of progression to clinical AD-dementia, and also correlated significantly better with severity of episodic memory deficits. These findings imply that microscopic changes are detectable within the hippocampi prior to definite

volumetric change; thus offering potential improvement in diagnostic sensitivity. Muller and colleagues went on to replicate these findings and showed that the manual segmentation and analysis technique had good intra-observer and inter-observer reliability (Muller et al., 2006, Muller et al., 2007, Fellgiebel et al., 2006).

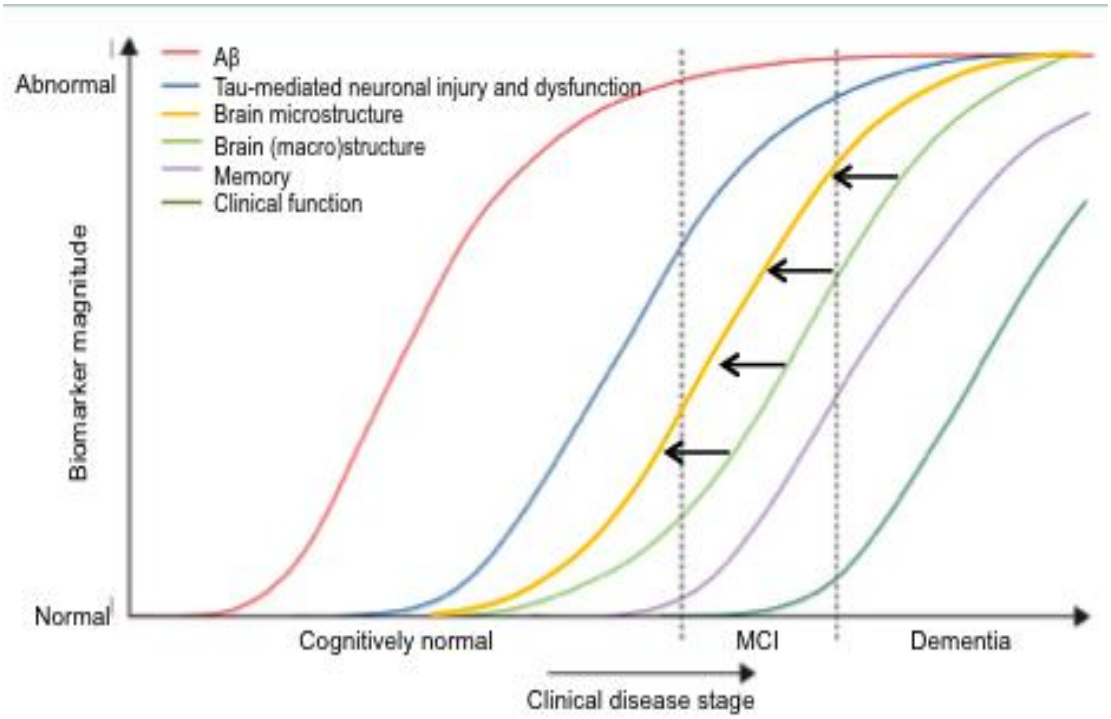

Figure 1-16. A graphical illustration of where microstructural cortical changes may lie in the sequence of biomarker changes in AD (adapted from the model proposed by Jack at al., 2010)

An additional curve has been added (in yellow) to represent where microstructural brain changes (the earliest of which may occur in the grey matter) are predicted to lie in the overall sequence. The black arrows show how the use of MRI to detect diffusivity changes in grey matter may allow significantly earlier detection of neurodegenerative change than is possible with conventional (macro)structural imaging methods.

Douaud et al used an automated voxel-wise analysis to assess both grey and white matter diffusion, again in a cohort of amnestic MCI patients (Douaud et al., 2013). They

also found hippocampal diffusivity to be a sensitive predictor of progression over a three-year follow-up period, with it being more sensitive than any changes to white matter tracts, and also a better predictor than CSF Aβ and tau measurements.

One small ROI study of presymptomatic *PSEN1* mutation carriers (n=10, mean EYO=5.6 years) found significant differences in hippocampal diffusivity compared to controls (Ryan et al., 2013). In the symptomatic phase, hippocampal MD was elevated, as has been seen in sporadic AD. In the presymptomatic phase hippocampal MD was also found to be abnormal and occurred prior to significant change in hippocampal volume.

1.4.4.5 Measuring neocortical diffusivity

Following the finding of early hippocampal diffusivity changes, the focus has broadened to neocortical areas. One study used whole brain voxel-wise analysis to assess cortical changes in clinically established AD (Rose et al., 2008). A number of cortical areas, beyond the hippocampi, were found to have elevated MD. Regions affected included the posterior cingulate cortex (with the greatest effect size), entorhinal cortex, amygdala, parahippocampal gyrus, middle temporal gyrus, superior and middle frontal gyrus and the supramarginal gyrus bilaterally; a pattern which is similar to that seen in studies of cortical thickness (Dickerson et al., 2009). A further study used both whole brain and manually segmented region of interest analyses to assess patients with MCI and with established AD (Scola et al., 2010). A significant trend was seen along the trajectory from normal controls, to MCI, to established AD, in terms of whole brain average grey matter MD. This was contrary to volume measurements, which were not able to accurately predict progression. Additionally, MD measurements in a number of regions of interest, including hippocampi, amygdala, parieto-occipital association cortices and frontal lobe cortical areas, were found to be

independently associated with disease progression. As discussed by the study's authors, the observed spreading of microstructural cortical involvement as the disease progresses fits well with the established histopathological staging of AD (Braak and Braak, 1998). A more recent study, assessing MD across the entire cortical mantle, found a similar pattern of progressive increase in MD, with more cortical regions affected with worsening clinical status (Lin et al., 2016).

Diffusion analysis of multiple cortical areas has demonstrated some value in differentiation of different types of dementia (Kantarci et al., 2010). Compared to patients with DLB, patients with probable AD had higher MD in the hippocampi, parahippocampal gyri, tempero-parietal association cortices, posterior cingulate cortex and the precuneus. In a logistic regression model the ability to differentiate the two diseases was significantly increased with the addition of MD measurements compared to volume measurements alone.

Patients with earlier stages of AD have also shown widespread patterns of change. One study of 20 patients with amnestic MCI found elevated diffusivity (with associated reduced FA) compared to controls, in a cortical distribution very similar to that described above (Jacobs et al., 2013). Again, the most marked effects were seen in the posterior cingulate cortex and precuneus, which are contiguous with one another. Unfortunately, the value of cortical diffusivity measurements, and particularly that of the posterior cingulate and precuneus, in predicting conversion from MCI to AD was not assessed. However, the importance of the posterior cingulate cortex has been confirmed by a large cortical diffusion study of healthy individuals and patients with different focal MCI syndromes (Kantarci et al., 2011). The study found that diffusivity changes in the posterior cingulate were independently associated with memory, language, executive function and visuospatial function.

In a study of presymptomatic FAD mutation carriers, widespread neocortical diffusion changes were demonstrated prior to the onset of symptoms (Fortea et al., 2010). These changes were most prominent posteriorly, affecting the precuneus, posterior cingulate cortex and inferior parietal cortex, similar to that which has been seen in early symptomatic sporadic patients (Jacobs et al., 2013). This distribution differed from symptomatic FAD patients, in whom MD changes were observed throughout the whole cortex.

1.4.4.6 Further findings in FAD

The two previous small studies of grey matter diffusivity in FAD – one of the hippocampus and one of the neocortex – also found diffusivity changes in the subcortical grey matter of the thalamus and caudate several years prior to predicted symptom onset (Fortea et al., 2010, Ryan et al., 2013). The presence of early changes in subcortical grey matter integrity is consistent with the early subcortical amyloid deposition and macrostructural volume loss in FAD, and serves to emphasise that it is not only cortical grey matter that is affected early in the disease process (Knight et al., 2011b, Klunk et al., 2007). However, whether assessment of similar subcortical grey matter areas would be useful in demonstrating early changes in sporadic AD, or whether early thalamostriatal change is unique to familial AD, has not yet been established.

The above studies detected in-vivo presymptomatic microstructural grey matter changes in limbic cortex, neocortex and subcortical grey matter structures. However, one key finding, consistent across all of these anatomical structures, was that the presymptomatic change in MD was not in the direction one would have expected, in that it was decreased rather than increased compared to controls. This is the opposite to the direction of change observed in symptomatic AD (both familial and sporadic).

This reduction in presymptomatic MD was also associated with marginally increased cortical thickness (discussed in section 1.4.3.5.). Although unexpected, and requiring further replication in larger studies, the finding of a presymptomatic fall in MD may suggest the presence of more than one pathological process affecting diffusion imaging changes: the presymptomatic reduction in MD may indicate an inflammatory response to amyloid accumulation (Figure 1-17), occurring prior to (or coincident with and obscuring) the onset of microstructural breakdown and macrostructural atrophy (Ryan et al., 2013, Fortea et al., 2010). A summary of AD research studies assessing diffusivity in grey matter is given in table 1-2.

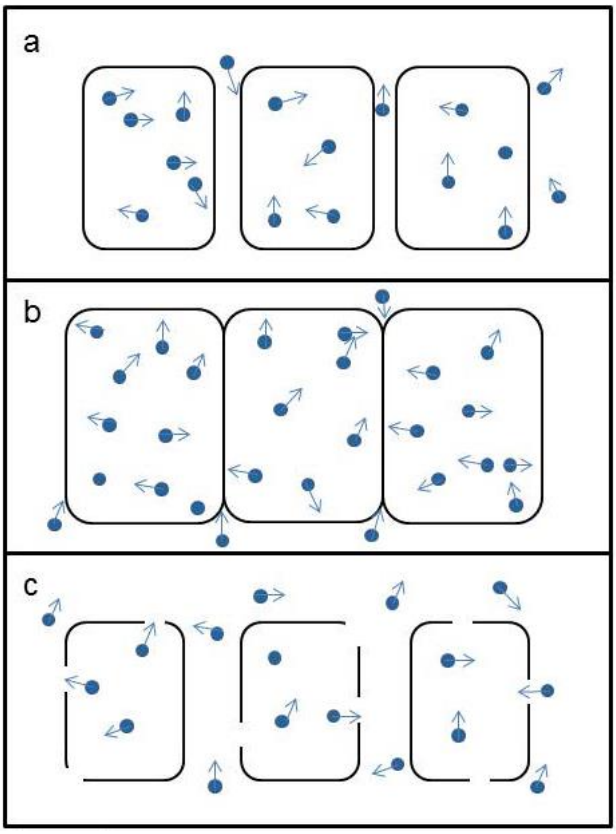

Figure 1-17. A simplified schematic representation of molecular diffusion in and around neurons and how this may change over time in AD (reproduced from Weston et al., 2015)

*In the early presymptomatic stage **(a)** water molecules are able to diffuse normally, with the MD being the same as a normal healthy individual. Evidence from familial AD studies suggests that in the period shortly before symptom onset **(b)** the MD falls, implying that diffusion is restricted. This restriction may be a result of cellular hypertrophy and/or inflammation, in response to amyloid deposition in the presymptomatic phase. During the symptomatic phase **(c)**, progressive cellular atrophy results in a breakdown in the usual barriers to diffusion, with studies showing an increase in MD compared to normal controls. The effects in (**c)** would be likely to progressively outweigh the effects in (**b)** as the disease progresses.*

Author	Familial or sporadic	n	Methods	Main findings
Kantarci et al., 2005	sporadic	21 MCI, 54 NC	Hippocampi manually segmented. Volume & MD measured. 36 month clinical follow-up	Hippocampal MD better than hippocampal volume for predicting conversion from MCI to AD over the 36 month follow-up
Muller et al., 2005	sporadic	18 MCI, 18 NC	Hippocampi manually segmented. Volume, MD + FA measured.	Increased MD in hippocampus is strongest independent predictor of episodic memory decline, and is more sensitive than volume loss.
Fellgiebel et al., 2006	sporadic	18 MCI	Hippocampi manually segmented. Volume and MD measured. 18-month clinical follow-up with convertors and non-convertors compared.	Increased left hippocampal MD at baseline in convertors compared to non-convertors.
Rose et al., 2008	sporadic	13 AD-D, 13 NC	Voxel-wise GM MD analysis	Elevated MD in hippocampus, amygdala, and medial temporal, parietal, and frontal GM in AD. Largest number of abnormal voxels in PCC.
Scola et al., 2010	sporadic	21 AD-D, 21 MCI, 20 NC	Whole brain GM + WM MD; followed by ROI analysis. 2-year clinical follow-up with MCI convertors and non-convertors compared.	Trend seen over normal/MCI/AD for GM + WM MD. Volume alone could not predict convertors, but diffusivity could.
Kantarci et al., 2010	sporadic	30 AD-D, 30 DLB, 60 NC	ROI analysis using FLAIR diffusion imaging, measuring MD (+ volumes) in GM	Compared to DLB, AD has elevated MD in hippocampi, parahippocampal gyri, amygdala, temporoparietal association cortices, PCC + precuneus. Measuring MD increases ability to identify AD.
Douaud et al., 2013	sporadic	35 MCI	Voxelwise GM MD measured, with convertors and non-convertors compared (36 month follow-up)	Elevated left hippocampal and amygdala MD in convertors. Left hippocampal MD was the best predictor of conversion.
Jacobs et al., 2013	sporadic	20 MCI, 20 NC	Whole-brain CTh, MD analysis on GM. ROI analysis then applied	MCI showed increased MD in precuneus, PCC, supramarginal + frontal cortices; largest effect in the PCC.
Lin et al., 2017	sporadic	28 AD-D, 41 MCI, 40 NC	Analysis of MD across 90 parcellated cortical regions and hippocampus.	Compared to NC, increased MD in AD in 40/90 cortical regions + hippocampus. MD values for MCI lay between those for AD and NC
Fortea et al., 2010	familial	6 PMC, 5 SMC, 18 NC	ROI analysis of cortical and subcortical GM MD (+ CTh and subcortical volumes)	Reduced MD (+CTh) in precuneus, PCC + parietotempral association cortices in PMCs Widespread elevated MD in SMCs
Ryan et al., 2013	familial	10 PMC, 10 SMC, 20 NC	ROI MD and FA (GM and WM) + GM volumes	In PMC, reduced MD in right hippocampus (without atrophy) + cingulum, with increased FA in thalamus and caudate. In SMCs MD rises.

Table 1-2. A summary of AD studies that have measured AD diffusion changes

NC=normal control; MCI=mild cognitive impairment; AD-D=Alzheimer's disease dementia (i.e. dementia presumed to be caused by AD); PMC=presymptomatic mutation carrier; SMC=symptomatic mutation carrier; MD=mean diffusivity; FA=fractional anisotropy; GM=grey matter; CTh=cortical thickness; PCC=posterior cingulate cortex.

1.4.4.7 Methodological considerations when measuring cortical diffusivity

Measuring molecular diffusion in grey matter structures is not without pitfalls. An important issue is the potential for results to be biased by partial volume effects (figure 1-18) (Muller et al., 2005, Kantarci et al., 2010). This problem is particularly important in cortical studies because the cortex has a thickness (generally 2-4mm) that is similar to the typical voxel size used in diffusion imaging (2-2.5mm isotropic); with the issue being complicated further by the fact that the cortex has a convoluted structure and is adjacent to CSF spaces. There is therefore a danger of cortical voxels also containing some CSF, with this risk increasing as the cortex atrophies.

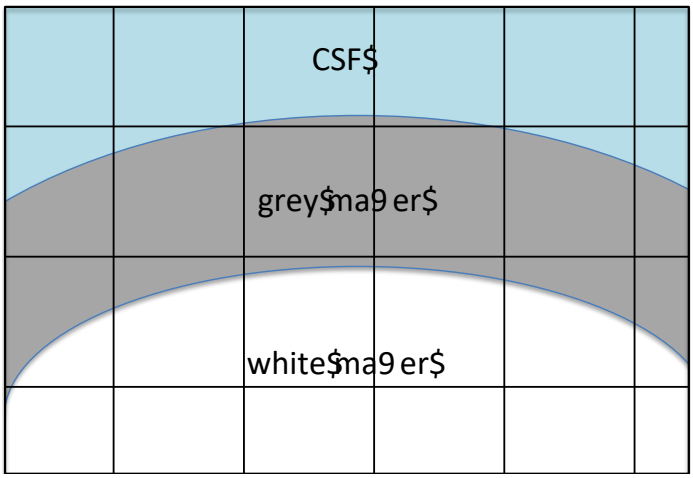

Figure 1-18. A schematic representation of partial volume

As voxel size increases (such as in most DWI acquisitions compared to T1-weighted acquisitions) the risk of partial volume effects, by which a single voxel contains more than one tissue type (e.g. both grey matter and CSF) increases. This leads to contamination of MRI signal within that voxel, as both grey matter and CSF will be contributing.

Investigators have addressed the issue of potential partial volume effects in a number of ways. Accurate segmentation, ensuring the region does not include any CSF, is

important (Fellgiebel et al., 2006, Muller et al., 2006, Rose et al., 2008). Setting inclusion thresholds that exclude any voxel with an MD approaching that of CSF has also been done (Rose et al., 2008). However, altering the characteristics of the distribution of MD measures by thresholding based on those same measures is questionable; this can give distinctly non-Gaussian distributions, which are difficult to analyse statistically. A further method used to reduce the risk of partial voluming has been to coregister the diffusion images to a fluid attenuated inversion recovery (FLAIR) sequence, as opposed to a T_2-weighted sequence as is conventionally done (Kantarci et al., 2010, Kantarci et al., 2011). By doing this, the signal from the CSF is suppressed, increasing the reliability of cortical diffusivity measurements. An additional consideration relates to how the diffusion image is spatially coregistered to the segmentations of the structural scan, which is itself not a trivial process, and can introduce further partial voluming if not done accurately (Alexander et al., 2001, Andersson and Skare, 2002).

It should also be noted that while detection of grey matter diffusivity changes in AD does show promise as a potential early marker of neurodegeneration, the number and size of the studies performed to date is relatively limited, particularly in presymptomatic disease.

1.4.5 Measuring neurodegeneration with fluorodeoxyglucose PET imaging

Whilst the use of PET imaging to detect the core pathological proteins of AD has been a relatively recent development, PET imaging using the radioligand FDG has been established since the 1980s as a means of identifying evidence of neurodegeneration in AD (Friedland et al., 1984, Foster et al., 1983). FDG is taken up by metabolically active tissue, with uptake reducing in brain regions undergoing neurodegenerative change. In AD, a characteristic pattern of hypometabolism is usually seen, with the

temporal and parietal regions most affected. The anatomical pattern of reduced tracer uptake has been shown to be closely associated with focal cognitive deficits (Foster et al., 1983). Also, in those with cognitive complaints, the efficacy of FDG PET in predicting future progressive decline is relatively high (Silverman et al., 2001). FDG PET may also have predictive power for the development of future symptomatic AD in individuals who as yet are asymptomatic (de Leon et al., 2001), and had been shown to correlate with early CSF Aβ and tau changes within this population (Petrie et al., 2009). However, when compared to structural MRI in its ability to detect AD in those with MCI and predict cognitive decline, FDG PET has been found to be inferior (Trzepacz et al., 2014). The clinical use of FDG PET is also limited by the availability of both scan facilities and tracer production.

FDG PET has been used to investigate presymptomatic neurodegenerative change in FAD mutation carriers. Presymptomatic hypometabolic change has been identified in a similar anatomical pattern to that seen in symptomatic sporadic AD, with hippocampus and temporoparietal neocortex significantly affected (Mosconi et al., 2006, Benzinger et al., 2013). These early changes seen on FDG PET appear to predate those seen on MRI. However one drawback to using PET to measure neurodegeneration is the fact that as each scan requires significant radiation exposure repeated use within the same subject might be limited, at least within relatively short intervals.

1.4.6 Measuring neurodegeneration with CSF biomarkers

Until now, at least in terms of routine clinical practice, the only fluid biomarkers available and validated for the investigation of AD are CSF $A\beta_{42}$, total tau and phosphotau (see section 1.4.2). However, as discussed previously, the measurement of downstream neurodegeneration, as opposed to simply measuring the primary molecular pathology, may link more closely to clinical outcomes. It can be argued that

total tau itself is a proxy marker of neurodegeneration in AD, as its anatomical deposition is associated with focal neuronal loss and focal cognitive decline (Arriagada et al., 1992), although its exact temporal relationship to clinically meaningful neurodegeneration is still not entirely certain.

Other than tau, a number of other potential markers have been investigated, the most promising of which appears to be neurofilament light (NfL). There are two major types of intermediate filaments in the nervous system: neurofilaments and glial filaments. Neurofilaments exist as 10 nm filaments in the axoplasm of neurons, where they give tensile strength to dendrites and axons and are an integral structural component of the neural cytoskeleton. Each neurofilament is made up of one NfL and either neurofilament medium (NfM) or neurofilament heavy (NfH) chains, arranged head-to-tail (Lee et al., 1993). Therefore, as neurons break down and their contents are released, concentrations of NfL in the surrounding CSF would be expected to rise. NfL was first shown to be increased in the CSF of AD patients over 20 years ago, using an enzyme-linked immunosorbent assay (ELISA) based method (Rosengren et al., 1996). ELISA involves antigens from the sample being attached to a surface. Then, a further specific antibody is applied over the surface so it can bind to the antigen. This antibody is linked to an enzyme, and, in the final step, a substance containing the enzyme's substrate is added. The subsequent reaction produces a detectable signal, most commonly a colour change in the substrate. Elevated CSF NfL is found in a number of neurological conditions, including AD, multiple sclerosis, motor neuron disease, FTD, and atypical parkinsonian disorders (Zetterberg et al., 2016, Teunissen et al., 2005, Tortelli et al., 2012, Scherling et al., 2014, Hall et al., 2012), and so is a marker of neurodegeneration rather than a specific underlying pathological entity.

Raised CSF NfL is associated with increased disease severity and shorter survival in individuals with dementia presumed to be due to AD (Skillback et al., 2014).

Furthermore, a recent study found increased CSF NfL to be predictive of subsequent progression to dementia in patients with MCI, showing that it has utility in early symptomatic disease (Zetterberg et al., 2016). The same study also found CSF NfL to be associated with quicker rates of brain atrophy (including whole brain, ventricular and hippocampal measurements), and reduced cognitive performance on the mini mental state examination (MMSE). A recent meta-analysis identified NfL as the only CSF marker other than the core AD molecular markers of $A\beta_{42}$, total tau and phosphotau to have good performance when it comes to separating AD dementia from controls (Olsson et al., 2016). It is possible though that when it comes to tracking progression, and correlating with cognitive performance in AD, that CSF NfL may outperform the core molecular markers. However, whilst the evidence for the use of CSF NfL in clinical disease appears to be strong, the utility of this measure in earlier disease prior to symptom onset has yet to be established.

A number of other putative CSF markers of neurodegeneration have been assessed in AD patients, including neuron-specific enolase, visilin-like protein-1 and heart fatty acid binding protein (Palumbo et al., 2008, Tarawneh et al., 2011, Olsson et al., 2013). However, so far the effect sizes produced by these measures when it comes to separating AD-dementia from controls appears to be moderate at best (Olsson et al., 2016), and they are unlikely to have any utility earlier in disease.

1.4.7 Measuring neurodegeneration with blood-based biomarkers

An area of great interest at present is the potential development of blood-based biomarkers that are able to detect and track neurodegenerative change in AD, ideally as early in the disease course as possible. A biomarker able to be measured in blood would be simpler to sample and generally more acceptable to research participants and/or patients than any of the neuroimaging or CSF-based methods discussed in

previous sections. However, there are currently no blood-based biomarkers proven to be sensitive to AD neurodegeneration, or to any other AD-related processes, even in the MCI phase (Olsson et al., 2016), and even less so in those who remain presymptomatic.

As discussed in section 1.4.2, a recent meta-analysis found the only biomarker measurable in blood to be able to reliably differentiate patients with AD-dementia from controls is total tau, measured in either plasma or serum (Zetterberg et al., 2013, Olsson et al., 2016). Higher plasma total tau has been found to be associated with AD-dementia, higher CSF tau, and lower CSF $A\beta_{42}$, but these correlations are relatively weak and differed between two independent study cohorts (Mattsson et al., 2016). Longitudinal analysis has shown associations between plasma tau and worsening cognition, increased atrophy, and more hypometabolism (as measured by FDG PET) during follow-up. However, while plasma tau does partly reflect AD pathology, the overlap between normal aging and AD is large, and there is no evidence that it is able to discriminate AD from controls in those who have not yet developed dementia.

Measurement of NfL, a marker of neurodegeneration, has shown promise in CSF, both as a diagnostic marker and prognostic indicator of future decline (Zetterberg et al., 2016). Two relatively recent studies aimed to measure blood concentrations of NfL in AD using electrochemiluminescence assays. Electrochemiluminescent labels generate light when stimulated by electricity in the appropriate chemical environment, with the light signal used to quantify the analyte of interest. Both studies found that NfL concentrations are significantly increased in the blood of patients with AD-dementia compared to controls, with CSF and blood levels correlating strongly (Gaiottino et al., 2013, Bacioglu et al., 2016) (figure 1-19b). However, as shown in figure, there is overlap between control and AD subjects. The same two studies also detected

significantly raised blood NfL concentrations in a number of other neurodegenerative diseases, including DLB, multisystem atrophy (MSA), PSP, and CBS.

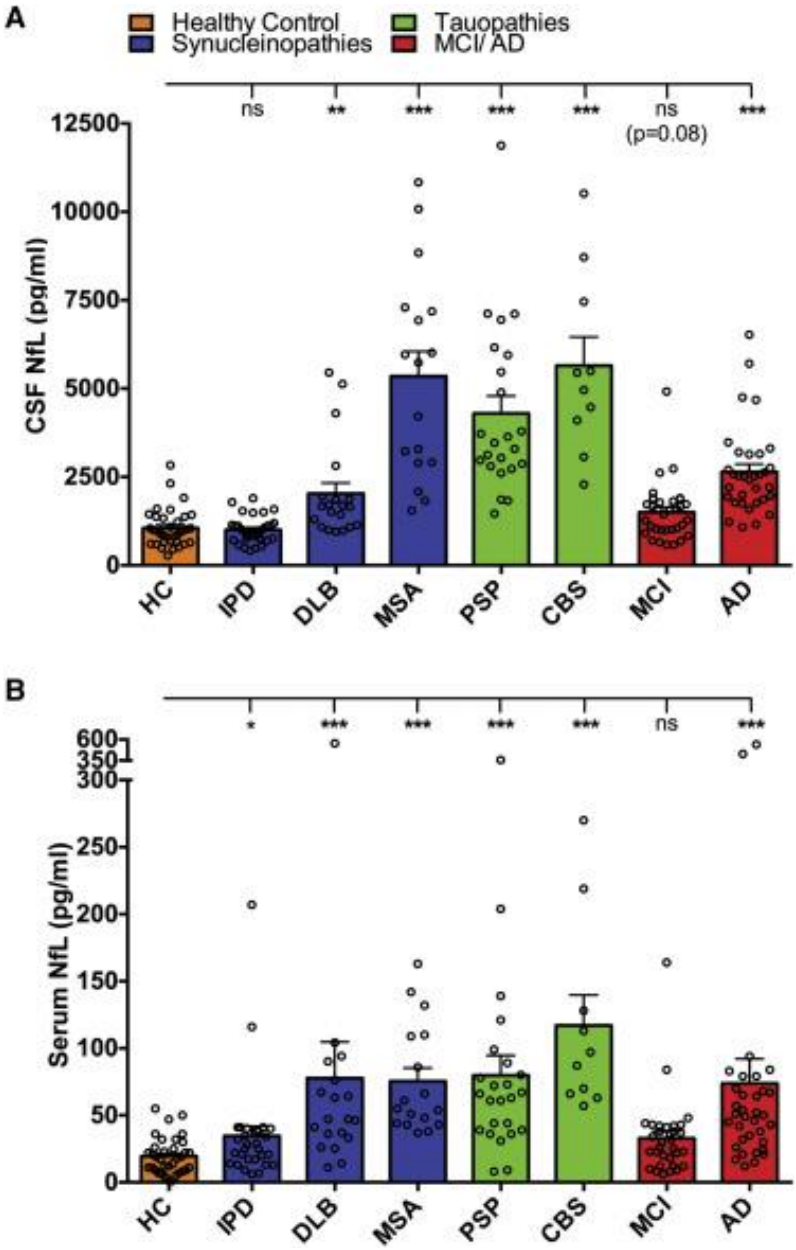

Figure 1-19. NfL in CSF and serum in a number of different neurodegenerative diseases (reporoduced from Bacioglu et al., 2016)

NfL concentrations are shown for (A) CSF, and (B) serum. HC=healthy control; IPD=idiopathic Parkinson's disease; DLB=dementia with Lewy bodies; MSA=multisystem atrophy; PSP=progressive supranuclear palsy; CBS=corticobasal syndrome; MCI=mild cognitive impairment; AD=Alzheimer's disease.

One potential problem when measuring NfL in blood is that, as concentrations are about 20-times lower than in CSF, control samples and many disease samples may have concentrations below the analytical sensitivity of the methods (Kuhle et al., 2016). This would be a particular problem in earlier disease, when it would be expected that less neurodegeneration would be occurring and so NfL concentrations would be much lower. A recently developed approach, known as the single molecule array (Simoa) technique, allows quantification down to subfemtomolar concentrations (below 1 pg/mL) (Rissin et al., 2010), and is 25-fold as sensitive as the previous electrochemiluminescence-based method for NfL (Kuhle et al., 2016). The technique is able to detect low-abundance proteins in blood by capturing them on microscopic beads decorated with specific antibodies and then labeling the immunocomplexes with an enzymatic reporter capable of generating a fluorescent product. After isolating the beads in reaction chambers designed to hold only a single bead, fluorescence imaging is used to detect single protein molecules. Serum NfL concentrations derived using Simoa correlate closely with CSF concentrations and are increased in HIV-associated dementia, progressive supranuclear palsy and FTD (Gisslen et al., 2016, Rojas et al., 2016, Rohrer et al., 2016). However, the technique has yet to be used to assess neurodegeneration during the presymptomatic disease stage.

No other direct blood-based biomarkers of neuronal loss have thus far been identified. However, rather than aiming to find a single blood-based biomarker of primary pathology or of neurodegeneration in AD, a number of studies have taken the alternative approach of assessing plasma or serum profiles to try and identify a pathological “fingerprint” of the disease. These studies have utilised a variety of different profiling approaches including proteomics, lipidomics and transcriptomics (Ray et al., 2007, Han et al., 2011, Booij et al., 2011, Uchida et al., 2015, Proitsi et al., 2016,

Sattlecker et al., 2016). A number of different biological pathways have been proposed as potentially contributing to biological abnormalities in AD, including APOE, complement and various cytokines. However, poor reproducibility remains an issue when assessing large panels of molecules involved in potentially diverse biological pathways, with initial non-hypothesis driven "discovery" analyses proving difficult to replicate (Soares et al., 2009, Mielke et al., 2011, Casanova et al., 2016). Therefore a single measure, linked more directly to AD neurodegeneration may be preferable to a "fingerprint" approach.

1.4.8 Measuring early cognitive change

1.4.8.1 Evidence from current testing methods

The final clinical manifestation of neurodegeneration in AD is progressive cognitive decline. In symptomatic individuals, both the severity and the neuroanatomical pattern of cognitive impairment is known to link closely to the severity and anatomical location of the underlying neuronal loss (Dickerson et al., 2009, Lehmann et al., 2011, Morra et al., 2009). In most cases of both sporadic and familial disease, the earliest and most prominent symptom noted by the patient, their family, and the clinicians assessing them is impairment of episodic memory for recent events, although phenotypic variability is well recognized (Graham et al., 2004, Dubois et al., 2014, Tang et al., 2016). These episodic memory symptoms are usually associated with impairment of both recall memory and recognition memory, which would imply that both retrieval and storage of information are affected (Bennett et al., 2006). Whilst the cognitive features of those in the symptomatic phase of AD have been well characterized, exactly when and how cognitive decline first begins remains less certain. At time of AD diagnosis the hippocampus is already on average ~10-20% smaller than age related control subjects, which implies neuronal loss has been already occurring for some years; Ridha et al estimated hippocampal loss to begin approximately five years before diagnosis (Ridha

et al., 2006). Tau pathology, known to be closely associated with neurodegeneration, accumulates in the medial temporal lobe structures a number of years before the onset of symptomatic disease; however whether this early pathology is completely silent from a functional point of view, or whether it has subtle cognitive effects is not known.

A number of neuropsychological studies have been performed in asymptomatic individuals who were followed up and later went on to be diagnosed clinically with sporadic AD. In these studies, verbal episodic delayed recall is consistently found to be the earliest cognitive domain to be affected, with short-term/working memory relatively preserved (Linn et al., 1995, Mistridis et al., 2015, Backman et al., 2001). Visual memory has also been found to show some presymptomatic decline, although usually later than in the verbal domain. It has also been reported that, along with verbal recall, executive function shows the greatest decline in the 1.5 years prior to diagnosis, although this has not been replicated consistently (Chen et al., 2001). One study identified a combination of eleven different cognitive test domains, which the authors proposed allowed the best discrimination between those who would and would not go on to develop symptomatic AD eight years prior to diagnosis (Schmid et al., 2013). Although even with all eleven test domains included, the correct classification was made only 60.4% of the time. Also, whilst longitudinal follow-up can sometimes demonstrate presymptomatic differences in group trajectories, it appears more difficult to demonstrate these differences on a single cross-sectional assessment. A further limitation of these studies is that, as they base the diagnosis of AD on clinical impression alone, it is likely that a proportion of people will have been erroneously labeled as AD when in fact there is another cause for their symptoms.

Other studies have separated the groups into probable presymptomatic AD and controls based on in-vivo evidence of Aβ pathology from either CSF or amyloid PET. Pike and colleagues found the presence of Aβ deposition to be associated with

reduced episodic memory, with another study finding episodic memory and also working memory to show decline (Pike et al., 2007, Lim et al., 2014). A further study found spatial navigation memory to also be impaired in amyloid positive individuals (Allison et al., 2016). However not all studies have found Aβ positivity to be discriminatory, with Doherty and colleagues not finding any statistically significant differences in performance between Aβ positive and Aβ negative individuals (Doherty et al., 2015).

Previous studies of FAD, where underlying pathology is much more certain and years to onset can be estimated, have shown conventional testing methods to first detect focal cognitive decline shortly before or even following the onset of clinical symptoms (Fox et al., 1998, Yau et al., 2015). Similar to studies of spradic disease, verbal episodic memory is usually the first domain to demonstrate decline, prior to more widespread symptomatic impairment. Much of the investigation of presymptomatic cognitive changes in FAD has been done in a large extended family of *PS1* E280A mutation carriers, originating from the Antioquia region of Colombia. These studies have found early deficits in episodic memory, occuring at least 2-3 years prior to symptom onset, although testing of individuals earlier in the presymptomatic period revealed no differences compared with non-carriers (Acosta-Baena et al., 2011, Ardila et al., 2000). Othe cognitive domains have also been found to be affected in the two years before symptom onset, including visual short term memory binding, dual task performance, and verbal semantic function (Parra et al., 2010, MacPherson et al., 2012, Arango-Lasprilla et al., 2007). One further cognitive test, found from a study at UCL to show presymptomatic decline approximately two years prior to symptom onset, is performance IQ (Fox et al., 1996).

Whlist presymptomatic decline in cognition, particulalrly in the episodic meory domain, has been demonstrated in both familial and sporadic disease, reliable detection of

cognitive abnormalities occuring at earlier points in the presymptomatic period, particularly with a single test perofrmed at a single time point, have so far proven elusive. There therefore remains a large gap between pathological change and currently measurable cognitive decline.

1.4.8.2 Potential limitations in current cognitive test methods

One possible reason for the difficulty in demonstrating significant cognitive impairment more than a couple of years before the time of symptom onset is that it is not present at this earlier disease stage. However, an alternative explanation could be that earlier cognitive decline does occur but current testing methods are insufficiently designed to detect it. While current standard cognitive tests are useful for detecting and characterizing cognitive decline at the stage of mild cognitive impairment and beyond, they were not designed for detecting the subtle cognitive variations that may be associated with presymptomatic disease (Rentz et al., 2013). Neuropsychologists have been attempting to meet this challenge by designing newer cognitive measures. As mentioned above, some recent studies have employed less conventional approaches, including testing short-term memory binding (the process of integrating multiple features within complex stimuli, such as shape-colour conjunctions) and dual task performance, with some success at identifying abnormalities in late presymptomatic disease (Parra et al., 2010, MacPherson et al., 2012).

However, as it is generally accepted that the first affected cognitive domain in AD is usually episodic memory, if we are to improve the sensitivity of cognitive testing in the presymptomatic phase of AD, it may be that directing our focus at trying to identify the earliest signal of subtle episodic memory decline is likely to provide the most promising results. Generally, currently used testing methods assess immediate recall and then delayed recall and/or recognition over a retention period of 5-30 minutes. Previously, it

has been shown that it is usually possible in patients with AD dementia to detect impairment in initial encoding (i.e. immediate recall), whilst those with MCI usually show no deficit on encoding tasks but do demonstrate impairment on delayed recall (Ally et al., 2013). However, if and how it may be possible to separate those with disease but who are currently asymptomatic from healthy individuals with no disease pathology is uncertain. One possibility may be to extend the retention period beyond 20-30 minutes. Evidence from studies that have used this approach in patients with non-AD temporal lobe pathology will now be discussed.

	Memory encoding	**Delayed recall**
AD dementia	↓	↓
MCI	↔	↓
Healthy aging	↔	↔

Table 1-3. Current understanding of how memory performance progresses as individuals progress through different symptomatic stages of AD

1.4.8.3 Accelerated long-term forgetting

Accelerated long-term forgetting (ALF) is a form of memory impairment that has been described primarily in patients with temporal lobe epilesy (Blake et al., 2000, Butler et al., 2007). It refers to a process in which new material appears to be encoded normally and retained normally over periods of up to 30 minutes but is then forgotten at an abnormally rapid rate over the following days to weeks. This observation applies to both verbal and visual material, and has also been shown to apply to real-life events as well as material learned in a test environment (Muhlert et al., 2010). Given that

information is retained normally over the initial 30-minute period, individuals who suffer with ALF generally demonstrate no impairment on standard memory tests. Amongst the epilepsy population, ALF has been shown to apply only to those with focal temporal lobe pathology, and is absent in those with more diffuse generalised disease (Muhlert et al., 2011).

It has been suggested that ALF represents a disruption in memory consolidation (Hoefeijzers et al., 2013), which refers to the gradual post-acquisition stabilization of long-term memories (Dudai et al., 2015). Although there does remain some debate as to whether deficits in initial encoding may also contribute (Cassel et al., 2016). Consolidation of memory has been described at two levels: the cellular/synaptic level, which is thought to last hours to days, and the brain systems level, which is thought to last days to months. For consolidation to be successful, and memory traces to be stored without disruption, it is thought to require interaction between the hippocampus and neocortex (Maviel et al., 2004). The exact structural and/or functional correlate for ALF has however yet to be established, with no direct association found with structural imaging changes (Butler et al., 2009).

No ALF studies of individuals with known AD pathology have yet to be performed. In order to reliably investigate ALF, and compare a disease group to controls, both groups would need to be equal for initial learning and delayed recall over 30 minutes, which for symptomatic AD, including MCI, would not be the case. Therefore, in AD, ALF would have most potential relevance and utility in presymptomatic disease. ALF has recently been assessed in a mouse model of presymptomatic FAD (Beglopoulos et al., 2016). The genetically modified mice, who were young and showed no outward signs of cognitive decline, were found to have abnormal retention over an interval of seven days, despite demonstrating normal learning and retention over ten minutes.

Testing for ALF is not without its potential pitfalls. A review article identified a number of important methodological considerations prior to undertaking an ALF study (Elliott et al., 2014). Such issues include the need to:

- ensure participants are equal for learning and initial recall.
- take into account IQ, which can influence memory performance.
- aim to avoid rehearsal effects (i.e. do not forewarn participants about later testing)
- ideally assess both recall and recognition, as it is currently unclear whether they are affected differently by ALF.

1.4.8.4 Subjective cognitive decline

In the previous studies of epilepsy patients, ALF was found, at least in a proportion of patients, to be associated with subjective cogntive concerns (Blake et al., 2000, Butler et al., 2007). Subjective cognitive concerns, often also referred to as subjective cognitive decline, refer to perceived cognitive difficulties experienced by an individual despite lack of objective impairment on cognitive testing. The most common subjective cognitive concerns described relate to perceived inefficiencies in episodic memory. As discussed above, current memory tests tend to test recall over no more than 30 minutes, and so may miss subtle changes.

The topic of subjective cognitive concerns has attracted increasing interest in the AD research community. Evidence suggests that early subjective changes, even in the absence of decline on conventional testing, may be a harbinger for future progressive cognitive impariemnt in AD (Dik et al., 2001, Reisberg et al., 2008, Jessen et al., 2014, Perrotin et al., 2016). In asymptomatic Aβ-positive individuals with normal cognitive testing at baseline, subjective cognitive decline has been found to be associated with greater rates of subsequent episodic memory decline (Koppara et al., 2015, Buckley et

al., 2016a). This has led to an acknowledgement from authors that cognitive testing methods may need to be improved in order to detect the early subtle changes that may underlie these subjective concerns (Buckley et al., 2016a). A number of conceptual frameworks have recently been published in order to promote the greater utilization of subjective cognitive decline assessment in AD research, including clinical trials (Jessen et al., 2014, Buckley et al., 2016b).

Whether the increase in subjective cognitive concerns observed in early sporadic AD, prior to objective decline, is 1) also evident in FAD, and 2) associated with ALF, as it is in epilepsy, is currently unknown.

1.4.9 Summary of the evidence in support of findings in FAD being applicable to sporadic disease

Although FAD and sporadic AD differ in their ages at clinical onset and underlying causative mechanisms, the evidence presented in the previous sections points to them being similar when it comes to pathological, radiologic, cognitive and fluid biomarker findings. Large cohort studies that have aimed to model the cascade of presymptomatic biological changes have found the order of key events to be the same (Bateman et al., 2012, Villemagne et al., 2013). The same order of events deduced from longitudinal statistical modeling has also been found to be the case in a smaller group of prospectively followed FAD mutation carriers, in whom intra-individual progression was tracked over a period of up to eleven years (Yau et al., 2015).

Certain differences have been identified, perhaps most notably that FAD mutation carriers appear to have increased early involvement of sub-cortical grey matter structures, including the thalami and basal ganglia, compared to those with sporadic

disease (Klunk et al., 2007, Ryan et al., 2013). As discussed, sporadic AD demonstrates a significant amount of phenotypic heterogeneity. This can also be the case in familial disease. However, as certain FAD studies tend to focus on a single mutation (e.g. E280A in the Colombian kindred), this heterogeneity is not always present, which may potentially affect how generalizable the results may be. Studies of FAD cohorts with a variety of different genes and mutations, producing more heterogeneity, may therefore be preferable if results are to be applied to the larger AD population.

Overall, the evidence does point towards findings gathered from presymptomatic mutation carriers having relevance for sporadic disease, although generalizability cannot be taken for granted.

1.5 Aims of this thesis

The preceding sections have outlined the need and the realistic hope for disease modifying treatments for AD. To facilitate such trials, and treat and monitor individuals in clinical practice, sensitive markers of early disease activity are required. Although not as disease-specific as measures of molecular pathology, measures of neurodegeneration (and resulting early cognitive change) offer the advantage of more closely reflecting disease stage and proximity to/from symptom onset. Whilst numerous markers across a number of different modalities have been developed, each has its own limitations/drawbacks.

This thesis presents a number of studies of asymptomatic and mildly symptomatic individuals from families affected by FAD, with the intention to develop improved methods of detecting and tracking presymptomatic neurodegeneration, and to build on

the findings of previous work. It is hoped that the outcomes of the research will serve two main purposes: 1) to enhance knowledge of the natural history of presymptomatic FAD, in order to improve understanding of when and how to try and intervene; and 2) to provide potential disease markers that may have utility in presymptomatic secondary prevention trials.

The work presented covers a number of different methodological modalities, with a particular focus on three currently unmet needs:

1. Utilising new approaches for the analysis of macrostructural and microstructural neuroimaging of the cerebral cortex to facilitate earlier and more reliable identification of AD-related neurodegeneration.
2. Development of blood-based measures of AD-related neurodegeneration, able to detect changes presymptomatically.
3. Adopting new approaches to the assessment of the earliest cognitive changes, to enable detection of presymptomatic decline.

Four studies are presented. The first uses volumetric T_1-weighted MRI to measure cortical thickness and identify a disease-specific cortical signature of FAD. Presymptomatic thinning is then assessed, both in terms of cross-sectional thickness measurement and longitudinal rate of thinning. Associations between baseline cortical signature thickness and both cognitive performance and future rates of thinning are assessed.

Following on from the cortical thickness study, the next study uses DWI to measure MD in the cortical grey matter of the FAD cortical signature regions. Presymptomatic changes are again assessed.

The third study uses a recently developed ultrasensitive assay to measure serum NfL in FAD mutation carriers; and assesses associations between serum NfL and numerous markers of disease stage and severity.

Finally, a study of long-term forgetting in presymptomatic mutation carriers is presented, assessing recall and recognition memory over a seven-day interval. Group differences (carriers versus non-carriers) are assessed and compared with standard cognitive testing. Associations between ALF and both subjective memory scores and structural imaging measures are assessed.

With the exception of cortical thickness measurement, the main methods used in the studies presented have never been used previously to assess presymptomatic AD. Hypotheses specific to each individual study are outlined at the beginning of each chapter.

1.6 Publications arising from this chapter

- Weston, P. S. J., Simpson, I. J., Ryan, N. S., Ourselin, S. & Fox, N. C. 2015. Diffusion imaging changes in grey matter in Alzheimer's disease: a potential marker of early neurodegeneration. *Alzheimers Res Ther*, 7, 47-54.

2 General methods

2.1 Study participants

2.1.1 Participant recruitment

The work in this thesis is drawn from studies of a cohort of individuals who come from families known to be affected by FAD, with genetic mutations in either *PSEN1* or *APP*. Individuals were recruited to an ongoing cohort study of FAD at the Dementia Research Centre (DRC), University College London (UCL) Institute of Neurology, between June 2009 and March 2016 (the recruitment and data collection periods for the different individual studies that form this thesis are given at the start of chapters three to six).

Participants came from a number of sources:

- Families already known to the DRC through previous participation in research.
- Individuals seen in the Specialist Cognitive Disorders Clinic at the National Hospital for Neurology and Neurosurgery.
- Individuals who contacted the DRC after being made aware of the research study through other means (e.g. department website or other media coverage).

Individuals were eligible if they had either i) a diagnosis of FAD, or ii) a parent affected by FAD. In addition, for the two neuroimaging studies (chapters three and four), healthy individuals with no family history of dementia were also recruited. Participants therefore fell in to one of the following groups:

- **Symptomatic FAD (n=24)** – individuals with a confirmed clinical diagnosis of FAD, with a confirmed mutation in either *PSEN1* or *APP*.
- **At-risk (n=55)** – asymptomatic individuals who, by virtue of having an affected parent (with a confirmed genetic diagnosis), are at 50% risk of having inherited a mutation, and thereby developing symptomatic FAD in the future. This group includes a small number of individuals who had decided to have clinical

predictive genetic testing, and so already know whether they are a mutation carrier.

- **Healthy controls (n=27) –** asymptomatic individuals with no family history of AD.

The number of participants stated for each category above refers to the total amount across the different studies reported (see individual chapters for the numbers relating to the individual studies). With regards to symptomatic FAD participants, where possible efforts were made to recruit controls who were age and gender matched; however in the case of *at-risk* participants from FAD families, for whom we did not know at the point of recruitment if they were mutation positive or negative, recruitment of matched controls was not possible, although it was expected that approximately 50% of at risk individuals would be non-carriers (essentially healthy controls), and that the ages of carriers and non-carriers should approximately balance out.

2.1.2 Family mutations

A total of 36 different FAD families, with 26 different mutations (28 *PSEN1*, eight *APP*), were involved across the four studies reported. Family mutations are listed in table 2-1.

Gene	Mutation	Number of families	Number of individuals
APP	p.A269G	1	1 S
	p.T712N	1	1 AR
	p.V717G	1	1 AR

	p.V717I	4	2 S, 4 AR
	p.V717L	1	4 AR
PSEN1	Intron 4	2	3 S, 4 AR
	p.Y115C	1	1 AR
	p.Y115H	1	2 S, 1 AR
	p.E120K	1	2 S
	p.S132A	1	2 AR
	p.Met139Val	2	1 S, 3 AR
	p.Met146Ile	2	1 S, 3 AR
	p.L171P	1	1 S, 1 AR
	p.E184D	2	6 AR
	p.I202F	1	4 AR
	p.H214T	1	1 AR
	p.L235V	1	1 AR
	p.L262F	1	1 AR
	p.P264L	2	2 S, 1 AR
	p.R269H	2	2 S
	p.Arg278Ile	1	1 S, 3 AR
	p.E280G	2	4 S, 9 AR
	p.F283L	1	3 AR
	p.S290C	1	1 AR
	ΔE9*	1	1 S
	p.G394V	1	1 S

Table 2-1. Family mutations represented in the cohort

*The number of individuals, across all four studies reported, from families with each mutation is given, divided in to either symptomatic (S) or asymptomatic but at risk (AR). Details of many at risk participants for each mutation were carriers is not given to preserve genetic blinding and ensure it is not possible for any at risk individual to deduce their mutation status. * The exon 9 deletion (NM_000021.3:c.869-1G>T; p.S290C;T_S319del) commonly referred to as ΔE9.*

2.1.3 Inclusion criteria

In addition to meeting the definition of one of the three participant groups outlined above, each participant was also required to meet the following criteria:

1. Able to provide informed consent.
2. Assessed as able to comply with the demands of the study.
3. Age over 18 at the time of enrolment.
4. Fluent in English (to allow reliable cognitive testing).
5. No contraindication to MRI scanning, such as ferrous metal implants.
6. Absence of significant active central nervous system or medical disorders (in order to avoid confounding effects on outcome measures) thought to be due to a cause other than FAD.

2.2 Consent and ethical considerations

All studies reported in this thesis were carried out at UCL's Institute of Neurology in conjunction with the National Hospital for Neurology and Neurosurgery, UCL Hospitals NHS Trust. All experiments were carried out in accordance with the declaration of Helsinki. The study was approved by University College London (UCL) / UCL Hospitals Joint Research Ethics Committee.

Most of the *at-risk* participants had not previously undergone predictive clinical genetic testing, and so were unaware of their genetic status, and wished this to remain the case. One particularly important consideration from an ethical perspective was therefore to ensure that any genetic testing done as part of the research was done in a way that ensured the participant would never be made aware of the result. A specific

standard operating procedure was put in place in relation to this point, with several steps taken to ensure this was the case, as outlined below:

- Those who performed the genetic analysis in the laboratory would only communicate the results to specific pre-determined individuals (i.e. the study statisticians), who would themselves never have direct contact with the participants.
- The clinicians, psychologists, and radiographers who carried out assessments on the participants, including the author, remained blind to the participants' genetic status, which prevented them from either accidentally indicating the genetic result to the participant, or allowing knowledge of the genetic result to bias their objective clinical assessment.
- Any publications resulting from the work would not depict results in any way that may make it be possible to attempt to deduce the genetic status of any at risk individual.

The study followed the framework provided by the Mental Capacity Act (2005) relating to research and capacity (Bray, 2005). Participants lacking capacity were not recruited to the study. Capacity was assessed on an individual basis by a clinician with experience in the assessment of patients with cognitive impairment. Detailed discussions with the participant and their informant formed the foundation of this assessment. Whilst individuals lacking capacity were not recruited, it was possible that a participant may lose capacity during the course of the study after previously giving informed consent. In such a case, and if the individual was still able to participate, the researcher would be responsible for identifying an appropriate consultee who knows the participant well, who would then be consulted regarding whether or not the participant should continue.

2.3 Structure of cohort study

2.3.1 Annual assessments

As part of the UCL's longitudinal FAD study, individuals attended the DRC at approximately one-year intervals. At each annual research visit participants underwent a number of assessments, usually over the period of a single day, including:

- Clinical assessment (including a separate interview with the collateral source)
- Detailed neuropsychological assessment
- MRI – including both structural and diffusion-weighted sequences
- Blood sampling for genetic testing, as well as for serum biomarker development

Details of the above assessment areas are given in the following sections.

2.3.2 Long-term forgetting sub-study

In addition to the above, an extra sub-study was performed between February 2015 and March 2016, which involved the implementation of a novel neuropsychological test of long-term forgetting (see chapter six). This additional assessment involved a separate session of face-to-face testing between one and three months after the participants' main study visit, with a further follow-up phone call seven days later. The test materials for the long-term forgetting assessment were drawn from the Adult Memory and Information Processing Battery (AMIPB) (Coughlan and Hollows, 1985). Participants involved in the sub-study also completed the Everyday Memory Questionnaire (EMQ), which assess an individual's subjective impression of their

memory (Thompson and Corcoran, 1992) (appendix 2). The EMQ gives a score between 0 and 90, with higher scores indicating worse subjective memory.

2.4 Clinical assessment and determination of diagnostic group

A semi-structured interview was conducted with each participant to ascertain information relating to both his or her general health and potential symptoms of cognitive decline. Additionally, each participant nominated a close informant, who was interviewed separately in order to gain additional insight into the participant's level of functioning.

The Clinical Dementia Rating (CDR) scale was used to provide further information relating to the participant's day-to-day functioning (appendix 1) (Morris, 1993). The CDR incorporates information obtained from both the individual being assessed (i.e. the participant) and the informant separately, and assesses a number of different areas, including i) memory, ii) orientation, iii) judgment and problem solving, iv) community affairs, v) homes and hobbies, and vi) personal care. A quantitative global score is calculated, which relates to the participant's degree of impairment, as follows:

- 0 no impairment
- 0.5 questionable impairment
- 1 mild impairment
- 2 moderate impairment
- 3 severe impairment

One can also combine the scores from each area separately, to give a CDR “sum of boxes” (SOB) score, between 0 and 18.

The mini-mental state examination (MMSE), which gives a score between 0 and 30 (30 being the best), was also used as part of the clinical assessment to provide further information to assist in forming the clinical impression (Folstein et al., 1975). The Hospital Anxiety and Depression Score (HADS) questionnaire was administered, providing separate quantitative scores for both depressive symptoms and symptoms of generalized anxiety (Zigmond and Snaith, 1983).

A detailed physical neurological examination was performed on each participant to assess for possible non-cognitive signs of FAD (see section 1.3.4.), or of any evidence of other central or peripheral nervous system pathology. A general examination of the cardiorespiratory and gastrointestinal systems was also performed as standard.

Individuals were defined as symptomatic if i) consistent symptoms of cognitive decline were reported by the participant and/or their informant, ii) the clinical impression was that the participant was experiencing progressive decline, and iii) the global CDR was >0. If these criteria were not met the participant was said to be asymptomatic. To minimize inter-rater variability the same clinician would perform all assessments over a given period, with the author undertaking all assessments from August 2013 onwards.

2.5 Neuropsychological testing

A comprehensive neuropsychological test battery was independently administered by a trained psychologist, which includes assessment of the following:

- General intellectual functioning – Wechsler Abbreviated Scale of Intelligence (WASI) (Wechsler, 1999)
- Estimation of premorbid IQ – National Adult Reading Test (NART)
- Verbal and visual recognition memory – Recognition Memory Test (RMT) for words and faces (Warrington, 1984)
- Verbal paired associate learning – Camden Paired Associate Learning (PAL) Test (Warrington, 1996)
- Short-term memory - forward digit span
- Executive function – backwards digit span
- Naming – Graded Naming Test (McKenna and Warrington, 1983)
- Calculation – Graded Difficulty Arithmetic Test (Jackson and Warrington, 1986)
- Visuoperceptual skills – Object Decision Test from the Visual Object and Space Perception battery (VOSP) (Warrington et al., 1991)

2.6 Magnetic resonance imaging

For each participant at each visit, MR imaging was obtained on the same 3 T Siemens TIM Trio scanner using a 32-channel phased array head-coil. Acquisition sequences included:

- **T1-weighted imaging (approx. 5 minutes)** – A sagittal 3D magnetization-prepared rapid gradient-echo (MP-RAGE) T_1-weighted volumetric MRI (echo time/repetition time/inversion time = 2.9/2200/900 ms, dimensions of 256 × 256 × 208, voxel size of 1.1 × 1.1 × 1.1 mm) was acquired.
- **Diffusion-weighted imaging (approx. 2 × 7 minutes)** – Two 64-direction DWI sequences were acquired with a single shot, spin-echo echo planar imaging (EPI) sequence (field of view 240mm; matrix 96×96; yielding a voxel size of 2.5

× 2.5 × 2.5 mm; 55 contiguous axial slices; repetition time: 6800 ms; echo time: 91ms; b-value: 1000s/mm^2). We acquired nine acquisitions without diffusion weighting (b=0s/mm^2). The two DWI acqisitions, obtained back-to-back were used in combination at the analysis stage to increase signal-to-noise ratio.

In addition to the above, other sequences not used in this thesis included T_2-weighted imaging, T2*-weighted, and resting-state functional MRI. The total scan acquisition time was approximately 45 minutes. At the time of acquisition images were checked for movement artifact and were repeated if necessary (as long as it was felt that the participant could tolerate this). Further details of image analysis are given in chapters 3 and 4.

2.7 Blood sample acquisition and processing

Blood samples were acquired for two reasons:

1. **DNA testing –** Samples were collected in 10ml ethylenediaminetetraacetic acid (EDTA) coated Vacutainer™ tubes (BD, Oxford, UK). DNA was extracted and Sanger sequencing performed to establish the presence or absence of a pathogenic FAD mutation, as has been described previously (Janssen et al., 2003).
2. **Storage as serum for subsequent biomarker development** – Samples were collected in uncoated tubes and allowed to clot. They were then spun at 2000rpm for 15 minutes to separate out the serum. The serum was then stored at -80°.

As described in section 2.2, Genetic test data for individual participants were provided

only to designated individuals performing the statistical analysis, thus ensuring that the participants and the clinicians assessing them remain blind to the result of the genetic blood test.

2.8 Estimating years to symptom onset

EYO was calculated for each participant from an FAD family by subtracting the participant's current age from the age at which their affected parent first developed progressive symptoms of cognitive decline. The age at which their parent developed progressive symptoms was determined by detailed discussion with all available family members. This is the same method for calculating EYO as is used in many other FAD studies, including the large international multicenter DIAN study (Bateman et al., 2012), and has been shown to provide relatively accurate estimates of time to onset (Ryman et al., 2014). EYO allows prediction of how far from symptom onset an asymptomatic individual is at a given time point, if they are indeed a carrier of a mutation.

EYO can be thought of as a proxy marker of disease stage, or estimated proximity to symptomatic disease. Therefore, knowledge of individuals' current EYO allows one to assess potential associations between EYO (i.e. disease stage) and candidate biomarkers. It also allows separation of individuals in to different *disease stage* sub-groups based on EYO, i.e. those who are further and closer to predicted onset.

2.9 Statistical analysis

2.9.1 General approach

Specific details of the statistical analyses used for each individual study described in chapters three to six are given in the individual chapters. Here a general outline of the approach to statistical analysis is given. Data were collated in Microsoft Excel (Microsoft Inc.), with statistical analyses being performed in Stata v13.0 or later (StataCorp. 2015). Due to the requirement for the author to remain blind to the genetic status of all at-risk participants, the process of performing the statistical analysis was done collaboratively between the author and the two departmental statisticians (JN and TP), with each statistician leading on two (of four) studies. Each analysis was prospectively planned by the author, in terms of outcome variables of interest and any necessary covariables, with the statistician then separating the participants in to mutation carriers and non-carriers to perform the analysis.

All studies reported in this thesis primarily describe comparisons between two main groups: 1) FAD mutation carriers, and 2) non-carriers. FAD mutation carriers are those who test positive for a mutation, and may be either symptomatic or presymptomatic. For cross-sectional analyses, symptomatic and presymptomatic individuals are separated, due to the interest in investigating early/presymptomatic change. Non-carriers are a combination of any healthy controls not from FAD families (chapters three and four only) and those at risk FAD family members who test negative for a mutation.

Healthy controls not from FAD families were the spouses/partners of the FAD family participants. A clinical history was taken from these individuals to ensure no indication of current or previous significant neurological or psychiatric disease.

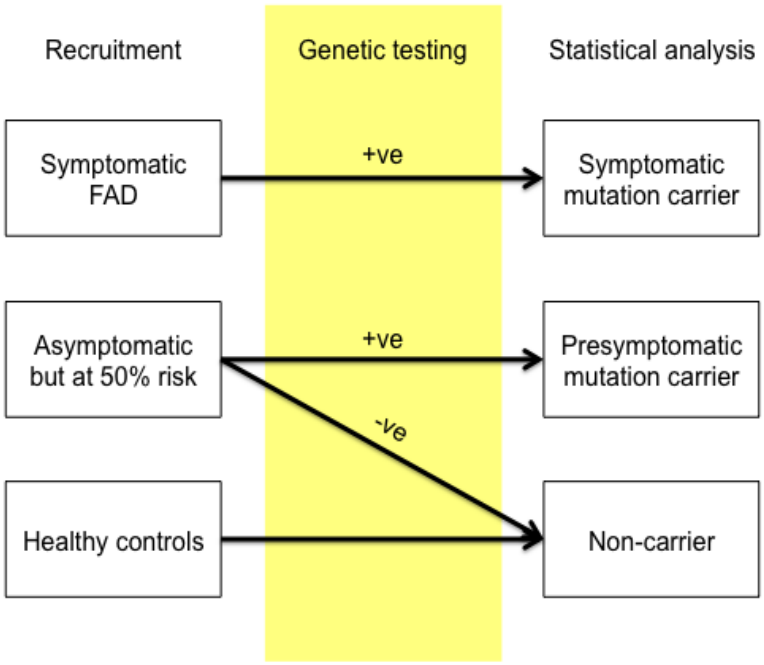

Figure 2-1. Separation of participants in to different groups for statistical analysis

Flow diagram illustrating how, following genetic testing, the different groups of individuals at recruitment are distributed in to the groups for the statistical analysis. Not all studies included healthy controls not from FAD families, in which case the non-carrier group was made up of mutation negative "at-risk" individuals only.

The general statistical approach to the evaluation of each candidate measure as a possible marker of AD-related neurodegeneration was then based on a number of analyses to determine the extent to which the measure fulfilled a number of traits:

1. Are there significant differences in the value of the measure between Symptomatic FAD and non-carriers?
2. Are there significant differences in the value of the measure between presymptomatic FAD and non-carriers?
3. Across all mutation carriers, does the measure demonstrate an association with

established measures of disease stage and/or severity – i.e. does it change progressively throughout the disease spectrum?

4. Within the presymptomatic group only, does the measure demonstrate an association with established measures of disease stage and/or severity?

Exactly if/how the above issues were investigated for each measure varied depending on the various characteristics of the measure being investigated and the number of data points available (including whether longitudinal or cross-sectional data were used). For the study described in chapter six (accelerated long-term forgetting) only asymptomatic at-risk participants were included due to the reasons discussed in the chapter.

2.9.2 Comparing baseline demographic characteristics between groups

As outlined in section 2.1.1, as mutation status was not known for the majority of participants at the time of recruitment, it was not possible to prospectively match the demographics of carriers and non-carriers. Also, as presymptomatic mutation carriers and symptomatic mutation carriers are at different stages of the disease, one would expect there to be a significant difference between their average ages, and so they could not both be matched to the age of the control group in any case. Group differences in age and gender, as well as other possible factors of interest such as cognitive performance, were generally assessed prior to undertaking more in-depth analysis.

2.9.3 Covariates

In advance of any analysis, variables that might theoretically be expected to have a systematic effect on the value of measures of interest were identified. These were then included as covariates in order to adjust for any confounding effects of these variables.

This approach was chosen because although the presence of a statistically significant difference between groups would indicate the need to adjust for this, the absence of a statistically significant difference does not rule out the possibility that the variable may still exert a confounding influence, particularly when small numbers of participants were being compared. For example, a group of presymptomatic mutation carriers and non-carriers may differ slightly but not statistically significantly in age, but if there is a large effect of age on rate of cortical thinning, this might produce a spurious difference in atrophy rates when these are compared between groups (a type 1 error). Thus, it is necessary to identify in advance those variables that might theoretically be expected to have a systematic effect on the value of measures of interest. Regression analysis allows these 'nuisance' variables to be adjusted for statistically.

Age is known to be closely associated with neuronal loss, both in normal aging and neurodegenerative disease (Scahill et al., 2003). Gender is known to have a significant influence on brain size, with men found to have larger brain volumes and thinner cortices (Barnes et al., 2010), although its influence on other blood-based and cognitive markers of neurodegeneration is less clear. For all analyses across all four studies reported, it was decided to include age as a covariable. Depending on the specific nature of the disease marker being investigated, other potentially confounding factors, such as gender, total intracranial volume (TIV) for brain volume measurement (but not for cortical thickness or DWI), and IQ for ALF, were also included as covariables in the statistical models.

In all statistical models, clustering of individuals from within the same family was accounted for, either by using a random effect or by using robust standard errors

2.9.4 Group comparisons

For cross-sectional analyses (i.e. chapters four, five, and six), regression modeling was used, adjusting for any predefined covariables, to compare group means for the measure of interest. Pairwise comparisons (i.e. presymptomatic mutation carriers vs. non-carriers; symptomatic mutation carriers vs. non-carriers; and symptomatic mutation carriers vs. presymptomatic mutation carriers could then be performed (figure 2-2). The exact nature of regression model chosen depended on a number of factors, including whether the data was normally distributed and how comparable the difference group variances were.

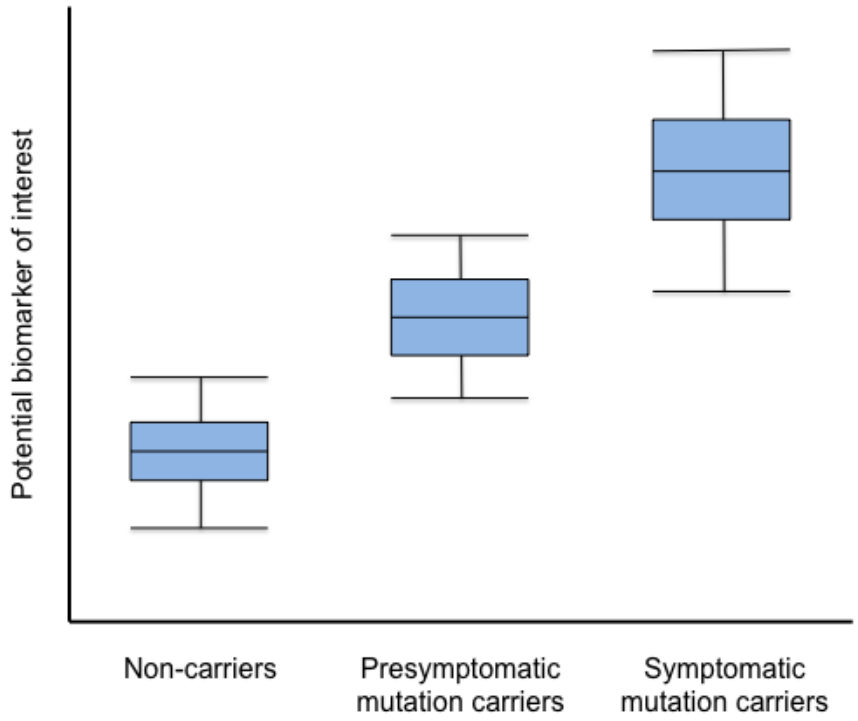

Figure 2-2. A box and whisker plot illustration of the different group measurements you may obtain for a disease marker of interest

A box and whisker plot illustration of the different group measurements you may obtain for a disease marker of interest. Regression analysis allows direct group-wise comparisons, with any necessary covariables accounted for, to assess how the variable of interest differs between the different groups. Such an approach is used for cross-sectional analyses.

For chapter 3, where longitudinal data were analysed (i.e. that data include repeated measures within the same individuals), a longitudinal mixed effects model, including both fixed and random effects, was used to examine how the measure of interest was associated with EYO in mutation carriers and with age in the non-carriers (figure 2-2-2).

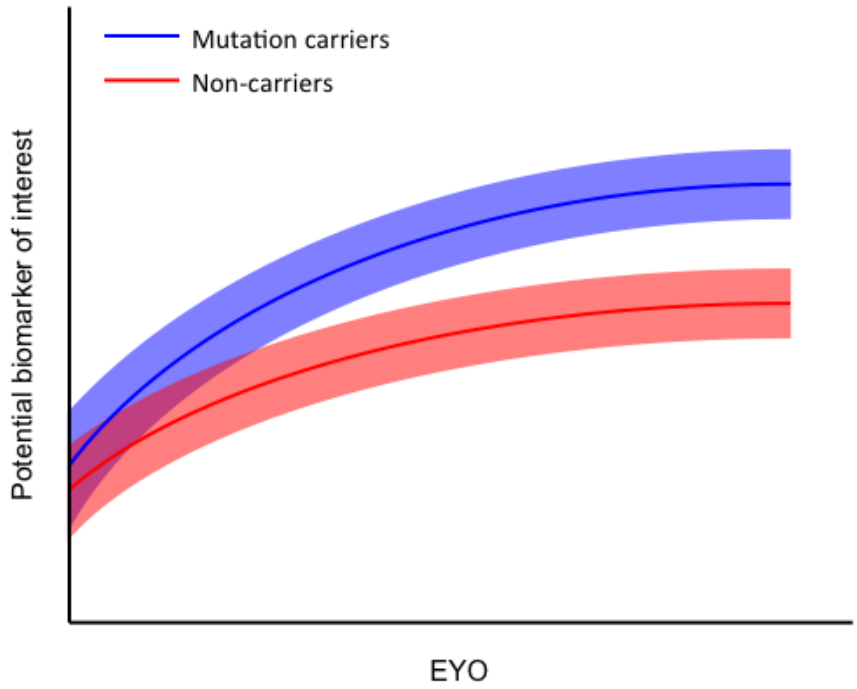

Figure 2-3. An illustration of how a longitudinal mixed effects model allows assessment of how a variable changes over time (measured as EYO in this case)

This approach is used for analysis of longitudinal (i.e. repeated measures) data. The approach allows assessment of when (i.e. how far to/from expected symptom onset) values for mutation carriers (blue) and non-carriers (red) diverge. The paler red and blue regions either side of the lines represent 95% CIs.

2.9.5 Assessing associations with other disease measures

After comparing between groups, the general approach taken has been to assess associations between the marker of interest and other previously validated markers of disease stage and/or severity, such as EYO (a marker of disease stage) or imaging and cognitive measures (markers of disease severity). This was performed within the mutation carriers only (i.e. those with AD pathology) to assess how well the marker of

interest is able to track the changes that occur over time as disease progresses. Such associations can be assessed visually on scatter plots (figure 2-3), and tested statistically using correlation coefficients (either Pearson or Spearman depending on whether there is a linear/parametric relationship).

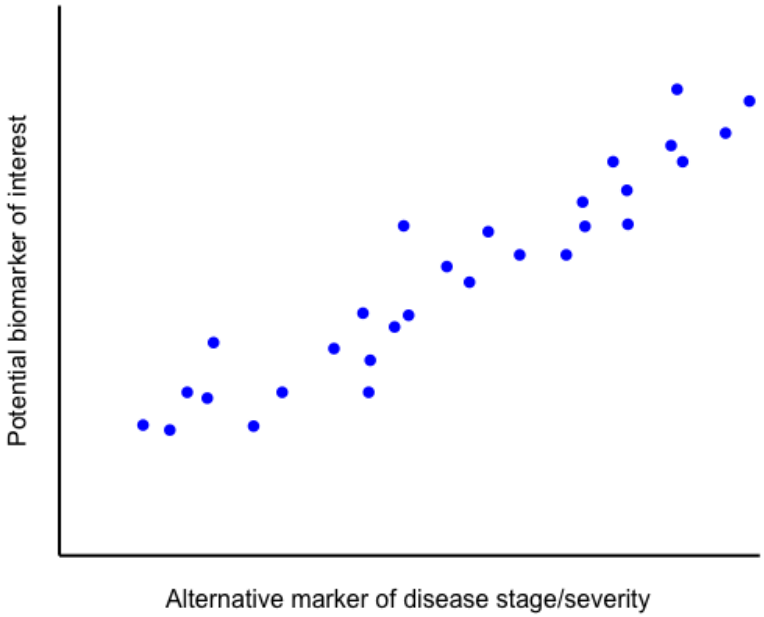

Figure 2-4. An illustration of how in mutation carriers a biomarker of interest may be associated with another separate marker of disease stage/severity

3 Macrostructural cortical imaging: assessment of longitudinal cortical thickness change

3.1 Introduction

Studies of volumetric MRI, using automated cortical thickness measurement, have suggested that sporadic AD is associated with cortical thinning in a relatively consistent pattern, or "signature", of cortical regions. (Dickerson et al., 2009, Bakkour et al., 2009). A composite signature is likely to be more robust to inter-individual variation than using a single region alone. However it has not yet been established whether a similar cortical signature pattern of loss could be used to track changes presymptomatically in FAD.

Previous imaging studies in FAD identified reductions in brain volumes before symptom onset, with longitudinal rates of change appearing more sensitive than cross-sectional measurement (Fox et al., 1996, Ridha et al., 2006).

This study is a longitudinal study of cortical thickness in FAD mutation carriers. Firstly, the identification of a cortical signature of FAD, determined in symptomatic participants, is described. The utility of this cortical signature approach in detecting presymptomatic change is then assessed, both in terms of absolute thickness and rates of thinning. Finally, whether baseline thickness can predict subsequent thinning is assessed, along with its correlation with preclinical cognitive changes.

3.2 Hypotheses

- Significant cortical thinning will be detectable in mutation carriers prior to symptom onset.
- Rates of change in cortical thinning will become abnormal prior to absolute thickness values.
- Regions identified as making up the cortical signature will correlate with early cognitive changes.

3.3 Contributions and collaborations

The study was conceived and designed by Professor N. Fox and the author. Participant recruitment and collection of imaging and clinical data was carried out by Dr N. Ryan, Dr Y. Liang and the author. Neuropsychology data were collected by Ms K. Macpherson. Processing and analysis of the imaging data was performed by Dr M. Lehmann and the author. The statistical analysis was planned by Dr J. Nicholas and the author, and then performed by Dr J. Nicholas (to prevent the author being unblinded to the genetic status of participants). SVM analysis was performed by the author, with assistance from Dr L. Harper. Interpretation of data and preparation of tables and figures was carried out by the author.

3.4 Methods

3.4.1 Participants

Eighty-five participants, recruited between July 2008 and June 2014 were included in the study. Twenty participants had symptomatic FAD at the time of recruitment, 38 were asymptomatic but by virtue of having an affected parent were at 50% risk of carrying a mutation, and 27 were healthy controls (i.e. a spouse of an individual from an FAD family) with no family history of AD.

The 58 participants from families affected by FAD (20 symptomatic, 38 at risk) came from a total of 28 different families. For these participants blinded genetic testing was performed to determine the presence or absence of a mutation, as described in sections 2.2 and 2.7. EYO was calculated as described in section 2.8.

At each time point, approximately annually, participants underwent magnetic resonance imaging (MRI), neurological examination, detailed neuropsychological assessment, and assessment with the MMSE and CDR, as described in chapter 2. The neuropsychological tests used in the analysis of this specific study were the WASI, RMT for words and faces, forward and backward digit span, the graded naming test, the graded difficulty arithmetic test; and the object decision test from VOSP.

3.4.2 MRI acquisition

All participants at all time points were scanned on the same 3 T Siemens TIM Trio scanner using a 32-channel phased array head-coil. A sagittal 3D MP-RAGE T1-weighted volumetric MRI (echo time/repetition time/inversion time = 2.9/2200/900 ms, dimensions of 256 × 256 × 208, voxel size of 1.1 × 1.1 × 1.1 mm) was acquired. For all

participants, images were assessed visually in all planes to ensure adequate coverage and to exclude significant motion, artifacts or unexpected pathology.

3.4.3 Image analysis

Cortical thickness was measured across the cortical mantle at approximately 300,000 vertices using Freesurfer v5.30's (http://surfer.nmr.mgh.harvard.edu) cross-sectional pipeline. The procedure used by Freesurfer for the surface construction has been described and validated previously (see section 1.4.3.5.) (Dale et al., 1999, Fischl and Dale, 2000). Two modifications to the standard Freesurfer processing stream were undertaken: a locally-generated brain mask was used for skull stripping and ventricular segmentations were added to the white matter mask to improve cortical segmentation. Cortical thickness was smoothed with a 20 mm full-width at half-maximum kernel. All cortical segmentations were visually inspected. Mean cortical thickness values were calculated for 34 parcellated cortical regions bilaterally.

3.4.4 Identifying the FAD cortical signature

Firstly, a literature review was undertaken in PubMed, using the search terms [familial Alzheimer's disease] OR [autosomal dominant Alzheimer's disease] AND [cortical thickness] OR [cortical volume], to identify articles that had previously examined cortical atrophy in FAD. The title and abstract of all articles identified by the search were assessed for suitability. For all suitable articles (i.e. original studies of FAD with data on cortical volumes/thickness) from the initial search, the titles and abstracts of articles in their reference lists were reviewed, and any additional suitable articles also included. Any articles that included any of the same participants as the current study were excluded. All regions previously found to show significant thinning ($p<0.05$) in FAD were identified.

In addition, data from symptomatic members of the study cohort were analysed to identify those regions that demonstrated the most significant bilateral thinning in the baseline scans of the ten mildest (according to MMSE) symptomatic FAD participants (mean age 49.0 (SD 10.8); 7 male/3 female) compared to the 42 non-carriers (43.9 (9.4); 24 male/18 female). The 10 mildly symptomatic participants had a mean CDR of 0.75 (SD 0.26) and MMSE of 24.1 (2.4). Freesurfer was used to measure cortical thickness in these individuals as described in section 3.2.3. An un-biased whole-brain analysis provided mean cortical thickness for 34 parcellated cortical regions bilaterally. Correcting for age and gender, a conservative statistical threshold ($p<0.001$ FWE corrected) was used to identify those cortical regions with evidence for significant thinning compared to controls. N.B. this analysis did not involve any presymptomatic at-risk individual)

A relatively liberal threshold ($p>0.05$ uncorrected) was purposely chosen when identifying regions in the initial literature search, to identify all regions that have previously been implicated as undergoing significant atrophy in FAD, prior to then applying much more stringent statistical criteria ($p<0.001$ FWE corrected) to the data-driven analysis that followed.

Comparing the results of the literature-driven and data-driven approaches, and including only regions identified by both approaches, cortical regions showing consistent thinning in FAD were identified (figure 3-2C), which were used to determine the final FAD cortical signature.

3.4.5 Longitudinal mixed effects modeling

Following blinded genetic testing, the 38 asymptomatic at-risk participants were divided in to either the mutation carrier group if mutation positive or the healthy control group

(i.e. non-carriers) if mutation negative. A longitudinal linear mixed effects framework was applied to assess longitudinal change within the cortical signature regions, in terms of both absolute cortical thickness and rates of change in cortical thickness, using data from all mutation carriers (symptomatic and presymptomatic) and non-carriers at all available time points.

The outcome (dependent variable) was cortical thickness in the region of interest in mm. The fixed effects predictor variables were age in years, gender, mutation carrier status, and polynomial terms for EYO in mutation carriers only. All models included a linear and quadratic term for EYO. A cubic term for EYO was also included if there was evidence that this provided a better model fit ($p<0.05$ Wald test), which was the case for the mean signature summary measure, inferior parietal cortex, superior parietal cortex and supramarginal gyrus.

Random effects included a family level random effect for intercept; and participant level random effects for intercept and EYO in all models with independent variance-covariance structure. A random effect for mutation carrier status was included if there was evidence that this provided a significantly better fit ($p<0.05$ likelihood ratio test), which was the case for inferior parietal cortex; precuneus and supramarginal gyrus. The random effects for years to onset and mutation carrier status had unstructured variance-covariance, to allow for a correlation between these two random effects.

Longitudinal mixed models were applied to investigate the association between the observed baseline thickness and subsequent post-baseline rate of thinning, based on methods outlined by Byth and Cox (Byth and Cox, 2005). These models were restricted to the data from the 33 mutation carriers with scans on at least two time points. The outcome (dependent variable) was cortical thickness in the region of interest in mm. The fixed effects predictor variables were duration of follow-up, gender, interaction

between duration and gender, and interaction between baseline cortical thickness (in mm) and duration. Random effects included a family level random effect for the intercept, and participant level random effects for intercept and duration with unstructured variance-covariance.

3.4.6 Support vector machine analysis – predicting diagnostic group

Following the longitudinal group-level analyses, a linear support vector machine (SVM) approach was used to assess how accurately, based on a single scan, the cortical signature is able to predict presymptomatically whether an individual is a mutation carrier or non-carrier. An SVM is a multivariate machine learning method that assesses several features, or *support vectors*, to determine the optimum decision boundary that divides the two populations (Falahati et al., 2014). The features used for the current analysis were the cortical thickness values for the six signature regions. The data were split in half into a *training set* and a *testing set*. The support vector algorithm was then first applied to the training set, to find the cortical thickness values that maximize the margin between two different groups – the so-called optimal hyperplane (figure 3-1). After modeling the hyperplane, the algorithm is then applied to the separate independent testing set, to assess how accurately it is able to classify the participants within that set as belonging to one of the two groups.

For the purpose of this analysis, the presymptomatic mutation carrier group was split in half at the median EYO (8 years) in to an early presymptomatic (EPS) group and a late presymptomatic (LPS) group.

Receiver operator curves (ROC) were produced for symptomatic individuals versus controls, all presymtpomatic individuals versus controls, LPS only versus controls and EPS only versus controls; with the area under the curve (AUC) calculated for each

contrast. It should be noted that, with regards to the symptomatic group, scans from ten of these individuals had earlier been used to help identify the cortical signature regions, which were then used as the features of interest in the support vector machine to try and separate the different groups. This means therefore that a degree of circularity is introduced with regards to the symptomatic individuals, which was taken in to account in any subsequent interpretation of results. The analyses involving the symptomatic group were not however of key interest, with the primary question being to what extent the SVM could discriminate between presymptomatic mutation carriers (either EPS or LPS) and non-carriers. SVM processing and analysis was performed using the Python libraries SciPy 0.14.0 and Scikit-Learn 0.15.2 (Pedregosa et al., 2011) on Python 2.7.6 – 64-bit.

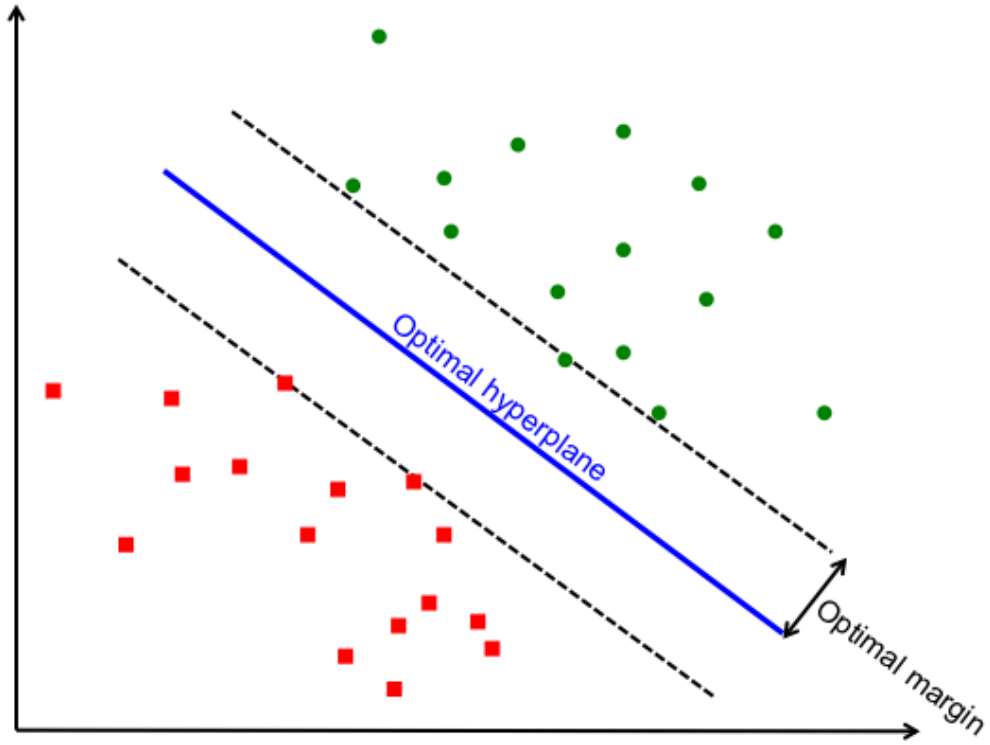

Figure 3-1. Schematic representation of support vector machine classification

The support vector machine finds a hyperplane that provides the best between group separation (in this case the two groups are represented by red squares and green circles). The optimal hyperplane provides the largest distance (optimal margin) between the two groups.

3.4.7 Assessing association between cortical signature change and neuropsychological performance

In order to assess the clinical implications of thinning within the cortical signature regions an analysis was undertaken to identify associations between cortical thickness and performance on neuropsychological testing in mutation carriers, both before and after symptom onset. Spearman correlation coefficients were used to assess cross-sectional correlation between mean cortical thickness across the six signature regions at baseline and score on each focal neuropsychological test. In addition, the following

specific correlations were examined, based on hypothesised associations between specific regions and specific focal tests:

- RMT (words and faces) and entorhinal cortex thickness.
- Digit span forwards and superior frontal cortex, supramarginal gyrus and inferior parietal cortex thickness.
- Digit span backwards and superior frontal cortex thickness.
- Arithmetic and supramarginal gyrus and inferior parietal cortex thickness.
- VOSP object decision and supramarginal gyrus, inferior parietal cortex and superior parietal lobule thickness.

As well as examining the above correlations amongst all mutation carriers, secondary analyses examined the correlation between cortical thickness and neuropsychological test scores in presymptomatic mutation carriers only. Cluster adjusted (robust) p-values were used to account for clustering of individuals within families.

3.5 Results

3.5.1 Participant demographics

Of the 38 asymptomatic at risk participants, 23 tested positive for a pathogenic mutation (presymptomatic mutation carriers) and 15 tested negative (non-carriers). Those who tested negative were combined with the healthy controls to form a non-carrier group. In total, 43 participants were carriers of pathogenic mutations in either *PSEN1* (n=36) or *APP* (n=7) and 42 were non-carriers. The mutation carrier group included a total of 14 different *PSEN1* mutations and four different *APP* mutations. At baseline 20 of the mutation carriers were symptomatic and 23 were presymptomatic.

Mutation carriers and non-carriers were well matched for age (43.2 years (SD 9.4) versus 43.9 (9.4)) and gender (15 male/28 female versus 18 male/24 female). The baseline group demographics, with mutation carriers broken down into symptomatic and presymptomatic, are shown in table 3-1.

	Controls	**Presymptomatic**	**Clinically affected**
N	42	23	20
Age, years (SD)	43.9 (9.4)	38.7 (7.8)	48.5 (8.8)
Gender, m/f	18/24	9/14	6/14
EYO years (SD)	-	7.5 (5.4)	-
Global CDR (SD)	0	0	1.1 (0.43)

Table 3-1. Demographics and baseline clinical characteristics of the participants

3.5.2 The FAD cortical signature

The literature search identified a total of seven articles, including a total of 260 FAD mutation carriers (Apostolova et al., 2011, Benzinger et al., 2013, Fortea et al., 2010, Lee et al., 2013, Quiroz et al., 2013, Reiman et al., 2012, Sala-Llonch et al., 2015). Cortical regions identified in these publications as showing significant differences ($p < 0.05$) in FAD compared to controls are outlined below in table 3-2, as well as in figure 3-2B.

Study	n= (mutation carriers)	Cortical regions identified
Apostolova et al.	25	Superior parietal, inferior parietal, supramarginal, precuneus, posterior cingulate
Benzinger et al.	137	Superior parietal, inferior parietal, superior temporal, middle temporal, entorhinal, precuneus
Fortea et al.	11	Banks of superior temporal sulcus, superior parietal, inferior parietal, supramarginal, fusiform
Lee et al.	25	Superior parietal, superior temporal, middle temporal, superior frontal
Quiroz et al.	18	Superior parietal, inferior parietal, precuneus
Reiman et al.	20	Superior parietal, inferior parietal, supramarginal, middle cingulate, superior temporal, parahippocampal, fusiform
Sala-Llonch et al.	24	Inferior parietal, superior temporal, middle temporal, middle frontal

Table 3-2. A summary of the cortical regions identified as undergoing significant atrophy in FAD from the seven studies identified by the literature search

When combining the results of the literature search with the additional data-driven analysis, six cortical regions were identified and chosen for inclusion as the FAD cortical signature (figure 3-1C):

- entorhinal cortex
- inferior parietal cortex
- precuneus
- superior frontal cortex
- superior parietal cortex
- supramarginal gyrus

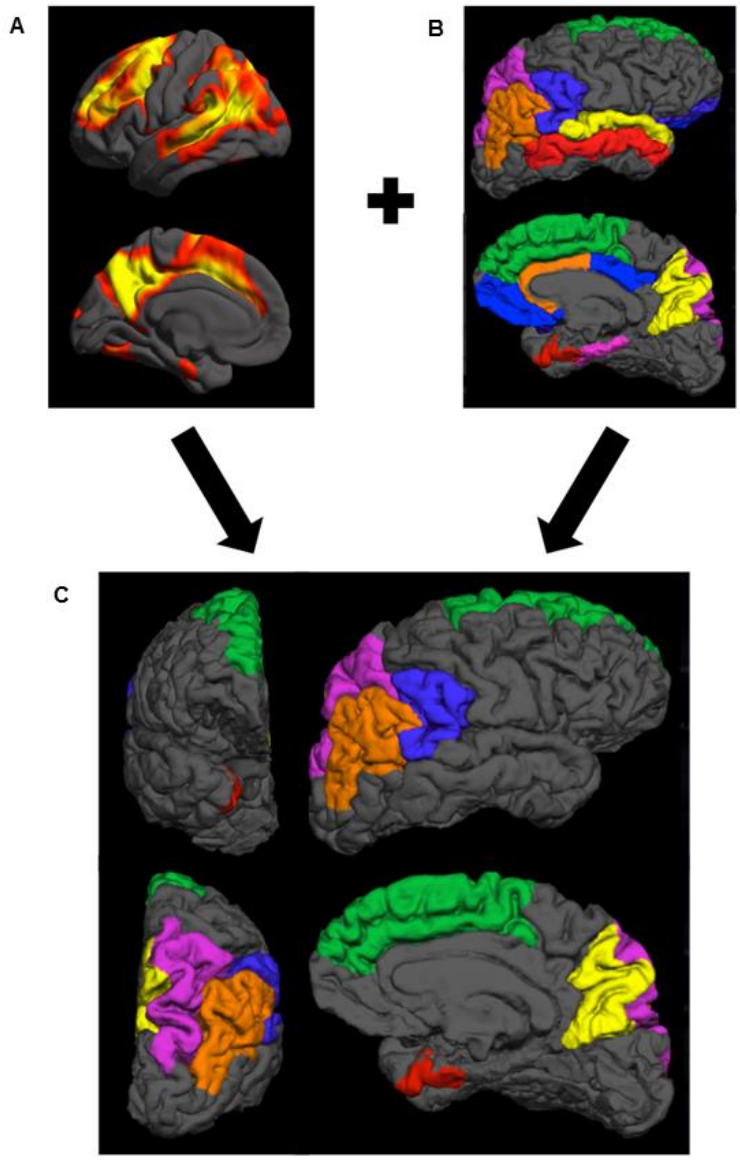

Figure 3-2.The FAD cortical signature

(A) *Results of Freesurfer analysis indicating regions exhibiting the most significant cortical thinning in the mildly symptomatic FAD individuals from our cohort (p<0.01 FWE corrected).* ***(B)*** *The result of a literature search, showing regions previously highlighted as showing significant atrophy in FAD. Regions were identified that were positive in both the literature driven and data driven approaches, and only these regions were included in the final FAD cortical signature* ***(C)****. A total of six regions were included: entorhinal cortex (red), inferior parietal cortex (orange), precuneus (yellow), superior frontal cortex (green), superior parietal lobule (purple) and supramarginal gyrus (blue).*

3.5.3 Assessment of presymptomatic cortical thinning across the cortical signature

Analysis of longitudinal cortical thickness change found that, for all six cortical signature regions there was strong evidence of a difference in cortical thickness between mutation carriers and non-carriers ($p<0.0001$ for all regions) and for a difference in rates of change in cortical thickness ($p<0.0001$ for all regions). Combining all signature regions to give a mean signature measure showed cortical signature thickness to be significantly lower in mutation carriers compared to controls by 3 years before predicted onset (table 3-3, figure 3-3). The earliest significant difference in cortical thickness in any individual region was detectable 4 years pre-onset, in the precuneus.

Earlier differences between mutation carriers and non-carriers were apparent, for all six signature regions, when comparing the rate of change in cortical thickness, rather than the absolute cortical thickness value alone (table 3-3, figure 3-3). Rates of thinning in the mean signature summary measure become nominally higher in mutation carriers compared with controls at around 9 years pre-predicted onset, with the difference becoming statistically significant by 5 years before predicted onset. The earliest significant difference in rate of change in an individual region was again observed in the precuneus, with significant differences in rates of thinning seen at 8 years pre-onset. A paired t-test, including all six signature regions, found the change in rate to be significantly earlier than the change in absolute thickness ($p=0.005$).

Across all mutation carriers, lower baseline cortical thickness predicted greater thinning in the subsequent follow-up period. This association was stronger for the mean signature summary measure than for any region individually (table 3-3). A significant association remained between mean signature thickness and future decline even when

only presymptomatic carriers were assessed (p=0.02); a similar association was also found in this group for the precuneus (p=0.03).

	Cortical Thickness (MC vs. NC)	Rate of change (MC vs. NC)	Association between baseline cortical thickness and subsequent rate of thinning (MC only)		
	Earliest significant (p<0.05) difference (EYO)	Earliest significant (p<0.05) difference (EYO)	Coefficient (mm/y for every additional mm at baseline)	95% CI	p-value
Mean signature summary measure	-3	-5	0.184	0.063 to 0.305	0.003
Entorhinal cortex	-2	-5	0.115	-0.104 to 0.335	0.30
Inferior parietal cortex	-3	-4	0.139	0.036 to 0.242	0.008
Precuneus	-4	-8	0.105	0.029 to 0.180	0.007
Superior frontal cortex	-3	-5	0.162	0.038 to 0.286	0.01
Superior parietal cortex	-2	-3	0.119	0.036 to 0.202	0.005
Supramarginal cortex	-2	-5	0.081	0.009 to 0.152	0.03

Table 3-3. Longitudinal cortical thinning in the cortical signature regions

A comparison between mutation carriers (MC) and non-carriers (NC), indicating the number of years prior to predicted symptom onset when a significant difference is detectable in (i) cortical thickness and (ii) the rate of change in cortical thickness. All regions show significant presymptomatic thinning, including a mean signature measure. For all regions, apart from the entorhinal cortex, there was a significant relationship between cortical thickness at a given time point and the subsequent rate of thinning; with lower baseline thickness associated with a greater rate of subsequent decline. This association was stronger for the mean cortical signature measure than for any individual region.

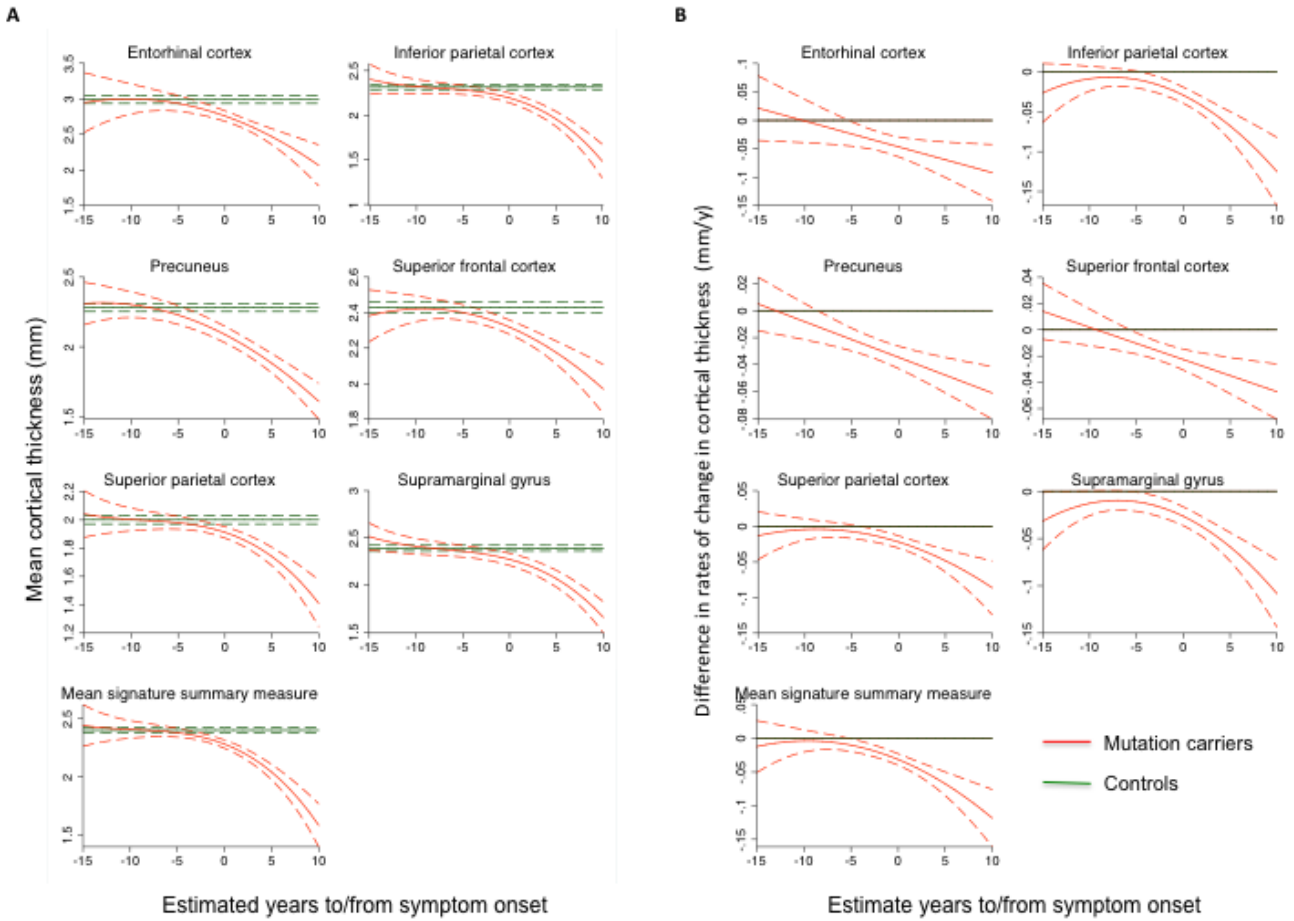

Figure 3-3. Longitudinal change in cortical thickness in the six cortical signature regions

Graphs comparing mutation carriers and controls for (A) absolute cortical thickness value, and (B) difference in rate of change in cortical thickness, with the x-axes representing estimated time to/from onset of progressive cognitive symptoms. Graphs are shown for each cortical signature region as well as the mean signature summary measure. Dotted lines indicate 95% CIs.

3.5.4 Assessing the utility of cortical signature thickness in predicting diagnostic group in individual people

Based on a single scan per participant, the cortical signature was able to differentiate AD from non-AD extremely accurately in symptomatic participants versus controls (AUC=1.00, 95% CI 0.84-1.00). When looking at all presymptomatic individuals versus controls, the AUC was 0.80 (0.59-0.91). When the presymptomatic group is divided in to LPS (EYO < 8) and EPS (EYO > 8) we see AUCs of 0.87 (0.61-0.96) and 0.65 (0.37-0.84) respectively (figure 3-3).

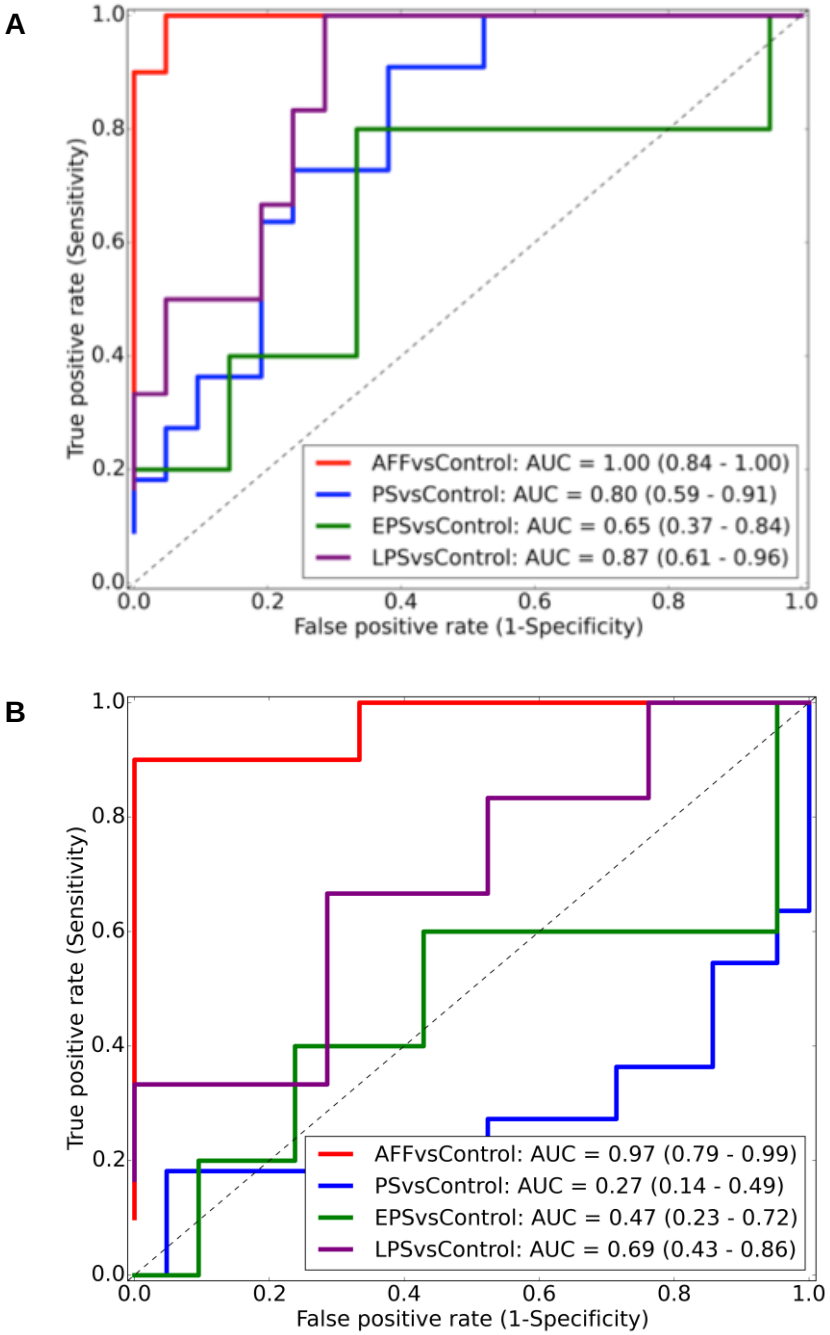

Figure 3-4. Predicting diagnostic group in individual people

*ROC show the results of a support vector machine analysis to assess the accuracy with which cortical thickness within **(A)** the cortical signature, and **(B)** the precuneus, measured from a single scan, is able to predict whether an individual is a mutation carrier or a non-carrier, at various different disease stages. Curves are shown for clinically affected individuals (AFF) versus controls; all presymptomatic (PS) individualls versus controls; LPS versus controls; and EPS versus controls. ROC=receiver operator curves; AFF=affected; PS=presymptomatic (all); LPS=late presymptomatic; EPS=early presymptomatic.*

3.5.5 Correlation between cortical signature thickness and neuropsychological performance

Across all mutation carriers, there were significant positive correlations between the mean cortical signature summary measure and cognitive performance across tests of a wide range of cognitive modalities (table 3-4). For each of these tests, there was also significant correlation between test performance and cortical thickness in specific hypothesised individual cortical region(s).

Looking at the presymptomatic participants only (median time to onset=8 years), there remained a statistically significant correlation between cortical thickness and performance in both verbal recognition memory and arithmetic, but not with other domains (table 3-4).

Despite the precuneus not being one of the pre-hypothesised regions for testing associations with cognitive decline, as it had demonstrated the earliest presymptomatic thinning of any individual region a post-hoc analysis was undertaken to assess its association with presymptomatic cognitive performance. It was found that, in presymptomatic individuals, precuneus thickness correlated with verbal recognition memory only (Spearman rho = 0.48, p = 0.02).

Test	Region	All mutation carriers		Presymptomatic carriers only	
		Spearman's rho	p-value	Spearman's rho	p-value
RMT faces	Mean signature	0.41	0.005	0.08	0.74
	Entorhinal	0.40	0.009	0.02	0.93
RMT words	Mean signature	0.67	<0.001	0.65	0.001
	Entorhinal	0.50	0.001	0.57	0.001
Digit span forwards	Mean signature	0.45	0.01	0.13	0.66
	Superior frontal	0.45	0.01	0.19	0.41
	Supramarginal	0.49	0.004	0.23	0.47
	Inferior parietal	0.47	0.009	0.08	0.78
Digit span backwards	Mean signature	0.60	<0.001	0.29	0.32
	Superior frontal	0.57	0.001	0.18	0.45
Arithmetic	Mean signature	0.77	<0.001	0.43	0.075
	Supramarginal	0.78	<0.001	0.51	0.03
	Inferior parietal	0.70	<0.001	0.28	0.27
VOSP	Mean signature	0.28	0.05	0.18	0.42
	Superior parietal	0.15	0.37	-0.03	0.90
	Inferior parietal	0.23	0.17	0.09	0.70
	Supramarginal	0.23	0.10	0.18	0.30

Table 3-4. Correlations between baseline cortical thickness and cognitive performance

Spearman correlation coefficients are shown for performance on a number of focal cognitive tests and cortical thickness, in mutation carriers only. Correlations were assessed between each cognitive test and the mean signature summary measure, as well as for certain specific individual regions. To limit the number of comparisons we constrained comparisons between focal tests and individual regions to only those for which we had a priori hypotheses (based on the previous literature). For each comparison correlations were assessed both across the entire cohort and in presymptomatic individuals only. For each cortical region (and cortical signature) the thickness was calculated as an average of left and right.

3.6 Discussion

Results are reported from the assessment of longitudinal cortical thickness change in presymptomatic FAD, within a disease-specific cortical signature. The FAD cortical signature that was identified would appear to closely resemble that previously identified for sporadic AD (Dickerson et al., 2009), and included medial parietal, lateral parietal, and medial temporal regions. By then applying this cortical signature to an independent group of presymptomatic mutation carriers, it was found that all six cortical signature regions showed significant thinning a number of years before the onset of cognitive symptoms.

The findings suggest, consistent with previous studies of FAD mutation carriers, that the precuneus is one of the earliest regions to show significantly reduced cortical thickness, at approximately 4 years pre-onset (Benzinger et al., 2013, Knight et al., 2011a). A previous cross-sectional study of FAD, which applied the sporadic AD cortical signature (rather than an FAD-specific one), identified presymptomatic thinning in three of the regions identified in our study, including the precuneus, at an average of 6 years prior to onset (Quiroz et al., 2013). The reason for the slightly earlier precuneus thinning in this study may have been the increased homogeneity of the participants, with all mutation carriers having the same mutation (*PSEN1* E280G).

Studies of presymptomatic FAD have reported an initial *increase* in cortical thickness, prior to later decline (Fortea et al., 2010, Sala-Llonch et al., 2015, Pegueroles et al., 2017). The authors acknowledged that this was unexpected, and speculated that it may indicate a presymptomatic inflammatory process. Here, in a larger sample, we find no evidence to support an early cortical thickness rise. However, the possibility that cortical thickness may increase in the earliest presymptomatic phase – perhaps even

earlier than the period the current study spanned – before falling as individuals come closer to symptom onset cannot be excluded.

Across all six signature regions, it was found that assessing the *rate* of change in cortical thickness allowed significantly earlier detection of neurodegeneration than a cross-sectional measure of thickness at a single time point (table 3-3). Previous imaging studies have similarly suggested that rate of loss rather than absolute volume/thickness may be more sensitive to early pathological change (Ridha et al., 2006, Knight et al., 2011a, Jack et al., 2005, Fox et al., 1996), although very few FAD studies have measured longitudinal change in cortical thickness specifically. The timing of the increase in rate of decline in cortical thickness from our study was slightly earlier than found for other longitudinal volumetric imaging measures (Ridha et al., 2006, Yau et al., 2015).

It is not only at the group level that the cortical signature appears able to discriminate between early AD and healthy aging. As disease modifying therapies become available, accurate presymptomatic screening of individual people (rather than merely separating groups) will become more important. At the level of the individual person, assessing thickness within the six signature regions shows promise for predicting whether or not an asymptomatic individual is destined to develop clinical AD, up to 8 years before the onset of any symptoms (AUC of 0.87). Such accurate discriminatory power for a neuroimaging measure has only previously been reported for identifying AD after patients are already clinically demented (Falahati et al., 2014, Casanova et al., 2013). The gradually progressive reduction in cortical thickness, beginning early in the disease process, is illustrated nicely by the progressive increase in AUC (for discriminating AD from controls) as the disease progresses. However, with regards to discriminating symptomatic individuals from controls, where the AUC was an improbably high 1.00, it is important to bear in mind the circularity outlined in section

3.4.6, which leads inevitably to a degree of bias that should be acknowledged. Such circularity did not apply however to the presymptomatic group analyses discussed above. The utility of a combined cortical signature approach, as opposed to using a single region alone, is underlined by the fact that the discriminatory performance when using the precuneus only – the individual region to show the earliest thinning – was significantly poorer than for the six-region signature.

It was found that, in mutation carriers, thickness across the cortical signature regions correlated with cognitive performance (table 3-4). This was true even prior to the onset of symptomatic decline, in individuals who were on average eight years from predicted symptom onset. In the presymptomatic mutation carriers the closest correlation was between cortical thickness and verbal episodic memory. This cognitive domain has previously been identified as being the earliest neuropsychological predictor of later decline (Fox et al., 1998, Linn et al., 1995, Lopera et al., 1997). Compared to the precuneus – the cortical region that showed the earliest thinning – the statistical significance of the correlation between mean signature thickness and verbal episodic memory was greater by an order of magnitude. (This also provides further support for the potential value in developing more sensitive methods for the detection of early episodic memory change, as is done in chapter six.)

The findings also suggest that cortical signature thickness at a given time point may have prognostic value, in that it correlates significantly with future rate of decline. When analysing all mutation carriers, assessing the mean thickness across a composite of preselected cortical regions provided stronger prediction of future decline than any single region alone (table 3-3); although when looking in presymptomatic individuals only the predictive value of the cortical signature and precuneus were similar. The finding that a multi-region signature provides predictive power and greater correlation with cognitive performance than any region in isolation is consistent with the concept

that in AD there is early breakdown of a vulnerable but distributed neural network of different interconnected regions; the variability between individuals in the patterns of loss and sequence of recruitment of different regions with progression means that a composite signature region may be a more robust measure than a single region (Pievani et al., 2011, Warren et al., 2012). This is also supported by the findings from the SVM analysis discussed above. A similar “cortical signature” approach to that used here for FAD has previously shown promise in identifying early symptomatic sporadic AD (Dickerson et al., 2009, Bakkour et al., 2009, Dickerson et al., 2013).

A composite cortical signature region may be useful in the recruitment to, and monitoring of, presymptomatic trials of disease modifying therapies (Bateman et al., 2011, Kozauer and Katz, 2013, Reiman et al., 2011). The use of a marker of AD-neurodegeneration, such as the cortical thickness signature, may allow presymptomatic disease staging, by allowing prediction of how close an individual is to symptom onset. A cortical signature could also provide a means of quantifying loss over time, a potentially valuable outcome biomarker.

Compared to previous imaging studies of FAD, this study has a number of novel features that provide insights into presymptomatic disease. Empiric evidence is provided of the value of assessing presymptomatic longitudinal rate of change in cortical thickness, rather than just cross-sectional measurement; of the potential predictive value of using a composite signature region; and that cortical signature thickness is related to cognitive performance even prior to symptom onset.

This study does however have a number of limitations. In the selection of our cortical signature, the regions to select from were restricted to those that had been identified previously in the literature as involved in FAD. Whilst such an approach has the potential to introduce bias, combining *a priori* information from the literature with an

independent data set can produce more robust results, with greater face-validity, when identifying specific features of interest (Chu et al., 2012). When using an SVM approach, as was done for part of the analysis in this study, a sample size such as the one used here (which is smaller than is ideal for this type of analysis) can potentially lead to over-fitting of the data (Falahati et al., 2014). The results from the SVM analysis should therefore be interpreted with caution. Future validation of the utility of the cortical signature would be valuable, ideally in a large cohort such as DIAN (Moulder et al., 2013). Also of interest would be a direct comparison between thinning patterns in familial and sporadic cases. If, as is likely, cortical losses reflect neuronal loss and dysfunction, the question is raised of whether there are compensatory cognitive mechanisms at play, given that many individuals are still asymptomatic despite damage. These findings therefore prompt consideration of more subtle cognitive tests to probe the consequences of these early losses (this is discussed further in chapter six).

3.7 Conclusion

FAD is characterized by cortical thinning that is detectable presymptomatically. Of the regions studied, the precuneus showed particularly early change. However, a composite signature of multiple vulnerable regions may provide more robust prediction of future decline, and closer correlation with preclinical cognitive change, than measuring a single region alone. Rates of thinning in the cortical signature became significantly abnormal about two years earlier than absolute cortical thickness. This imaging measure may have utility in presymptomatic trials.

3.8 Publications arising from this chapter

Data included in this chapter have been published in the following:

Weston, P. S., Nicholas, J. M., Lehmann, M., Ryan, N. S., Liang, Y., Macpherson, K., Modat, M., Rossor, M. N., Schott, J. M., Ourselin, S. & Fox, N. C. 2017. Presymptomatic cortical thinning in familial Alzheimer disease: A longitudinal MRI study. *Neurology*, 87, 2050-2057.

4 Microstructural cortical imaging: measurement of cortical mean diffusivity

4.1 Introduction

In the previous chapter, a disease-specific anatomical and temporal "signature" of early macrostructural cortical atrophy in FAD was identified. The finding that early neurodegeneration can produce a relatively consistent pattern of cortical loss, which can be measured using T_1-weighted MRI, is consistent with previous studies (Dickerson et al., 2009, Quiroz et al., 2013). Whilst assessment of cortical thickness allows detection of early change at the macrostructural level, DWI allows assessment at the microscopic level (Le Bihan, 2003), which may predate macrostructural changes atrophy such as that assessed by cortical thickness. Whilst most diffusion studies in AD have focused on white matter (Ringman et al., 2007), diffusion-weighted MRI of cerebral grey matter has been shown to differentiate patients with MCI from healthy controls (see section1.4.4), with the most significant difference occurring in the precuneus (i.e. the same region that also seems to show the earliest thinning) (Jacobs et al., 2013).

However, the current body of evidence to support the use of cortical diffusion measurement remains relatively small, with a number of methodological issues, particularly how to deal with partial volume effects, still outstanding. Partial volume effects are particularly important to account for in individuals who may also be undergoing macrostructual volume/thickness loss, as progressive loss of cortex may cause CSF (which has greater diffusivity than brain tissue) to occupy a higher proportion of many of the cortical voxels, which would artificially increase MD values in those voxels (see section 1.4.4.7). Moreover, the ability of DWI to detect

presymptomatic cortical changes, and to predict conversion to AD dementia, has not yet been established.

MD is a diffusion imaging metric that increases with microstructural breakdown, and has been used to investigate cortical integrity in both symptomatic AD and healthy aging (Lin et al., 2016, Elman et al., 2017). Unlike other DWI metrics, MD measures diffusion in all directions equally, and so should be well suited to measurement of diffusivity within the cortex where neurons are not thought to be aligned in any one specific direction and so diffusion is isotropic (unlike in white matter tracts).

In this study, the aim was to measure cortical MD in symptomatic and presymptomatic FAD mutation carriers, and compare them to non-carriers, to assess the earliest microstructural changes. A method was devised to correct for potential volume effects, which have been overlooked in most of the previous studies. Following on from the previous chapter, an ROI approach was taken, with the six cortical regions previously identified as showing the earliest macrostructural thinning thought to be the best candidates to detect early microstructural breakdown.

4.2 Hypothesis

- MD within the cerebral cortex can be measured in individuals with FAD, producing results with high face validity.
- Cortical MD increases presymptomatically in FAD within the regions identified as making up the FAD cortical signature, and correlates with early disease stage.
- Sensitivity to early microstructural cortical changes is improved by introducing a method for correcting for partial volume effects.

4.3 Contributions and collaborations

The study was conceived and designed by Professor N. Fox, Dr I. Simpson and the author. Participant recruitment and collection of imaging and clinical data was carried out by Dr N. Ryan, Dr Y. Liang and the author. Neuropsychology data were collected by Ms K Macpherson. Processing and analysis of the imaging data was performed by Dr M Lehmann, Dr N. Toussaint and the author. Dr G. Zhang provided advice regarding image analysis. The statistical analysis was planned by Ms T. Poole and the author, and then performed by Ms T. Poole (to prevent the author being unblinded to the genetic status of participants). SVM analysis was performed by the author, with assistance from Dr L. Harper. Interpretation of data and preparation of tables and figures was carried out by the author.

4.4 Methods

4.4.1 Participants

Seventy-seven participants were included, between April 2009 and June 2014, with 52 of them being from FAD families and 25 being healthy controls. Of those who came from FAD families, 17 already had progressive symptoms of FAD and 35 were asymptomatic but at 50% risk. A total of 27 different FAD families were represented. All participants underwent a neurological examination, neuropsychological assessment, and assessment with the CDR as outlined in chapter 2. EYO was calculated for all participants who came from FAD families as outlined in section 2.8.

4.4.2 MRI acquisition

All participants were scanned on the same 3-Tesla Siemens TIM Trio scanner using a 32-channel phased array head-coil. A sagittal 3D MP-RAGE T1-weighted volumetric MRI (echo time/repetition time/inversion time = 2.9/2200/900ms, dimensions of 256×256×208, voxel size of 1.1mm isotropic) was acquired. Two 64-direction diffusion-weighted image (DWI) sequences were acquired with a single shot, spin-echo echo planar imaging (EPI) sequence (field of view 240mm; matrix 96×96; yielding a voxel size of 2.5mm isotropic; 55 contiguous axial slices; repetition time: 6800 ms; echo time: 91ms; b-value: 1000s/mm^2). Nine acquisitions without diffusion weighting were also acquired (b=0s/mm^2).

4.4.3 Image analysis

Cortical parcellation was performed using Freesurfer v5.30 (http://surfer.nmr.mgh.harvard.edu) (Fischl and Dale, 2000). For the DWI, images were registered to the first B=0 image using niftyreg (Modat et al., 2014) and corrected for susceptibility (Daga et al., 2014), motion and eddy current distortion. The two DWI acquisitions for each participant were combined to increase the signal-to-noise ratio, with tensor fitting performed using the single tensor model, to produce MD maps.

As the method used (i.e. cortical MD measurement) is relatively new, and has not yet been validated to the same extent as cortical thickness, it was decided to perform cross-sectional analysis only, with one scan used from each participant.

4.4.4 Regions of interest analysis

We restricted our analysis to six *a priori* cortical regions of interest (ROI), based on those identified in the previous chapter as making up the FAD cortical signature. The

six regions are: entorhinal cortex, inferior parietal cortex, precuneus, superior frontal cortex, superior parietal cortex and supramarginal gyrus. Following cortical parcellation, the Freesurfer label for each ROI was warped into diffusion space and registered to the MD map, to allow extraction of mean MD within that region (figure 4-1).

Additionally, to reduce potential CSF-grey matter partial volume effects when calculating regional MD, a weighted mean was calculated, with the relative weighting given to each individual voxel depending on the degree of partial voluming within it. Weights were derived from interpolation of the T_1 space binarised label map towards the lower resolution diffusion space. For example, if eight adjacent voxels from the higher resolution T_1 space, six of which contained cerebral cortex and two of which contained CSF, were combined in to the same single voxel in the lower resolution diffusion space results, the weighting given would be 0.75 (as 75% of the T_1 space voxels contained cortical tissue). The MD results produced both with and without this partial volume correction were compared.

Cortical thickness for each region was calculated using the same procedure as described in chapter 3.

4.4.5 Statistical analysis

Following genetic testing, the asymptomatic at-risk individuals were split in to those who were presymptomatic mutation carriers and those who were non-carriers. The non-carriers were combined with the healthy controls that were recruited to form a non-carrier group. The presymptomatic mutation carriers were split at the median EYO (8.1 years) into an early presymptomatic (EPS) group and a late presymptomatic (LPS) group, resulting in a total of four subgroups: symptomatic; LPS; EPS; and controls.

Cortical MD was averaged across left and right hemispheres for the reported analyses. Linear regression was used to compare MD between the subgroups, with all models adjusting for age and gender. “Family” was included as a random effect to assess any impact of clustering within a family. Pairwise differences in means were then used to examine the evidence for a difference in MD between each pair of subgroups.

In mutation carriers, Spearman correlation coefficients were calculated to assess association between EYO and cortical MD in each of the ROIs, first across all mutation carriers and then in presymptomatic carriers only.

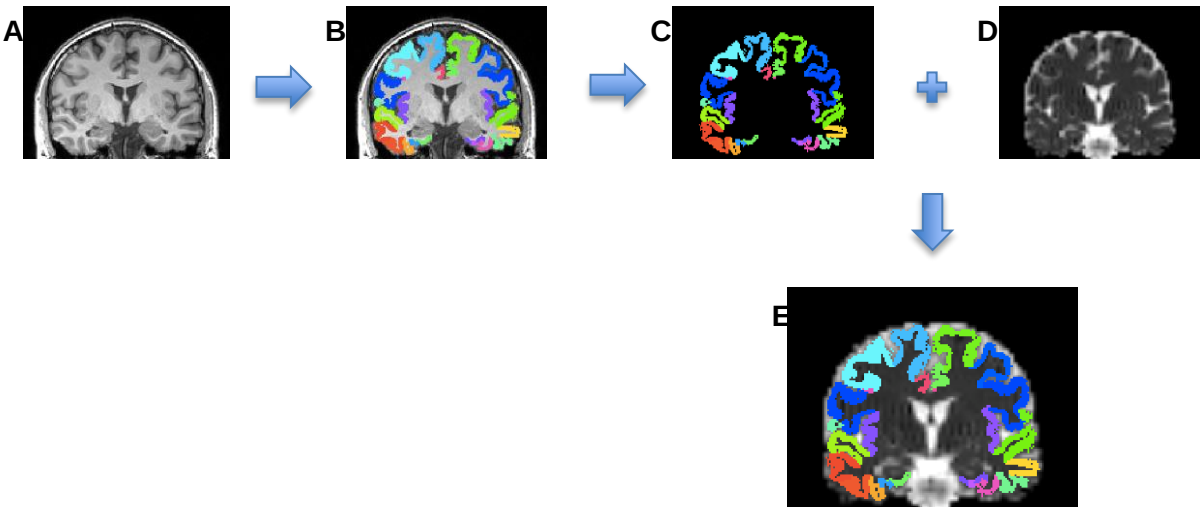

Figure 4-1. Cortical parcellation and measurement of cortical MD

Each T1 image (A) underwent cortical parcellation using Freesurfer (v5.30) (B). The Freesurfer label for each ROI was warped into diffusion space (C) and registered to the MD map (D) to allow extraction of mean MD within that region (E).

All of the above was done on both the partial volume corrected data and the non-partial volume corrected data. Investigation of how applying partial volume correction altered

the results was done by assessing pair-plots of each individual's mean cortical signature MD both before and after partial volume correction, and also performing Bland-Altman plot analysis (Bland and Altman, 1986).

Spearman coefficients were also calculated to assess the association in mutation carriers between cortical MD (corrected for partial volume) and cortical thickness.

4.4.6 Support vector machine analysis

Following the group-wise statistical analysis of MD, a linear SVM approach was used to assess how accurately, based on a single scan, measuring MD (with correction for partial volume) across the six cortical signature regions is able to predict whether an individual is a mutation carrier (and therefore has underlying AD pathology) or a non-carrier. The method used is the same as that described in section 3.3.6. Receiver operator curves (ROC) were produced for symptomatic individuals versus controls, all presymptomatic individuals versus controls, LPS only versus controls and EPS only versus controls; with the area under the curve (AUC) calculated for each contrast. SVC processing and analysis was performed using the Python libraries SciPy 0.14.0 and Scikit-Learn 0.15.2 (Pedregosa et al., 2011) on Python 2.7.6 – 64-bit.

4.5 Results

4.5.1 Participant demographics

Of the 35 at-risk participants, 21 were found to be mutation carriers. There were therefore a total of 38 participants with pathogenic FAD mutations (21 presymptomatic, 17 symptomatic) and 39 non-carriers. Participant demographics and clinical information are shown in table 4-1.

	Non-carriers	Early presymptomatic	Late presymptomatic	Symptomatic
N	39	10	11	17
Mean age, years (SD)	44.6 (9.5)	34.8 (5.5)	41.9 (8.4)	47.6 (9.0)
Gender, m/f	15/24	3/8	5/6	10/6
Mean EYO (SD)	-	11.8 (2.6)	3.3 (4.6)	-4.8 (4.0)
Mean global CDR (SD)	0	0	0	0.88 (0.38)

Table 4-1. Participant demographics and clinical characteristics

4.5.2 Cortical MD without partial volume correction

The analysis was first performed using MD data that had not been corrected for partial volume effects (table 4-2). After adjusting for age and gender, symptomatic individuals had significantly higher MD compared with controls in all six cortical regions ($p<0.001$). When comparing the LPS group with controls, there was a trend towards higher cortical MD in all six regions, although this reached statistical significance only in the inferior parietal cortex ($p=0.03$). No statistically significant differences in MD were found between the EPS group compared with controls. Allowing for clustering within a family had no impact on results.

Across all mutation carriers, a positive correlation was found between cortical MD and proximity to/from symptom onset (EYO) ($p=0.03$ for entorhinal cortex, <0.0001 in all other ROIs). When including presymptomatic individuals only, there remained a correlation between MD and EYO in the precuneus ($p=0.03$) but not in the other regions.

4.5.3 Cortical MD with partial volume correction

When the analysis was repeated, but this time using MD values adjusted for partial volume effects by applying a weighted mean, similar results were found, but with some differences. After adjusting for age and gender, symptomatic individuals had significantly higher MD compared with controls in all six cortical regions (p<0.001) (Fig. 4-3, table 4-2). When comparing the LPS group (late presymptomatic – i.e. nearer to expected onset) with non-carriers, there was a trend towards higher cortical MD in all six regions, reaching statistical significance in the inferior parietal cortex as previously, but this time with the group difference being more significant by an order of magnitude (p=0.003). In addition, significant group difference for LPS vs. non-carriers was also now seen for the precuneus (p=0.04). No statistically significant differences in MD were found between the EPS group (further from onset) compared with controls.

Across all mutation carriers, a positive correlation was found between cortical MD and proximity to/from symptom onset (EYO) (p<0.0001) in all ROIs except entorhinal cortex (where p=0.14). When including presymptomatic individuals only, there remained a correlation between MD and EYO in the precuneus (p=0.04) but not in the other regions.

	Mean MD (SD)				p-values for group differences (based on linear regression)			Correlation between MD and EYO, rho (p-value)	
	NC	EPS	LPS	Symp	EPS vs. NC	LPS vs. NC	Symp vs. NC	All MCs	PS only
Entorhinal	268 (18)	277 (20)	267 (27)	304 (33)	0.16	0.90	<0.0001	0.38 (0.03)	-0.38 (0.09)
Inferior parietal	272 (12)	271 (17)	280 (11)	323 (26)	0.21	0.03	<0.0001	0.77 (<0.0001)	0.29 (0.20)
Precuneus	284 (14)	279 (16)	292 (13)	336 (29)	0.66	0.08	<0.0001	0.84 (<0.0001)	0.47 (0.03)
Superior frontal	286 (16)	277 (11)	288 (15)	319 (22)	0.52	0.44	<0.0001	0.76 (<0.0001)	0.41 (0.06)
Superior parietal	298 (20)	292 (19)	301 (15)	302 (30)	0.53	0.24	<0.0001	0.75 (<0.0001)	0.33 (0.14)
Supra-marginal	284 (23)	273 (17)	284 (12)	328 (25)	0.96	0.33	<0.0001	0.76 (<0.0001)	0.15 (0.50)
Mean signature	282 (12)	278 (13)	286 (12)	325 (25)	0.44	0.16	<0.0001	0.80 (<0.0001)	0.20 (0.38)

Table 4-2. Cortical mean diffusivity measurement without correcting for partial volume effects

MD measurements (mean of left and right) are given for the six individual cortical signature regions, as well as a mean value for the six regions combined. No correction for partial volume effects has been made. Pairwise analysis of differences in group means are shown for each mutation carrier sub-group compared with non-carriers. Spearman correlation coefficients and corresponding p-values are shown for the association between cortical MD and EYO, across all mutation carriers and in presymptomatic carriers only. MD=mean diffusivitity; EYO=estimated years to/from onset; NC=non-carriers; EPS=early presymptomatic mutation carriers (i.e. EYO>8.1); LPS=late presymptomatic mutation carriers; symp=symptomatic mutation carriers; PS=presymptomatic.

	Mean MD (SD)				p-values for group differences (based on linear regression)			Association between MD and EYO, rho (p-value)	
	NC	EPS	LPS	Symp	EPS vs. NC	LPS vs. NC	Symp vs. NC	All MCs	PS only
Entorhinal	248 (17)	258 (15)	250 (21)	283 (34)	0.11	0.60	<0.0001	0.25 (0.14)	-0.43 (0.06)
Inferior parietal	263 (8)	264 (12)	273 (9)	309 (18)	0.15	0.003	<0.0001	0.74 (<0.0001)	0.28 (0.23)
Precuneus	273 (9)	269 (11)	281 (14)	317 (21)	0.91	0.04	<0.0001	0.80 (<0.0001)	0.46 (0.04)
Superior frontal	266 (9)	261 (7)	266 (12)	296 (19)	0.68	0.79	<0.0001	0.71 (<0.0001)	0.40 (0.07)
Superior parietal	278 (12)	277 (12)	284 (12)	319 (22)	0.51	0.15	<0.0001	0.75 (<0.0001)	0.32 (0.16)
Supra-marginal	268 (12)	265 (12)	272 (10)	308 (21)	0.78	0.31	<0.0001	0.70 (<0.0001)	0.11 (0.63)
Mean signature	266 (9)	266 (9)	271 (10)	305 (19)	0.36	0.11	<0.0001	0.75 (<0.0001)	0.16 (0.49)

Table 4-3. Cortical mean diffusivity measurement with weighted mean partial volume correction

MD measurements (calculated as a mean of left and right) are given for the six individual cortical signature regions, as well as a mean value for the six regions combined. Partial volume effects were (at least partially) corrected for by applying a weighted mean to each voxel in the analysis, based on the proportion of that voxel thought to contain cortical tissue vs. CSF. Pairwise analysis of differences in group means (based on linear regression) are shown for each mutation carrier sub-group compared with non-carriers. Spearman correlation coefficients and corresponding p-values are shown for the association between cortical MD and EYO, across all mutation carriers and in presymptomatic carriers only. MD=mean diffusivitity; EYO=estimated years to/from onset; NC=non-carriers; EPS=early presymptomatic mutation carriers (i.e. >8.1 years from predicted onset); LPS=late presymptomatic mutation carriers; symp=symptomatic mutation carriers; PS=presymptomatic.

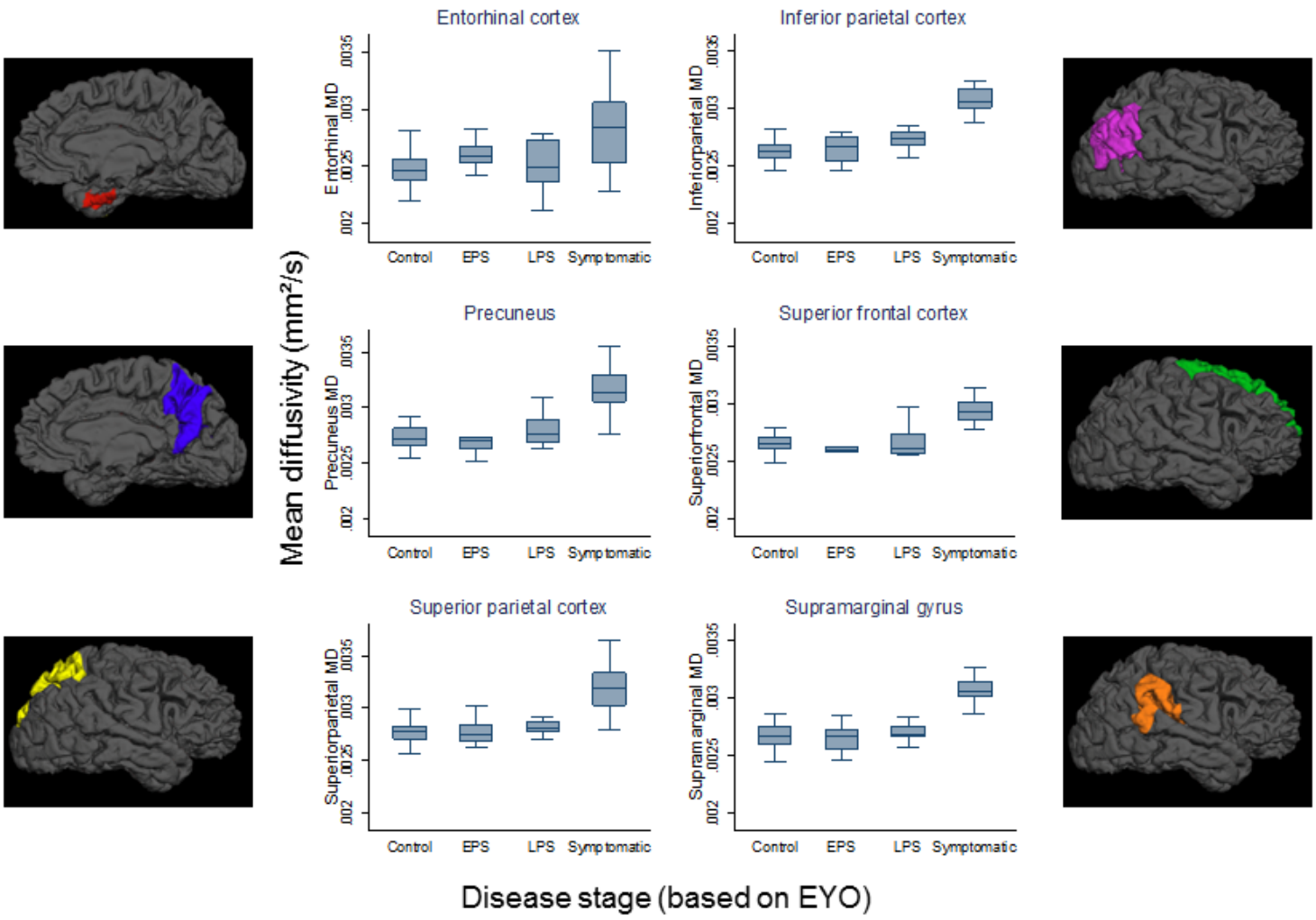

Figure 4-2. Box plots of cortical MD (with correction for partial volume effects) in the six cortical signature regions of interest across the different disease stages.

4.5.4 The effect of correcting for partial volume on MD values

Whilst results for cortical MD both before and after partial volume correction were generally similar, there were some significant differences. For all except one of the 77 participants, MD values were lower following partial volume correction (figure 4-3 A). Bland-Altman plot analysis (figure 4-3 B) showed that those individuals for whom the MD value changed most (i.e. the difference between the value obtained from one method and the other was greatest), were those individuals who had the highest initial (i.e. *uncorrected*) MD values; with the effect being that the MD was reduced after attempting to correct for partial volume.

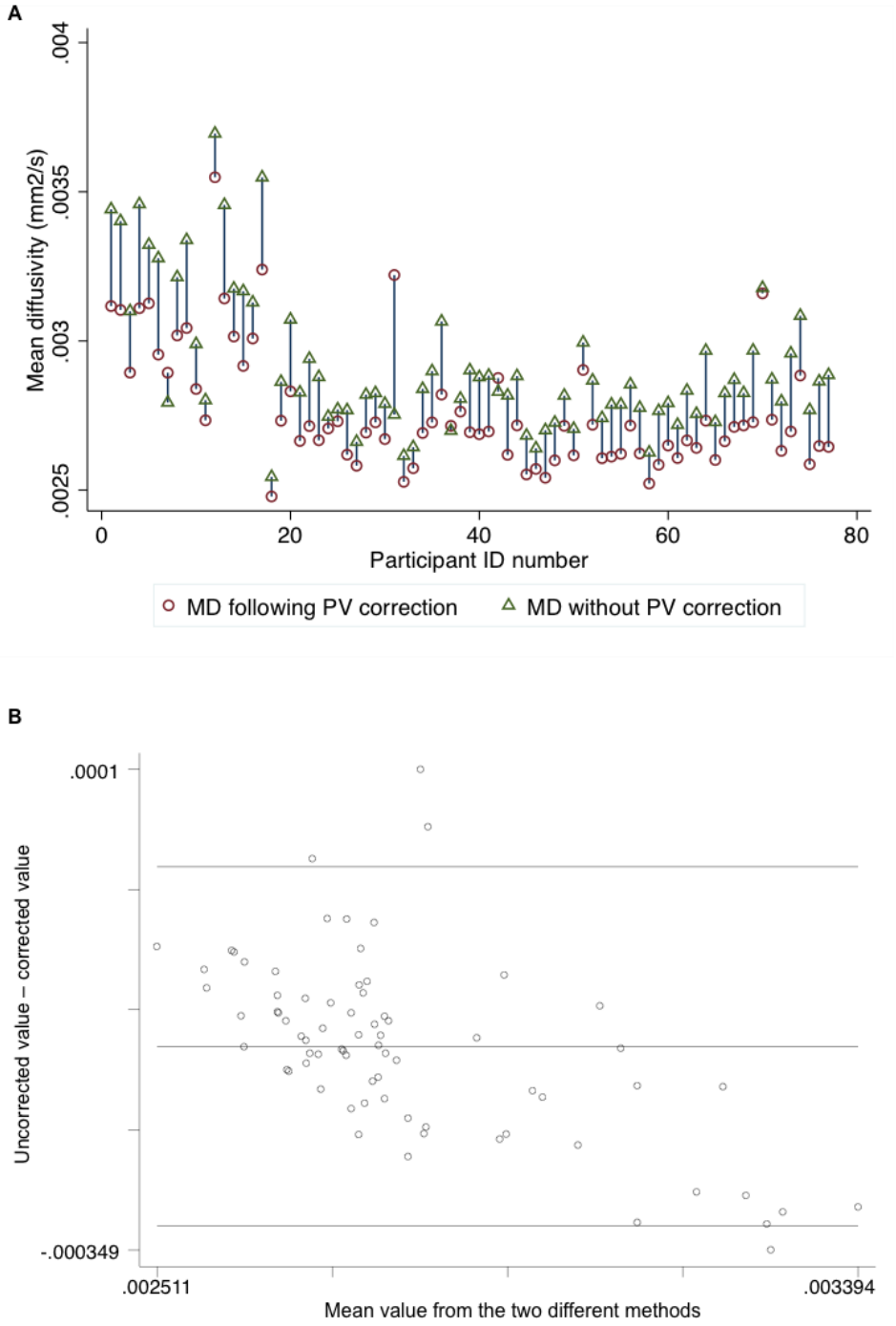

Figure 4-3. A comparison between MD values obtained with and without correcting for partial volume effects

A pair-plot of each participant's mean cortical signature MD, both before and after correction for partial volume effects. ***(B)*** *A Bland-Altman plot, with the three horizontal lines represent the mean +/- 1 SD difference between values. Partial volume correction altered the MD value most for those with the highest initial values.*

4.5.5 The association between cortical MD and cortical thickness

In mutation carriers, cortical MD demonstrated a significant correlation with cortical thickness (p<0.0001) in all ROIs except entorhinal cortex (p=0.240) (figure 4.4)

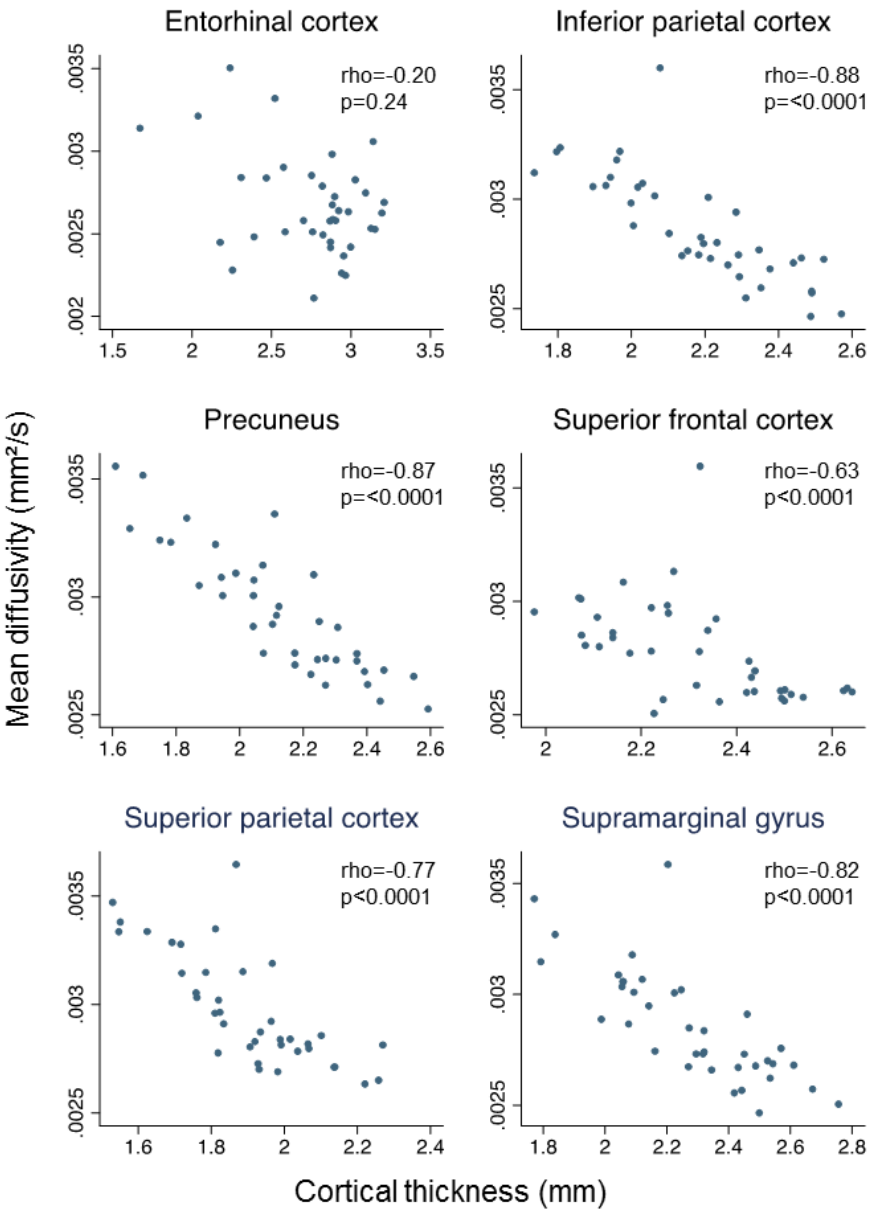

Figure 4-4. The association between cortical MD and cortical thickness

Scatter plots are shown, with accompanying Spearman coefficients, for the association between MD (corrected for partial volume) and cortical thickness in mutation carriers.

4.5.6 Assessing the utility of cortical MD thickness in predicting diagnostic group in individual people

Based on a single scan per participant, the cortical MD measurement (with partial volume correction) within the cortical signature regions was able to differentiate AD from non-AD relatively accurately in symptomatic participants versus controls (AUC=0.82, 95% CI 0.58-0.93). When looking at all presymptomatic individuals versus controls, the AUC was 0.44 (0.26-0.65). When the presymptomatic group is divided in to LPS (EYO < 8) and EPS (EYO > 8) we see AUCs of 0.59 (0.32-0.81) and 0.57 (0.31-0.79) respectively (figure 4-5).

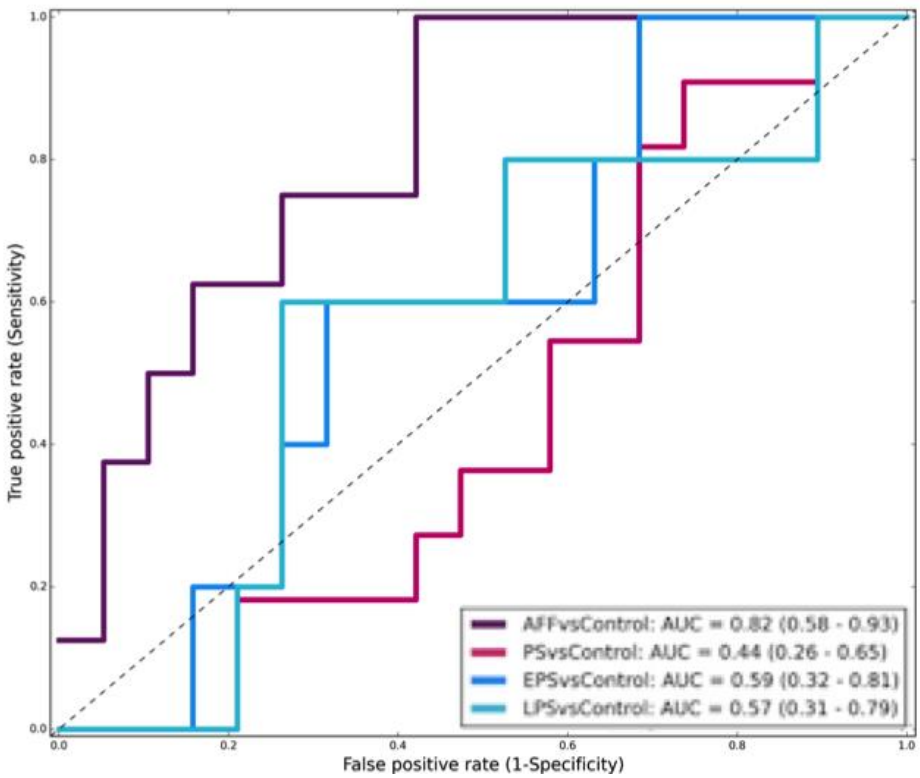

Figure 4-5. Predicting diagnostic group in individual people

Receiver operating curves (ROC) show the results of a support vector machine analysis to assess the accuracy with which cortical MD within the six cortical signature regions is able to predict whether an individual is a mutation carrier or a non-carrier, at various different disease stages. Curves are shown for clinically affected individuals (AFF) versus controls; all presymptomatc individuals versus controls; EPS versus controls; and LPS versus controls. ROC=receiver operator curves; AFF=affected; PS=presymptomatic (all); LPS=late presymptomatic; EPS=early presymptomatic.

4.6 Discussion

The main findings of this study were that asymptomatic FAD mutation carriers, on average 3.3 years from predicted symptom onset, have significantly increased cortical MD compared with controls, in precuneus and inferior parietal cortex. Furthermore, among mutation carriers as a group, cortical MD correlates with proximity to expected symptom onset, but when looking in presymptomatic carriers only this is only true for the precuneus.

It has previously been shown that using DWI to measure cortical diffusivity provides a means of separating patients with MCI and AD dementia from controls (Jacobs et al., 2013, Scola et al., 2010, Rose et al., 2008). Here we replicate this finding, in a group of symptomatic individuals who on average are only mildly clinically affected (mean CDR = 0.88). We also extend these findings to show that cortical diffusivity changes are identifiable in presymptomatic FAD a number of years before the onset of cognitive symptoms.

Of the six ROIs, the most significant presymptomatic MD changes were seen in the inferior parietal cortex and precuneus. Both of these regions have been identified as being affected early in symptomatic AD (Bakkour et al., 2009), with a previous study of cortical diffusivity in MCI showing the precuneus to undergo the most significant change (Jacobs et al., 2013). Studies of cortical thickness have also identified both of these regions as undergoing early thinning (Benzinger et al., 2013). The finding of early change in the precuneus is also consistent with the findings of the previous chapter, which showed the precuneus to undergo early thinning.

One previous much smaller study also investigated cortical diffusivity change in presymptomatic FAD (Fortea et al., 2010). However, while they too found changes in

the precuneus, they observed a fall in MD rather than an increase. The authors speculated that this may indicate a presymptomatic inflammatory process (similar to the findings of presymptomatic increased thickness discussed previously). Here, in a larger sample, we find no conclusive evidence to support an early MD reduction (although we did see nominal but non-significant increases in MD in the early presymptomatic period in four of the six regions), with the MD rise we observe being consistent with what one would expect to see during a neurodegenerative process. However, as with the cortical thickness finding, the possibility that MD may reduce in the earliest presymptomatic phase before rising as individuals approach symptom onset cannot be excluded.

The one region in which MD did not show significant correlation with disease progression was the entorhinal cortex, where there was greater inter-individual variability in MD than for other regions (Fig. 4-2). The anatomical location of the entorhinal cortex, which can make it more difficult to accurately parcellate, may mean that its MD signal is particularly vulnerable to CSF contamination, which could explain the greater variability. When looking in presymptomatic participants only, the association between entorhinal cortex MD and EYO, although not reaching statistical significance, was in the opposite direction to the trend seen in the other five regions measured, in that MD appeared to go down with increasing proximity to onset. This anomaly may again be due to issues regarding accurate parcellation, or alternatively could point to a presymptomatic reduction in MD (in entorhinal cortex only), as discussed above.

An additional way in which this study advances on many of the previous studies of cortical diffusion changes, is the effort made to correct, at least in part, for the effects of partial voluming. By moving from high resolution T_1-space to the much lower resolution DWI space, with voxels not much thinner than the cortex itself, a degree of partial

volume is inevitable. As the cortex interfaces with CSF, where diffusion is significantly freer, any CSF contamination of DWI cortical voxels could cause significant alteration to the measured MD. A weighted mean was therefore applied to mitigate any such effect, with the effect being that the average MD was reduced, particularly in those voxels that had the highest MD to begin with (i.e. those that were likely to have been most influenced by CSF contamination). The fact that we saw a significant presymptomatic MD increase in more regions after correction for partial volume would imply that the MD signal we were measuring was not simply a proxy measure of CSF contamination, but rather an actual biological change in the cortical tissue (likely due to microstructural cellular breakdown). This adds validity to both the method and the results.

A close association was found between cortical MD and cortical thickness in the mutation carriers for the majority of the regions assessed. This provides further face-validity for cortical MD being a feasible marker of cortical degeneration, with both reduction in thickness and increasing MD likely being part of the same pathological continuum.

Microstructual changes such as MD, which indicate loss of neuronal integrity, may lie upstream to macrostructural volume and thickness changes (Ringman et al., 2007, Muller et al., 2005), and so could provide an earlier measure of change; however further studies, ideally with longitudinal assessment, will be required to confirm this. The study in the previous chapter, which measured cortical thickness, used a different statistical approach (i.e. longitudinal mixed effects modeling) to the study of cortical MD, meaning that it is difficult to directly compare the results. However, it would be reasonable to say that the current cortical MD results do not appear to offer a clear improvement in terms detecting early change, compared to cortical thickness. Indeed, when looking at the results of the SVM analysis, unlike in the cortical thickness study,

cortical MD does not seem to be able to identify an individual person's diagnostic group at a level any better than chance, other than for those who are already symptomatic. As mentioned in the previous chapter, the results of any such SVM analysis, particularly in sample sizes such as those used in the imaging studies reported, do have to be interpreted with a degree of caution (Falahati et al., 2014). However as it stands, cortical MD measurement, whilst providing promising group level results for what is a relatively novel approach, is likely to require further study and development (as was done previously with cortical thickness), before its use can be recommended above cortical thickness measurement for the reliable detection of early neurodegenerative change. However it may well be that, rather than choosing one or the other, the best results may come by using both cortical thickness measurement and cortical MD measurement in combination, with it having been suggested that the two provide different but complimentary information (Elman et al., 2017).

This study has a number of limitations. While steps were taken to minimise the effects of partial volume, this cannot be eliminated completely. The study used only cross-sectional data. One key limitation with regards to DWI in general, is that previous studies have found its test-retest reliability to be sub-optimal, particularly with regards to (relatively isotropic) grey matter, which is perhaps the reason that no DWI approach of any form has so far entered widespread clinical trial use. Assessing and refining the test-retest reliability of cortical MD measurement, and its ability to reliably track longitudinal change, will be important. The use in future studies of more advanced diffusion imaging acquisition methods, such as multi-shell acquisitions, would reduce this issue significantly by allowing modelling within each voxel of each separate tissue type (i.e. intraneuronal, extraneuronal and CSF) (Zhang et al., 2012). As with many FAD studies, the sample size is relatively modest, primarily due to the rarity of the disease. However, this is the largest DWI study of presymptomatic FAD to date.

4.7 Conclusion

Measurement of cortical MD provides consistent and biologically plausible results. Cortical MD measurement was able to detect presymptomatic microstructural breakdown, which may precede later macrostructural atrophy, or provide complementary information. Measurement of cortical MD, particularly within the precuneus and inferior parietal cortex, may have potential as a method for detecting early change, and may prove useful in future AD prevention trials, both in terms of identifying those at risk of symptom onset and as a complementary measure of progression. However, whilst the findings are encouraging, significant further work is required to further develop and validate this method, and to understand the biological implications of the findings.

5 A blood-based biomarker of early neurodegeneration: serum neurofilament-light

5.1 Introduction

Detection of early AD pathogenic change has until now largely relied on either cerebrospinal fluid (CSF) analysis or neuroimaging. However, criteria for the ideal AD biomarker include being minimally invasive, inexpensive, and simple to acquire (Disease", 1998); which it could be argued current markers do not fulfill. Blood-based biomarkers offer greater convenience and patient acceptability, but have proven more challenging than CSF measures for several reasons, including much lower blood concentration of the target analyte making reliable quantification more difficult. Recent systematic reviews were not able to identify any blood biomarkers with utility in early disease (Olsson et al., 2016, Henriksen et al., 2014).

One promising neurodegeneration biomarker in CSF is neurofilament light (NfL) (Zetterberg et al., 2016). NfL can also be detected in serum using standard immunoassay formats (Gaiottino et al., 2013, Bacioglu et al., 2016) but control samples and many disease samples have concentrations below the analytical sensitivity of these methods (Kuhle et al., 2016). We therefore used a recently developed immunoassay based on the Single molecule array (Simoa) technique that allows quantification down to subfemtomolar concentrations (below 1 pg/mL) of the analyte (Rissin et al., 2010), and is 25-fold as sensitive as the previous electrochemiluminescence-based method for NfL (Kuhle et al., 2016). Serum NfL concentrations derived using Simoa correlate closely with CSF concentrations and are increased in HIV-associated dementia, PSP and FTD (Gisslen et al., 2016, Rojas et al., 2016, Rohrer et al., 2016).

In this study serum NfL concentration was measured in FAD mutation carriers (both symptomatic and presymptomatic) and mutation negative relatives, and NfL concentrations between the groups compared. We also assessed, in mutation carriers, the association between serum NfL concentration and EYO (a proxy marker of disease stage), and the association between NfL and various cognitive and imaging measures of disease severity, before and after the onset of symptoms.

5.2 Hypothesis

- With the more sensitive assay, serum NfL concentration would be elevated in mutation carriers compared to healthy non-carriers prior to symptom onset.
- Serum NfL would correlate with markers of disease stage and severity.

5.3 Contributions and collaborations

The study was performed in collaboration with Professor H Zetterberg and Professor K. Blennow (University of Gothenburg). The study was conceived by Professor N. Fox, Professor H. Zetterberg and the author. Participant recruitment and collection of blood and imaging and clinical data were carried out by Dr N Ryan, Dr Y Liang and the author. Neuropsychology data were collected by Ms K Macpherson and Ms E Donnachie. Processing of serum samples to measure serum NfL was overseen by Zetterberg and Professor K. Blennow. Processing of imaging data was overseen by Dr I. Malone. The statistical analysis was planned by Ms T Poole and the author, and then performed by Ms T. Poole (to prevent the author being unblinded to the genetic status of participants). Interpretation of data and preparation of tables and figures was carried out by the author.

5.4 Methods

5.4.1 Study design and participants

Forty-eight participants, recruited between 2010 and 2015 were included in the study. Eighteen participants had symptomatic FAD and 30 individuals were asymptomatic but, by virtue of having an affected parent, were at 50% risk of developing symptomatic disease in the future. No additional healthy controls not from FAD families were included, as blood samples were not routinely collected from these people. For all participants, blinded genetic testing was performed to determine the presence or absence of a mutation as described in sections 2.2 and 2.7.

As outlined in section 2, each participant underwent blood sampling for collection of serum, MRI, neurological assessment (including a separate in interview with a close friend or relative), and neuropsychological assessment. For each participant all assessments were done within four months of blood sample collection. The neuropsychological assessments included in the analysis were the WASI, the NART (a measure of predicted premorbid IQ), RMT for faces and words, the MMSE, and the CDR. As previously, EYO was calculated as described in section 2.8. Individuals were defined as symptomatic if the global CDR was >0 and consistent symptoms of cognitive decline were reported by the participant and/or their informant.

5.4.2 Measurement of serum NfL concentrations

Serum samples were collected, processed, aliquoted and frozen at −80°C according to standardized procedures. Serum NfL concentrations were measured using the same

monoclonal antibodies and bovine NfL calibrator as in the NF-Light assay from Uman Diagnostics (UmanDiagnostics, Umeå, Sweden), transferred onto the Simoa platform as described previously (Rohrer et al., 2016). The lower limits of detection and quantification, as defined by the concentration derived from the signal of blank samples (sample diluent) + 3 and 10 standard deviations, were 0.97 and 2.93 pg/mL, respectively. For a QC sample with a concentration of 13.0 pg/mL, repeatability was 14.0% and intermediate precision was 15.7%. For a QC sample with a concentration of 131.8 pg/mL, repeatability was 13.3% and intermediate precision was 13.3%. All measurements were performed by board-certified laboratory technicians in one round of experiments using one batch of reagents.

5.4.3 MRI acquisition and analysis

MR imaging was obtained on 43 of the 48 participants at the time of the blood sample. For the five participants for whom a scan was not obtained, this was due to either the participant declining to have a scan or an inability to tolerate the scan (e.g. claustrophobia). For 33 of the 43 participants who had an initial scan, a second MRI scan was performed at a separate visit (mean interval ± SD=1.3 ± 0.46 years), with the other ten individuals not having a second scan due to either leaving the study (n=5) or data collection finishing prior to their second scan date (n=5).

All scans were performed on the same 3T Siemens TIM Trio scanner using a 32-channel phased array head-coil. A sagittal 3D MP-RAGE T1-weighted volumetric MRI (echo time/repetition time/inversion time = 2.9/2200/900 ms, dimensions of 256×256×208, voxel size 1.1×1.1×1.1 mm) was acquired. Images were visually checked for artifacts. Four of the baseline scans and two of the follow-up scans were excluded due to either movement or metallic dental artifact, with a total of 39 scans

being available for baseline volume measurements and 30 pairs of scans for rates of atrophy measurements. Whole brain, ventricular, and hippocampal volumes were calculated using semi-automated methods (Freeborough et al., 1997). For ventricles and hippocampi, measurements from both right and left hemispheres were averaged to give a mean value. All volumes were corrected for TIV by dividing a participant's volume by their TIV and multiplying by the group mean TIV. Annualized rates of brain, ventricular, and hippocampal volume change during the inter-scan interval were calculated using the boundary shift interval (BSI) – a registration-based measure of within-subject volume change (Freeborough and Fox, 1997).

5.4.4 Statistical analysis

The primary objective of the study was to compare serum NfL between symptomatic mutation carriers, presymptomatic mutation carriers, and non-carrier controls. A generalised least squares linear regression model, an extension of the t-test/ANOVA model that allows different group-specific residual variances, was used to compare NfL between the groups, adjusting for age and gender. "Family" was included as a random effect to assess any impact of clustering within a family.

Spearman correlation coefficients were calculated to assess the association between NfL and EYO, first across all mutation carriers and then in presymptomatic carriers only and symptomatic carriers only. This rank-based approach, which can be used with bounded variables and is less sensitive to non-normality and outliers, was also used for NfL and cognitive measures, including estimated change in IQ (WASI IQ minus NART-predicted premorbid IQ), recognition memory (an average of scores from RMT faces and RMT words), MMSE and CDR SOB. Associations between NfL and the MRI measures were also assessed. For each association, we first calculated the Spearman

correlation coefficient using all available data points, and then repeated it using data from only those individuals who completed all assessments.

Spearman correlation coefficients between EYO and each cognitive and imaging measure were calculated, including only presymptomatic participants. To allow results to be comparable, these analyses were done using only individuals with all available data points. For all analyses, missing values were assumed to be missing completely at random.

5.5 Results

5.5.1 Participant demographics

Participants' demographic details, cognitive scores, neuroimaging measures, and serum NfL values are shown in table 5-1 and figure 5-1. Of the asymptomatic participants, 19 were mutation carriers and 11 were non-carriers; with non-carriers used as healthy controls. The mean EYO of the presymptomatic mutation carriers was −9.6 years.

5.5.2 Comparing NfL between groups

Adjusting for age, gender, serum NfL concentration was significantly higher in symptomatic mutation carriers compared with presymptomatic mutation carriers (estimated difference in means 23.2pg/mL, 95% CI 13.1−33.2; $p<0.0001$) and with non-carrier controls (29.2pg/mL, 19.3−39.1; $p<0.0001$). Presymptomatic mutation carriers had significantly higher NfL concentrations than non-carriers (6.1pg/mL, 1.6−10.5, $p=0.007$). Allowing for clustering within a family had no impact on the results.

	Non-carriers	Presymptomatic carriers	Symptomatic carriers
N	11	19	18
Age, years (SD)	38.9 (9.5)	36.0 (5.7)	46.6 (9.3)
Gender, m/f	3/8	10/9	13/5
EYO, years	–	–9.6 (5.5)	+3.4 (3.3)
MMSE /30 [IQR]	30.0 [30.0, 30.0]	29.0 [29.0, 30.0]	20.0 [19.0, 27.0] (n=17)
Global CDR	0 [0, 0]	0 [0, 0]	0.5 [0.5, 1.0] (n=16)
CDR SOB	0 [0, 0]	0 [0, 0]	3.75 [2, 4.75] (n=16)
NART predicted IQ	101.0 (7.1) (n=10)	97.3 (11.9)	98.8 (13.9) (n=13)
WASI IQ	110.1 (10.2) (n=10)	98.7 (10.4)	85.7 (20.0) (n=13)
Estimated change in IQ (WASI-NART)	9.1 (8.0) (n=10)	1.4 (2)	–13.2 (14.2) (n=13)
Combined RMT average/50	46.5 [45.5, 47.5] (n=10)	44.5 [41.5, 47.0]	38.0 [32.0, 41.0] (n=13)
Baseline brain vol. (corrected for TIV), mL	1230 (56) (n=9)	1220 (67) (n=17)	1110 (59) (n=13)
Rate of whole brain atrophy, %/year	0.1 (0.4) (n=8)	0.1 (0.7) (n=13)	1.3 (1.6) (n=9)
Baseline ventricular vol. (corrected for TIV), mL	10.5 (5) (n=9)	13.2 (7.5) (n=17)	24.3 (9.2) (n=12)
Rate of change in ventricular vol., %/year	0.6 (6.5) (n=8)	1.3 (5.6) (n=13)	16.4 (10.5) (n=9)
Baseline hippocampal vol. (corrected for TIV), mL	2.8 (0.3) (n=8)	3.0 (0.2) (n=17)	2.5 (0.3) (n=12)
Rate of hippocampal atrophy, %/year	1.0 (0.1) (n=8)	0.6 (1.5) (n=13)	3.9 (2.5) (n=8)
Serum NfL, pg/mL	12.7 (7.2)	16.7 (7.7)	46.0 (20.8)

Table 5-1. Participant demographics, cognitive test scores, imaging measures and serum NfL concentration

All values are group means (with SD), except for constrained variables (MMSE, global CDR, CDR SOB and combined RMT), which are shown as median (with interquartile range). Measures are uncorrected for any covariables. For variables with missing data points, the number of observations is shown underneath the group average value (e.g. n=x). EYO=estimated years from onset. MMSE=Mini-Mental State Examination. CDR=Clinical Dementia Rating Scale. SOB=sum of boxes. NART=National Adult Reading Test. WASI=Wechsler Abbreviated Scale of Intelligence. RMT=Recognition Memory Test. TIV=Total intracranial volume. Estimated change in IQ was calculated by subtracting the current IQ (measured by the WASI) from the predicted premorbid IQ (measured by the NART).

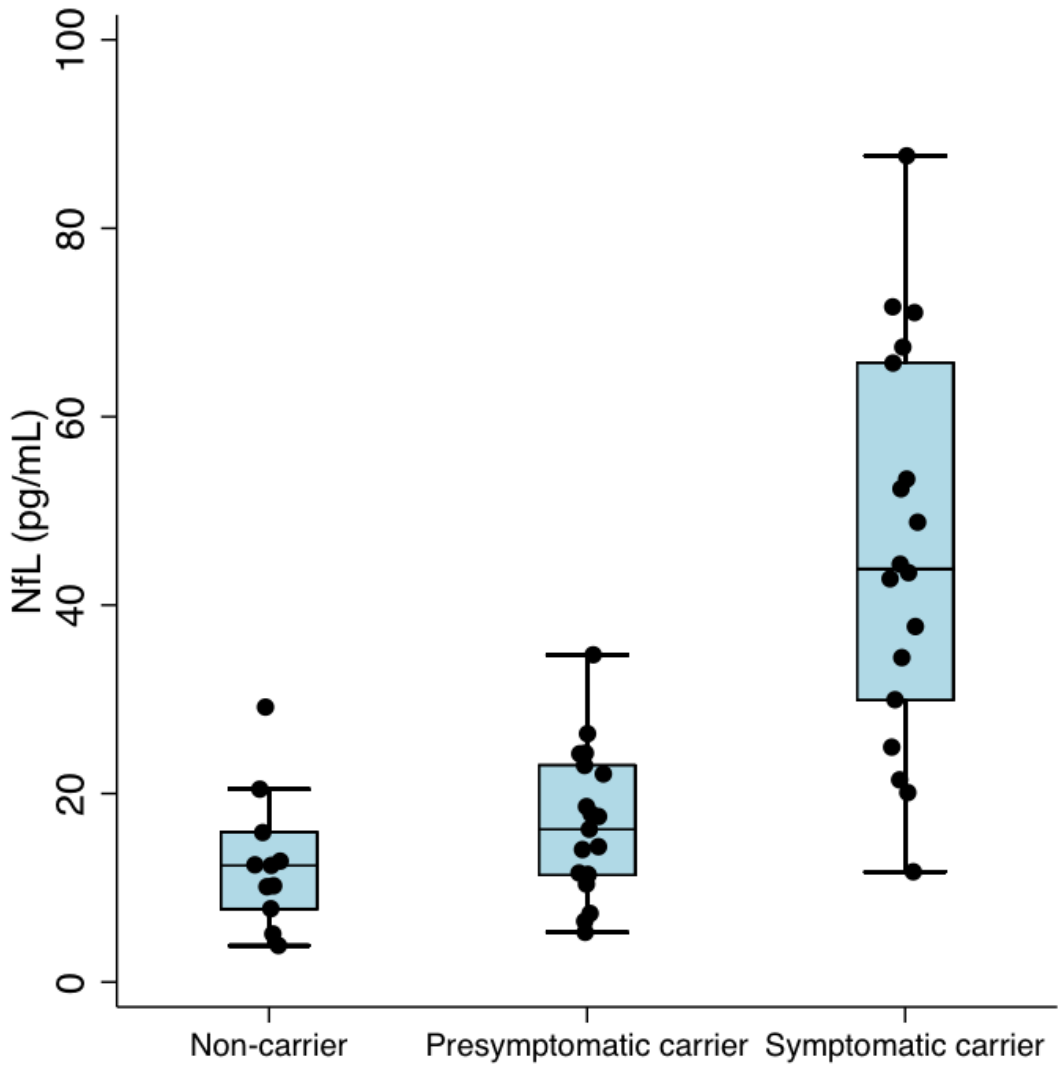

Figure 5-1. Box and whisker plots for serum NfL across the three groups

Mutation carriers have been divided into those who are symptomatic and those who are presymptomatic. Adjusting for age, gender, and allowing for within family clustering, serum NfL concentrations were higher in symptomatic mutation carriers compared with presymptomatic mutation carriers ($p<0.0001$) and non-carrier controls ($p<0.0001$). Presymptomatic mutation carriers had higher NfL concentrations than non-carriers ($p=0.007$).

5.5.3 Associations with measures of disease stage and severity

Across all mutation carriers, serum NfL concentrations correlated with EYO (Spearman's rho=0.81, p<0.0001), as illustrated in figure 5-2. Furthermore, this correlation was significant when calculated separately for both the presymptomatic (rho=0.55, p=0.01) and symptomatic (rho=0.49, p=0.04) groups.

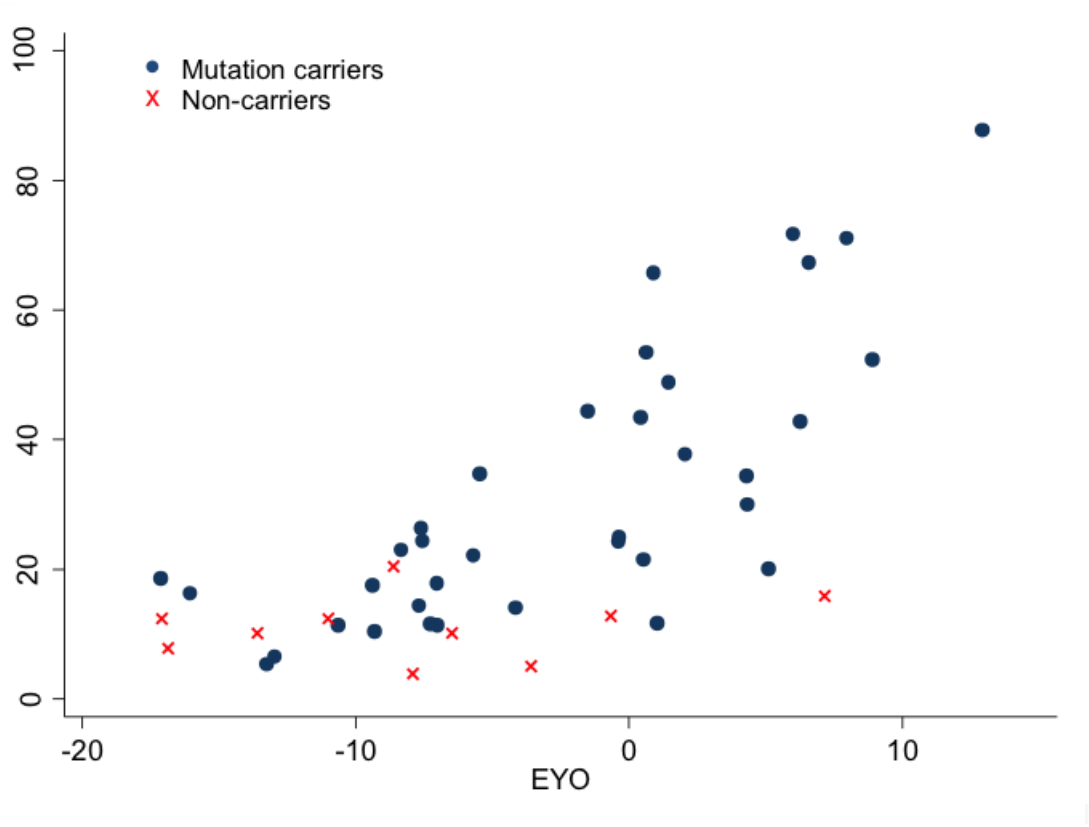

Figure 5-2. Scatter plot of serum NfL against EYO

Mutation carriers are represented by dots, and non-carriers by crosses. To ensure it is not possible to identify any of the individual asymptomatic participants (based on their EYO) and so determine their mutation status, two outlying participants have been removed and a jitter of up to +/– 2 years has been applied to all remaining participants.

Figure 5-3 shows scatter plots of serum NfL against different cognitive and imaging measures for all mutation carriers, with NfL concentration showing a relatively continuous distribution throughout the spectrum of disease severity. There were significant correlations between serum NfL and cognitive measures, including MMSE (rho=−0.62, p=0.0001), CDR SOB (rho=0.79, p<0.0001), and estimated change in IQ (rho=−0.48, p=0.005), with weak evidence for a correlation with recognition memory score (rho=−0.34, p=0.06). In mutation carriers, there was a significant correlation between NfL and cross-sectional neuroimaging measures, including baseline brain volume (rho=−0.62, p=0.0002), baseline ventricular volume (rho=0.56, p=0.002), and baseline hippocampal volume (rho=−0.54, p=0.003). There was also a significant correlation between serum NfL and subsequent rate of change in both brain volume (rho=0.53, p=0.01) and ventricular volume (rho=0.60, p=0.003); there was a non-significant trend for correlation with rate of change in hippocampal volume (rho=0.37, p=0.09). Repeating the analysis including data only from individuals who completed all assessments (i.e. no missing data) did not lead to material change in results, other than for the correlation between NfL and combined RMT (p-value changed from 0.06 to 0.6).

When including presymptomatic participants only, there was weak evidence of a significant correlation between NfL and baseline ventricular volume (rho=0.43, p=0.08) and between NfL and CDR SOB (rho=0.40, p=0.08), but no evidence of correlations with any other neuroimaging or cognitive measures.

When including only the 13 presymptomatic individuals who also had serial imaging, there remained a significant correlation between serum NfL and EYO (rho=0.73, p=0.005). However, when assessing the correlations between each of the six imaging

measures and EYO in the same individuals, none were statistically significant (table 5-2).

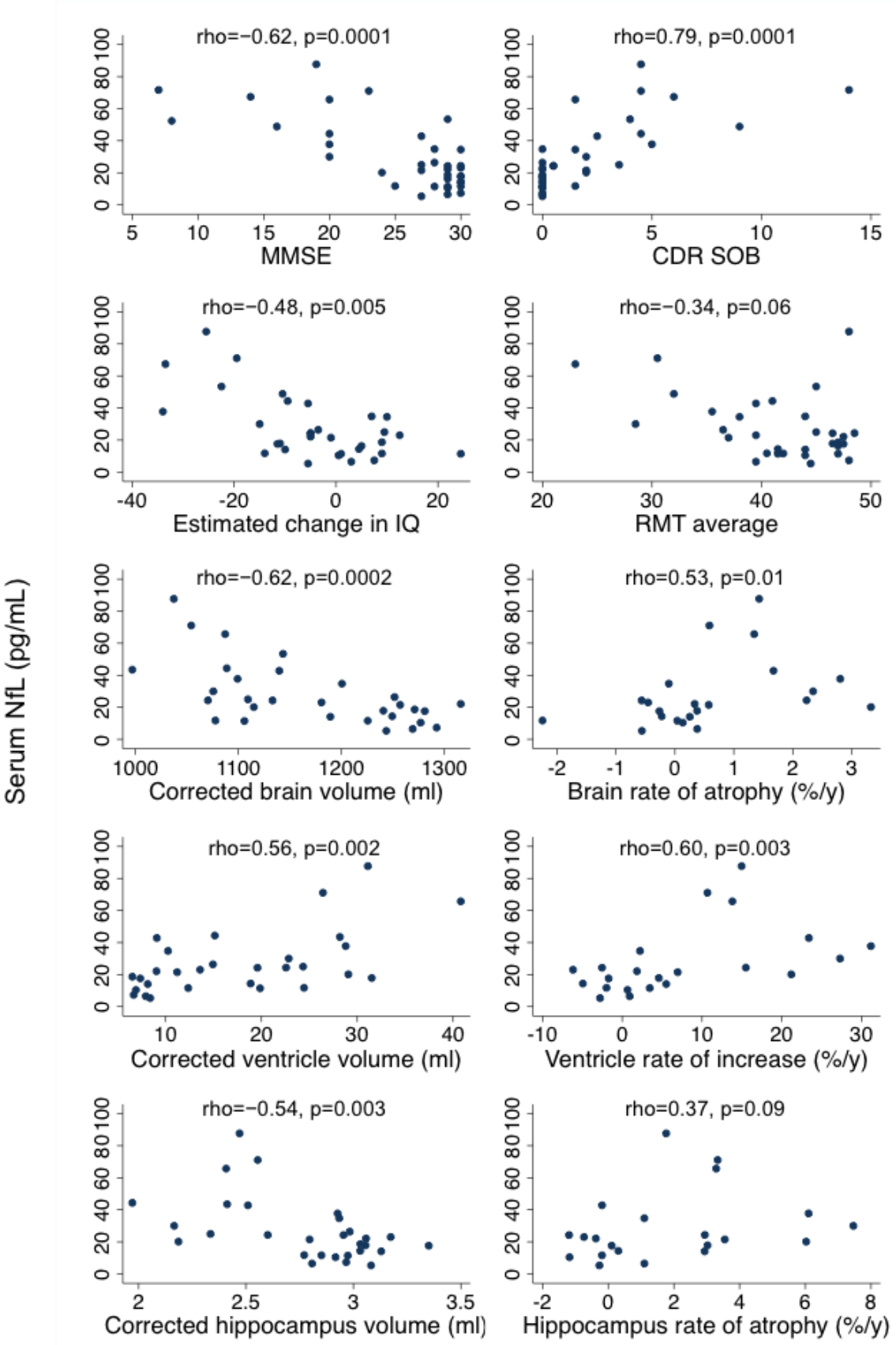
Serum NfL (pg/mL)
rho=−0.62, p=0.0001
MMSE
rho=0.79, p=0.0001
CDR SOB
rho=−0.48, p=0.005
Estimated change in IQ
rho=−0.34, p=0.06
RMT average
rho=−0.62, p=0.0002
Corrected brain volume (ml)
rho=0.53, p=0.01
Brain rate of atrophy (%/y)
rho=0.56, p=0.002
Corrected ventricle volume (ml)
rho=0.60, p=0.003
Ventricle rate of increase (%/y)
rho=−0.54, p=0.003
Corrected hippocampus volume (ml)
rho=0.37, p=0.09
Hippocampus rate of atrophy (%/y)

Figure 5-3. Scatter plots of serum NfL against cognitive and imaging measures across all mutation carriers

Spearman's rho and the associated p-vale are shown for each scatter plot. EYO=estimated years from onset. MMSE=Mini-Mental State Examination. CDR SOB=Clinical Dementia Rating Scale sum of boxes. RMT=Recognition Memory Test. TIV=Total intracranial volume. Estimated change in IQ was calculated by subtracting the current IQ (measured by the Wechsler Abbreviated Scale of Intelligence) from the predicted premorbid IQ (measured by the National Adult Reading Test).

Correlation between EYO and:	Spearman's R	p-value
Serum NfL	0.73	0.005
MMSE	0.09	0.8
CDR SOB	0.51	0.07
Estimated change in IQ	–0.23	0.5
Average RMT	0.52	0.07
Baseline brain volume (corrected for TIV), mL	–0.43	0.1
Rate of whole brain atrophy, %/year	0.09	0.8
Baseline ventricular vol., (corrected for TIV), mL	0.36	0.2
Rate of change in ventricular vol., %/year	0.52	0.07
Baseline hippocampal vol., (corrected for TIV), mL	–0.07	0.8
Rate of hippocampal atrophy, %/year	0.18	0.6

Table 5-2. Presymptomatic correlations between biomarkers and EYO

Spearman correlation coefficients for serum NfL, cognitive test scores, and imaging measures against EYO, in presymptomatic participants only. To allow for direct comparisons between the different measures, only the 13 presymptomatic mutation carriers for whom serum NfL and serial imaging measures were available are included. EYO=estimated years from onset. MMSE=Mini-Mental State Examination. CDR SOB=Clinical Dementia Rating Scale sum of boxes. RMT=Recognition Memory Test. TIV=Total intracranial volume. Estimated change in IQ was calculated by subtracting the current IQ (measured by the WASI) from the predicted premorbid IQ (measured by the NART).

5.6 Discussion

Using a recently developed, ultrasensitive immunoassay, this study shows show that serum NfL concentrations are increased in symptomatic FAD mutation carriers, in a group of individuals who are only mildly clinically affected (median CDR=0.5); we also found increased NfL concentrations in presymptomatic individuals who were on average nine years from their predicted symptom onset. Serum NfL correlated significantly with the estimated years to/from symptom onset (EYO) across all mutation carriers, as well as in the symptomatic and presymptomatic groups separately (although figure 5-2 shows clearly that the relationship is less pronounced in the presymptomatic disease phase than the symptomatic disease phase).

Across all carriers, serum NfL also correlated with CDR SOB and several cognitive measures. There was also a correlation between serum NfL and MRI measures of AD-related neurodegeneration, both in terms of cross-sectional volume loss and subsequent rates of atrophy. This suggests serum NfL concentrations may relate to disease severity and/or rate of progression.

The serum NfL concentrations measured in symptomatic FAD are similar to those in previous studies of sporadic AD (Gaiottino et al., 2013, Bacioglu et al., 2016). However, the current study extends on previous findings by showing for the first time that measurable increases in serum NfL precede the onset of symptomatic disease, and are correlated with predicted time to symptom onset. The observed progressive presymptomatic rise is consistent with proposed models of presymptomatic AD neurodegeneration (Jack et al., 2010), with NfL rise likely to reflect early axonal breakdown (Sjogren et al., 2001).

The correlation of serum NfL with cognitive measures known to be sensitive to AD-related decline supports the clinical relevance of NfL. While early cognitive changes in FAD most commonly involve episodic memory (Fox et al., 1998), it was found that serum NfL correlated more strongly with global cognitive measures than with memory scores. This may relate to the physiological role of NfL throughout the brain as an essential component of axonal stability, with initial rise possibly reflecting subtle widespread breakdown of neural networks, rather than focal, hippocampal (grey matter) atrophy. The possibility that elevated serum NfL levels more closely reflect global neurodegeneration is also supported by its correlation, across all carriers, with whole brain and ventricular atrophy.

It is notable that while serum NfL correlated significantly with disease stage (i.e. EYO) even when including only the presymptomatic participants, imaging and cognitive measures did not; serum NfL may therefore be a more sensitive marker of early neurodegeneration.

When measured in the CSF of individuals with mild cognitive impairment, NfL has been found to be predictive of subsequent progression to AD dementia (Zetterberg et al., 2016), with a recent meta-analysis showing it to have comparable discriminatory power to the well-established CSF AD biomarkers of $A\beta_{1-42}$, total tau and phosphorylated tau (Olsson et al., 2016). Recent studies comparing NfL measurement in CSF and serum have shown close correlation (Gaiottino et al., 2013, Bacioglu et al., 2016), implying that serum NfL may similarly have the ability to predict subsequent progression, in keeping with our data.

A study in an FAD mouse model, which knocked out the NfL gene, showed that NfL deficiency significantly increased AD-related neurodegeneration, a finding that might suggest a role for NfL in maintaining neuronal structure in patients with AD

(Fernandez-Martos et al., 2015). Moreover in *APP/PS1* mice, serum NfL concentrations have been shown to increase early in the disease, and to be closely associated with the progression of underlying AD-like pathology (Bacioglu et al., 2016). The same study showed serum NfL concentrations decreased in response to anti-Aβ immunotherapy, with the authors suggesting that serum NfL may serve as a biomarker of treatment response.

There are obvious benefits to identifying AD biomarkers that can be measured in blood (Disease", 1998), with numerous candidates proposed (Lista et al., 2015). However, recent comprehensive meta-analyses of blood-based markers showed only total tau was able reliably to differentiate AD from healthy controls (Zetterberg et al., 2013, Olsson et al., 2016). Moreover blood tau has only proven useful in identifying AD in established dementia cases, with no evidence that it is useful earlier in the disease, and there is often overlap between patient and control groups (Lista et al., 2015, Olsson et al., 2016). Studies attempting to measure blood concentrations of $A\beta_{1-42}$, the other core molecular marker of AD pathology, have so far produced conflicting results, with no strong overall evidence of a difference between AD and controls (Olsson et al., 2016, Lista et al., 2015). Futhermore, even if β-amyloid moieties could be reliably identified and quantified, as cerebral Aβ deposition is thought to plateau some time before symptom onset (Bateman et al., 2011, Villemagne et al., 2013), it may not be effective in tracking progression unless very early in disease. By contrast, a marker of downstream neurodegeneration, such as NfL, which may reflect ongoing (global) disease activity, might be useful as a trial outcome measure, from presymptomatic through to symptomatic phases of the disease. A blood test for neurodegeneration might also be useful clinically in identifying those individuals with cognitive concerns who are more or less likely to require more detailed investigation.

A number of studies have investigated plasma or serum profiles in an attempt to identify a pathological fingerprint of AD, using different profiling approaches including proteomics, lipidomics and transcriptomics (Ray et al., 2007, Han et al., 2011, Booij et al., 2011). However, poor reproducibility remains an issue when assessing large panels of molecules involved in potentially diverse biological pathways, with several follow-on studies showing negative results (Soares et al., 2009, Mielke et al., 2011, Casanova et al., 2016). Although our findings find support from previous studies of serum NfL in symptomatic AD (Bacioglu et al., 2016, Gaiottino et al., 2013), it will be important a) to replicate the presymptomatic findings, before now shown only in mice (Bacioglu et al., 2016), in other *at risk* FAD and sporadic AD cohorts (e.g. in amyloid positive older controls) and b) to determine the clinical outcomes in these individuals to assess the predictive value and time course of increases in serum NfL.

While the results of this study are encouraging, there are a number of issues to consider with regards to the utility of NfL as a biomarker of early AD. Although, as a group, the presymptomatic carriers had a higher mean NfL concentration than non-carriers, there was a degree of overlap in observed values between the two groups. The utility of serum NfL to diagnose presymptomatic AD at the individual level therefore remains uncertain, and needs reassessment in independent cohorts. A prospective decision was made not to use an SVM approach to assess serum NfL's ability to identify diagnostic group in individuals (as was done in the studies reported in chapters 3 and 4), as the lower number of participants in the current study (particularly in terms of controls) would have made the results of such analysis unreliable. The changes in serum NfL through the course of the disease were analysed in cross-sectional data only, so it is also not known whether serum NfL tracks progression at an individual level. A further consideration, with regards to the implementation of NfL testing in either clinical trials or clinical practice, is that it is quite possible that the pattern of change in NfL through the course of the disease will be non-linear. Such a possibility is indeed

suggested by the distribution of values in figure 5-2, with the rate of increase appearing to be greater later in the disease. However, longitudinal data will be needed in order to confirm this. Any such non-linear relationship would add an additional layer of complexity when it comes to interpreting changes in clinical trials, and comparing individuals at different disease stages. This is however also the case for all other markers on neurodegeneration in AD, including for example hippocampal volume, with change known to accelerate with increasing proximity to symptom onset (Ridha et al., 2006).

Also, while the findings support the use of serum NfL as a marker of neurodegeneration in AD, NfL is not a specific marker to AD and has been shown to rise in a number of other conditions (Gisslen et al., 2016, Rojas et al., 2016, Rohrer et al., 2016). It may therefore be that serum NfL will be most useful for identifying and tracking AD-related neurodegeneration when used in combination with a test to confirm underlying AD molecular pathology, such as CSF tau/Aβ_{1-42} or amyloid PET.

The study has a number of limitations. The non-carrier group was smaller than would have been expected (i.e. <50% of all at risk participants). As a result of this we had relatively few mutation negative individuals. It had been hoped that a group of additional controls samples (from another study) could have been used to increase the number of non-carriers, but these were not available at the time of performing the NfL measurements. For a number of participants not all cognitive and imaging assessments were completed, which resulted in missing data. However, minimal changes were seen when re-running the analyses to include only those participants who had completed all assessments.

5.7 Conclusion

In conclusion, this study shows, using a new ultrasensitive assay, that serum NfL concentration is increased in FAD prior to symptomatic disease, and correlates with the number of years to/from predicted symptom onset. Serum NfL also correlated with neuroimaging and cognitive markers of disease severity. The findings support the further investigation of serum NfL as an easily accessible biomarker of early AD-related neurodegeneration.

5.8 Publications arising from this chapter

Data included in this chapter have been published in the following:

Weston, P. S. J., Poole, T., Ryan, N. S., Nair, A., Liang, Y., Macpherson, K., Druyeh, R., Malone, I. B., Ahsan, R. L., Pemberton, H., Klimova, J., Mead, S., Blennow, K., Rossor, M. N., Schott, J. M., Zetterberg, H. & Fox, N. C. 2016. Serum neurofilament light in familial Alzheimer's disease: a marker of early neurodegeneration. *Neurology*, 89, 2167-2175.

6 Assessment of early cognitive change: accelerated long-term forgetting and subjective cognitive decline

6.1 Introduction

As discussed in earlier sections, there have been significant recent advances, in areas such as cerebrospinal fluid analysis and neuroimaging techniques, in detecting early AD pathology and neurodegeneration. The recognition of the long period of "presymptomatic" changes in CSF and imaging prompt further studies on the onset and progression of the earliest downstream cognitive changes. The medial temporal lobe (MTL), which plays an important role in memory function, is an early site of NFT deposition and atrophy (Braak and Braak, 1998, Brier et al., 2016, Ridha et al., 2006). Whilst this pathology predates the development of overt cognitive symptoms, Subtle cognitive impairment may be present much earlier than symptoms – cognitive measures sensitive to such very early change would be valuable both diagnostically and for presymptomatic trials. However current standardized tests are not designed to detect the subtle changes that may occur during the early disease stage (Rentz et al., 2013), with studies of familial and sporadic AD showing conventional testing methods to detect the presence of focal cognitive decline only shortly before or following the onset of clinical symptoms (Fox et al., 1998, Yau et al., 2015, Lopera et al., 1997, Linn et al., 1995).

As outlined in section 1.4.9.3, ALF is a form of memory impairment described primarily in patients with temporal lobe epilesy (Blake et al., 2000, Butler et al., 2007). It refers to a process where new material is encoded and retained normally over periods of up to 30 minutes – consistent with normal performance on standard memory tests – but is then forgotten at an abormally rapid rate over the following days to weeks. ALF has

recently been assessed in a mouse model of presymptomatic FAD (Beglopoulos et al., 2016), with the genetically modified mice found to have abnormal retention over an interval of seven days, despite demonstrating normal learning and retention over a short interval.

In studies of patients with epilepsy, ALF was found to be associated with subjective cognitive concerns (Blake et al., 2000, Butler et al., 2007). Evidence suggests that subjective cognitive concerns may also be a possible preclinical marker of AD (Dik et al., 2001, Reisberg et al., 2008, Jessen et al., 2014, Perrotin et al., 2016).

This study investigates long-term forgetting in presymptomatic FAD mutation carriers and non-carriers. Participants were assessed on three memory tasks – list recall, story recall and figure recall – immediately, at 30 minutes and at seven days. The performance of carriers and non-carriers was compared, and the association between ALF and subjective cognitive decline assessed.

6.2 Hypotheses

- ALF is present in presymptomatic FAD mutation carriers.
- An increase in subjective cognitive concerns is present in FAD mutation carriers, even prior to the onset of overt symptoms.
- ALF is associated with subjective cognitive concerns.

6.3 Contributions and collaborations

The study was conceived by Professor A. Zeman, Dr C. Butler, Professor N. Fox and Dr S. Crutch. Dr Y. Liang, Dr S. Henley and the author designed the ALF testing paradigm. Standard neuropsychology data were collected by Ms K Macpherson and Ms E. Donnachie. The statistical analysis was planned by Dr J. Nicholas and the author, and then performed by Dr J. Nicholas (to prevent the author being unblinded to the genetic status of the participants). Image processing and analysis was performed by Dr L.Harper and the author. All other aspects of the study, including recruitment of participants, collection of all ALF, clinical, and imaging data, and interpretation of the data was performed by the author.

6.4 Methods

6.4.1 Study design and participants

Thirty-five asymptomatic individuals from 19 different FAD families were assessed between February 2015 and March 2016. All participants, by virtue of having an affected parent, were at 50% risk of carrying a pathogenic FAD mutation. Blinded genetic testing was performed, to determine the presence or absence of a mutation as outlined in sections 2.2 and 2.7. Nine participants (five mutation positive, four mutation negative) had however previously chosen to have clinical predictive genetic testing, and so were already aware of their genetic status.

As detailed in chapter 2, participants each underwent neurological assessment, neuropsychological assessment, MMSE, and completion of the CDR (Morris, 1993). The global CDR and CDR SOB were calculated. The neuropsychological tests used in

the analysis included measures of general intellectual functioning (WASI) (Wechsler, 1999), verbal and visual recognition memory (RMT) for words and faces (Warrington, 1984), and paired associate learning (Camden PAL) (Warrington, 1996). Symptoms of depression and anxiety were assessed using the HADS (Zigmond and Snaith, 1983). All individuals identified a close informant who was interviewed separately to gain a collateral history. EYO was calculated as outlined in section 2.8.

Subjective memory was assessed using the EMQ (Thompson and Corcoran, 1992), which gives a subjective memory score between 0 and 90, with higher scores indicating worse subjective memory.

6.4.2 Long-term forgetting assessment

Long-term forgetting was evaluated separately from the other assessments, using test materials from the Adult Memory and Information Processing Battery (AMIPB) (Coughlan and Hollows, 1985). Participants were assessed on three separate tests: learning and recall of a 15-item word list, learning and recall of a short story, and learning and recall of a complex visual figure. For each of the three tests there were two possible test versions, with each participant being tested on either set one or set two. For the word list, participants had to learn the material to a minimum required accuracy of 80% over a minimum of four and maximum of ten trials. For the story a similar approach was taken, with participants having to learn the material to a minimum required accuracy of 80% over a minimum of two and maximum of ten trials. For the visual figure, participants were first asked to copy the figure as accurately as possible on to a separate piece of paper; the figure and their drawing were then removed and they were asked to draw the figure again from memory. Participants were then tested on free recall of the word list, story and figure, each at a standard interval of 30 minutes after presentation of the last learning trial. Participants were randomly assigned to

either test set one or test set two, although within families from which two members were participating the assignment was not entirely random, as the second participant in a family was always assessed on a different version from the first participant. This procedure was intended to prevent the possibility of relearning the stimuli within families during the retention interval. Participants were requested not to discuss details of the tests with other participants.

Following assessment of initial learning the participants were told that they would be telephoned seven days later and asked a few follow-up questions; but it was not explicitly stated that their memory of the test materials would be retested. The participants were given an envelope, which they were asked not to open until when asked to do so during the phone call seven days later. At the time of the seven-day phone call participants' free recall of the test materials was reassessed. For the visual figure test this was done by asking them to draw the figure on a blank piece of paper included in the envelope they had been given. Following assessment of free recall, we also assessed forced choice recognition memory. For the word list, recognition memory was assessed by verbally giving the participant 15 pairs of semantically unrelated words, one of which was from the original list and one of which was not, and asking them to select the correct one. A similar procedure was done for 12 separate aspects of the story, but with the participant given three possible options rather than two. For the figure, the participants were asked to look at a piece of paper (contained in a separate envelope within the first envelope) showing four sets of three similar illustrations. For each set of three, one of the illustrations exactly resembled a part of the original figure, with the participants having to mark on the paper, which one they thought was correct. A stamped addressed envelope was also included in the participant's envelope; with the participants asked to post back the sheets of paper containing their seven day figure recall and recognition assessments. As well as assessing seven-day recall and recognition raw scores, seven-day recall/30-minute

recall was also calculated, in order to assess what proportion of information retained at 30 minutes was retained seven days later.

All participants completed all assessments. However, for the seven-day figure recall and figure recognition assessments, four participants failed to send back the assessment documents, so these could not be included in the analysis.

6.4.3 MRI acquisition and hippocampal volumetry

Volumetric MRI scans were obtained on 27 participants. All scans were performed on the same 3T Siemens TIM Trio scanner using a 32-channel phased array head-coil. A sagittal 3D MP-RAGE T_1-weighted volumetric MRI (echo time/repetition time/inversion time = 2.9/2200/900 ms, dimensions of 256 × 256 × 208, voxel size of 1.1 × 1.1 × 1.1 mm) was acquired. Images were visually checked for artifact.

Hippocampal volumes were calculated using a semi-automated method (Freeborough et al., 1997), with subsequent manual checking and editing performed as needed.

6.4.4 Statistical analysis

Scores on standard cognitive tests, HADS, EMQ and scores on each accelerated forgetting test for initial learning (i.e. score on the final learning trial), number of learning trials to reach criterion, 30-minute recall, seven-day recall, seven-day/30-minute score, and seven-day recognition were compared between mutation carriers and non-carriers using linear regression with robust standard errors to account for clustering of participants within families. If diagnostic plots of model residuals indicated a departure from the assumption of normal distribution with constant variance,

statistical inference was based on non-parametric bias-corrected and accelerated 95% confidence intervals (CIs) from 2000 bootstrap replications clustered on family.

Analysis of HAD anxiety, HAD depression, MMSE, RMT faces, RMT words Camden PAL and EMQ was adjusted for age (years) and IQ (WASI total score). Analysis of WASI performance IQ and WASI verbal IQ was unadjusted, since these measures were corrected for age. Analysis of forgetting tests (list, story and figure) scores was adjusted for age (years), IQ (WASI total score) and test version.

In mutation carriers only, the association between the score on each long-term forgetting test and EYO was assessed using the non-parametric Spearman correlation coefficient with cluster adjusted (robust) p-values, due to anticipation that there may not be a linear relationship between the two variables. Also in mutation carriers only, Spearman correlation coefficients were also calculated for the association between each long-term forgetting test and EMQ score. For all analyses involving EMQ score, only participants who were unaware of their mutation status were included, since knowledge of mutation status might bias an individual's perception of their memory.

Spearman correlation coefficients were calculated for mean hippocampal volume against each of the three long-term forgetting tests (for seven day recall/30 minute recall). Additionally, the correlation was assessed between the left hippocampal volume and list and story recall, and between right hippocampal volume and figure recall.

6.4.5 Voxel based morphometry

Whole brain voxel base morphometry was carried out using SPM12 (Statistical Parametric Mapping, version 12; Wellcome Trust Centre for Neuroimaging, London,

UK). The T_1-weighted scans were segmented into grey and white matter using the segment toolbox with default settings (Weiskopf et al., 2011). Grey and white matter segmentations were then iteratively registered by DARTEL to an evolving estimate of their group-wise average (Ashburner and Friston, 2009). The native space tissue segments were then normalized to MNI space using the DARTEL transformations, modulated to account for volume changes. A smoothing kernel of 6 mm full-width at half-maximum was applied. Total intracranial volume was calculated for each subject using Jacobian integration of deformation fields created by the new segment toolbox (Ridgway et al., 2011).

Voxel-wise statistical analysis was performed, with multiple-regression analyses used to assess whether, in the mutation carriers, there were any brain regions in which local grey matter volume covaried linearly with scores on the ALF assessments. Additional covariables included in the models were age, gender, TIV, and IQ (total score on WASI). Resultant t-statistic maps were thresholded of $p<0.05$ with family-wise error correction for multiple comparisons across the whole brain.

6.5 Results

6.5.1 Participant demographics and performance on standard cognitive tests

Of the 35 participants, 21 were mutation carriers. All participants scored 0 for both global CDR and CDR SOB. Mutation carriers and non-carriers were well matched for age, gender, and years in education (table 6-1); all were right-handed. Mutation carriers were on average (±SD) 7.3±4.5years from estimated symptom onset. There were no significant inter-group differences in mood and on conventional tests of memory and global intelligence, except for recognition memory for words, which was

higher in carriers ($p<0.05$), and performance IQ, which was higher in non-carriers ($p=0.04$) (table 6-2).

	Mutation carriers	**Non-carriers**
n	21	14
Gender (m/f)	11/10	6/8
Mean age (SD)	38.0 (5.9)	39.2 (7.9)
Mean estimated years to symptom onset (SD)	7.2 (4.5)	N/A
Mean years of education (SD)	13.8 (2.5)	14.4 (2.2)

Table 6-1. Participant demographics

	Mutation carriers	Non-carriers	p-value
HADS anxiety score /21	6.0 (3.0-9.0)	4.5 (4.0-7.0)	0.47
HADS depression score /21	2.0 (0-2.0)	1.0 (0-2.0)	0.59
MMSE /30	29.0 (29.0-30.0)	29.5 (29.0-30.0)	>0.05
WASI verbal IQ	106 (91-108)	103 (95-103)	0.37
WASI performance IQ	104 (100-116)	119 (106-121)	0.03
RMT words /50	49.0 (49.0-50.0)	48.0 (46.0-50.0)	<0.05
RMT faces /50	45.0 (43.0-48.0)	45.5 (44.0-47.0)	>0.05
Camden PAL /24	19.0 (16.0-22.0)	19.0 (17.0-22.0)	>0.05

Table 6-2. Results of mood assessment and standard tests of intelligence and memory

Group median scores (with inter-quartile ranges) are shown. Exact p-values are shown for those variables that satisfied the assumptions of the linear regression model. For other variables, parametric assumptions were not met and therefore p < or > than 0.05 was inferred from bootstrapped 95% confidence intervals. For HAD anxiety, HAD depression, MMSE, RMT faces, RMT words and Camden PAL, p-values reflect the group differences after adjusting for age (years) and IQ (WASI total score). Analysis of WASI performance IQ and WASI verbal IQ was unadjusted, since these measures were corrected for age. Robust standard errors accounted for clustering of participants within families. HADS=Hospital Anxiety and Depression Scale. MMSE=Mini Mental State Examination. WASI=Wechsler Abbreviated Scale of Intelligence. RMT=Recognition Memory Test. PAL=Paired Associate Learning.

6.5.2 Performance on ALF assessment

Across all three ALF tests, adjusting for age, IQ and test version, and accounting for potential clustering within families, there was no evidence of a difference between the mutation carriers and non-carriers in their ability to learn the material, either in terms of initial score or number of learning trials to criterion (table 6-3). All participants learned the word list and story to the required 80% accuracy within the allowed number of trials. There were no significant between-group differences for 30-minute recall score on any task (table 6-3, figure 6-1). For seven-day/30 minute recall scores, there was evidence that mutation carriers performed worse than non-carriers for list (estimated difference in means = 30.9 percentage points, 95% CI 16.7−45.2; p=0.0002), story (20.1, 6.9-33.3; p=0.005) and figure (15.4, 3.9-26.9; p=0.01). Mutation carriers' seven-day recall scores were also worse than non-carriers for list (24.6, 10.1-39.0; p=0.002) and story (18.0, 6.9-29.1; p=0.003), but not for figure (8.7, -5.6-22.9; p=0.22). Mutation carriers performed significantly less well than non-carriers on seven-day recognition for list (5.8, 2.6-9.9; $p<0.05$), story (6.8, 3.3-11.0; $p<0.05$) and figure (17.6, 8.0-27.6; $p<0.05$).

		Mutation carriers	Non-carriers	p-value
List	Learning trials	5.0 (4.0-6.0)	4.0 (4.0-6.0)	> 0.05
	Learning score %	80.0 (80.0-86.7)	86.7 (80.0-93.3)	> 0.05
	30-min. recall %	80.0 (73.3- 80.0)	80.0 (73.3-86.7)	0.85
	7-day recall %	26.7 (20.0- 46.7)	56.7 (46.7- 66.7)	0.002 *
	7-day/30-min recall	36.4 (30.0-58.3)	71.8 (55.6-81.8)	0.0002 *
	7-day recognition %	93.3 (86.7-100.0)	100.0 (100.0-100.0)	<0.05 *
Story	Learning trials	3.0 (2.0-3.0)	2.0 (2.0-3.0)	> 0.05
	Learning score %	87.5 (83.3-91.1)	90.5 (87.5-94.6)	0.67
	30-min. recall %	83.3 (80.0-87.5)	87.9 (80.4-91.1)	0.76
	7-day recall %	56.7 (50.0-68.3)	79.3 (71.4-83.9)	0.003 *
	7-day/30-min recall	66.7 (58.8-81.3)	92.2 (81.1- 95.7)	0.005 *
	7-day recognition %	91.7 (91.7-100.0)	100.0 (100.0-100.0)	<0.05 *
Figure	Learning score %	100.0 (97.4-100.0)	100.0 (99.3-100.0)	>0.05
	30-min. recall %	92.5 (72.4- 97.4)	88.4 (72.4- 96.7)	0.34
	7-day recall %	59.2 (48.8- 73.7)	74.3 (62.5-83.2)	0.22
	7-day/30-min recall	70.3 (63.2-82.1)	87.6 (76.9-96.4)	0.01 *
	7-day recognition %	75.0 (75.0-100.0)	100.0 (100.0-100.0)	<0.05 *
Mean	7-day/30-min recall	56.9 (51.8- 74.2)	84.1 (75.2- 88.8)	0.001 *

Table 6-3. Results of long-term forgetting assessments

*Uncorrected group median values (with interquartile range) are shown. Exact p-values are shown for those variables that satisfied the assumptions of the linear regression model. For other variables, parametric assumptions were not met and therefore p < or > than 0.05 was inferred from bootstrapped 95% confidence intervals. P-values reflect the group differences after adjusting for age, IQ (WASI total score), and test version. Robust standard errors accounted for clustering of participants within families. For the list and story, "learning score" refers to the score from the final learning trial. * indicates statistically significant results.*

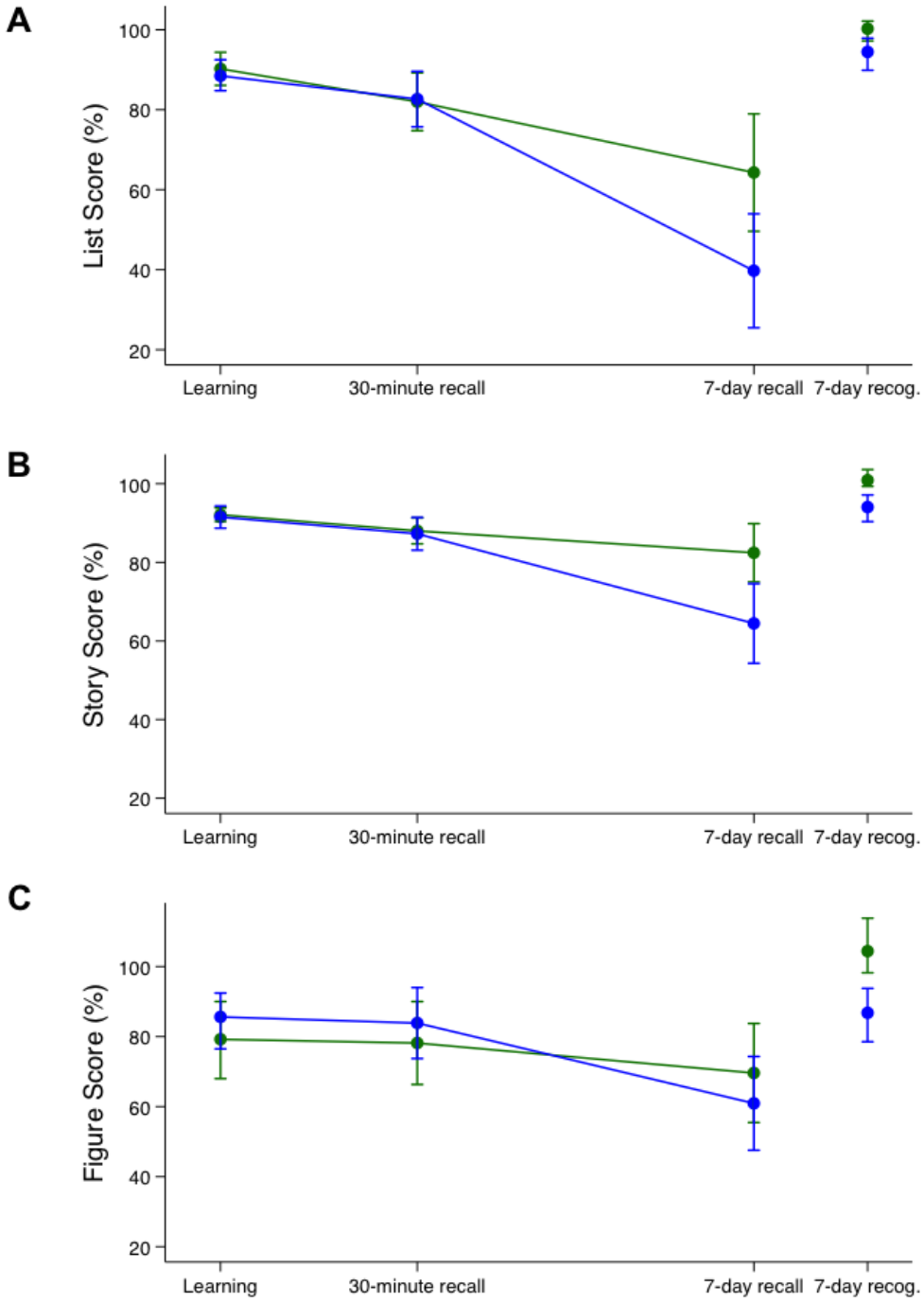

Figure 6-1. Results of long-term forgetting assessments

Adjusted mean scores for mutation carriers are shown in blue and non-carriers in green. Scores are adjusted for age, IQ (WASI total score), and test version. Robust standard errors accounted for within family clustering. Recall percentage scores are shown at initial learning, 30 minutes and seven days for (A) word list, (B) story, and (C) figure. 7-day recognition scores are also shown, on the right hand side of each graph.

Performance on each long-term forgetting recall test (calculated as seven-day/30 minutes score) showed an association with EYO, in that the performance progressively worsened with increased proximity to estimated symptom onset, reaching statistical significance for both list and story recall assessments, and trend significance for figure recall (table 6-3).

	Spearman's rho	p-value
Story (seven day/30 minutes)	0.41	0.03
List (seven day/30 minutes)	0.38	0.04
Figure (seven day/30 minutes)	0.37	0.08
Summary score	0.37	0.06

Table 6-4. Spearman correlation coefficients for the association between each ALF recall assessment (calculated as seven day score/30 minute score) and EYO

6.5.3 ALF and subjective memory

Neither mutation carriers (median=18·5/90) nor non-carriers (12·5/90) had high scores on the EMQ (having excluded participants who knew their genetic status). However, the difference was statistically significant, with mutation carriers having more subjective memory concerns than non-carriers (7·9, 1·36−14·41; p=0·02) (figure 6-2).

In mutation carriers, poorer long-term retention (7-day/30-minute recall score) was significantly associated with higher EMQ score for list (rho=−0·43, p=0·04), with a non-significant trend towards an association for story (rho=−0·38, p=0·08), for figure

(rho=−0·39, p=0·11) (figure 6-3), and a mean score all three tasks (rho=−0·50, p=0·05).

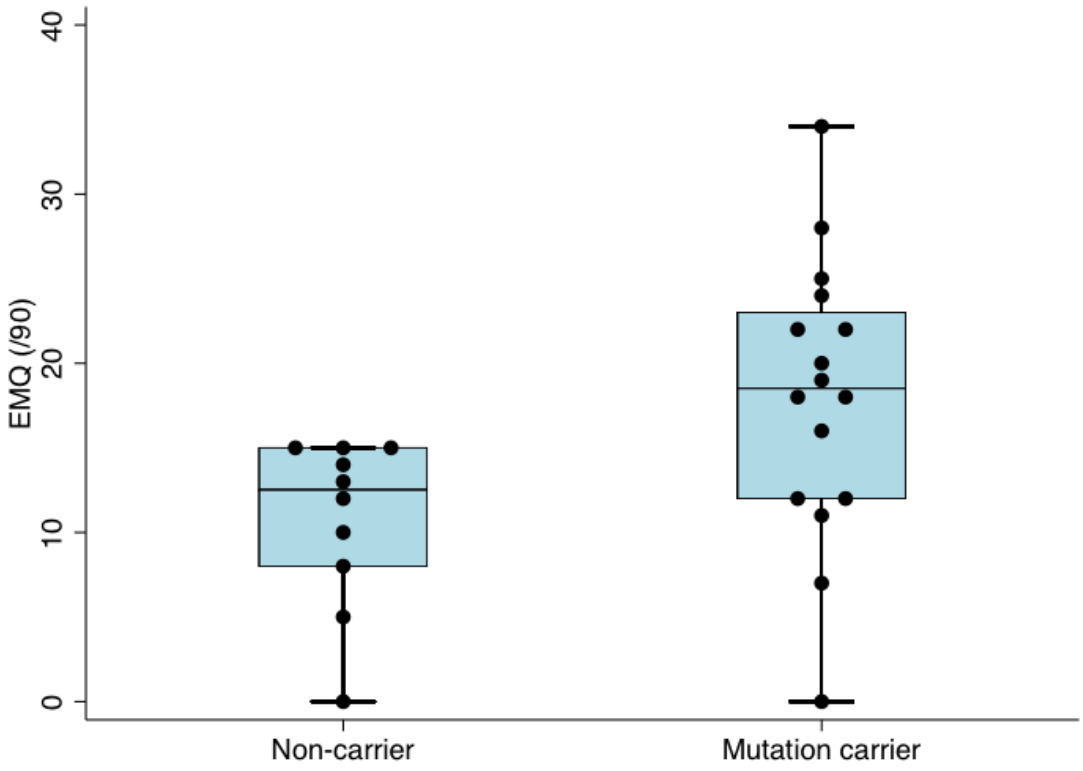

Figure 6-2. Box and whisker plots of Everyday Memory Questionnaire score

Results of the EMQ, assessing subjective memory concerns, are shown for mutation carriers and non-carriers, with individual data points also shown. The score is out of a maximum of 90, with higher scores indicating greater subjective cognitive concerns. Only individuals who did not know their genetic status are included. EMQ=Everyday Memory Questionnaire.

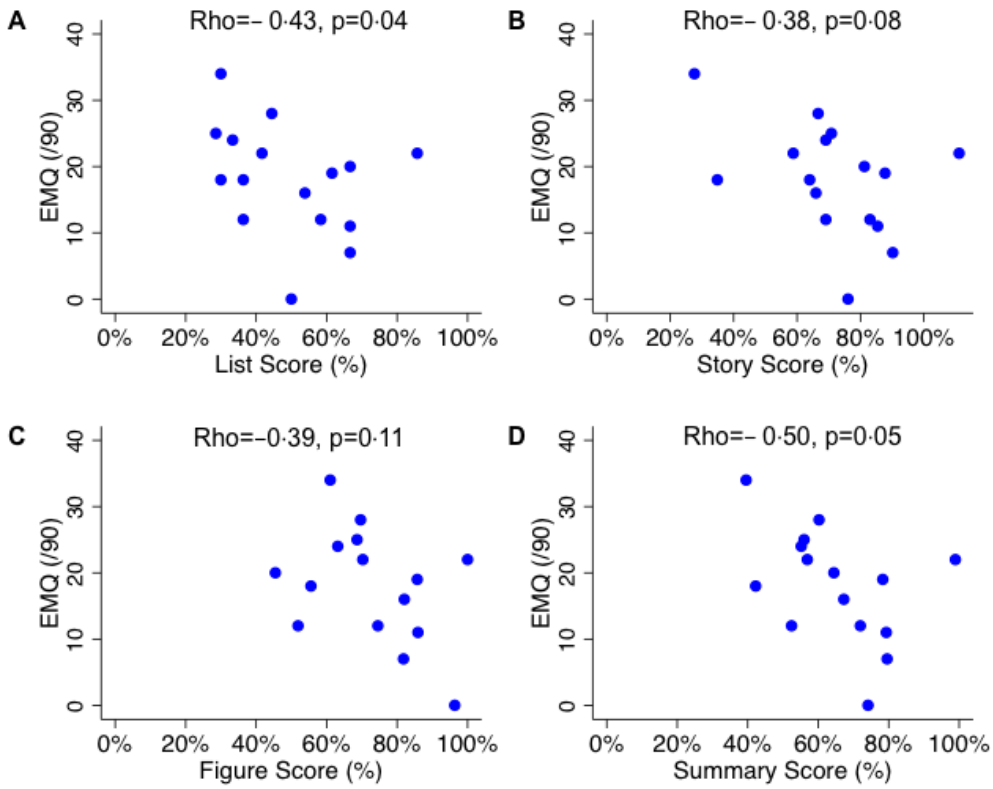

Figure 6-3. Scatter plots for EMQ score against long-term recall scores in mutation carriers

Comparison of EMQ score with long-term forgetting score (7-day recall/30-minute recall) for (A) word list, (B) story, (C) figure and (D) a mean score across the three separate tests. Only the 16 mutation carriers who did not know their genetic status are included.

6.5.4 ALF and brain imaging measures

There was no significant correlation between the volume of the hippocampal parcellations and performance on any of the individual tests of long-term forgetting, or for a mean score of the three ALF tests. On VBM analysis, no brain regions were found that correlated with performance on any of the individual tests of long-term forgetting, or for a mean score of the three accelerated forgetting tests.

6.6 Discussion

This study shows that ALF is a feature of presymptomatic FAD, in a group of individuals who on average were seven years from estimated symptom onset. Despite a lack of difference in initial learning or in recall over a short interval, reassessment seven days later demonstrated that the presymptomatic mutation carriers had forgotten significantly more than the non-carriers. This finding was consistent for recall and recognition memory, and for both verbal and non-verbal material. To the author's knowledge this is the first study to demonstrate such marked and consistent differences on a cross-sectional measure of cognition this early in the presymptomatic disease phase.

In marked contrast to the ALF findings, mutation carriers and non-carriers showed similar performance on conventional memory tests, which included both recognition memory for words and faces and paired associate learning, with the only significant group difference being that recognition memory for words was actually slightly higher in the mutation carriers. This provides further evidence that the differences seen in long-term forgetting are unlikely to be due to a problem with encoding or early retention, but rather are caused by an impairment of long-term memory consolidation. Whilst impairment of episodic memory is recognized as a central component of the clinical phenotype of AD, relatively little is known about how long-term consolidation of memory is affected. Some studies have tried to demonstrate consolidation deficits in MCI presumed to be due to AD (Koivunen et al., 2012), but it is difficult to measure long-term retention of memory and compare a disease group with controls, unless the groups are equal for initial encoding and short interval retention (Elliott et al., 2014), which would not be the case in the symptomatic phase of AD (including MCI). By recruiting a presymptomatic cohort, in whom underlying AD pathology is certain, and testing retention over a much longer period than would usually be done in standard

neuropsychological assessment, we were able to demonstrate that impairment of long-term retention is an early amnestic feature of AD; and indeed may be the earliest feature of AD-related cognitive decline.

There was a clear ceiling effect on testing of seven-day recognition memory, particularly for the non-carriers. However, the fact that it was still possible to demonstrate significant group differences in seven-day recognition memory across all three tests despite these ceiling effects, provides further support that long-term recognition memory, as well as recall memory, is significantly impaired in the presymptomatic mutation carriers. The presence of impaired recognition, which implies a “storage” deficit as opposed to an isolated “retrieval” deficit, would be consistent with pathology primarily affecting the medial temporal lobe (Simons and Spiers, 2003), the brain region known to be affected early in AD.

The process of long-term memory consolidation is known to involve both the hippocampus and neocortex (Dudai et al., 2015, Bontempi et al., 1999, Nestor et al., 2002). However, there was no evidence of any direct correlation between accelerated forgetting and either hippocampal volume or grey matter volume in other focal brain regions. This is perhaps not entirely surprising when one considers that the presymptomatic mutation carriers are over seven years from predicted onset, which is likely to be before significant macrostructural atrophy has occurred, consistent with the findings from chapters two and three as well as the results of previous imaging studies (Fox et al., 1996, Cash et al., 2013). This would suggest therefore that assessment of accelerated long-term forgetting might be more sensitive to presymptomatic neurodegenerative change than current gold standard structural imaging techniques. The finding of no correlation between accelerated long-term forgetting and focal volumetric change is consistent with previous findings in epilepsy patients (Butler et al., 2009). It may be that accelerated long-term forgetting, in the absence of any other

demonstrable memory deficit, is caused by early, diffuse, microstructural breakdown of the network connecting the different interacting brain regions involved in the consolidation process. This would be consistent with the concept that in AD there is early breakdown of a vulnerable but distributed neural network of different interconnected regions (Warren et al., 2013).

	Memory encoding	**Early retention**	**Long-term retention**
AD dementia	↓	↓	↓
MCI	↔	↓	↓
Presymptomatic AD	↔	↔	↓
Healthy aging	↔	↔	↔

Table 6-5. Proposed stages of progressive memory impairment in AD

Previous studies have established differences in memory function between AD dementia, AD-MCI and healthy aging, based on tests of memory encoding and retention over a short interval. The results of our study allow us to propose a third column, for long-term retention, which demonstrates impairment a number of years prior to the onset of noticeable symptoms. MCI=mild cognitive impairment. ↓=reduced relative to healthy aging. ↔=normal/unchanged relative to healthy aging. MCI=mild cognitive impairment.

The findings advance existing understanding of the stages of memory decline in AD. It has previously been reported that it is possible to discriminate AD dementia from AD-MCI based on initial encoding of memory being impaired in the dementia stage but not in MCI; whilst it is possible to separate AD-MCI from presymptomatic disease and healthy aging by the fact that those with MCI would usually demonstrate difficulty with

short-term retention (e.g. over 30 minutes) (Ally et al., 2013). With the introduction of testing of long-term retention it may be possible to discriminate those with presymptomatic AD (but without conventional deficits) from healthy aging (table 6-5, figure 6-4).

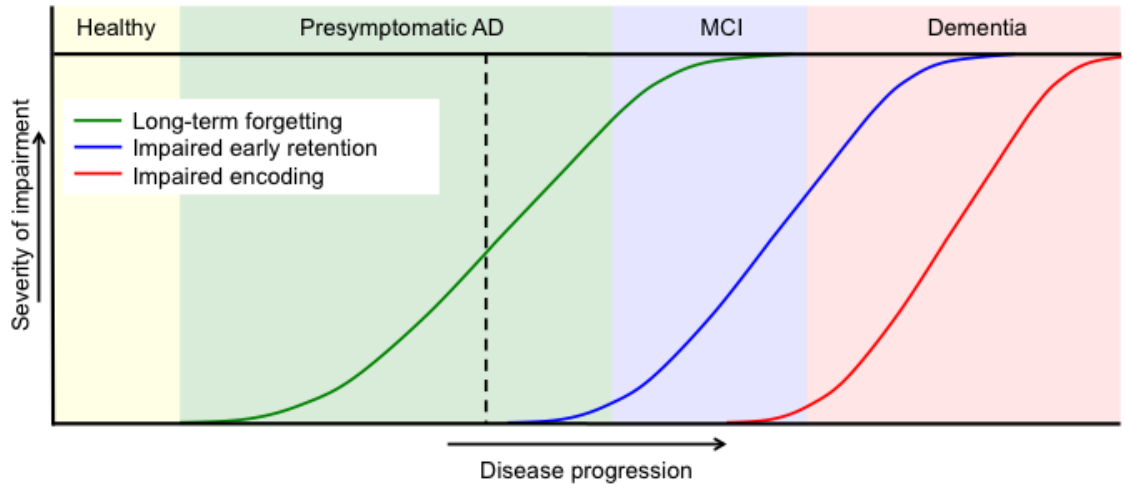

Figure 6-4. The sequential decline in different aspects of episodic memory as AD progresses

A schematic representation of the order in which different aspects of episodic memory function may be sequentially affected by AD pathology. Prior to any symptoms, in individuals who perform normally on standard tests, deficits would appear to be detectable by testing long-term forgetting over intervals of days to weeks. Early retention (e.g. over 30 minutes) then becomes progressively affected as individuals enter the AD-MCI stage, whilst deficits in memory encoding generally only develop in individuals with AD-dementia. An approximate position on where (on average) the mutation carriers in the current study sit on the AD disease spectrum is indicated by the black dotted line.

Other than for ALF, the only group difference we observed on cognitive testing where non-carriers performed better than carriers, was for performance IQ. This is consistent

with previous findings in FAD that, along with episodic memory, reduced performance IQ is one of the earliest cognitive changes (Fox et al., 1998). However, the proportional difference in performance IQ between groups was much smaller than for the ALF testing, with the subsequent p-value being less significant by an order of magnitude. As WASI score was corrected for in all regression analyses, it is unlikely that the difference in performance IQ had any influence on our main study findings.

It was found that, despite reporting no overall concerns about their memory and being unaware of their genetic status, presymptomatic mutation carriers had significantly worse subjective memory scores than non-carriers, which support emerging evidence that subtle subjective cognitive concerns may be a harbinger of AD-related cognitive decline (Dik et al., 2001, Reisberg et al., 2008). A consistent trend was found across all three ALF tasks that, in mutation carriers, there was an association between subjective cognitive concerns and accelerated long-term forgetting, although it was only for list recall that this reached statistical significance. This is consistent with findings from previous epilepsy studies (Blake et al., 2000, Butler et al., 2007), and also one small study of non-epilepsy individuals (Manes et al., 2008). Whilst requiring further investigation, this suggests that early subjective changes in AD, in the absence of objective findings on conventional cognitive tests, may reflect impairments in ALF.

The findings support those in a recent study of *APP* transgenic mice (Beglopoulos et al., 2016). The study assessed very young mice, which had yet to develop any signs of cognitive decline on standard assessment. The authors reported that, despite normal learning of a spatial navigation task and normal retention over a short interval, compared to wild-type mice FAD mice had significantly reduced retention when retested seven days later. It was also found that this impairment in long-term retention was associated with reduced glucose uptake at seven days (despite normal uptake during the learning task). The authors hypothesised that this represented early

metabolic impairment of brain regions subserving long-term consolidation. Furthermore, it appeared that the deficit in long-term retention could potentially be rescued by anti-amyloid β immunotherapy. These results, in mice, alongside the findings of our study, suggest that assessment of long-term forgetting in humans may have utility as a marker of treatment response in presymptomatic therapeutic trials.

This study has a number of limitations. First, while the participants were told not to discuss the testing following the initial learning and 30-minute recall task, and were not explicitly told that they would be retested seven days later, it is possible that some individuals may have rehearsed the material during the intervening period; an inherent difficulty with ALF testing (Elliott et al., 2014). However, when asked following the 7-day testing, all participants said that they had not rehearsed. We did not assess issues relating to the participants' sleep between the initial learning and seven-day testing. Sleep is thought to play an important role in memory consolidation (Rasch and Born, 2013). However, a previous study in epilepsy patients found sleep quality to have no direct effect on ALF (Atherton et al., 2014). Also, we found no significant group difference in mood, which usually correlates closely with sleep (Boivin et al., 1997). Future validation of the utility of ALF testing in FAD and sporadic AD, including assessment of its reliability at the individual level, will be essential.

6.7 Conclusion

The findings show that accelerated long term forgetting is present in FAD mutation carriers who were on average seven years from predicted symptom onset, and may be a very early feature of AD-related cognitive decline. A subtle but significant increase in subjective cognitive concerns is also a presymptomatic feature of FAD. It is possible that ALF may underpin the subjective cognitive difficulties that are often reported prior

to the onset of objective decline. ALF may have utility as an inclusion criterion or outcome marker in presymptomatic AD trials.

6.8 Publications arising from this chapter

Data included in this chapter have been published in the following:

- Weston, P. S. J., Nicholas, J. M., Henley S. M. D., Liang, Y., Macpherson, K., Donnachie, E., Schott, J. M., Rossor, M. N., Crutch, S. J., Butler, C. R., Zeman, A. Z., Fox, N. C. 2018. Accelerated long-term forgetting in presymptomatic autosomal dominant Alzheimer's disease: A cross-sectional study. *Lancet Neurology*, 17, 123-132.

7 Summary and future work arising from this thesis

7.1 The study of FAD to develop biomarkers of early neurodegeneration

In describing the clinical features of AD and the devastating effect it has on patients and their families, the introductory chapter of this thesis set out the pressing need for disease modifying treatments that slow the disease's progression. The same chapter also presented overwhelming evidence in support of AD having a long presymptomatic phase, with progressive deposition of molecular pathology followed by progressive neurodegeneration, beginning years before the onset of symptomatic disease. If future trials of putative disease modifying therapies are to be more successful than those to date, it is likely that intervention will be required earlier than has been attempted so far, prior to clinically significant irreversible neuronal loss. For such trials to be successful, it is essential that understanding of the progressive biological changes that occur during the presymptomatic period is improved, so that 1) we know when intervention is likely to be most effective, and 2) we have methods available to detect and track early disease activity, particularly neurodegeneration. The chapter went on to describe current models of presymptomatic disease and what is understood about the timing and order of early changes, and current methods of measuring them.

The work presented in this thesis has aimed to address the needs outlined above, by studying FAD mutation carriers, using a variety of different modalities. Whilst FAD is much rarer than sporadic AD, the two share many characteristics, with neuropathological, radiological, and clinical studies (discussed in chapter one) suggesting that findings in FAD are likely to be largely applicable to the sporadic form of the disease. Furthermore, the study of individuals with presymptomatic FAD offers certain advantages over studying presymptomatic sporadic AD, including knowing with

almost certainty what the underlying pathology is (without requiring post-mortem examination) and being able to predict with relatively high accuracy when symptom onset is likely to occur (Ryman et al., 2014).

The key difference between FAD and sporadic AD is that on average FAD has a significantly younger age at onset. This means that, in general, the young/middle-aged adults who suffer with FAD have significantly fewer co-morbidities, both in terms of co-existing cerebral pathology and extra-cerebral pathology, than their elderly counterparts with sporadic AD. Whether this should be viewed as a strength or a weakness, in terms of findings from FAD being generalizable to the wider AD population, is open to debate. On the one hand, it could be argued that the lack of co-morbidities should be seen as a strength, as one can be confident that any abnormalities observed – cognitive, radiological or otherwise – are very likely to be a direct downstream consequence of AD pathology. Studying FAD could therefore be thought of as the study of a more "pure" form of AD than late onset sporadic disease, with no additional *confounds* present (in the form of co-morbidities) to potentially influence the results. However, it could also be argued that the fact FAD patients do not usually have additional pathologies or illnesses, makes it less reflective of the reality of late-onset sporadic disease, and therefore to what extent findings can be directly translated is questionable. This point is particularly pertinent when it comes to co-exisitng cerebrovascular pathology. It is now recognised that small vessel arteriolosclerotic lesions are present in a significant proportion of individuals with sporadic AD, with evidence suggesting that it may be an integral part of the AD pathophysiological cascade, as opposed to simply a mutually exclusive co-existing phenomenon (de la Torre, 2002, Thal et al., 2003, Iadecola, 2004). Apart from in certain specific mutations (outlined in section 1.3.), the same degree of vascular pathology is not generally observed in individuals with FAD. Understanding how the presence of such vascular pathology affects the measurement of the various disease

markers investigated in this thesis would be important, before one could confidently use the same markers in a sporadic AD population.

However, notwithstanding the above, the overall balance of evidence points to findings in FAD being generally applicable to and useful in sporadic AD.

7.2 Assessment of longitudinal cortical thickness change

The work presented in chapter three utilised a widely used and well-validated method of measuring cortical thickness – a measure of cortical macrostructure – to identify a disease-specific "signature" pattern of cortical thinning in FAD. It followed on from previous work in sporadic AD that took the approach of identifying a combination of cortical regions that tend to be affected preferentially in the majority of individuals with the disease (Dickerson et al., 2009). Whilst individuals with sporadic and familial AD were not directly compared, the six region FAD cortical signature identified was similar to that reported previously for sporadic disease, but with some subtle differences.

All six signature regions, identified in mildly symptomatic mutation carriers, demonstrated presymptomatic thinning in a separate group of presymptomatic individuals, with changes in the precuneus detectable almost a decade before predicted symptom onset – earlier than for many other structural imaging measures. Importantly though, whilst all six independent regions underwent cortical thinning prior to symptom onset, assessing all six regions in combination provided more clinically relevant results (i.e. greater correlation with cognition) and also allowed greater ability to discriminate between individual mutation carriers and non-carriers (on the basis of SVM analysis), than assessing any single region in isolation. Measurement of the cortical signature also had prognostic value, in that baseline measurement was

associated with future rate of thinning. The study replicated previous imaging studies in FAD, which used volumetric rather than thickness measures (Fox et al., 1996, Ridha et al., 2006), in finding longitudinal assessment of rate of loss to be more sensitive to detecting early neurodegeneration than cross-sectional measurement alone.

The findings of the study would suggest that the FAD composite cortical signature may be useful in the recruitment to, and monitoring of, presymptomatic trials of disease modifying therapies, and potentially also in more routine clinical assessment in the future. This is particularly the case given that structural MRI is available in most clinical centres, and the software used for the cortical thickness measurement (Freesurfer v5.30 (http://surfer.nmr.mgh.harvard.edu)) is freely available in the public domain, and allows automated measurement. The ability to quantify the degree of thinning across the cortical signature as individuals become progressively closer to onset may allow presymptomatic disease staging, which may be important when stratifying/prioritizing potential trial recruits and/or assessing treatment efficacy.

The findings of this study may also potentially have implications beyond AD. Although neurodegeneration is a process common to a large number of conditions, it has been shown previously that by using an accurate and reliable method of cortical thickness measurement to assess the anatomical pattern of loss it is possible to distinguish symptomatic individuals with neurodegeneration due to AD from other pathological processes such as FTD or DLB (Blanc et al., 2015, Du et al., 2007). The results of the current study suggest that identifying the disease-specific composite pattern of neurodegeneration for a particular condition may allow one to discriminate between those with and without a particular neurodegenerative disease some years before the onset of symptoms, without necessarily requiring assessment of the underlying molecular pathology.

Future work is required to validate the FAD cortical signature, ideally by assessing its utility in a larger independent cohort of FAD mutation carriers, before it can be used in presymptomatic clinical trials, at least two of which have already begun (Reiman et al., 2011, Mills et al., 2013). The need for further validation is particularly required when it comes to assessing the cortical signature's discriminatory value at the individual level, with the SVM approach used being at risk of over-fitting when small samples are used (Falahati et al., 2014). The results suggest that longitudinal assessment of annualized thinning rates may be more sensitive than cross-sectional assessment. The mean inter-scan interval for the study was over one year, but in certain trial situations it may be preferable to reduce this interval. However, exactly how small the inter-scan interval can be to still provide useful results is currently uncertain, and requires further investigation. Lastly, further longitudinal assessment of thinning in presymptomatic sporadic AD will be useful, in order to assess how similar the longitudinal rates of presymptomatic cortical neurodegeneration are between the two forms of the disease.

7.3 Assessment of cortical mean diffusivity

In any neurodegenerative process it would follow that, prior to there being macrostructural atrophy evident to the naked eye or on conventional structural MRI (such as cortical thinning), changes in tissue microstructure are likely to occur. It is these changes in cortical microstructure that the study reported in chapter 4 sought to identify. Although there was a strong theoretical basis for why assessment of cortical microstructure in presymptomatic AD could be useful and informative, there was no one widely accepted and validated optimum method for assessing cortical diffusivity, not least because the combination of the lower resolution of DWI (compared to T_1-weighted imaging) and the close interface between cortical grey matter and CSF, meant there was a high risk of significant partial volume effects influencing the results.

It was therefore important to ensure the method used sought to mitigate any such effects, and produced sensible results with face-validity, before considering any specific implications for the results in FAD.

The study was able to show that measuring diffusion changes – through the metric of MD – in cortical grey matter is a feasible approach to assessing cortical microstructure, with the use of a weighted-mean to reduce any partial volume effects increasing the face validity of the final regional MD values. Following on from the study reported in Chapter 3, a region of interest approach was taken, focusing on the six cortical regions identified from the cortical thickness study as comprising the FAD cortical signature. This hypothesis-driven approach reduced the risk of a type 1 error, but on the other hand possibly prevented the identification of regions outside of the cortical signature that may have legitimately undergone early microstructural change. However, as the regions that show the greatest macroostrucutal change (e.g. the six cortical signature regions) could be reasonably expected to also be the first to undergo microstructural change (as measured by DWI) the risk of such a type 2 error was felt to be low.

Consistent with a previous study of individuals with sporadic AD-MCI (Jacobs et al., 2013), the precuneus was identified in the cortical MD study as being one of the most significantly affected regions (along with the inferior parietal cortex) during the presymptomatic period; which is also consistent with the cortical thickness findings reported earlier in this thesis. However, given that much of the focus of the cortical MD work was on identifying and refining the methodological approach to the image analysis, with further work in this area likely to be needed, the study focused on assessment of cross-sectional differences only (as opposed to longitudinal differences), and so employed a completely different statistical analysis approach to that described for cortical thickness in chapter three. Therefore, whilst the study provides evidence that presymptomatic change in cortical MD can be detected, it is not

possible based on the current evidence to say whether it can detect changes earlier than cortical thickness, with it being quite possible that it may not do so using the current image acquisition and analysis approach. It is therefore not possible to recommend the use of cortical MD measurement above cortical thickness measurement in presymptomatic clinical trials or in the clinical setting at the present time, with cortical thickness measurement having undergone far more robust validation to date.

There is however significant potential in the further development and use of cortical diffusivity measurement in the future. A methodological development that offers potential benefits for the measurement of grey matter diffusivity is the advent of multiband MRI (Larkman et al., 2001). By simultaneously acquiring MRI data from multiple slices, this technique significantly increases the acquisition speed and offers the possibility of reducing the voxel size (albeit at the cost of signal-to-noise ratio), from the 2-2.5mm isotropic that is currently most common, down to 1-1.5mm isotropic, without having to substantially increase the duration of the scan. This improvement in spatial resolution significantly reduces partial voluming, and is increasingly used (Sotiropoulos et al., 2013, Feinberg and Setsompop, 2013).

One further potential way of enhancing the current analysis technique may be to acquire multi-shell DWI (i.e. multiple diffusion sequences each using a different B-value), which would allow the use of more sophisticated modeling in the analysis, such as composite hindered and restricted model of diffusion (CHARMED) or neurite orientation dispersion and density imaging (NODDI) (Zhang et al., 2012, Assaf and Basser, 2005). Such approaches are able to model neural tissue in terms of multiple separate compartments, e.g. intracellular, extracellular and CSF, within the same voxel (see figure 7-1). This allows these techniques to model the partial volume effect, which is not possible with conventional single-shell techniques, and therefore offers potential

for more precise and reliable diffusion metrics. The use of both multiband and multi-shell approaches going forward is likely to lead to greater precision and reliability.

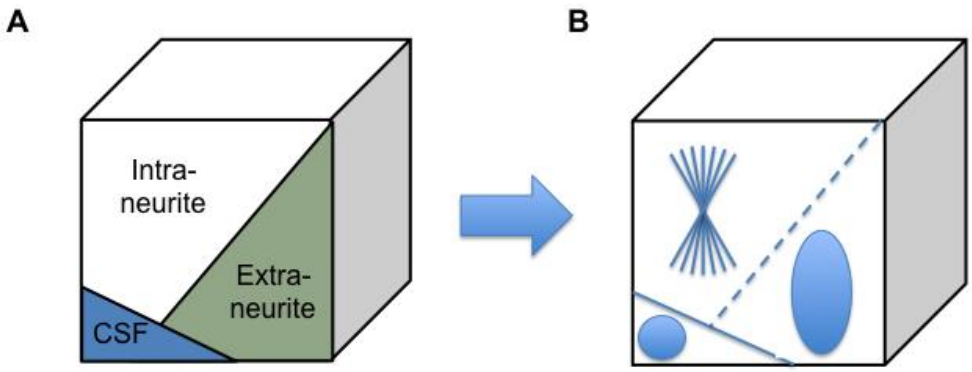

Figure 7-1. Multi-shell DWI modelling

An illustration of how multi-shell analysis approaches make it possible to model different tissue compartments within the same voxel to be modeled separately.

As methods are refined and potential sources of bias mitigated, one could reasonably envisage that the assessment of cortical changes using DWI may become the most sensitive method of detecting early cortical neurodegeneration in AD, much as it is already in another neurodegenerative disease – CJD (Demaerel et al., 1999, Zerr et al., 2009). However, an additional factor to consider if grey matter diffusion is to enter widespread clinical use in AD assessment is the time and expertise often required to register T_1-weighted cortical parcellations to diffusivity maps. Grey matter diffusivity analysis would ideally be automated (Fellgiebel and Yakushev, 2011). Such methodology has recently been used successfully in studies of cortical and subcortical grey matter diffusivity in AD and other neurodegenerative conditions (Barbagallo et al.,

2014, Ryan et al., 2013, Cardoso et al., 2013), and could potentially be transferred to the clinical setting.

7.4 Measuring serum neurofilament light

A sensitive and reliable method of detecting neurodegeneration in blood would offer clear advantages over the neuroimaging techniques used in Chapters three and four, particularly in terms of cost and ease/speed of acquisition. The study reported in Chapter five used a recently developed ultrasensitive assay to measure the concentration of NfL, which plays an important role in maintaining neuronal structural integrity, in the serum of FAD mutation carriers, both pre- and post-symptom onset. The results are very encouraging in that, not only is serum NfL higher in symptomatic mutation carriers compared to controls, despite them being on average only mildly affected (mean global CDR = 0.5), but it was also raised in carriers who were presymptomatic. Also, within the mutation carriers, serum NfL correlated with a proxy measure of disease stage (EYO) and numerous validated and widely used imaging and cognitive measures of disease severity.

Whilst no direct comparison of FAD and sporadic AD was made, the measured NfL concentrations in FAD are similar to those reported previously in sporadic AD (Bacioglu et al., 2016), providing support for findings relating to FAD being relevant to sporadic disease also.

The results suggest that, following further validation in larger cohorts, serum NfL measurement could be a very useful tool in the assessment and on-going monitoring of individuals thought to be at risk of AD, either in clinical trials or even as part of routine clinical assessment. Indeed, compared to other previously proposed blood-based

markers of AD disease activity (Olsson et al., 2016), NfL would appear to be the most promising, especially in the assessment of early (i.e. presymptomatic or mildly symptomatic) neurodegeneration. One potential clinical application would be to "screen" individuals who present with symptoms of cognitive dysfunction, in order to allow stratification of who should and should not go on to have more in-depth, time-consuming and expensive investigations (as the negative predictive value of a low serum NfL is likely to be quite high).

However, an important point to keep in mind is NfL's lack of disease specificity, with it being raised across a range of neurodegenerative conditions (Gisslen et al., 2016, Rojas et al., 2016, Rohrer et al., 2016). This is an issue common to most measures of neuronal injury/loss, but is even more the case with serum NfL than it is with neuroimaging measures, as with neuroimaging you can at least look for disease-specific anatomical patterns of loss. It is therefore more likely that NfL will be used as a marker of disease severity and/or intensity, and to track disease progression, rather than as a diagnostic test. A recent study has found serum NfL is also be elevated in individuals with recent small vessel infarcts, independent of any neurodegeneration (Gattringer et al., 2017). Given the recognition that small vessel pathology is present in a significant proportion of older people with AD, this adds a further layer of complexity when it comes to interpreting NfL measurements in such individuals. Further studies will therefore likely be needed in order to clarify the separate relative contributions of both neurodegenerative and vascular pathology to the final NfL measurement.

Another current limitation of using this assay for the widespread measurement of serum NfL concentrations is that the technology required (i.e. Simoa) is currently limited to just a few centres worldwide; although it is envisaged that this will change in the future.

Whilst NfL is known to form an important part of axonal structural integrity (Lee et al., 1993), the precise anatomical correlate of what raised NfL represents has not previously been investigated in-vivo. The current study found raised NfL levels to be associated with macrostructural atrophy, but it is possible that NfL changes may also be associated with earlier, more specific, and more subtle neuroimaging abnormalities, particularly those linked to early axonal degeneration. Another further study arising from the current work will therefore be to assess the association between serum NfL and DWI metrics in those individuals who are yet to undergo macrostructural atrophy.

7.5 Assessment of accelerated long-term forgetting and subjective cognitive change

Whilst a blood-based marker of neurodegeneration provides a minimally invasive assessment of neuronal loss in AD, an even less invasive assessment modality, which requires no high-tech processing of samples, is to test cognitive performance. The novel approach to cognitive assessment in AD described in chapter six was able to demonstrate consistent differences in the long-term memory retention of presymptomatic mutation carriers (mean EYO > 7 years) and non-carriers, despite there being no difference in initial learning or short interval retention. What was also striking was that the accelerated forgetting that occurred in mutation carriers between 30 minutes and seven days was consistent across verbal and non-verbal domains, and for both recall and recognition.

As outlined in table 6-5 and figure 6-4, this novel finding has significant implications for our understanding of the evolution of cognitive (and particularly episodic memory) impairment in AD. From a practical point of view though it also provides a means of detecting early subtle cognitive decline, potentially at an earlier stage in the disease

than was possible previously. However, one potential issue when considering the widespread use of ALF assessment to track progressive cognitive change over time by taking repeated measurements, is the high potential for individuals anticipating the re-testing at seven days post-learning (or whatever the long interval is set at), and so rehearsing the material in the interim period. The issue of rehearsing, which is a significant methodological consideration whenever one assesses long-term retention (Elliott et al., 2014), was unlikely to have significantly confounded the results presented in chapter six, as none of the participants were told they would be re-tested at seven days. However if the same assessment paradigm were to be used repeatedly in the same individual the potential for rehearsing could become a major issue, which may mean that potentially further revision of the paradigm used in the current study will be needed, although how best to do this would appear to be unclear.

The other main focus of Chapter six was to investigate subjective concerns in presymptomatic mutation carriers, and whether these might be related to ALF. Whilst no participants reported any overt symptoms of decline, and had relatively low scores on a questionnaire of everyday memory (appendix 2) (Thompson and Corcoran, 1992), the mutation carriers did have significantly more subjective concerns than the non-carriers, which is consistent with findings from sporadic AD that subjective decline in cognition is an early feature (Dik et al., 2001, Reisberg et al., 2008, Jessen et al., 2014, Perrotin et al., 2016). Moreover, in carriers, there was a consistent trend towards an association between ALF and subjective cognitive concerns, suggesting that ALF may underpin subtle subjective changes. Therefore, it may also be useful for presymptomatic trials to include detailed assessment of participants' subjective view of their cognition as well as objective testing.

7.6 Common limitations to methodological approaches taken

Whilst specific limitations of the different studies presented in this thesis are discussed in the relevant chapters, there are some over-arching issues, common to all the studies presented, which should be acknowledged. Firstly, the sample sizes available for each study were not large, especially when data was only collected on individuals from FAD families (i.e. no separate healthy controls) such as in Chapters five and six. The sample sizes were primarily limited by the rarity of FAD, limiting the number of eligible participants it was possible to recruit within the data collection window of each study. However, the cohort of FAD families from which the study samples were drawn does remain one of the largest single centre FAD cohorts reported worldwide, and did provide adequate statistical power to demonstrate significant group-level differences in each case. The sample sizes did however prohibit reliable analysis at the level of individual participants. This was attempted for the studies in Chapters three and four (by way of an SVM analysis), although the reliability of the results cannot be certain given the sample sizes. For Chapters five and six such an analysis was not attempted, as the sample sizes were smaller still. Therefore, although the results presented in Chapters three to six give cause for optimism, before any of the disease markers identified in this thesis can be taken forward in to the trial or clinical setting, further validation in larger cohorts, which will enable formal sensitivity and specificity analysis at the level of individual participants, will be required. This is particularly the case if a disease biomarker is to be used for diagnostic purposes (i.e. as a binary discriminator), as opposed to being used to monitor progression only. The requirement for robust evidence in support of a biomarker's use is discussed in detail in a recent document published by the Foundation for the National Institutes of Health (FNIH) (Health, 2016), which outlines the evidentiary criteria that should be met prior to a biomarker receiving regulatory approval.

Another limitation of the studies presented is that three out of four of them involved cross-sectional analysis only, with each participant providing only one data point from a single time point. The exception to this was the cortical thickness study reported in Chapter three, where a longitudinal mixed effects framework was used to quantify progressive change in the marker of interest (i.e. cortical thickness) over time. This mixed effects approach, which used data collected at multiple time points from the same individuals, has the advantage of allowing estimation of the specific point in time (i.e. number of years prior to symptom onset) when significant differences become detectable between those with AD pathology and those without AD pathology. The main reason this was done for the cortical thickness study but not for the others (apart from the increased time that would have been required to collect longitudinal data), is that the methodologies utilised in chapters four, five and six – i.e. measurement of cortical MD, serum NfL and ALF – were all much more novel than cortical thickness, with far less of a prior evidence base to support their efficacy. Therefore, for these newer assessment methods, it was felt to be prudent to carry out cross-sectional studies only in the first instance to assess whether or not cross-sectional group differences are apparent. It is however envisaged that further studies will follow, which will build on what was learned from these initial studies, including assessing evidence of longitudinal change.

The FAD families represented in the studies reported in this thesis are affected by pathogenic mutations in one of two genes – either *PSEN1* or *APP* – with 26 separate mutations represented amongst the 36 families studied. As discussed in section 1.3.5, there can be significant variability in clinical and radiological phenotype, both between mutations within the same gene as well as across the two different genes (Ryan et al., 2016, Scahill et al., 2013). It would have been interesting to compare findings between mutations in *PSEN1* and *APP*, with a view to what it may tell us about differences in

their underlying biology; but this was unfortunately not feasible due to the relatively small number of *APP* (five) mutations compared to *PSEN1* (21). This proportional difference does however mirror the prevalence of mutations in the two genes across the global FAD population (Tang et al., 2016). On one hand, the clinical heterogeneity between the different mutations from the different families studied could be seen as a weakness; however the ability of the different disease markers studied to detect group differences between mutation carriers and non-carriers despite this heterogeneity could also be seen as further validation of the robustness of the markers. Such robustness to inter-individual variability is likely to be valuable if the same markers are to be used in sporadic AD, where significant clinical heterogeneity is known to exist (Warren et al., 2012, Dubois et al., 2014).

The studies reported in this thesis each used the same method of estimating the number of years to/from symptom onset (EYO) that a participant is at a given time point, which was predicted by calculating the difference between the participant's age at assessment and the age at which their affected parent first developed symptoms of progressive decline (see section 2.8). Whilst parental age at onset has been shown to correlate closely with actual age at onset, and to closely relate to other methods of estimating disease onset (e.g. based on family mean or mutation mean age at onset), this remains a proxy measure only (Ryman et al., 2014). It would only be through longer-term follow-up, with each individual being prospectively followed until they themselves developed progressive symptoms, that the actual age at symptom onset can be confirmed. However as in some cases participants were over twenty years from expected onset results from such longitudinal follow-up was not feasible for this thesis

In order to assess the accuracy of EYO calculation, an analysis was performed on those individuals from across the studies reported in chapters three to six who had already developed symptoms or who have since developed symptoms (n=28), to

assess the difference between the estimated age at symptom onset (AAO) (based on parental age at onset) and the actual age at symptom onset. The mean difference between the predicted and actual ages at onset was ±1.9 years (SD=1.6), with only four of the 28 individuals having a discrepancy of greater than 3 years (figure 7-2). Across all 28 individuals, the mean predicted AAO and mean actual AAO were identical (both 43), meaning that there was no systematic tendency to either under or over predict the AAO, with the degree of error centring around zero. Therefore, at the group level, for each of the studies in this thesis, the mean EYO is likely to have been relatively accurate. These findings support the published evidence that, whilst not perfect, estimating AAO based on parental AAO provides in the majority of cases a reasonably accurate prediction of at what age symptoms are likely to begin, and therefore how far away an individual is at a given time point (Ryman et al., 2014). One has to be aware though that in a small proportion of cases the estimated may be inaccurate, but not to the extent that it is likely to invalidate the results.

Whilst the same method being used to calculate EYO across all the studies reported allows direct comparison between the results of the different studies (in terms of how close to onset significant group differences appear to be evident); it can become more difficult when trying to make similar comparisons between other FAD studies reported in the literature. This is because a consistent definition of what is meant by disease "onset" does not appear to exist. A significant number of studies, including the ones presented in this thesis, define onset as being the first point at which symptoms of progressive cognitive decline become evident to either the patient or to those around them (Bateman et al., 2012, Benzinger et al., 2013). However other published studies talk only in terms of time to/from diagnosis of AD (Acosta-Baena et al., 2011, Reiman et al., 2012). The potential downside of the approach to defining onset taken in this thesis (i.e. defining it as first onset of symptoms) is that identification of such an onset is often difficult at the time, given the slow insidious way in which AD progresses, and

so often only becomes clearer in retrospect. However the significant advantage of this method compared to using time to/from AD diagnosis is that (1) symptom onset can usually be identified by anyone (e.g. other family members) regardless of clinical training, and 2) the time between onset of symptoms and what an individual clinician decides as meeting diagnostic criteria for AD can be highly variable. Also, some individuals may present to medical services long after passing the point when they would have first met such diagnostic criteria, leading to further delay in diagnosis. Therefore, despite some potential limitations, the method used for EYO calculation was and still is felt to be the optimum method.

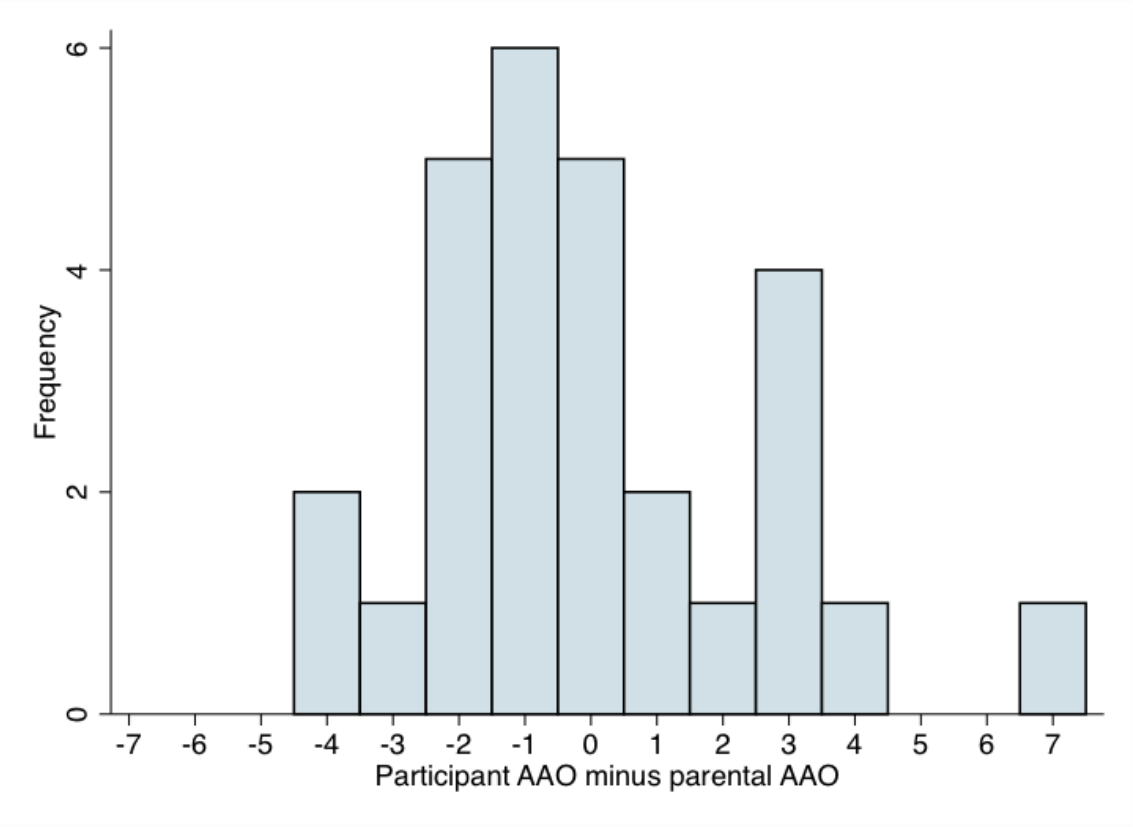

Figure 7-2. Accuracy of predicted AAO vs. actual AAO

A histogram showing the difference between actual and predicted age at onset for the 28 individuals involved in studies reported in this thesis who have already had symptom onset.

7.7 When to test therapeutic interventions and how best to utilize the markers described in this thesis

As discussed in chapter one, there is a growing consensus that new disease-modifying therapies for AD may be most successful at stopping or slowing the disease if they are given early in the disease process, prior to clinically significant neuronal loss. Intervening prior to the onset of clinical symptoms is therefore likely to be preferable, however exactly how close/far from symptom onset a drug will to be most effective will likely depend on a significant number of different factors, including importantly what aspect of the AD pathological cascade the drug is targeting (Sperling et al., 2011b).

To carry out presymptomatic trials, methods of measuring disease activity sensitive enough to detect presymptomatic changes will be required. According to a recently published framework, such disease markers can be categorized as follows (Health, 2016):

- susceptibility/risk biomarker – a measure that indicates the potential for developing a disease or medical condition in an individual without clinically apparent disease.
- diagnostic biomarker – a measure used to identify individuals with the disease or condition of interest or to define a subset of the disease.
- monitoring biomarker – a measure assessed serially and used to detect a change in the degree or extent of disease.
- prognostic biomarker – a measure used to identify likelihood of progression
- predictive biomarker – a measure used to identify individuals who are more likely than similar patients without the biomarker to experience a favorable or unfavorable effect from a specific intervention or exposure.

- pharmacodynamic/response biomarker – a measure used to show that a biological response has occurred in an individual who has received an intervention or exposure.

Based on the results reported earlier in this thesis, each of the four measures of neurodegeneration (or its downstream cognitive effects) assessed in chapters three to six fulfill the criteria of two or more of the above categories (table 7-1), and may therefore each be of value in presymptomatic AD clinical trials in one way or another. Between the four measures, all six of the categories described above are covered, with the greatest body of evidence thus far existing for cortical signature thickness measurement. Ideally though one would want to be certain that the neurodegeneration being detected is due to AD rather than another separate neurodegenerative process, and therefore you would ideally want to combine markers of neurodegeneration with a molecular marker of AD pathology (e.g. PET or CSF). As discussed earlier, assessing AD molecular pathology only is not necessarily enough to stage the disease (Bateman et al., 2012, Villemagne et al., 2013), as Aβ load shows little correlation with underlying neuronal loss or proximity to symptom onset; hence why measures of neurodegeneration are so important.

All four markers could be used to assess which asymptomatic FAD individuals are most susceptible (i.e. at greatest risk) to developing clinical AD in the relatively near future, by assessing which people have already developed sub-clinical neurodegeneration and/or early mild cognitive decline (i.e. ALF), which may help to stratify selection to trials. It is possible that the optimum approach may be to combine one of the three neurodegeneration markers (cortical thickness, cortical MD or serum NfL) with a test of ALF and/or subjective cognitive decline, so that you have evidence not only that an individual is undergoing early neurodegeneration, but also that the neuronal loss is already beginning to have (subtle) downstream effects on their

cognition. Such individuals could be considered to be particularly vulnerable to developing symptomatic disease in the coming years. Other than for cortical signature thickness, for which longitudinal modeling was possible, it is not possible to say for the other markers exactly how far from symptom onset a marker first becomes significantly abnormal, so precisely predicting proximity to onset based on these markers would be difficult. Also, although none of the four markers are specific markers of AD molecular pathology, they would all in theory be capable of defining a subset of the disease – i.e. individuals who have developed early neurodegenerative change but have not yet developed symptomatic decline – and thereby fulfilling criteria for a diagnostic marker.

As cortical thickness measurement (within the cortical signature) has been shown to progressively change within individuals as the disease (i.e. neurodegeneration) progresses it would also be reasonable to consider this as a marker able to monitor progression. Also, if a drug is aiming to slow or halt AD-related neurodegeneration, then a slowing of the rate of cortical thinning could be used as a treatment response biomarker. It is possible that the other markers, or at least cortical MD and NfL, would also be able to serve these functions, although empiric evidence is not yet available. Due to the issues discussed in section 7.5, further work will be needed before repeated measures of ALF, and hence its use to repeatedly monitor disease progression, could be considered as a feasible possibility.

Baseline cortical signature thickness measurement and baseline serum NfL concentration have both been shown to have an association with subsequent rate of neuronal loss (as measured by MRI), and therefore could both also be considered as potential prognostic biomarkers.

Table 7-1 outlines how, based on the current evidence, each of the four individual measures might be helpful in future presymptomatic trials, and ultimately also in the

clinical setting. Following further study, including longitudinal study of cortical MD, serum NfL and ALF, it is likely that these measures will be able to be included in more categories than they are currently. However the table only includes a disease marker in a specific category if there already exists evidence from human study that it is able, at least at the group level, to perform the specific function listed. A further consideration when deciding which, if any of the disease markers studied in this thesis should be used in a particular trial will also depend on certain practical factors, including what resources, including financial, technological, and human expertise, are available.

	Susceptibility/ risk biomarker	Diagnostic biomarker	Monitoring biomarker	Prognostic biomarker	Pharmacodynamic/ response biomarker
Cortical signature thickness	X	X	X	X	X
Cortical MD measurement	X	X			
Serum NfL	X	X		X	
Accelerated long-term forgetting	X	X			

Table 7-1. Current potential biomarker categories for the markers assessed in this thesis based on the current available evidence

7.8 Translational work in sporadic Alzheimer's disease

While the results presented in this thesis are interesting and have helped advance our knowledge and understanding of early neurodegenerative change in FAD, a crucial step in ensuring the findings have maximum impact will be their translation to the much more common sporadic form of AD. Although there is strong evidence that the temporal pattern of early neurodegenerative change is very similar between FAD and sporadic AD, empirical evidence of the utility for each of the individual markers studied here in the sporadic AD setting will be required before their widespread use in sporadic AD could be considered.

As has been discussed, a specific "cortical signature" pattern of thinning has already been identified in sporadic AD (Dickerson et al., 2009, Bakkour et al., 2009), although has not been employed as yet to any significant extent in individuals who are yet to develop clinical symptoms. This is similarly the case for blood measures of neurofilament light, with a resent study demonstrating that it is elevated in symptomatic sporadic AD in a very similar way to what we found in symptomatic FAD (Mattsson et al., 2017); however further work in presymptomatic sporadic AD is required. Following on from the accelerated long-term forgetting work reported here, a recent small study of asymptomatic ApoE4 homozygotes (i.e. individuals at relatively high genetic risk of developing symptomatic sporadic AD in the future) found a similar pattern of forgetting, which suggests that accelerated long-term forgetting is likely to also be a feature of presymptomatic sporadic AD (Zimmermann and Butler, 2018). However, a larger study of ALF in presymptomatic sporadic AD would ideally be required in order to confirm this.

A current on-going study at UCL will hopefully help address some of the unanswered questions outlined above, in terms of assessing the utility of the disease markers

identified in this thesis in a large cohort of individuals with presymptomatic sporadic AD. The Insight 46 study aims to obtain clinical, neuropsychological, MRI, amyloid PET, and blood-based biomarker data on 500 individuals in there 70s (members of an MRC study birth cohort all born during the same week in 1946) at two time-points two years apart (Lane et al., 2017). It is anticipated that approximately 20% (i.e. 100) of the participants will have presymptomatic sporadic AD (as measured by amyloid PET). There are plans to include assessment cortical signature thinning, serum NfL and accelerated long-term forgetting, which will hopefully demonstrate direct translation of findings reported in this thesis to sporadic AD.

7.9 Conclusions

Whilst the global burden AD imposes on society is greater than it has ever been, and is likely to get worse before it gets better, there is cause for cautious optimism. More is known about the disease now than ever before, and work aimed at further advancing knowledge, developing new treatments, and improving methods of assessing the efficacy of those treatments, continues around the world on a greater scale than at any point previously. The move towards conducting therapeutic trials earlier in the disease is a positive one. Study of presymptomatic individuals who carry FAD genetic mutations, both in terms of observational research and now also clinical trials, has and will continue to provide valuable insights that will likely have applicability to sporadic disease. I hope the work presented in this thesis will contribute in some small part to continue to advance understanding of the disease and development of presymptomatic disease markers. The work has prompted a number of further questions, providing a basis for future follow-on studies, in the on-going search for the most effective ways of assessing disease modifying treatments for Alzheimer's disease.

8 Publications arising from this thesis

- Weston, P. S. J, Simpson, I. J., Ryan, N. S., Ourselin, S. & Fox, N. C. 2015. Diffusion imaging changes in grey matter in Alzheimer's disease: a potential marker of early neurodegeneration. *Alzheimers Res Ther*, 7, 47-54.

- Ryan, N. S., Nicholas, J. M., Weston, P. S. J., Liang, Y., Lashley, T., Guerreiro, R., Adamson, G., Kenny, J., Beck, J., Chavez-Gutierrez, L., De Strooper, B., Revesz, T., Holton, J., Mead, S., Rossor, M. N. & Fox, N. C. 2016. Clinical phenotype and genetic associations in autosomal dominant familial Alzheimer's disease: a case series. *Lancet Neurol*, 15, 1326-1335.

- Weston, P. S. J, Nicholas, J. M., Lehmann, M., Ryan, N. S., Liang, Y., Macpherson, K., Modat, M., Rossor, M. N., Schott, J. M., Ourselin, S. & Fox, N. C. 2016a. Presymptomatic cortical thinning in familial Alzheimer disease: A longitudinal MRI study. *Neurology*, 87, 2050-2057.

- Weston, P. S. J., Poole, T., Ryan, N. S., Nair, A., Liang, Y., Macpherson, K., Druyeh, R., Malone, I. B., Ahsan, R. L., Pemberton, H., Klimova, J., Mead, S., Blennow, K., Rossor, M. N., Schott, J. M., Zetterberg, H. & Fox, N. C. 2017. Serum neurofilament light in familial Alzheimer’s disease: a marker of early neurodegeneration. *Neurology*, 89, 2167-2175.

- Weston, P. S. J., Nicholas, J. M., Henley S. M. D., Liang, Y., Macpherson, K., Donnachie, E., Schott, J. M., Rossor, M. N., Crutch, S. J., Butler, C. R., Zeman, A. Z., Fox, N. C. 2018. Accelerated long-term forgetting in presymptomatic

autosomal dominant Alzheimer's disease: A cross-sectional study. *Lancet Neurology*, 17, 123-132.

Appendix 1: The Clinical Dementia Rating Scale scoring structure

Scoring for each domain is as outlined below:

Categories	None: 0	Questionable: 0.5	Mild: 1	Moderate: 2	Severe: 3
Memory (major category)	No memory loss or slight inconsistent forgetfulness	Consistent slight forgetfulness, partial recollection of events, "benign" forgetfulness	Moderate memory loss; more marked for recent events; defect interferes with everyday activities	Severe memory loss; only highly learned material retained; new material rapidly lost	Severe memory less; only fragments remain
Orientation	Fully oriented	Fully oriented except for slight difficulty with time relationships	Moderate difficulty with time relationships; oriented for place at examination; may have geographic disorientation elsewhere	Severe difficulty with time relationships; usually disoriented to time, often to place	Oriented to person only
Judgment and problem solving	Solves everyday problems and handles business and financial affairs, well; judgment good in relation to past performance	Slight impairment in solving problems, similarities, and differences	Moderate difficulties in handling problems, similarities, and differences; social judgment usually maintained	Severely impaired in handling problems, similarities, and differences; social judgment usually impaired	Unable to make judgements or solve problems
Community affairs	Independent function at usual level in job, shopping, and volunteer and social groups	Slight impairment in these activities	Unable to function independently at these activities although may still be engaged in some; appears normal to casual inspection	No pretense of independent function outside home. Appears well enough to be taken to function outside a family home	No pretense of independent function outside home. Appears too ill to be taken to function outside a family home
Home and hobbies	Life at home, hobbies, and intellectual interests are well maintained	Life at home, hobbies, and intellectual interests slightly impaired	Mild but definite impairment in function at home, more difficult chores abandoned, more complicated hobbies and interests abandoned	Only simple chores preserved; very restricted interests, poorly maintained	No significant function at home
Personal care	Fully capable of self-care	Fully capable of self-care	Needs prompting	Requires assistance in dressing, hygiene, keeping of personal effects	Requires much help with personal care; frequent incontinence

The scores for each of the six CDR domains are calculated based on standardized structured interviews with both the participant and a close informant. The scores can be used to calculate both a global CDR, which is based on the most common score an individual receives across the domains (when there is an equal number of two scores the score for memory generally takes precedence) and a CDR sum of boxes (SOB), which is based on the total cumulative score across the six domains.

Appendix 2: Everyday memory questionnaire

In the below questions, please circle your answer according to the following scheme:

A = not at all; B = about once in last 3 months; C = about once a month; D = about once a week; E = about once a day; F = more than once a day

1. forget where you put something, eg. losing something around the house?	A B C D E F
2. fail to recognise places that you are told you have been to often before?	A B C D E F
3. fail to remember a change in your daily routine such as a change in the place where something is kept or a change in the time something happens?	A B C D E F
4. have to go back to check whether you had done something you meant to do?	A B C D E F
5. forget that you were told something yesterday, or a few days ago, and maybe had to be reminded of it	A B C D E F
6. let yourself ramble on to speak about unimportant or irrelevant things?	A B C D E F
7. have difficulty picking up a new skill, eg. finding it hard to learn a new game or to work some gadget after you had practised it once or twice?	A B C D E F
8. find that a word is 'on the tip of your tongue', you know what it is but cannot find it?	A B C D E F
9. forget important details of what you did or forget what happened to you the day before?	A B C D E F
10. forget important details about yourself, eg date of birth, where you live?	A B C D E F
11. when talking to someone, forget what you had just said, maybe saying "what was I talking about?"	A B C D E F
12. when reading a newspaper or magazine, being unable to follow the thread of the story, lose track of what it was about?	A B C D E F
13. forget to tell somebody something important. Perhaps forget to pass on a message or remind someone of something?	A B C D E F
14. get the details of what somebody has told you mixed up or confused?	A B C D E F
15. forget people's names?	A B C D E F
16. get lost or turn in the wrong direction on a journey, on a walk, or in a building you have only been to once or twice before?	A B C D E F
17. repeat to someone what you have told them or ask the same question twice?	A B C D E F
18. fail to recognise by sight a close relative?	A B C D E F

Appendix 3: Accelerated long-term forgetting test materials

AMIPB list recall (list 1)

Date……..

Name……

ID……...

	1	2	3	4	5	6	7	8	9	10	40s	30m	7d
Butter													
Orange													
Ink													
Fire													
Shell													
Salad													
Kitchen													
Goat													
Thunder													
Bag													
Temple													
Needle													
Train													
Skirt													
Hedge													
Score													

AMIPB list recall (list 2)

Date……..

Name……

ID……...

	1	2	3	4	5	6	7	8	9	10	40s	30m	7d
Plant													
Bell													
Perfume													
King													
Coffee													
Thief													
Finger													
Prize													
Mouse													
Window													
Flame													
Bible													
Kiss													
Whistle													
Hammer													
Score													

List recognition (list 1)

Date……..

Name……

ID……...

Correct	**Alternative**	
Butter	Barrel	
Orange	Earth	
Ink	Gun	
Fire	Hall	
Shell	Hammer	
Salad	Frost	
Kitchen	Diamond	
Goat	Flag	
Thunder	Church	
Bag	Hen	
Temple	Ocean	
Needle	Marble	
Train	Lion	
Skirt	Honey	
Hedge	Pigeon	
Score		

List recognition (list 2)

Date……..

Name……

ID……...

Correct	**Alternative**	
Plant	Ankle	
Bell	Crab	
Perfume	Driver	
King	Flag	
Coffee	Hotel	
Thief	Insect	
Finger	Lemon	
Prize	Marble	
Mouse	Ocean	
Window	Pencil	
Flame	Paper	
Bible	Pigeon	
Kiss	Rain	
Whistle	Shower	
Hammer	Worm	
Score		

AMIPB story recall (story 1

Participant ID: …… Date of assessment: initial __ __/__ __/__ __

F/U __ __/__ __/__ __

Trial no:	
Mrs Angela	
Harper	
was sitting in her bedroom	
mending the curtains	
when she heard a noise	
coming from the kitchen.	
She rushed to investigate	
and found a boy	
climbing out of the window	
with her handbag.	
She threw a vase at him	
but it missed	
and he ran off laughing.	
She chased after him	
past the shops	
and into the park	
but he got away	
by squeezing through some railings.	
On her way back home	
Mrs Harper phoned	
the Police.	
She described	
the thief as quite tall	
and neatly dressed.	
He had a scar	
on his face	
But she could not remember	
the colour of his hair.	
Total score (out of 56)	

AMIPB story recall (story 2)

Participant ID: …… Date of assessment: initial __ __/__ __/__ __

F/U __ __/__ __/__ __

Trial no:	
Mr Peter	
Williams	
who died last month	
has left two hundred thousand pounds	
to a charity that provides	
seaside outings	
for the children	
of refugees.	
His younger	
brother,	
who lives in Canada,	
will inherit	
his house,	
his yacht	
and his Rolls-Royce car.	
Mr Williams came from a poor family	
but he was determined to do well.	
He worked extremely hard	
and everyone liked him.	
His first job	
was as a butchers boy	
but he earned extra money	
by doing night work	
in a laundry.	
When he was thirty	
he bought a van	
and started a removals business.	
However, he eventually made his fortune	
selling paintings	
and antique clocks.	
Total score (out of 60)	

Story recognition (story 1)

Date……..
Name……
ID……...

1. What was the lady's name?

a) **Angela** b) Rebecca c) Chloe

2. And her second name?

a) Taylor b) **Harper** c) Andrews

3. What was she doing?

a) **mending the curtains** b) sewing some clothes c) knitting a jumper

4. Where did she hear a noise coming from?

a) the hall b) the dining room c) **the kitchen**

5. What did the boy steal?

a) her husband's wallet b) **her handbag** c) her savings box

6. What did she throw at him?

a) umberella b) plate c) **vase**

7. What happened then?

a) **she chased after him** b) police chased after him c) a neighbor chased after him

8. Where to?

a) past the library b) **past the shops** c) past the bust stop

9. And where into?

a) **the park** b) some flats c) a supermarket

10. How did he get away/escape?

a) by climbing over a fence b) by jumping over a wall? c) **by squeezing through some railings**

11. How did she describe the thief?

a) untidily dressed b) wore glasses c) **neatly dressed**

12. How else did she describe the thief?

a) had threckles on her face b) **had a scar on his face** c) had a ring through his nose

Score /12

Story recognition (story 2)

Date……..
Name……
ID……...

1. What was his name?

a) Mark b) **Peter** c) Jonathan

2. And his second name?

a) **Williams** b) Stevenson c) Jeffrey

3. How much money did he leave?

a) 10 thousand b) **200 thousand** c) 125 thousand

4. What did he leave it to?

a) a charity for sick children b) a charity for endangered animals c) **a charity for the children of refugees**

5. Where does his younger brother live?

a) **Canada** b) America c) China

6. And what will he inherit?

a) helicopter b) **yacht** c) aeroplane

7. And what else?

a) Jeep b) motorbike c) **Rolls-Royce car**

8. What was his first job?

a) **a butcher's boy** b) a baker's boy c) an errand boy

9. Where did he earn extra money?

a) **in a laundry** b) in a pub c) in a shop

10. What did he do next?

a) start a catering business b) start a gardening business c) **start a removals business**

11. What did he sell to eventually make his fortune?

a) marble floors b) **paintings** c) fireplaces

12. And what else?

a) jewellery b) statues c) **antique clocks**

Score /12

AMIPB visual figure (figure 1)

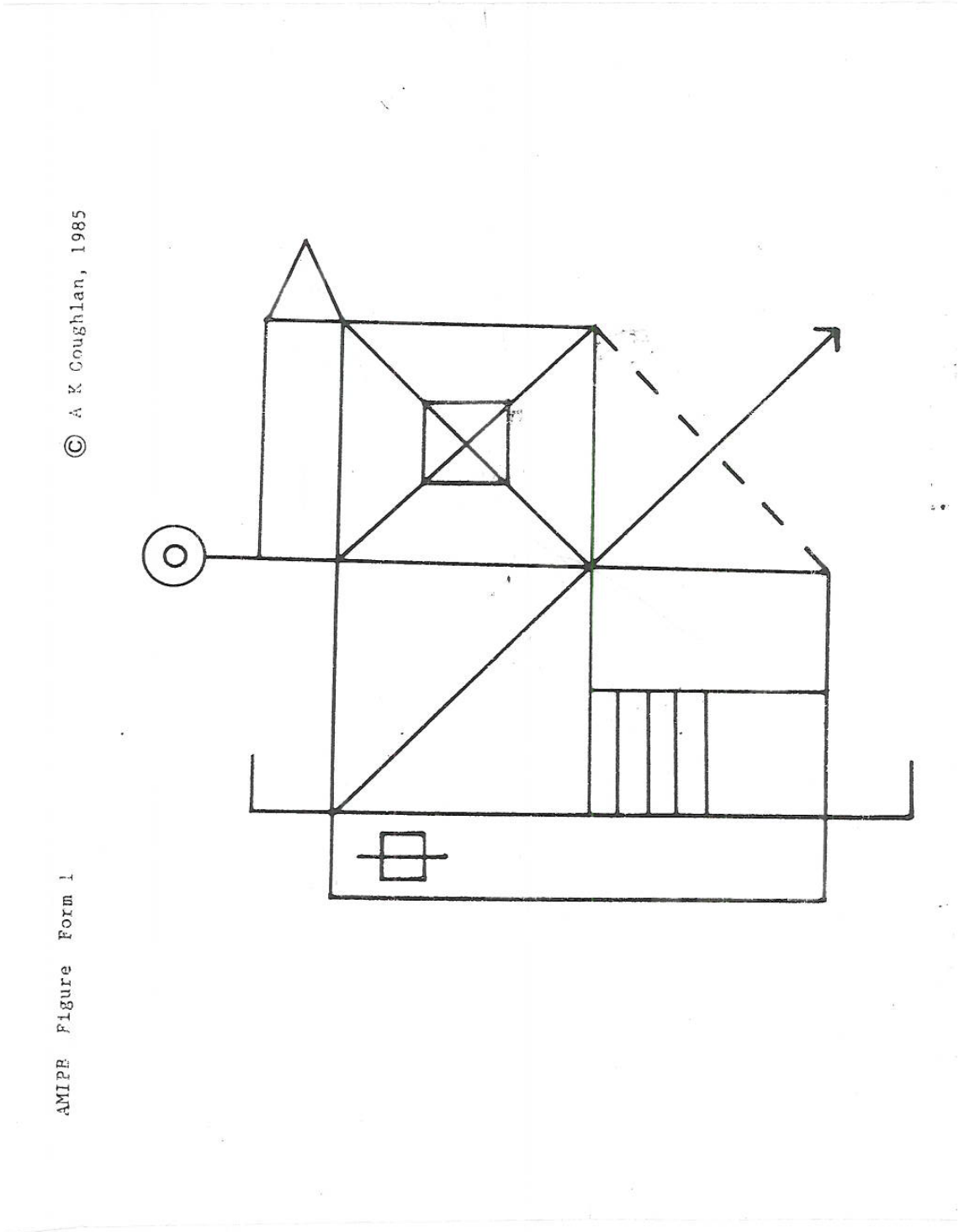

AMIPB visual figure (figure 2)

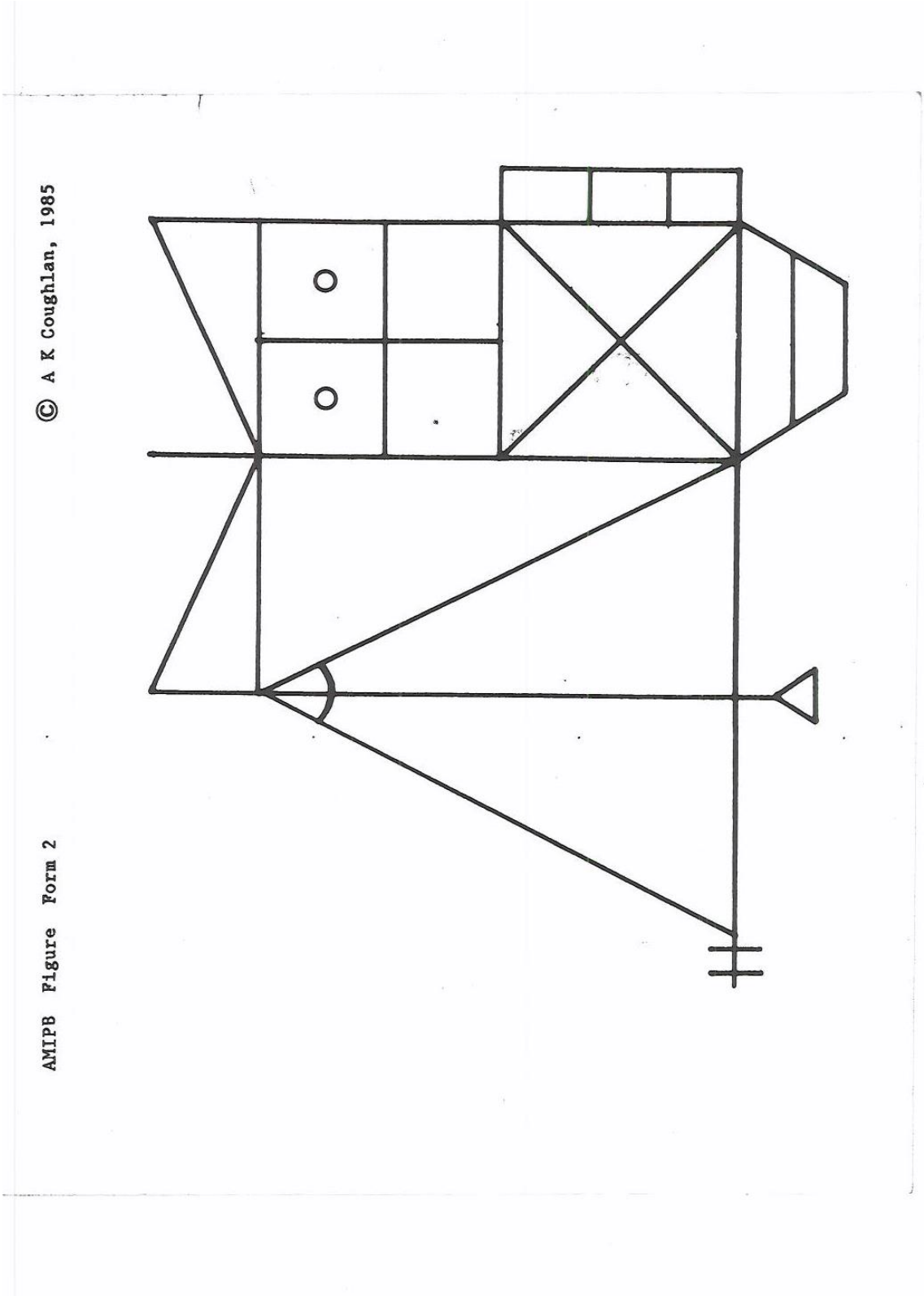

Figure recognition (figure 1)

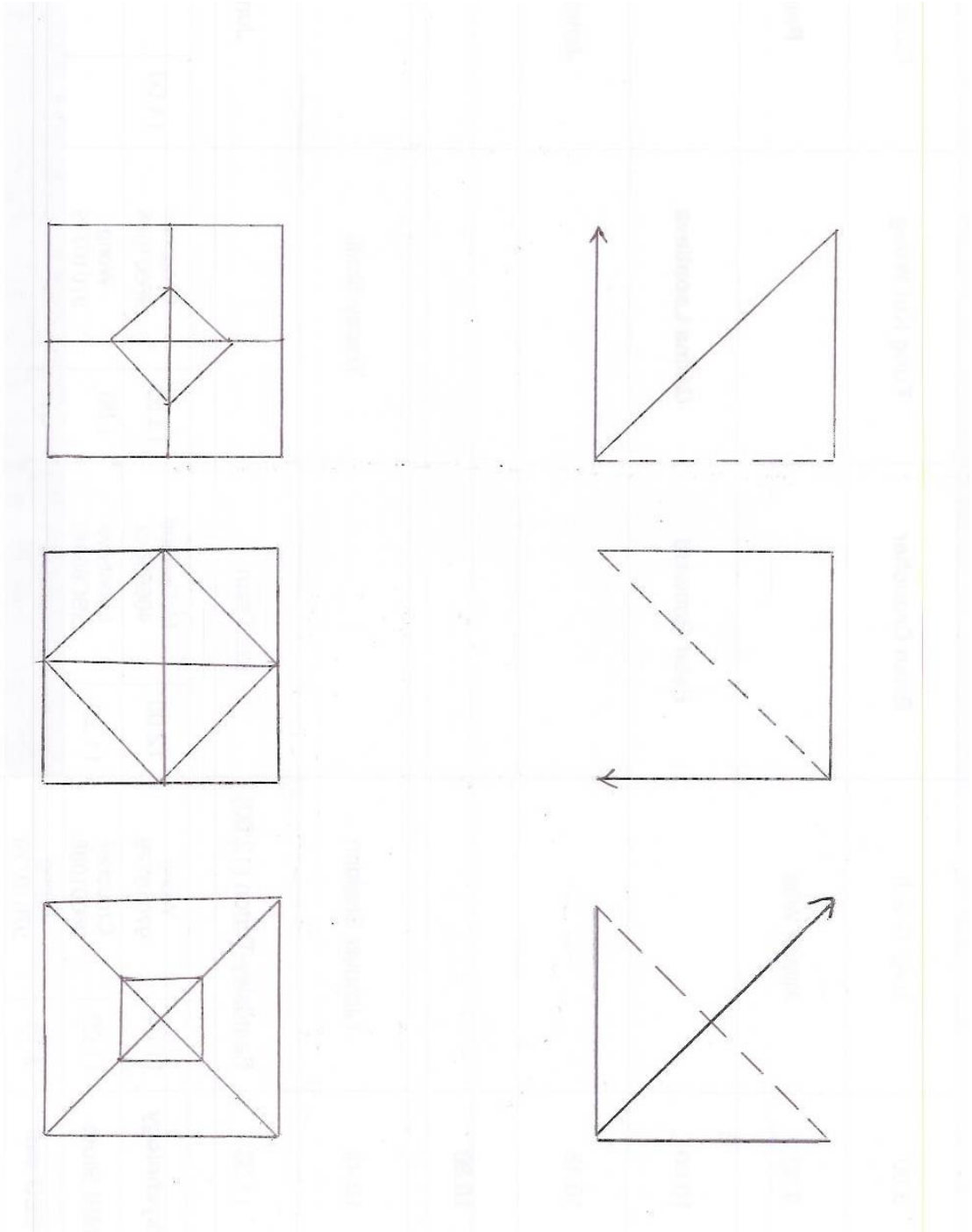

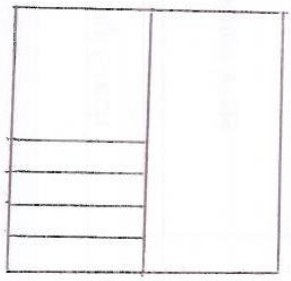

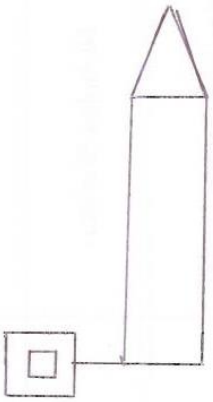

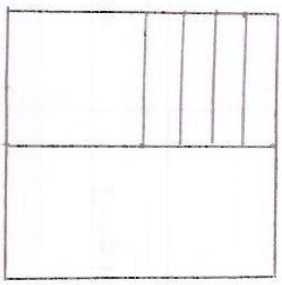

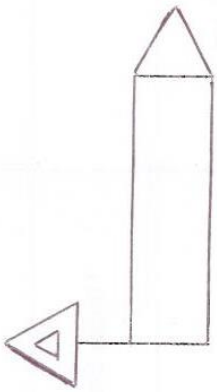

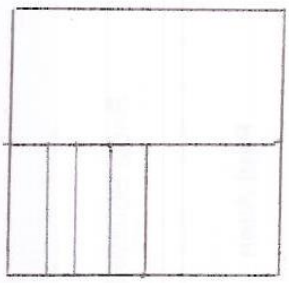

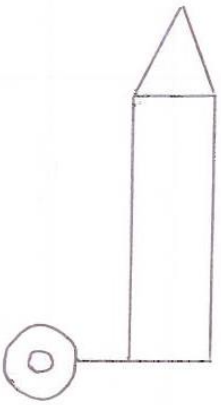

Figure recognition (figure 2)

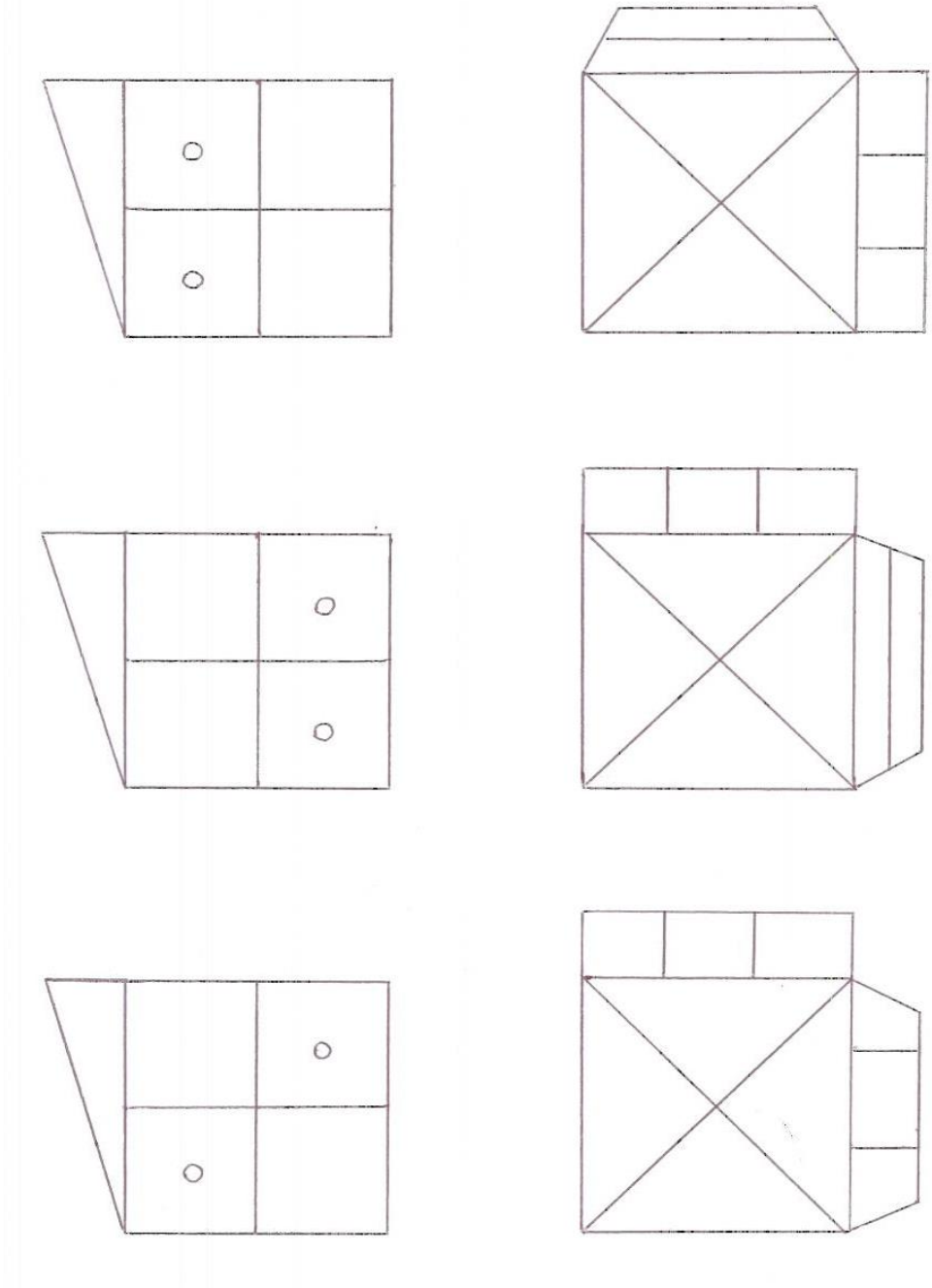

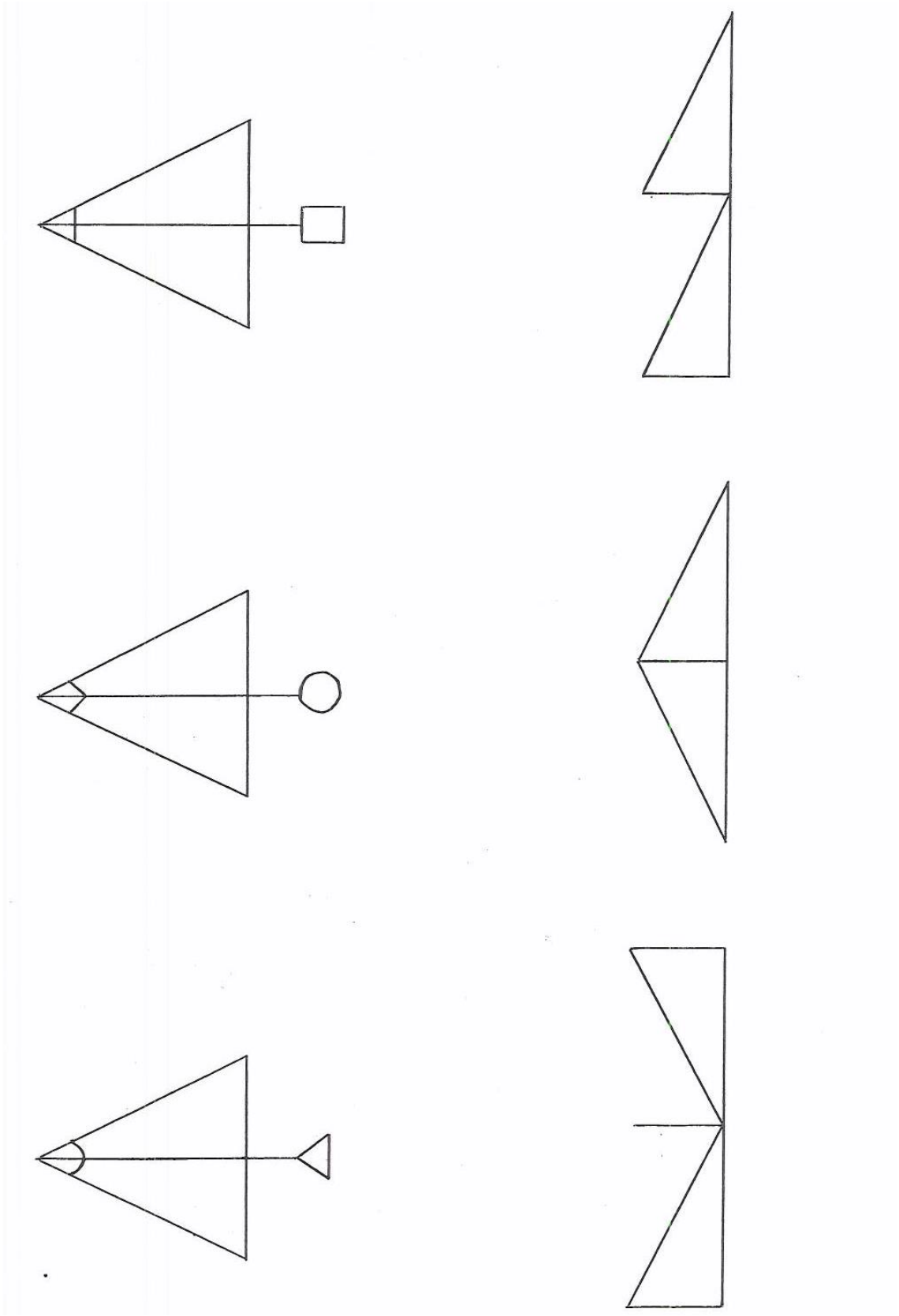

References

Acosta-Baena, N., Sepulveda-Falla, D., Lopera-Gomez, C. M., Jaramillo-Elorza, M. C., Moreno, S., Aguirre-Acevedo, D. C., Saldarriaga, A. & Lopera, F. 2011. Pre-dementia clinical stages in presenilin 1 E280A familial early-onset Alzheimer's disease: a retrospective cohort study. *Lancet Neurol,* 10**,** 213-20.

Alexander, D. C., Pierpaoli, C., Basser, P. J. & Gee, J. C. 2001. Spatial transformations of diffusion tensor magnetic resonance images. *IEEE Trans Med Imaging,* 20**,** 1131-9.

Allison, S. L., Fagan, A. M., Morris, J. C. & Head, D. 2016. Spatial Navigation in Preclinical Alzheimer's Disease. *J Alzheimers Dis,* 52**,** 77-90.

Ally, B. A., Hussey, E. P., Ko, P. C. & Molitor, R. J. 2013. Pattern separation and pattern completion in Alzheimer's disease: evidence of rapid forgetting in amnestic mild cognitive impairment. *Hippocampus,* 23**,** 1246-58.

Andersson, J. L. & Skare, S. 2002. A model-based method for retrospective correction of geometric distortions in diffusion-weighted EPI. *Neuroimage,* 16**,** 177-99.

Anstey, K. J., Cherbuin, N., Budge, M. & Young, J. 2011. Body mass index in midlife and late-life as a risk factor for dementia: a meta-analysis of prospective studies. *Obes Rev,* 12**,** e426-37.

Anstey, K. J., Mack, H. A. & Cherbuin, N. 2009. Alcohol consumption as a risk factor for dementia and cognitive decline: meta-analysis of prospective studies. *Am J Geriatr Psychiatry,* 17**,** 542-55.

Apostolova, L. G., Hwang, K. S., Medina, L. D., Green, A. E., Braskie, M. N., Dutton, R. A., Lai, J., Geschwind, D. H., Cummings, J. L., Thompson, P. M. & Ringman, J. M. 2011. Cortical and hippocampal atrophy in patients with autosomal dominant familial Alzheimer's disease. *Dement Geriatr Cogn Disord,* 32**,** 118-25.

Arango-Lasprilla, J. C., Cuetos, F., Valencia, C., Uribe, C. & Lopera, F. 2007. Cognitive changes in the preclinical phase of familial Alzheimer's disease. *J Clin Exp Neuropsychol,* 29**,** 892-900.

Ardila, A., Lopera, F., Rosselli, M., Moreno, S., Madrigal, L., Arango-Lasprilla, J. C., Arcos, M., Murcia, C., Arango-Viana, J. C., Ossa, J., Goate, A. & Kosik, K. S. 2000. Neuropsychological

profile of a large kindred with familial Alzheimer's disease caused by the E280A single presenilin-1 mutation. *Arch Clin Neuropsychol,* 15**,** 515-28.

Arriagada, P. V., Growdon, J. H., Hedley-Whyte, E. T. & Hyman, B. T. 1992. Neurofibrillary tangles but not senile plaques parallel duration and severity of Alzheimer's disease. *Neurology,* 42**,** 631-9.

Ashburner, J. & Friston, K. J. 2000. Voxel-based morphometry--the methods. *Neuroimage,* 11**,** 805-21.

Assaf, Y. & Basser, P. J. 2005. Composite hindered and restricted model of diffusion (CHARMED) MR imaging of the human brain. *Neuroimage,* 27**,** 48-58.

Association, A. S. 2015. 2015 Alzheimer's disease facts and figures. *Alzheimers Dement,* 11**,** 332-84.

Atherton, K. E., Nobre, A. C., Zeman, A. Z. & Butler, C. R. 2014. Sleep-dependent memory consolidation and accelerated forgetting. *Cortex,* 54**,** 92-105.

Bacioglu, M., Maia, L. F., Preische, O., Schelle, J., Apel, A., Kaeser, S. A., Schweighauser, M., Eninger, T., Lambert, M., Pilotto, A., Shimshek, D. R., Neumann, U., Kahle, P. J., Staufenbiel, M., Neumann, M., Maetzler, W., Kuhle, J. & Jucker, M. 2016. Neurofilament Light Chain in Blood and CSF as Marker of Disease Progression in Mouse Models and in Neurodegenerative Diseases. *Neuron*.

Backman, L., Small, B. J. & Fratiglioni, L. 2001. Stability of the preclinical episodic memory deficit in Alzheimer's disease. *Brain,* 124**,** 96-102.

Bakkour, A., Morris, J. C. & Dickerson, B. C. 2009. The cortical signature of prodromal AD: regional thinning predicts mild AD dementia. *Neurology,* 72**,** 1048-55.

Barbagallo, G., Nicoletti, G., Cherubini, A., Trotta, M., Tallarico, T., Chiriaco, C., Nistico, R., Salvino, D., Bono, F., Valentino, P. & Quattrone, A. 2014. Diffusion tensor MRI changes in gray structures of the frontal-subcortical circuits in amyotrophic lateral sclerosis. *Neurol Sci*.

Barnes, J., Ridgway, G. R., Bartlett, J., Henley, S. M., Lehmann, M., Hobbs, N., Clarkson, M. J., Macmanus, D. G., Ourselin, S. & Fox, N. C. 2010. Head size, age and gender adjustment in MRI studies: a necessary nuisance? *Neuroimage,* 53**,** 1244-55.

Baron, J. C., Chetelat, G., Desgranges, B., Perchey, G., Landeau, B., De La Sayette, V. & Eustache, F. 2001. In vivo mapping of

gray matter loss with voxel-based morphometry in mild Alzheimer's disease. *Neuroimage,* 14**,** 298-309.

Barthel, H., Gertz, H. J., Dresel, S., Peters, O., Bartenstein, P., Buerger, K., Hiemeyer, F., Wittemer-Rump, S. M., Seibyl, J., Reininger, C., Sabri, O. & Florbetaben Study, G. 2011. Cerebral amyloid-beta PET with florbetaben (18F) in patients with Alzheimer's disease and healthy controls: a multicentre phase 2 diagnostic study. *Lancet Neurol,* 10**,** 424-35.

Bartus, R. T., Dean, R. L., 3rd, Beer, B. & Lippa, A. S. 1982. The cholinergic hypothesis of geriatric memory dysfunction. *Science,* 217**,** 408-14.

Bateman, R. J., Aisen, P. S., De Strooper, B., Fox, N. C., Lemere, C. A., Ringman, J. M., Salloway, S., Sperling, R. A., Windisch, M. & Xiong, C. 2011. Autosomal-dominant Alzheimer's disease: a review and proposal for the prevention of Alzheimer's disease. *Alzheimers Res Ther,* 3**,** 1.

Bateman, R. J., Xiong, C., Benzinger, T. L., Fagan, A. M., Goate, A., Fox, N. C., Marcus, D. S., Cairns, N. J., Xie, X., Blazey, T. M., Holtzman, D. M., Santacruz, A., Buckles, V., Oliver, A., Moulder, K., Aisen, P. S., Ghetti, B., Klunk, W. E., Mcdade, E., Martins, R. N., Masters, C. L., Mayeux, R., Ringman, J. M., Rossor, M. N., Schofield, P. R., Sperling, R. A., Salloway, S., Morris, J. C. & Dominantly Inherited Alzheimer, N. 2012. Clinical and biomarker changes in dominantly inherited Alzheimer's disease. *N Engl J Med,* 367**,** 795-804.

Bayer, T. A., Cappai, R., Masters, C. L., Beyreuther, K. & Multhaup, G. 1999. It all sticks together--the APP-related family of proteins and Alzheimer's disease. *Mol Psychiatry,* 4**,** 524-8.

Beglopoulos, V., Tulloch, J., Roe, A. D., Daumas, S., Ferrington, L., Watson, R., Fan, Z., Hyman, B. T., Kelly, P. A., Bard, F. & Morris, R. G. 2016. Early detection of cryptic memory and glucose uptake deficits in pre-pathological APP mice. *Nat Commun,* 7**,** 11761.

Bennett, I. J., Golob, E. J., Parker, E. S. & Starr, A. 2006. Memory evaluation in mild cognitive impairment using recall and recognition tests. *J Clin Exp Neuropsychol,* 28**,** 1408-22.

Benzinger, T. L., Blazey, T., Jack, C. R., Jr., Koeppe, R. A., Su, Y., Xiong, C., Raichle, M. E., Snyder, A. Z., Ances, B. M., Bateman, R. J., Cairns, N. J., Fagan, A. M., Goate, A., Marcus, D. S., Aisen, P. S., Christensen, J. J., Ercole, L., Hornbeck, R. C., Farrar, A. M., Aldea, P., Jasielec, M. S., Owen, C. J., Xie, X., Mayeux, R., Brickman, A., Mcdade, E., Klunk, W., Mathis, C. A., Ringman, J., Thompson, P. M.,

Ghetti, B., Saykin, A. J., Sperling, R. A., Johnson, K. A., Salloway, S., Correia, S., Schofield, P. R., Masters, C. L., Rowe, C., Villemagne, V. L., Martins, R., Ourselin, S., Rossor, M. N., Fox, N. C., Cash, D. M., Weiner, M. W., Holtzman, D. M., Buckles, V. D., Moulder, K. & Morris, J. C. 2013. Regional variability of imaging biomarkers in autosomal dominant Alzheimer's disease. *Proc Natl Acad Sci U S A,* 110**,** E4502-9.

Bergem, A. L. & Lannfelt, L. 1997. Apolipoprotein E type epsilon4 allele, heritability and age at onset in twins with Alzheimer disease and vascular dementia. *Clin Genet,* 52**,** 408-13.

Bierer, L. M., Hof, P. R., Purohit, D. P., Carlin, L., Schmeidler, J., Davis, K. L. & Perl, D. P. 1995. Neocortical neurofibrillary tangles correlate with dementia severity in Alzheimer's disease. *Arch Neurol,* 52**,** 81-8.

Biomarkers Definitions Working, G. 2001. Biomarkers and surrogate endpoints: preferred definitions and conceptual framework. *Clin Pharmacol Ther,* 69**,** 89-95.

Blake, R. V., Wroe, S. J., Breen, E. K. & Mccarthy, R. A. 2000. Accelerated forgetting in patients with epilepsy: evidence for an impairment in memory consolidation. *Brain,* 123 Pt 3**,** 472-83.

Blanc, F., Colloby, S. J., Philippi, N., De Petigny, X., Jung, B., Demuynck, C., Phillipps, C., Anthony, P., Thomas, A., Bing, F., Lamy, J., Martin-Hunyadi, C., O'brien, J. T., Cretin, B., Mckeith, I., Armspach, J. P. & Taylor, J. P. 2015. Cortical Thickness in Dementia with Lewy Bodies and Alzheimer's Disease: A Comparison of Prodromal and Dementia Stages. *PLoS One,* 10**,** e0127396.

Bland, J. M. & Altman, D. G. 1986. Statistical methods for assessing agreement between two methods of clinical measurement. *Lancet,* 1**,** 307-10.

Blessed, G., Tomlinson, B. E. & Roth, M. 1968. The association between quantitative measures of dementia and of senile change in the cerebral grey matter of elderly subjects. *Br J Psychiatry,* 114**,** 797-811.

Boivin, D. B., Czeisler, C. A., Dijk, D. J., Duffy, J. F., Folkard, S., Minors, D. S., Totterdell, P. & Waterhouse, J. M. 1997. Complex interaction of the sleep-wake cycle and circadian phase modulates mood in healthy subjects. *Arch Gen Psychiatry,* 54**,** 145-52.

Bontempi, B., Laurent-Demir, C., Destrade, C. & Jaffard, R. 1999. Time-dependent reorganization of brain circuitry underlying long-term memory storage. *Nature,* 400**,** 671-5.

Booij, B. B., Lindahl, T., Wetterberg, P., Skaane, N. V., Saebo, S., Feten, G., Rye, P. D., Kristiansen, L. I., Hagen, N., Jensen, M., Bardsen, K., Winblad, B., Sharma, P. & Lonneborg, A. 2011. A gene expression pattern in blood for the early detection of Alzheimer's disease. *J Alzheimers Dis,* 23**,** 109-19.

Boutajangout, A., Ingadottir, J., Davies, P. & Sigurdsson, E. M. 2011a. Passive immunization targeting pathological phospho-tau protein in a mouse model reduces functional decline and clears tau aggregates from the brain. *J Neurochem,* 118**,** 658-67.

Boutajangout, A., Sigurdsson, E. M. & Krishnamurthy, P. K. 2011b. Tau as a therapeutic target for Alzheimer's disease. *Curr Alzheimer Res,* 8**,** 666-77.

Bozzali, M., Cercignani, M., Sormani, M. P., Comi, G. & Filippi, M. 2002a. Quantification of brain gray matter damage in different MS phenotypes by use of diffusion tensor MR imaging. *AJNR Am J Neuroradiol,* 23**,** 985-8.

Bozzali, M., Falini, A., Franceschi, M., Cercignani, M., Zuffi, M., Scotti, G., Comi, G. & Filippi, M. 2002b. White matter damage in Alzheimer's disease assessed in vivo using diffusion tensor magnetic resonance imaging. *J Neurol Neurosurg Psychiatry,* 72**,** 742-6.

Braak, H. & Braak, E. 1991. Neuropathological stageing of Alzheimer-related changes. *Acta Neuropathol,* 82**,** 239-59.

Braak, H. & Braak, E. 1995. Staging of Alzheimer's disease-related neurofibrillary changes. *Neurobiol Aging,* 16**,** 271-8; discussion 278-84.

Braak, H. & Braak, E. 1998. Evolution of neuronal changes in the course of Alzheimer's disease. *J Neural Transm Suppl,* 53**,** 127-40.

Bray, K. 2005. Mental Capacity Act 2005 England and Wales: a short summary. *Nurs Crit Care,* 10**,** 300-1.

Brier, M. R., Gordon, B., Friedrichsen, K., Mccarthy, J., Stern, A., Christensen, J., Owen, C., Aldea, P., Su, Y., Hassenstab, J., Cairns, N. J., Holtzman, D. M., Fagan, A. M., Morris, J. C., Benzinger, T. L. & Ances, B. M. 2016. Tau and Abeta imaging, CSF measures, and cognition in Alzheimer's disease. *Sci Transl Med,* 8**,** 338ra66.

Brodaty, H., Seeher, K. & Gibson, L. 2012. Dementia time to death: a systematic literature review on survival time and years of life lost in people with dementia. *Int Psychogeriatr,* 24**,** 1034-45.

Brun, A. & Englund, E. 1981. Regional pattern of degeneration in Alzheimer's disease: neuronal loss and histopathological grading. *Histopathology,* 5**,** 549-64.

Buckley, R. F., Maruff, P., Ames, D., Bourgeat, P., Martins, R. N., Masters, C. L., Rainey-Smith, S., Lautenschlager, N., Rowe, C. C., Savage, G., Villemagne, V. L., Ellis, K. A. & Study, A. 2016a. Subjective memory decline predicts greater rates of clinical progression in preclinical Alzheimer's disease. *Alzheimers Dement,* 12**,** 796-804.

Buckley, R. F., Villemagne, V. L., Masters, C. L., Ellis, K. A., Rowe, C. C., Johnson, K., Sperling, R. & Amariglio, R. 2016b. A Conceptualization of the Utility of Subjective Cognitive Decline in Clinical Trials of Preclinical Alzheimer's Disease. *J Mol Neurosci,* 60**,** 354-361.

Buee, L., Bussiere, T., Buee-Scherrer, V., Delacourte, A. & Hof, P. R. 2000. Tau protein isoforms, phosphorylation and role in neurodegenerative disorders. *Brain Res Brain Res Rev,* 33**,** 95-130.

Butler, C. R., Bhaduri, A., Acosta-Cabronero, J., Nestor, P. J., Kapur, N., Graham, K. S., Hodges, J. R. & Zeman, A. Z. 2009. Transient epileptic amnesia: regional brain atrophy and its relationship to memory deficits. *Brain,* 132**,** 357-68.

Butler, C. R., Graham, K. S., Hodges, J. R., Kapur, N., Wardlaw, J. M. & Zeman, A. Z. 2007. The syndrome of transient epileptic amnesia. *Ann Neurol,* 61**,** 587-98.

Byth, K. & Cox, D. R. 2005. On the relation between initial value and slope. *Biostatistics,* 6**,** 395-403.

Cardoso, J. M., Leung, K., Modat, M., Keihaninejad, S., Cash, D., Barnes, J., Fox, N. C., Ourselin, S. & Alzheimer's Disease Neuroimaging, I. 2013. STEPS: Similarity and Truth Estimation for Propagated Segmentations and its application to hippocampal segmentation and brain parcelation. *Med Image Anal,* 17**,** 671-84.

Casanova, R., Hsu, F. C., Sink, K. M., Rapp, S. R., Williamson, J. D., Resnick, S. M., Espeland, M. A. & Alzheimer's Disease Neuroimaging, I. 2013. Alzheimer's disease risk assessment using large-scale machine learning methods. *PLoS One,* 8**,** e77949.

Casanova, R., Varma, S., Simpson, B., Kim, M., An, Y., Saldana, S., Riveros, C., Moscato, P., Griswold, M., Sonntag, D., Wahrheit, J., Klavins, K., Jonsson, P. V., Eiriksdottir, G., Aspelund, T., Launer, L. J., Gudnason, V., Quigley, C. L. & Thambisetty, M. 2016. Blood metabolite markers of preclinical Alzheimer's

disease in two longitudinally followed cohorts of older individuals. *Alzheimers Dement,* 12**,** 815-22.

Cash, D. M., Ridgway, G. R., Liang, Y., Ryan, N. S., Kinnunen, K. M., Yeatman, T., Malone, I. B., Benzinger, T. L., Jack, C. R., Jr., Thompson, P. M., Ghetti, B. F., Saykin, A. J., Masters, C. L., Ringman, J. M., Salloway, S. P., Schofield, P. R., Sperling, R. A., Cairns, N. J., Marcus, D. S., Xiong, C., Bateman, R. J., Morris, J. C., Rossor, M. N., Ourselin, S., Fox, N. C. & Dominantly Inherited Alzheimer, N. 2013. The pattern of atrophy in familial Alzheimer disease: volumetric MRI results from the DIAN study. *Neurology,* 81**,** 1425-33.

Cassel, A., Morris, R., Koutroumanidis, M. & Kopelman, M. 2016. Forgetting in temporal lobe epilepsy: When does it become accelerated? *Cortex,* 78**,** 70-84.

Chavez-Gutierrez, L., Bammens, L., Benilova, I., Vandersteen, A., Benurwar, M., Borgers, M., Lismont, S., Zhou, L., Van Cleynenbreugel, S., Esselmann, H., Wiltfang, J., Serneels, L., Karran, E., Gijsen, H., Schymkowitz, J., Rousseau, F., Broersen, K. & De Strooper, B. 2012. The mechanism of gamma-Secretase dysfunction in familial Alzheimer disease. *EMBO J,* 31**,** 2261-74.

Chen, P., Ratcliff, G., Belle, S. H., Cauley, J. A., Dekosky, S. T. & Ganguli, M. 2001. Patterns of cognitive decline in presymptomatic Alzheimer disease: a prospective community study. *Arch Gen Psychiatry,* 58**,** 853-8.

Chiapponi, C., Piras, F., Piras, F., Fagioli, S., Caltagirone, C. & Spalletta, G. 2013. Cortical grey matter and subcortical white matter brain microstructural changes in schizophrenia are localised and age independent: a case-control diffusion tensor imaging study. *PLoS One,* 8**,** e75115.

Chu, C., Hsu, A. L., Chou, K. H., Bandettini, P., Lin, C. & Alzheimer's Disease Neuroimaging, I. 2012. Does feature selection improve classification accuracy? Impact of sample size and feature selection on classification using anatomical magnetic resonance images. *Neuroimage,* 60**,** 59-70.

Clark, C. M., Schneider, J. A., Bedell, B. J., Beach, T. G., Bilker, W. B., Mintun, M. A., Pontecorvo, M. J., Hefti, F., Carpenter, A. P., Flitter, M. L., Krautkramer, M. J., Kung, H. F., Coleman, R. E., Doraiswamy, P. M., Fleisher, A. S., Sabbagh, M. N., Sadowsky, C. H., Reiman, E. P., Zehntner, S. P., Skovronsky, D. M. & Group, A. a. S. 2011. Use of florbetapir-PET for imaging beta-amyloid pathology. *JAMA,* 305**,** 275-83.

Clarkson, M. J., Cardoso, M. J., Ridgway, G. R., Modat, M., Leung, K. K., Rohrer, J. D., Fox, N. C. & Ourselin, S. 2011. A comparison of voxel and surface based cortical thickness estimation methods. *Neuroimage,* 57**,** 856-65.

Cleveland, D. W., Hwo, S. Y. & Kirschner, M. W. 1977. Physical and chemical properties of purified tau factor and the role of tau in microtubule assembly. *J Mol Biol,* 116**,** 227-47.

Corder, E. H., Saunders, A. M., Strittmatter, W. J., Schmechel, D. E., Gaskell, P. C., Small, G. W., Roses, A. D., Haines, J. L. & Pericak-Vance, M. A. 1993. Gene dose of apolipoprotein E type 4 allele and the risk of Alzheimer's disease in late onset families. *Science,* 261**,** 921-3.

Coughlan, A. K. & Hollows, S. E. 1985. *The adult memory and information processing battery (AMIPB) : test manual,* Leeds, A K Coughlin, Psychology Dept, St James' Hosp.

Courtney, C., Farrell, D., Gray, R., Hills, R., Lynch, L., Sellwood, E., Edwards, S., Hardyman, W., Raftery, J., Crome, P., Lendon, C., Shaw, H., Bentham, P. & Group, A. D. C. 2004. Long-term donepezil treatment in 565 patients with Alzheimer's disease (AD2000): randomised double-blind trial. *Lancet,* 363**,** 2105-15.

Coyle, J. T., Price, D. L. & Delong, M. R. 1983. Alzheimer's disease: a disorder of cortical cholinergic innervation. *Science,* 219**,** 1184-90.

Crutch, S. J., Lehmann, M., Schott, J. M., Rabinovici, G. D., Rossor, M. N. & Fox, N. C. 2012. Posterior cortical atrophy. *Lancet Neurol,* 11**,** 170-8.

Cummings, J. L. 2000. Cholinesterase inhibitors: A new class of psychotropic compounds. *Am J Psychiatry,* 157**,** 4-15.

Daga, P., Pendse, T., Modat, M., White, M., Mancini, L., Winston, G. P., Mcevoy, A. W., Thornton, J., Yousry, T., Drobnjak, I., Duncan, J. S. & Ourselin, S. 2014. Susceptibility artefact correction using dynamic graph cuts: application to neurosurgery. *Med Image Anal,* 18**,** 1132-42.

Dale, A. M., Fischl, B. & Sereno, M. I. 1999. Cortical surface-based analysis. I. Segmentation and surface reconstruction. *Neuroimage,* 9**,** 179-94.

De La Torre, J. C. 2002. Alzheimer disease as a vascular disorder: nosological evidence. *Stroke,* 33**,** 1152-62.

De Leon, M. J., Convit, A., Wolf, O. T., Tarshish, C. Y., Desanti, S., Rusinek, H., Tsui, W., Kandil, E., Scherer, A. J., Roche, A., Imossi, A., Thorn, E., Bobinski, M., Caraos, C., Lesbre, P., Schlyer, D., Poirier, J., Reisberg, B. & Fowler, J. 2001.

Prediction of cognitive decline in normal elderly subjects with 2-[(18)F]fluoro-2-deoxy-D-glucose/poitron-emission tomography (FDG/PET). *Proc Natl Acad Sci U S A,* 98**,** 10966-71.

De Strooper, B. 2010. Proteases and proteolysis in Alzheimer disease: a multifactorial view on the disease process. *Physiol Rev,* 90**,** 465-94.

De Strooper, B., Annaert, W., Cupers, P., Saftig, P., Craessaerts, K., Mumm, J. S., Schroeter, E. H., Schrijvers, V., Wolfe, M. S., Ray, W. J., Goate, A. & Kopan, R. 1999. A presenilin-1-dependent gamma-secretase-like protease mediates release of Notch intracellular domain. *Nature,* 398**,** 518-22.

De Strooper, B., Saftig, P., Craessaerts, K., Vanderstichele, H., Guhde, G., Annaert, W., Von Figura, K. & Van Leuven, F. 1998. Deficiency of presenilin-1 inhibits the normal cleavage of amyloid precursor protein. *Nature,* 391**,** 387-90.

Demaerel, P., Heiner, L., Robberecht, W., Sciot, R. & Wilms, G. 1999. Diffusion-weighted MRI in sporadic Creutzfeldt-Jakob disease. *Neurology,* 52**,** 205-8.

Diaz-De-Grenu, L. Z., Acosta-Cabronero, J., Chong, Y. F., Pereira, J. M., Sajjadi, S. A., Williams, G. B. & Nestor, P. J. 2014. A brief history of voxel-based grey matter analysis in Alzheimer's disease. *J Alzheimers Dis,* 38**,** 647-59.

Dickerson, B. C., Bakkour, A., Salat, D. H., Feczko, E., Pacheco, J., Greve, D. N., Grodstein, F., Wright, C. I., Blacker, D., Rosas, H. D., Sperling, R. A., Atri, A., Growdon, J. H., Hyman, B. T., Morris, J. C., Fischl, B. & Buckner, R. L. 2009. The cortical signature of Alzheimer's disease: regionally specific cortical thinning relates to symptom severity in very mild to mild AD dementia and is detectable in asymptomatic amyloid-positive individuals. *Cereb Cortex,* 19**,** 497-510.

Dickerson, B. C., Fenstermacher, E., Salat, D. H., Wolk, D. A., Maguire, R. P., Desikan, R., Pacheco, J., Quinn, B. T., Van Der Kouwe, A., Greve, D. N., Blacker, D., Albert, M. S., Killiany, R. J. & Fischl, B. 2008. Detection of cortical thickness correlates of cognitive performance: Reliability across MRI scan sessions, scanners, and field strengths. *Neuroimage,* 39**,** 10-8.

Dickerson, B. C., Stoub, T. R., Shah, R. C., Sperling, R. A., Killiany, R. J., Albert, M. S., Hyman, B. T., Blacker, D. & Detoledo-Morrell, L. 2011. Alzheimer-signature MRI biomarker predicts AD dementia in cognitively normal adults. *Neurology,* 76**,** 1395-402.

Dickerson, B. C., Wolk, D. A. & Alzheimer's Disease Neuroimaging, I. 2012. MRI cortical thickness biomarker predicts AD-like CSF and cognitive decline in normal adults. *Neurology,* 78**,** 84-90.

Dickerson, B. C., Wolk, D. A. & Alzheimer's Disease Neuroimaging, I. 2013. Biomarker-based prediction of progression in MCI: Comparison of AD signature and hippocampal volume with spinal fluid amyloid-beta and tau. *Front Aging Neurosci,* 5**,** 55.

Dik, M. G., Jonker, C., Comijs, H. C., Bouter, L. M., Twisk, J. W., Van Kamp, G. J. & Deeg, D. J. 2001. Memory complaints and APOE-epsilon4 accelerate cognitive decline in cognitively normal elderly. *Neurology,* 57**,** 2217-22.

Diniz, B. S., Butters, M. A., Albert, S. M., Dew, M. A. & Reynolds, C. F., 3rd 2013. Late-life depression and risk of vascular dementia and Alzheimer's disease: systematic review and meta-analysis of community-based cohort studies. *Br J Psychiatry,* 202**,** 329-35.

Disease", W. G. O. M. a. B. M. O. a. S. 1998. Consensus report of the Working Group on: "Molecular and Biochemical Markers of Alzheimer's Disease". The Ronald and Nancy Reagan Research Institute of the Alzheimer's Association and the National Institute on Aging Working Group. *Neurobiol Aging,* 19**,** 109-16.

Doherty, B. M., Schultz, S. A., Oh, J. M., Koscik, R. L., Dowling, N. M., Barnhart, T. E., Murali, D., Gallagher, C. L., Carlsson, C. M., Bendlin, B. B., Larue, A., Hermann, B. P., Rowley, H. A., Asthana, S., Sager, M. A., Christian, B. T., Johnson, S. C. & Okonkwo, O. C. 2015. Amyloid burden, cortical thickness, and cognitive function in the Wisconsin Registry for Alzheimer's Prevention. *Alzheimers Dement (Amst),* 1**,** 160-169.

Doody, R. S., Dunn, J. K., Huang, E., Azher, S. & Kataki, M. 2004. A method for estimating duration of illness in Alzheimer's disease. *Dement Geriatr Cogn Disord,* 17**,** 1-4.

Doody, R. S., Raman, R., Farlow, M., Iwatsubo, T., Vellas, B., Joffe, S., Kieburtz, K., He, F., Sun, X., Thomas, R. G., Aisen, P. S., Alzheimer's Disease Cooperative Study Steering, C., Siemers, E., Sethuraman, G., Mohs, R. & Semagacestat Study, G. 2013. A phase 3 trial of semagacestat for treatment of Alzheimer's disease. *N Engl J Med,* 369**,** 341-50.

Doody, R. S., Raman, R., Sperling, R. A., Seimers, E., Sethuraman, G., Mohs, R., Farlow, M., Iwatsubo, T., Vellas, B., Sun, X., Ernstrom, K., Thomas, R. G., Aisen, P. S. & Alzheimer's Disease Cooperative, S. 2015. Peripheral and central effects

of gamma-secretase inhibition by semagacestat in Alzheimer's disease. *Alzheimers Res Ther,* 7**,** 36.

Doody, R. S., Thomas, R. G., Farlow, M., Iwatsubo, T., Vellas, B., Joffe, S., Kieburtz, K., Raman, R., Sun, X., Aisen, P. S., Siemers, E., Liu-Seifert, H., Mohs, R., Alzheimer's Disease Cooperative Study Steering, C. & Solanezumab Study, G. 2014. Phase 3 trials of solanezumab for mild-to-moderate Alzheimer's disease. *N Engl J Med,* 370**,** 311-21.

Douaud, G., Menke, R. A., Gass, A., Monsch, A. U., Rao, A., Whitcher, B., Zamboni, G., Matthews, P. M., Sollberger, M. & Smith, S. 2013. Brain microstructure reveals early abnormalities more than two years prior to clinical progression from mild cognitive impairment to Alzheimer's disease. *J Neurosci,* 33**,** 2147-55.

Dovey, H. F., John, V., Anderson, J. P., Chen, L. Z., De Saint Andrieu, P., Fang, L. Y., Freedman, S. B., Folmer, B., Goldbach, E., Holsztynska, E. J., Hu, K. L., Johnson-Wood, K. L., Kennedy, S. L., Kholodenko, D., Knops, J. E., Latimer, L. H., Lee, M., Liao, Z., Lieberburg, I. M., Motter, R. N., Mutter, L. C., Nietz, J., Quinn, K. P., Sacchi, K. L., Seubert, P. A., Shopp, G. M., Thorsett, E. D., Tung, J. S., Wu, J., Yang, S., Yin, C. T., Schenk, D. B., May, P. C., Altstiel, L. D., Bender, M. H., Boggs, L. N., Britton, T. C., Clemens, J. C., Czilli, D. L., Dieckman-Mcginty, D. K., Droste, J. J., Fuson, K. S., Gitter, B. D., Hyslop, P. A., Johnstone, E. M., Li, W. Y., Little, S. P., Mabry, T. E., Miller, F. D. & Audia, J. E. 2001. Functional gamma-secretase inhibitors reduce beta-amyloid peptide levels in brain. *J Neurochem,* 76**,** 173-81.

Du, A. T., Schuff, N., Kramer, J. H., Rosen, H. J., Gorno-Tempini, M. L., Rankin, K., Miller, B. L. & Weiner, M. W. 2007. Different regional patterns of cortical thinning in Alzheimer's disease and frontotemporal dementia. *Brain,* 130**,** 1159-66.

Dubois, B., Feldman, H. H., Jacova, C., Hampel, H., Molinuevo, J. L., Blennow, K., Dekosky, S. T., Gauthier, S., Selkoe, D., Bateman, R., Cappa, S., Crutch, S., Engelborghs, S., Frisoni, G. B., Fox, N. C., Galasko, D., Habert, M. O., Jicha, G. A., Nordberg, A., Pasquier, F., Rabinovici, G., Robert, P., Rowe, C., Salloway, S., Sarazin, M., Epelbaum, S., De Souza, L. C., Vellas, B., Visser, P. J., Schneider, L., Stern, Y., Scheltens, P. & Cummings, J. L. 2014. Advancing research diagnostic criteria for Alzheimer's disease: the IWG-2 criteria. *Lancet Neurol,* 13**,** 614-29.

Dubois, B., Hampel, H., Feldman, H. H., Scheltens, P., Aisen, P., Andrieu, S., Bakardjian, H., Benali, H., Bertram, L., Blennow, K., Broich, K., Cavedo, E., Crutch, S., Dartigues, J. F., Duyckaerts, C., Epelbaum, S., Frisoni, G. B., Gauthier, S., Genthon, R., Gouw, A. A., Habert, M. O., Holtzman, D. M., Kivipelto, M., Lista, S., Molinuevo, J. L., O'bryant, S. E., Rabinovici, G. D., Rowe, C., Salloway, S., Schneider, L. S., Sperling, R., Teichmann, M., Carrillo, M. C., Cummings, J., Jack, C. R., Jr., Proceedings of the Meeting of the International Working, G., The American Alzheimer's Association on "the Preclinical State Of, A. D., July & Washington Dc, U. S. A. 2016. Preclinical Alzheimer's disease: Definition, natural history, and diagnostic criteria. *Alzheimers Dement,* 12**,** 292-323.

Dudai, Y., Karni, A. & Born, J. 2015. The Consolidation and Transformation of Memory. *Neuron,* 88**,** 20-32.

Duits, F. H., Teunissen, C. E., Bouwman, F. H., Visser, P. J., Mattsson, N., Zetterberg, H., Blennow, K., Hansson, O., Minthon, L., Andreasen, N., Marcusson, J., Wallin, A., Rikkert, M. O., Tsolaki, M., Parnetti, L., Herukka, S. K., Hampel, H., De Leon, M. J., Schroder, J., Aarsland, D., Blankenstein, M. A., Scheltens, P. & Van Der Flier, W. M. 2014. The cerebrospinal fluid "Alzheimer profile": easily said, but what does it mean? *Alzheimers Dement,* 10**,** 713-723 e2.

Elliott, G., Isaac, C. L. & Muhlert, N. 2014. Measuring forgetting: A critical review of accelerated long-term forgetting studies. *Cortex,* 54C**,** 16-32.

Elman, J. A., Panizzon, M. S., Hagler, D. J., Jr., Fennema-Notestine, C., Eyler, L. T., Gillespie, N. A., Neale, M. C., Lyons, M. J., Franz, C. E., Mcevoy, L. K., Dale, A. M. & Kremen, W. S. 2017. Genetic and environmental influences on cortical mean diffusivity. *Neuroimage,* 146**,** 90-99.

Fagan, A. M., Roe, C. M., Xiong, C., Mintun, M. A., Morris, J. C. & Holtzman, D. M. 2007. Cerebrospinal fluid tau/beta-amyloid(42) ratio as a prediction of cognitive decline in nondemented older adults. *Arch Neurol,* 64**,** 343-9.

Fahrenholz, F. & Postina, R. 2006. Alpha-secretase activation--an approach to Alzheimer's disease therapy. *Neurodegener Dis,* 3**,** 255-61.

Falahati, F., Westman, E. & Simmons, A. 2014. Multivariate data analysis and machine learning in Alzheimer's disease with a focus on structural magnetic resonance imaging. *J Alzheimers Dis,* 41**,** 685-708.

Farrer, L. A., Cupples, L. A., Haines, J. L., Hyman, B., Kukull, W. A., Mayeux, R., Myers, R. H., Pericak-Vance, M. A., Risch, N. & Van Duijn, C. M. 1997. Effects of age, sex, and ethnicity on the association between apolipoprotein E genotype and Alzheimer disease. A meta-analysis. APOE and Alzheimer Disease Meta Analysis Consortium. *JAMA,* 278**,** 1349-56.

Feinberg, D. A. & Setsompop, K. 2013. Ultra-fast MRI of the human brain with simultaneous multi-slice imaging. *J Magn Reson,* 229**,** 90-100.

Fellgiebel, A., Dellani, P. R., Greverus, D., Scheurich, A., Stoeter, P. & Muller, M. J. 2006. Predicting conversion to dementia in mild cognitive impairment by volumetric and diffusivity measurements of the hippocampus. *Psychiatry Res,* 146**,** 283-7.

Fellgiebel, A. & Yakushev, I. 2011. Diffusion tensor imaging of the hippocampus in MCI and early Alzheimer's disease. *J Alzheimers Dis,* 26 Suppl 3**,** 257-62.

Fernandez-Martos, C. M., King, A. E., Atkinson, R. A., Woodhouse, A. & Vickers, J. C. 2015. Neurofilament light gene deletion exacerbates amyloid, dystrophic neurite, and synaptic pathology in the APP/PS1 transgenic model of Alzheimer's disease. *Neurobiol Aging,* 36**,** 2757-67.

Fernandez-Tome, P., Brera, B., Arevalo, M. A. & De Ceballos, M. L. 2004. Beta-amyloid25-35 inhibits glutamate uptake in cultured neurons and astrocytes: modulation of uptake as a survival mechanism. *Neurobiol Dis,* 15**,** 580-9.

Ferri, C. P., Prince, M., Brayne, C., Brodaty, H., Fratiglioni, L., Ganguli, M., Hall, K., Hasegawa, K., Hendrie, H., Huang, Y., Jorm, A., Mathers, C., Menezes, P. R., Rimmer, E., Scazufca, M. & Alzheimer's Disease, I. 2005. Global prevalence of dementia: a Delphi consensus study. *Lancet,* 366**,** 2112-7.

Fischl, B. & Dale, A. M. 2000. Measuring the thickness of the human cerebral cortex from magnetic resonance images. *Proc Natl Acad Sci U S A,* 97**,** 11050-5.

Fleisher, A. S., Chen, K., Quiroz, Y. T., Jakimovich, L. J., Gomez, M. G., Langois, C. M., Langbaum, J. B. S., Ayutyanont, N., Roontiva, A., Thiyyagura, P., Lee, W., Mo, H., Lopez, L., Moreno, S., Acosta-Baena, N., Giraldo, M., Garcia, G., Reiman, R. A., Huentelman, M. J., Kosik, K. S., Tariot, P. N., Lopera, F. & Reiman, E. M. 2012. Florbetapir PET analysis of amyloid-β deposition in the presenilin 1 E280A autosomal dominant Alzheimer's disease kindred: a cross-sectional study. *The Lancet Neurology,* 11**,** 1057-1065.

Folstein, M. F., Folstein, S. E. & Mchugh, P. R. 1975. "Mini-mental state". A practical method for grading the cognitive state of patients for the clinician. *J Psychiatr Res,* 12**,** 189-98.

Fortea, J., Sala-Llonch, R., Bartres-Faz, D., Bosch, B., Llado, A., Bargallo, N., Molinuevo, J. L. & Sanchez-Valle, R. 2010. Increased cortical thickness and caudate volume precede atrophy in PSEN1 mutation carriers. *J Alzheimers Dis,* 22**,** 909-22.

Foster, N. L., Chase, T. N., Fedio, P., Patronas, N. J., Brooks, R. A. & Di Chiro, G. 1983. Alzheimer's disease: focal cortical changes shown by positron emission tomography. *Neurology,* 33**,** 961-5.

Fotiadis, P., Van Rooden, S., Van Der Grond, J., Schultz, A., Martinez-Ramirez, S., Auriel, E., Reijmer, Y., Van Opstal, A. M., Ayres, A., Schwab, K. M., Alzheimer's Disease Neuroimaging Initiative, A., Hedden, T., Rosand, J., Viswanathan, A., Wermer, M., Terwindt, G. M., Sperling, R. A., Polimeni, J. R., Johnson, K. A., Van Buchem, M. A., Greenberg, S. M. & Gurol, M. E. 2016. Cortical atrophy in patients with cerebral amyloid angiopathy: a case-control study. *Lancet Neurol,* 15**,** 811-9.

Fox, N. C., Black, R. S., Gilman, S., Rossor, M. N., Griffith, S. G., Jenkins, L., Koller, M. & Study, A. N. 2005. Effects of Abeta immunization (AN1792) on MRI measures of cerebral volume in Alzheimer disease. *Neurology,* 64**,** 1563-72.

Fox, N. C., Warrington, E. K., Freeborough, P. A., Hartikainen, P., Kennedy, A. M., Stevens, J. M. & Rossor, M. N. 1996. Presymptomatic hippocampal atrophy in Alzheimer's disease. A longitudinal MRI study. *Brain,* 119 (Pt 6)**,** 2001-7.

Fox, N. C., Warrington, E. K., Seiffer, A. L., Agnew, S. K. & Rossor, M. N. 1998. Presymptomatic cognitive deficits in individuals at risk of familial Alzheimer's disease. A longitudinal prospective study. *Brain,* 121 (Pt 9)**,** 1631-9.

Freeborough, P. A. & Fox, N. C. 1997. The boundary shift integral: an accurate and robust measure of cerebral volume changes from registered repeat MRI. *IEEE Trans Med Imaging,* 16**,** 623-9.

Freeborough, P. A., Fox, N. C. & Kitney, R. I. 1997. Interactive algorithms for the segmentation and quantitation of 3-D MRI brain scans. *Comput Methods Programs Biomed,* 53**,** 15-25.

Friedland, R. P., Budinger, T. F., Brant-Zawadzki, M. & Jagust, W. J. 1984. The diagnosis of Alzheimer-type dementia. A

preliminary comparison of positron emission tomography and proton magnetic resonance. *JAMA,* 252**,** 2750-2.

Frisoni, G. B., Testa, C., Zorzan, A., Sabattoli, F., Beltramello, A., Soininen, H. & Laakso, M. P. 2002. Detection of grey matter loss in mild Alzheimer's disease with voxel based morphometry. *J Neurol Neurosurg Psychiatry,* 73**,** 657-64.

Gaiottino, J., Norgren, N., Dobson, R., Topping, J., Nissim, A., Malaspina, A., Bestwick, J. P., Monsch, A. U., Regeniter, A., Lindberg, R. L., Kappos, L., Leppert, D., Petzold, A., Giovannoni, G. & Kuhle, J. 2013. Increased neurofilament light chain blood levels in neurodegenerative neurological diseases. *PLoS One,* 8**,** e75091.

Gattringer, T., Pinter, D., Enzinger, C., Seifert-Held, T., Kneihsl, M., Fandler, S., Pichler, A., Barro, C., Grobke, S., Voortman, M., Pirpamer, L., Hofer, E., Ropele, S., Schmidt, R., Kuhle, J., Fazekas, F. & Khalil, M. 2017. Serum neurofilament light is sensitive to active cerebral small vessel disease. *Neurology,* 89**,** 2108-2114.

Gauthier, S., Feldman, H. H., Schneider, L. S., Wilcock, G. K., Frisoni, G. B., Hardlund, J. H., Moebius, H. J., Bentham, P., Kook, K. A., Wischik, D. J., Schelter, B. O., Davis, C. S., Staff, R. T., Bracoud, L., Shamsi, K., Storey, J. M., Harrington, C. R. & Wischik, C. M. 2016. Efficacy and safety of tau-aggregation inhibitor therapy in patients with mild or moderate Alzheimer's disease: a randomised, controlled, double-blind, parallel-arm, phase 3 trial. *Lancet,* 388**,** 2873-2884.

Gauthier, S., Reisberg, B., Zaudig, M., Petersen, R. C., Ritchie, K., Broich, K., Belleville, S., Brodaty, H., Bennett, D., Chertkow, H., Cummings, J. L., De Leon, M., Feldman, H., Ganguli, M., Hampel, H., Scheltens, P., Tierney, M. C., Whitehouse, P., Winblad, B. & International Psychogeriatric Association Expert Conference on Mild Cognitive, I. 2006. Mild cognitive impairment. *Lancet,* 367**,** 1262-70.

Giacobini, E. & Gold, G. 2013. Alzheimer disease therapy--moving from amyloid-beta to tau. *Nat Rev Neurol,* 9**,** 677-86.

Giannakopoulos, P., Herrmann, F. R., Bussiere, T., Bouras, C., Kovari, E., Perl, D. P., Morrison, J. H., Gold, G. & Hof, P. R. 2003. Tangle and neuron numbers, but not amyloid load, predict cognitive status in Alzheimer's disease. *Neurology,* 60**,** 1495-500.

Gilman, S., Koller, M., Black, R. S., Jenkins, L., Griffith, S. G., Fox, N. C., Eisner, L., Kirby, L., Rovira, M. B., Forette, F., Orgogozo, J. M. & Team, A. N. S. 2005. Clinical effects of

Abeta immunization (AN1792) in patients with AD in an interrupted trial. *Neurology,* 64**,** 1553-62.
Gisslen, M., Price, R. W., Andreasson, U., Norgren, N., Nilsson, S., Hagberg, L., Fuchs, D., Spudich, S., Blennow, K. & Zetterberg, H. 2016. Plasma Concentration of the Neurofilament Light Protein (NFL) is a Biomarker of CNS Injury in HIV Infection: A Cross-Sectional Study. *EBioMedicine,* 3**,** 135-40.
Goate, A., Chartier-Harlin, M. C., Mullan, M., Brown, J., Crawford, F., Fidani, L., Giuffra, L., Haynes, A., Irving, N., James, L. & Et Al. 1991. Segregation of a missense mutation in the amyloid precursor protein gene with familial Alzheimer's disease. *Nature,* 349**,** 704-6.
Goedert, M. & Jakes, R. 1990. Expression of separate isoforms of human tau protein: correlation with the tau pattern in brain and effects on tubulin polymerization. *EMBO J,* 9**,** 4225-30.
Goedert, M., Spillantini, M. G., Jakes, R., Rutherford, D. & Crowther, R. A. 1989. Multiple isoforms of human microtubule-associated protein tau: sequences and localization in neurofibrillary tangles of Alzheimer's disease. *Neuron,* 3**,** 519-26.
Gomez-Isla, T., Hollister, R., West, H., Mui, S., Growdon, J. H., Petersen, R. C., Parisi, J. E. & Hyman, B. T. 1997. Neuronal loss correlates with but exceeds neurofibrillary tangles in Alzheimer's disease. *Ann Neurol,* 41**,** 17-24.
Gorno-Tempini, M. L., Brambati, S. M., Ginex, V., Ogar, J., Dronkers, N. F., Marcone, A., Perani, D., Garibotto, V., Cappa, S. F. & Miller, B. L. 2008. The logopenic/phonological variant of primary progressive aphasia. *Neurology,* 71**,** 1227-34.
Graham, N. L., Emery, T. & Hodges, J. R. 2004. Distinctive cognitive profiles in Alzheimer's disease and subcortical vascular dementia. *J Neurol Neurosurg Psychiatry,* 75**,** 61-71.
Grannell, P. K. & Mansfield, P. 1975. Microscopy in vivo by nuclear magnetic resonance. *Phys Med Biol,* 20**,** 477-82.
Green, R. C., Schneider, L. S., Amato, D. A., Beelen, A. P., Wilcock, G., Swabb, E. A., Zavitz, K. H. & Tarenflurbil Phase 3 Study, G. 2009. Effect of tarenflurbil on cognitive decline and activities of daily living in patients with mild Alzheimer disease: a randomized controlled trial. *JAMA,* 302**,** 2557-64.
Grignon, Y., Duyckaerts, C., Bennecib, M. & Hauw, J. J. 1998. Cytoarchitectonic alterations in the supramarginal gyrus of late onset Alzheimer's disease. *Acta Neuropathol,* 95**,** 395-406.
Group, A.-F. R. 2015. Follow-up evaluation of cognitive function in the randomized Alzheimer's Disease Anti-inflammatory

Prevention Trial and its Follow-up Study. *Alzheimers Dement,* 11**,** 216-25 e1.
Gudala, K., Bansal, D., Schifano, F. & Bhansali, A. 2013. Diabetes mellitus and risk of dementia: A meta-analysis of prospective observational studies. *J Diabetes Investig,* 4**,** 640-50.
Gurol, M. E., Viswanathan, A., Gidicsin, C., Hedden, T., Martinez-Ramirez, S., Dumas, A., Vashkevich, A., Ayres, A. M., Auriel, E., Van Etten, E., Becker, A., Carmasin, J., Schwab, K., Rosand, J., Johnson, K. A. & Greenberg, S. M. 2013. Cerebral amyloid angiopathy burden associated with leukoaraiosis: a positron emission tomography/magnetic resonance imaging study. *Ann Neurol,* 73**,** 529-36.
Hall, S., Ohrfelt, A., Constantinescu, R., Andreasson, U., Surova, Y., Bostrom, F., Nilsson, C., Hakan, W., Decraemer, H., Nagga, K., Minthon, L., Londos, E., Vanmechelen, E., Holmberg, B., Zetterberg, H., Blennow, K. & Hansson, O. 2012. Accuracy of a panel of 5 cerebrospinal fluid biomarkers in the differential diagnosis of patients with dementia and/or parkinsonian disorders. *Arch Neurol,* 69**,** 1445-52.
Han, X., Jovicich, J., Salat, D., Van Der Kouwe, A., Quinn, B., Czanner, S., Busa, E., Pacheco, J., Albert, M., Killiany, R., Maguire, P., Rosas, D., Makris, N., Dale, A., Dickerson, B. & Fischl, B. 2006. Reliability of MRI-derived measurements of human cerebral cortical thickness: the effects of field strength, scanner upgrade and manufacturer. *Neuroimage,* 32**,** 180-94.
Han, X., Rozen, S., Boyle, S. H., Hellegers, C., Cheng, H., Burke, J. R., Welsh-Bohmer, K. A., Doraiswamy, P. M. & Kaddurah-Daouk, R. 2011. Metabolomics in early Alzheimer's disease: identification of altered plasma sphingolipidome using shotgun lipidomics. *PLoS One,* 6**,** e21643.
Hardy, J. & Allsop, D. 1991. Amyloid deposition as the central event in the aetiology of Alzheimer's disease. *Trends Pharmacol Sci,* 12**,** 383-8.
Hardy, J. A. & Higgins, G. A. 1992. Alzheimer's disease: the amyloid cascade hypothesis. *Science,* 256**,** 184-5.
Harold, D., Abraham, R., Hollingworth, P., Sims, R., Gerrish, A., Hamshere, M. L., Pahwa, J. S., Moskvina, V., Dowzell, K., Williams, A., Jones, N., Thomas, C., Stretton, A., Morgan, A. R., Lovestone, S., Powell, J., Proitsi, P., Lupton, M. K., Brayne, C., Rubinsztein, D. C., Gill, M., Lawlor, B., Lynch, A., Morgan, K., Brown, K. S., Passmore, P. A., Craig, D., Mcguinness, B., Todd, S., Holmes, C., Mann, D., Smith, A. D., Love, S., Kehoe, P. G., Hardy, J., Mead, S., Fox, N., Rossor,

M., Collinge, J., Maier, W., Jessen, F., Schurmann, B., Heun, R., Van Den Bussche, H., Heuser, I., Kornhuber, J., Wiltfang, J., Dichgans, M., Frolich, L., Hampel, H., Hull, M., Rujescu, D., Goate, A. M., Kauwe, J. S., Cruchaga, C., Nowotny, P., Morris, J. C., Mayo, K., Sleegers, K., Bettens, K., Engelborghs, S., De Deyn, P. P., Van Broeckhoven, C., Livingston, G., Bass, N. J., Gurling, H., Mcquillin, A., Gwilliam, R., Deloukas, P., Al-Chalabi, A., Shaw, C. E., Tsolaki, M., Singleton, A. B., Guerreiro, R., Muhleisen, T. W., Nothen, M. M., Moebus, S., Jockel, K. H., Klopp, N., Wichmann, H. E., Carrasquillo, M. M., Pankratz, V. S., Younkin, S. G., Holmans, P. A., O'donovan, M., Owen, M. J. & Williams, J. 2009. Genome-wide association study identifies variants at CLU and PICALM associated with Alzheimer's disease. *Nat Genet,* 41**,** 1088-93.

Harris, M. E., Wang, Y., Pedigo, N. W., Jr., Hensley, K., Butterfield, D. A. & Carney, J. M. 1996. Amyloid beta peptide (25-35) inhibits Na+-dependent glutamate uptake in rat hippocampal astrocyte cultures. *J Neurochem,* 67**,** 277-86.

Head, D., Buckner, R. L., Shimony, J. S., Williams, L. E., Akbudak, E., Conturo, T. E., Mcavoy, M., Morris, J. C. & Snyder, A. Z. 2004. Differential vulnerability of anterior white matter in nondemented aging with minimal acceleration in dementia of the Alzheimer type: evidence from diffusion tensor imaging. *Cereb Cortex,* 14**,** 410-23.

Health, F. F. T. N. I. O. 2016. Framework for Defining Evidentiary Criteria for Biomarker Qualification.

Helath, D. O. 2009. National dementia strategy (accesible summary).

Hendriks, L., Van Duijn, C. M., Cras, P., Cruts, M., Van Hul, W., Van Harskamp, F., Warren, A., Mcinnis, M. G., Antonarakis, S. E., Martin, J. J. & Et Al. 1992. Presenile dementia and cerebral haemorrhage linked to a mutation at codon 692 of the beta-amyloid precursor protein gene. *Nat Genet,* 1**,** 218-21.

Heneka, M. T., Carson, M. J., El Khoury, J., Landreth, G. E., Brosseron, F., Feinstein, D. L., Jacobs, A. H., Wyss-Coray, T., Vitorica, J., Ransohoff, R. M., Herrup, K., Frautschy, S. A., Finsen, B., Brown, G. C., Verkhratsky, A., Yamanaka, K., Koistinaho, J., Latz, E., Halle, A., Petzold, G. C., Town, T., Morgan, D., Shinohara, M. L., Perry, V. H., Holmes, C., Bazan, N. G., Brooks, D. J., Hunot, S., Joseph, B., Deigendesch, N., Garaschuk, O., Boddeke, E., Dinarello, C. A., Breitner, J. C., Cole, G. M., Golenbock, D. T. & Kummer, M. P. 2015.

Neuroinflammation in Alzheimer's disease. *Lancet Neurol,* 14**,** 388-405.

Henriksen, K., O'bryant, S. E., Hampel, H., Trojanowski, J. Q., Montine, T. J., Jeromin, A., Blennow, K., Lonneborg, A., Wyss-Coray, T., Soares, H., Bazenet, C., Sjogren, M., Hu, W., Lovestone, S., Karsdal, M. A., Weiner, M. W. & Blood-Based Biomarker Interest, G. 2014. The future of blood-based biomarkers for Alzheimer's disease. *Alzheimers Dement,* 10**,** 115-31.

Hinshaw, W. S., Bottomley, P. A. & Holland, G. N. 1977. Radiographic thin-section image of the human wrist by nuclear magnetic resonance. *Nature,* 270**,** 722-3.

Hoefeijzers, S., Dewar, M., Della Sala, S., Zeman, A. & Butler, C. 2013. Accelerated long-term forgetting in transient epileptic amnesia: an acquisition or consolidation deficit? *Neuropsychologia,* 51**,** 1549-55.

Hofman, A., Rocca, W. A., Brayne, C., Breteler, M. M., Clarke, M., Cooper, B., Copeland, J. R., Dartigues, J. F., Da Silva Droux, A., Hagnell, O. & Et Al. 1991. The prevalence of dementia in Europe: a collaborative study of 1980-1990 findings. Eurodem Prevalence Research Group. *Int J Epidemiol,* 20**,** 736-48.

Holmes, C. 2002. Genotype and phenotype in Alzheimer's disease. *Br J Psychiatry,* 180**,** 131-4.

Howard, R., Mcshane, R., Lindesay, J., Ritchie, C., Baldwin, A., Barber, R., Burns, A., Dening, T., Findlay, D., Holmes, C., Hughes, A., Jacoby, R., Jones, R., Jones, R., Mckeith, I., Macharouthu, A., O'brien, J., Passmore, P., Sheehan, B., Juszczak, E., Katona, C., Hills, R., Knapp, M., Ballard, C., Brown, R., Banerjee, S., Onions, C., Griffin, M., Adams, J., Gray, R., Johnson, T., Bentham, P. & Phillips, P. 2012. Donepezil and memantine for moderate-to-severe Alzheimer's disease. *N Engl J Med,* 366**,** 893-903.

Hulstaert, F., Blennow, K., Ivanoiu, A., Schoonderwaldt, H. C., Riemenschneider, M., De Deyn, P. P., Bancher, C., Cras, P., Wiltfang, J., Mehta, P. D., Iqbal, K., Pottel, H., Vanmechelen, E. & Vanderstichele, H. 1999. Improved discrimination of AD patients using beta-amyloid(1-42) and tau levels in CSF. *Neurology,* 52**,** 1555-62.

Hyman, B. T., Van Hoesen, G. W., Damasio, A. R. & Barnes, C. L. 1984. Alzheimer's disease: cell-specific pathology isolates the hippocampal formation. *Science,* 225**,** 1168-70.

Iadecola, C. 2004. Neurovascular regulation in the normal brain and in Alzheimer's disease. *Nat Rev Neurosci,* 5**,** 347-60.

Ihara, Y., Nukina, N., Miura, R. & Ogawara, M. 1986. Phosphorylated tau protein is integrated into paired helical filaments in Alzheimer's disease. *J Biochem,* 99**,** 1807-10.

Iqbal, K., Alonso Adel, C., Chen, S., Chohan, M. O., El-Akkad, E., Gong, C. X., Khatoon, S., Li, B., Liu, F., Rahman, A., Tanimukai, H. & Grundke-Iqbal, I. 2005. Tau pathology in Alzheimer disease and other tauopathies. *Biochim Biophys Acta,* 1739**,** 198-210.

Jack, C. R., Jr., Bennett, D. A., Blennow, K., Carrillo, M. C., Feldman, H. H., Frisoni, G. B., Hampel, H., Jagust, W. J., Johnson, K. A., Knopman, D. S., Petersen, R. C., Scheltens, P., Sperling, R. A. & Dubois, B. 2016a. A/T/N: An unbiased descriptive classification scheme for Alzheimer disease biomarkers. *Neurology,* 87**,** 539-47.

Jack, C. R., Jr., Knopman, D. S., Jagust, W. J., Petersen, R. C., Weiner, M. W., Aisen, P. S., Shaw, L. M., Vemuri, P., Wiste, H. J., Weigand, S. D., Lesnick, T. G., Pankratz, V. S., Donohue, M. C. & Trojanowski, J. Q. 2013. Tracking pathophysiological processes in Alzheimer's disease: an updated hypothetical model of dynamic biomarkers. *Lancet Neurol,* 12**,** 207-16.

Jack, C. R., Jr., Knopman, D. S., Jagust, W. J., Shaw, L. M., Aisen, P. S., Weiner, M. W., Petersen, R. C. & Trojanowski, J. Q. 2010. Hypothetical model of dynamic biomarkers of the Alzheimer's pathological cascade. *Lancet Neurol,* 9**,** 119-28.

Jack, C. R., Jr., Petersen, R. C., O'brien, P. C. & Tangalos, E. G. 1992. MR-based hippocampal volumetry in the diagnosis of Alzheimer's disease. *Neurology,* 42**,** 183-8.

Jack, C. R., Jr., Petersen, R. C., Xu, Y. C., O'brien, P. C., Smith, G. E., Ivnik, R. J., Boeve, B. F., Waring, S. C., Tangalos, E. G. & Kokmen, E. 1999. Prediction of AD with MRI-based hippocampal volume in mild cognitive impairment. *Neurology,* 52**,** 1397-403.

Jack, C. R., Jr., Petersen, R. C., Xu, Y. C., Waring, S. C., O'brien, P. C., Tangalos, E. G., Smith, G. E., Ivnik, R. J. & Kokmen, E. 1997. Medial temporal atrophy on MRI in normal aging and very mild Alzheimer's disease. *Neurology,* 49**,** 786-94.

Jack, C. R., Jr., Shiung, M. M., Weigand, S. D., O'brien, P. C., Gunter, J. L., Boeve, B. F., Knopman, D. S., Smith, G. E., Ivnik, R. J., Tangalos, E. G. & Petersen, R. C. 2005. Brain atrophy rates predict subsequent clinical conversion in normal elderly and amnestic MCI. *Neurology,* 65**,** 1227-31.

Jack, C. R., Jr., Therneau, T. M., Wiste, H. J., Weigand, S. D., Knopman, D. S., Lowe, V. J., Mielke, M. M., Vemuri, P., Roberts, R. O., Machulda, M. M., Senjem, M. L., Gunter, J. L., Rocca, W. A. & Petersen, R. C. 2016b. Transition rates between amyloid and neurodegeneration biomarker states and to dementia: a population-based, longitudinal cohort study. *Lancet Neurol,* 15**,** 56-64.

Jackson, M. & Warrington, E. K. 1986. Arithmetic skills in patients with unilateral cerebral lesions. *Cortex,* 22**,** 611-20.

Jacobs, H. I., Van Boxtel, M. P., Gronenschild, E. H., Uylings, H. B., Jolles, J. & Verhey, F. R. 2013. Decreased gray matter diffusivity: a potential early Alzheimer's disease biomarker? *Alzheimers Dement,* 9**,** 93-7.

Janssen, J. C., Beck, J. A., Campbell, T. A., Dickinson, A., Fox, N. C., Harvey, R. J., Houlden, H., Rossor, M. N. & Collinge, J. 2003. Early onset familial Alzheimer's disease: Mutation frequency in 31 families. *Neurology,* 60**,** 235-9.

Jessen, F., Amariglio, R. E., Van Boxtel, M., Breteler, M., Ceccaldi, M., Chetelat, G., Dubois, B., Dufouil, C., Ellis, K. A., Van Der Flier, W. M., Glodzik, L., Van Harten, A. C., De Leon, M. J., Mchugh, P., Mielke, M. M., Molinuevo, J. L., Mosconi, L., Osorio, R. S., Perrotin, A., Petersen, R. C., Rabin, L. A., Rami, L., Reisberg, B., Rentz, D. M., Sachdev, P. S., De La Sayette, V., Saykin, A. J., Scheltens, P., Shulman, M. B., Slavin, M. J., Sperling, R. A., Stewart, R., Uspenskaya, O., Vellas, B., Visser, P. J., Wagner, M. & Subjective Cognitive Decline Initiative Working, G. 2014. A conceptual framework for research on subjective cognitive decline in preclinical Alzheimer's disease. *Alzheimers Dement,* 10**,** 844-52.

Jonsson, T., Atwal, J. K., Steinberg, S., Snaedal, J., Jonsson, P. V., Bjornsson, S., Stefansson, H., Sulem, P., Gudbjartsson, D., Maloney, J., Hoyte, K., Gustafson, A., Liu, Y., Lu, Y., Bhangale, T., Graham, R. R., Huttenlocher, J., Bjornsdottir, G., Andreassen, O. A., Jonsson, E. G., Palotie, A., Behrens, T. W., Magnusson, O. T., Kong, A., Thorsteinsdottir, U., Watts, R. J. & Stefansson, K. 2012. A mutation in APP protects against Alzheimer's disease and age-related cognitive decline. *Nature,* 488**,** 96-9.

Jorm, A. F., Korten, A. E. & Henderson, A. S. 1987. The prevalence of dementia: a quantitative integration of the literature. *Acta Psychiatr Scand,* 76**,** 465-79.

Josephs, K. A., Whitwell, J. L., Ahmed, Z., Shiung, M. M., Weigand, S. D., Knopman, D. S., Boeve, B. F., Parisi, J. E., Petersen, R.

C., Dickson, D. W. & Jack, C. R., Jr. 2008. Beta-amyloid burden is not associated with rates of brain atrophy. *Ann Neurol,* 63**,** 204-12.

Kantarci, K., Avula, R., Senjem, M. L., Samikoglu, A. R., Zhang, B., Weigand, S. D., Przybelski, S. A., Edmonson, H. A., Vemuri, P., Knopman, D. S., Ferman, T. J., Boeve, B. F., Petersen, R. C. & Jack, C. R., Jr. 2010. Dementia with Lewy bodies and Alzheimer disease: neurodegenerative patterns characterized by DTI. *Neurology,* 74**,** 1814-21.

Kantarci, K., Petersen, R. C., Boeve, B. F., Knopman, D. S., Weigand, S. D., O'brien, P. C., Shiung, M. M., Smith, G. E., Ivnik, R. J., Tangalos, E. G. & Jack, C. R., Jr. 2005. DWI predicts future progression to Alzheimer disease in amnestic mild cognitive impairment. *Neurology,* 64**,** 902-4.

Kantarci, K., Senjem, M. L., Avula, R., Zhang, B., Samikoglu, A. R., Weigand, S. D., Przybelski, S. A., Edmonson, H. A., Vemuri, P., Knopman, D. S., Boeve, B. F., Ivnik, R. J., Smith, G. E., Petersen, R. C. & Jack, C. R., Jr. 2011. Diffusion tensor imaging and cognitive function in older adults with no dementia. *Neurology,* 77**,** 26-34.

Kennedy, M. E., Stamford, A. W., Chen, X., Cox, K., Cumming, J. N., Dockendorf, M. F., Egan, M., Ereshefsky, L., Hodgson, R. A., Hyde, L. A., Jhee, S., Kleijn, H. J., Kuvelkar, R., Li, W., Mattson, B. A., Mei, H., Palcza, J., Scott, J. D., Tanen, M., Troyer, M. D., Tseng, J. L., Stone, J. A., Parker, E. M. & Forman, M. S. 2016. The BACE1 inhibitor verubecestat (MK-8931) reduces CNS beta-amyloid in animal models and in Alzheimer's disease patients. *Sci Transl Med,* 8**,** 363ra150.

Kim, D. H., Yeo, S. H., Park, J. M., Choi, J. Y., Lee, T. H., Park, S. Y., Ock, M. S., Eo, J., Kim, H. S. & Cha, H. J. 2014. Genetic markers for diagnosis and pathogenesis of Alzheimer's disease. *Gene,* 545**,** 185-93.

Klunk, W. E., Engler, H., Nordberg, A., Wang, Y., Blomqvist, G., Holt, D. P., Bergstrom, M., Savitcheva, I., Huang, G. F., Estrada, S., Ausen, B., Debnath, M. L., Barletta, J., Price, J. C., Sandell, J., Lopresti, B. J., Wall, A., Koivisto, P., Antoni, G., Mathis, C. A. & Langstrom, B. 2004. Imaging brain amyloid in Alzheimer's disease with Pittsburgh Compound-B. *Ann Neurol,* 55**,** 306-19.

Klunk, W. E., Price, J. C., Mathis, C. A., Tsopelas, N. D., Lopresti, B. J., Ziolko, S. K., Bi, W., Hoge, J. A., Cohen, A. D., Ikonomovic, M. D., Saxton, J. A., Snitz, B. E., Pollen, D. A., Moonis, M., Lippa, C. F., Swearer, J. M., Johnson, K. A., Rentz, D. M.,

Fischman, A. J., Aizenstein, H. J. & Dekosky, S. T. 2007. Amyloid deposition begins in the striatum of presenilin-1 mutation carriers from two unrelated pedigrees. *J Neurosci,* 27**,** 6174-84.

Knight, W. D., Kim, L. G., Douiri, A., Frost, C., Rossor, M. N. & Fox, N. C. 2011a. Acceleration of cortical thinning in familial Alzheimer's disease. *Neurobiol Aging,* 32**,** 1765-73.

Knight, W. D., Okello, A. A., Ryan, N. S., Turkheimer, F. E., Rodriguez Martinez De Llano, S., Edison, P., Douglas, J., Fox, N. C., Brooks, D. J. & Rossor, M. N. 2011b. Carbon-11-Pittsburgh compound B positron emission tomography imaging of amyloid deposition in presenilin 1 mutation carriers. *Brain,* 134**,** 293-300.

Koivunen, J., Karrasch, M., Scheinin, N. M., Aalto, S., Vahlberg, T., Nagren, K., Helin, S., Viitanen, M. & Rinne, J. O. 2012. Cognitive decline and amyloid accumulation in patients with mild cognitive impairment. *Dement Geriatr Cogn Disord,* 34**,** 31-7.

Koppara, A., Wagner, M., Lange, C., Ernst, A., Wiese, B., Konig, H. H., Brettschneider, C., Riedel-Heller, S., Luppa, M., Weyerer, S., Werle, J., Bickel, H., Mosch, E., Pentzek, M., Fuchs, A., Wolfsgruber, S., Beauducel, A., Scherer, M., Maier, W. & Jessen, F. 2015. Cognitive performance before and after the onset of subjective cognitive decline in old age. *Alzheimers Dement (Amst),* 1**,** 194-205.

Kozauer, N. & Katz, R. 2013. Regulatory innovation and drug development for early-stage Alzheimer's disease. *N Engl J Med,* 368**,** 1169-71.

Kuhle, J., Barro, C., Andreasson, U., Derfuss, T., Lindberg, R., Sandelius, A., Liman, V., Norgren, N., Blennow, K. & Zetterberg, H. 2016. Comparison of three analytical platforms for quantification of the neurofilament light chain in blood samples: ELISA, electrochemiluminescence immunoassay and Simoa. *Clin Chem Lab Med,* 54**,** 1655-1661.

Laakso, M. P., Lehtovirta, M., Partanen, K., Riekkinen, P. J. & Soininen, H. 2000. Hippocampus in Alzheimer's disease: a 3-year follow-up MRI study. *Biol Psychiatry,* 47**,** 557-61.

Lambert, J. C., Heath, S., Even, G., Campion, D., Sleegers, K., Hiltunen, M., Combarros, O., Zelenika, D., Bullido, M. J., Tavernier, B., Letenneur, L., Bettens, K., Berr, C., Pasquier, F., Fievet, N., Barberger-Gateau, P., Engelborghs, S., De Deyn, P., Mateo, I., Franck, A., Helisalmi, S., Porcellini, E., Hanon, O., European Alzheimer's Disease Initiative, I., De

Pancorbo, M. M., Lendon, C., Dufouil, C., Jaillard, C., Leveillard, T., Alvarez, V., Bosco, P., Mancuso, M., Panza, F., Nacmias, B., Bossu, P., Piccardi, P., Annoni, G., Seripa, D., Galimberti, D., Hannequin, D., Licastro, F., Soininen, H., Ritchie, K., Blanche, H., Dartigues, J. F., Tzourio, C., Gut, I., Van Broeckhoven, C., Alperovitch, A., Lathrop, M. & Amouyel, P. 2009. Genome-wide association study identifies variants at CLU and CR1 associated with Alzheimer's disease. *Nat Genet,* 41**,** 1094-9.

Lambert, M. P., Barlow, A. K., Chromy, B. A., Edwards, C., Freed, R., Liosatos, M., Morgan, T. E., Rozovsky, I., Trommer, B., Viola, K. L., Wals, P., Zhang, C., Finch, C. E., Krafft, G. A. & Klein, W. L. 1998. Diffusible, nonfibrillar ligands derived from Abeta1-42 are potent central nervous system neurotoxins. *Proc Natl Acad Sci U S A,* 95**,** 6448-53.

Lane, C. A., Parker, T. D., Cash, D. M., Macpherson, K., Donnachie, E., Murray-Smith, H., Barnes, A., Barker, S., Beasley, D. G., Bras, J., Brown, D., Burgos, N., Byford, M., Jorge Cardoso, M., Carvalho, A., Collins, J., De Vita, E., Dickson, J. C., Epie, N., Espak, M., Henley, S. M. D., Hoskote, C., Hutel, M., Klimova, J., Malone, I. B., Markiewicz, P., Melbourne, A., Modat, M., Schrag, A., Shah, S., Sharma, N., Sudre, C. H., Thomas, D. L., Wong, A., Zhang, H., Hardy, J., Zetterberg, H., Ourselin, S., Crutch, S. J., Kuh, D., Richards, M., Fox, N. C. & Schott, J. M. 2017. Study protocol: Insight 46 - a neuroscience sub-study of the MRC National Survey of Health and Development. *BMC Neurol,* 17**,** 75.

Larkman, D. J., Hajnal, J. V., Herlihy, A. H., Coutts, G. A., Young, I. R. & Ehnholm, G. 2001. Use of multicoil arrays for separation of signal from multiple slices simultaneously excited. *J Magn Reson Imaging,* 13**,** 313-7.

Larson, E. B., Shadlen, M. F., Wang, L., Mccormick, W. C., Bowen, J. D., Teri, L. & Kukull, W. A. 2004. Survival after initial diagnosis of Alzheimer disease. *Ann Intern Med,* 140**,** 501-9.

Le Bihan, D. 2003. Looking into the functional architecture of the brain with diffusion MRI. *Nat Rev Neurosci,* 4**,** 469-80.

Lee, G. J., Lu, P. H., Medina, L. D., Rodriguez-Agudelo, Y., Melchor, S., Coppola, G., Braskie, M. N., Hua, X., Apostolova, L. G., Leow, A. D., Thompson, P. M. & Ringman, J. M. 2013. Regional brain volume differences in symptomatic and presymptomatic carriers of familial Alzheimer's disease mutations. *J Neurol Neurosurg Psychiatry,* 84**,** 154-62.

Lee, H. G., Zhu, X., Castellani, R. J., Nunomura, A., Perry, G. & Smith, M. A. 2007. Amyloid-beta in Alzheimer disease: the null versus the alternate hypotheses. *J Pharmacol Exp Ther,* 321**,** 823-9.

Lee, M. K., Xu, Z., Wong, P. C. & Cleveland, D. W. 1993. Neurofilaments are obligate heteropolymers in vivo. *J Cell Biol,* 122**,** 1337-50.

Lehmann, M., Crutch, S. J., Ridgway, G. R., Ridha, B. H., Barnes, J., Warrington, E. K., Rossor, M. N. & Fox, N. C. 2011. Cortical thickness and voxel-based morphometry in posterior cortical atrophy and typical Alzheimer's disease. *Neurobiol Aging,* 32**,** 1466-76.

Lesne, S., Koh, M. T., Kotilinek, L., Kayed, R., Glabe, C. G., Yang, A., Gallagher, M. & Ashe, K. H. 2006. A specific amyloid-beta protein assembly in the brain impairs memory. *Nature,* 440**,** 352-7.

Levy, E., Carman, M. D., Fernandez-Madrid, I. J., Power, M. D., Lieberburg, I., Van Duinen, S. G., Bots, G. T., Luyendijk, W. & Frangione, B. 1990. Mutation of the Alzheimer's disease amyloid gene in hereditary cerebral hemorrhage, Dutch type. *Science,* 248**,** 1124-6.

Levy-Lahad, E., Wasco, W., Poorkaj, P., Romano, D. M., Oshima, J., Pettingell, W. H., Yu, C. E., Jondro, P. D., Schmidt, S. D., Wang, K. & Et Al. 1995. Candidate gene for the chromosome 1 familial Alzheimer's disease locus. *Science,* 269**,** 973-7.

Lewczuk, P., Esselmann, H., Otto, M., Maler, J. M., Henkel, A. W., Henkel, M. K., Eikenberg, O., Antz, C., Krause, W.-R., Reulbach, U., Kornhuber, J. & Wiltfang, J. 2004. Neurochemical diagnosis of Alzheimer’s dementia by CSF Aβ42, Aβ42/Aβ40 ratio and total tau. *Neurobiology of Aging,* 25**,** 273-281.

Lim, Y. Y., Maruff, P., Pietrzak, R. H., Ellis, K. A., Darby, D., Ames, D., Harrington, K., Martins, R. N., Masters, C. L., Szoeke, C., Savage, G., Villemagne, V. L., Rowe, C. C. & Group, A. R. 2014. Abeta and cognitive change: examining the preclinical and prodromal stages of Alzheimer's disease. *Alzheimers Dement,* 10**,** 743-751 e1.

Lin, S. H., Hsu, W. C., Ng, S. H., Cheng, J. S., Khegai, O., Huang, C. C., Chen, Y. L., Chen, Y. C. & Wang, J. J. 2016. Increased Water Diffusion in the Parcellated Cortical Regions from the Patients with Amnestic Mild Cognitive Impairment and Alzheimer's Disease. *Front Aging Neurosci,* 8**,** 325.

Linn, R. T., Wolf, P. A., Bachman, D. L., Knoefel, J. E., Cobb, J. L., Belanger, A. J., Kaplan, E. F. & D'agostino, R. B. 1995. The 'preclinical phase' of probable Alzheimer's disease. A 13-year prospective study of the Framingham cohort. *Arch Neurol,* 52**,** 485-90.

Lista, S., O'bryant, S. E., Blennow, K., Dubois, B., Hugon, J., Zetterberg, H. & Hampel, H. 2015. Biomarkers in Sporadic and Familial Alzheimer's Disease. *J Alzheimers Dis,* 47**,** 291-317.

Liu, C. C., Kanekiyo, T., Xu, H. & Bu, G. 2013. Apolipoprotein E and Alzheimer disease: risk, mechanisms and therapy. *Nat Rev Neurol,* 9**,** 106-18.

Lopera, F., Ardilla, A., Martinez, A., Madrigal, L., Arango-Viana, J. C., Lemere, C. A., Arango-Lasprilla, J. C., Hincapie, L., Arcos-Burgos, M., Ossa, J. E., Behrens, I. M., Norton, J., Lendon, C., Goate, A. M., Ruiz-Linares, A., Rosselli, M. & Kosik, K. S. 1997. Clinical features of early-onset Alzheimer disease in a large kindred with an E280A presenilin-1 mutation. *JAMA,* 277**,** 793-9.

Macpherson, S. E., Parra, M. A., Moreno, S., Lopera, F. & Della Sala, S. 2012. Dual task abilities as a possible preclinical marker of Alzheimer's disease in carriers of the E280A presenilin-1 mutation. *J Int Neuropsychol Soc,* 18**,** 234-41.

Mak, H. K., Zhang, Z., Yau, K. K., Zhang, L., Chan, Q. & Chu, L. W. 2011. Efficacy of voxel-based morphometry with DARTEL and standard registration as imaging biomarkers in Alzheimer's disease patients and cognitively normal older adults at 3.0 Tesla MR imaging. *J Alzheimers Dis,* 23**,** 655-64.

Manes, F., Serrano, C., Calcagno, M. L., Cardozo, J. & Hodges, J. 2008. Accelerated forgetting in subjects with memory complaints. A new form of Mild Cognitive Impairment? *J Neurol,* 255**,** 1067-70.

Mann, D. M., Pickering-Brown, S. M., Takeuchi, A., Iwatsubo, T. & Members of the Familial Alzheimer's Disease Pathology Study, G. 2001. Amyloid angiopathy and variability in amyloid beta deposition is determined by mutation position in presenilin-1-linked Alzheimer's disease. *Am J Pathol,* 158**,** 2165-75.

Masters, C. L., Simms, G., Weinman, N. A., Multhaup, G., Mcdonald, B. L. & Beyreuther, K. 1985. Amyloid plaque core protein in Alzheimer disease and Down syndrome. *Proc Natl Acad Sci U S A,* 82**,** 4245-9.

Matthews, F. E., Stephan, B. C., Robinson, L., Jagger, C., Barnes, L. E., Arthur, A., Brayne, C., Cognitive, F. & Ageing Studies,

C. 2016. A two decade dementia incidence comparison from the Cognitive Function and Ageing Studies I and II. *Nat Commun,* 7**,** 11398.

Mattsson, N., Andreasson, U., Zetterberg, H., Blennow, K. & Alzheimer's Disease Neuroimaging, I. 2017. Association of Plasma Neurofilament Light With Neurodegeneration in Patients With Alzheimer Disease. *JAMA Neurol,* 74**,** 557-566.

Mattsson, N., Zetterberg, H., Janelidze, S., Insel, P. S., Andreasson, U., Stomrud, E., Palmqvist, S., Baker, D., Tan Hehir, C. A., Jeromin, A., Hanlon, D., Song, L., Shaw, L. M., Trojanowski, J. Q., Weiner, M. W., Hansson, O., Blennow, K. & Investigators, A. 2016. Plasma tau in Alzheimer disease. *Neurology,* 87**,** 1827-1835.

Maviel, T., Durkin, T. P., Menzaghi, F. & Bontempi, B. 2004. Sites of neocortical reorganization critical for remote spatial memory. *Science,* 305**,** 96-9.

May, P. C., Willis, B. A., Lowe, S. L., Dean, R. A., Monk, S. A., Cocke, P. J., Audia, J. E., Boggs, L. N., Borders, A. R., Brier, R. A., Calligaro, D. O., Day, T. A., Ereshefsky, L., Erickson, J. A., Gevorkyan, H., Gonzales, C. R., James, D. E., Jhee, S. S., Komjathy, S. F., Li, L., Lindstrom, T. D., Mathes, B. M., Martenyi, F., Sheehan, S. M., Stout, S. L., Timm, D. E., Vaught, G. M., Watson, B. M., Winneroski, L. L., Yang, Z. & Mergott, D. J. 2015. The potent BACE1 inhibitor LY2886721 elicits robust central Abeta pharmacodynamic responses in mice, dogs, and humans. *J Neurosci,* 35**,** 1199-210.

Mckenna, P. & Warrington, E. K. 1983. *Graded naming test,* Windsor, NFER-Nelson.

Mckhann, G., Drachman, D., Folstein, M., Katzman, R., Price, D. & Stadlan, E. M. 1984. Clinical diagnosis of Alzheimer's disease: report of the NINCDS-ADRDA Work Group under the auspices of Department of Health and Human Services Task Force on Alzheimer's Disease. *Neurology,* 34**,** 939-44.

Mclean, C. A., Cherny, R. A., Fraser, F. W., Fuller, S. J., Smith, M. J., Beyreuther, K., Bush, A. I. & Masters, C. L. 1999. Soluble pool of Abeta amyloid as a determinant of severity of neurodegeneration in Alzheimer's disease. *Ann Neurol,* 46**,** 860-6.

Mega, M. S., Cummings, J. L., Fiorello, T. & Gornbein, J. 1996. The spectrum of behavioral changes in Alzheimer's disease. *Neurology,* 46**,** 130-5.

Meng, X. & D'arcy, C. 2012. Education and dementia in the context of the cognitive reserve hypothesis: a systematic review with

meta-analyses and qualitative analyses. *PLoS One,* 7**,** e38268.

Meng, X. F., Yu, J. T., Wang, H. F., Tan, M. S., Wang, C., Tan, C. C. & Tan, L. 2014. Midlife vascular risk factors and the risk of Alzheimer's disease: a systematic review and meta-analysis. *J Alzheimers Dis,* 42**,** 1295-310.

Mielke, M. M., Haughey, N. J., Bandaru, V. V., Weinberg, D. D., Darby, E., Zaidi, N., Pavlik, V., Doody, R. S. & Lyketsos, C. G. 2011. Plasma sphingomyelins are associated with cognitive progression in Alzheimer's disease. *J Alzheimers Dis,* 27**,** 259-69.

Mills, S. M., Mallmann, J., Santacruz, A. M., Fuqua, A., Carril, M., Aisen, P. S., Althage, M. C., Belyew, S., Benzinger, T. L., Brooks, W. S., Buckles, V. D., Cairns, N. J., Clifford, D., Danek, A., Fagan, A. M., Farlow, M., Fox, N., Ghetti, B., Goate, A. M., Heinrichs, D., Hornbeck, R., Jack, C., Jucker, M., Klunk, W. E., Marcus, D. S., Martins, R. N., Masters, C. M., Mayeux, R., Mcdade, E., Morris, J. C., Oliver, A., Ringman, J. M., Rossor, M. N., Salloway, S., Schofield, P. R., Snider, J., Snyder, P., Sperling, R. A., Stewart, C., Thomas, R. G., Xiong, C. & Bateman, R. J. 2013. Preclinical trials in autosomal dominant AD: implementation of the DIAN-TU trial. *Rev Neurol (Paris),* 169**,** 737-43.

Mistridis, P., Krumm, S., Monsch, A. U., Berres, M. & Taylor, K. I. 2015. The 12 Years Preceding Mild Cognitive Impairment Due to Alzheimer's Disease: The Temporal Emergence of Cognitive Decline. *J Alzheimers Dis,* 48**,** 1095-107.

Mitchell, A. J. & Shiri-Feshki, M. 2009. Rate of progression of mild cognitive impairment to dementia--meta-analysis of 41 robust inception cohort studies. *Acta Psychiatr Scand,* 119**,** 252-65.

Modat, M., Cash, D. M., Daga, P., Winston, G. P., Duncan, J. S. & Ourselin, S. 2014. Global image registration using a symmetric block-matching approach. *J Med Imaging (Bellingham),* 1**,** 024003.

Morgan, D., Diamond, D. M., Gottschall, P. E., Ugen, K. E., Dickey, C., Hardy, J., Duff, K., Jantzen, P., Dicarlo, G., Wilcock, D., Connor, K., Hatcher, J., Hope, C., Gordon, M. & Arendash, G. W. 2000. A beta peptide vaccination prevents memory loss in an animal model of Alzheimer's disease. *Nature,* 408**,** 982-5.

Morra, J. H., Tu, Z., Apostolova, L. G., Green, A. E., Avedissian, C., Madsen, S. K., Parikshak, N., Hua, X., Toga, A. W., Jack, C. R., Jr., Schuff, N., Weiner, M. W., Thompson, P. M. & Alzheimer's Disease Neuroimaging, I. 2009. Automated 3D

mapping of hippocampal atrophy and its clinical correlates in 400 subjects with Alzheimer's disease, mild cognitive impairment, and elderly controls. *Hum Brain Mapp,* 30**,** 2766-88.

Morris, J. C. 1993. The Clinical Dementia Rating (CDR): current version and scoring rules. *Neurology,* 43**,** 2412-4.

Mosconi, L., Sorbi, S., De Leon, M. J., Li, Y., Nacmias, B., Myoung, P. S., Tsui, W., Ginestroni, A., Bessi, V., Fayyazz, M., Caffarra, P. & Pupi, A. 2006. Hypometabolism exceeds atrophy in presymptomatic early-onset familial Alzheimer's disease. *J Nucl Med,* 47**,** 1778-86.

Moulder, K. L., Snider, B. J., Mills, S. L., Buckles, V. D., Santacruz, A. M., Bateman, R. J. & Morris, J. C. 2013. Dominantly Inherited Alzheimer Network: facilitating research and clinical trials. *Alzheimers Res Ther,* 5**,** 48.

Muhlert, N., Grunewald, R. A., Hunkin, N. M., Reuber, M., Howell, S., Reynders, H. & Isaac, C. L. 2011. Accelerated long-term forgetting in temporal lobe but not idiopathic generalised epilepsy. *Neuropsychologia,* 49**,** 2417-26.

Muhlert, N., Milton, F., Butler, C. R., Kapur, N. & Zeman, A. Z. 2010. Accelerated forgetting of real-life events in Transient Epileptic Amnesia. *Neuropsychologia,* 48**,** 3235-44.

Mullan, M., Houlden, H., Crawford, F., Kennedy, A., Rogues, P. & Rossor, M. 1993. Age of onset in familial early onset Alzheimer's disease correlates with genetic aetiology. *Am J Med Genet,* 48**,** 129-30.

Muller, M. J., Greverus, D., Dellani, P. R., Weibrich, C., Wille, P. R., Scheurich, A., Stoeter, P. & Fellgiebel, A. 2005. Functional implications of hippocampal volume and diffusivity in mild cognitive impairment. *Neuroimage,* 28**,** 1033-42.

Muller, M. J., Greverus, D., Weibrich, C., Dellani, P. R., Scheurich, A., Stoeter, P. & Fellgiebel, A. 2007. Diagnostic utility of hippocampal size and mean diffusivity in amnestic MCI. *Neurobiol Aging,* 28**,** 398-403.

Muller, M. J., Mazanek, M., Weibrich, C., Dellani, P. R., Stoeter, P. & Fellgiebel, A. 2006. Distribution characteristics, reproducibility, and precision of region of interest-based hippocampal diffusion tensor imaging measures. *AJNR Am J Neuroradiol,* 27**,** 440-6.

Naj, A. C., Jun, G., Beecham, G. W., Wang, L. S., Vardarajan, B. N., Buros, J., Gallins, P. J., Buxbaum, J. D., Jarvik, G. P., Crane, P. K., Larson, E. B., Bird, T. D., Boeve, B. F., Graff-Radford, N. R., De Jager, P. L., Evans, D., Schneider, J. A.,

Carrasquillo, M. M., Ertekin-Taner, N., Younkin, S. G., Cruchaga, C., Kauwe, J. S., Nowotny, P., Kramer, P., Hardy, J., Huentelman, M. J., Myers, A. J., Barmada, M. M., Demirci, F. Y., Baldwin, C. T., Green, R. C., Rogaeva, E., St George-Hyslop, P., Arnold, S. E., Barber, R., Beach, T., Bigio, E. H., Bowen, J. D., Boxer, A., Burke, J. R., Cairns, N. J., Carlson, C. S., Carney, R. M., Carroll, S. L., Chui, H. C., Clark, D. G., Corneveaux, J., Cotman, C. W., Cummings, J. L., Decarli, C., Dekosky, S. T., Diaz-Arrastia, R., Dick, M., Dickson, D. W., Ellis, W. G., Faber, K. M., Fallon, K. B., Farlow, M. R., Ferris, S., Frosch, M. P., Galasko, D. R., Ganguli, M., Gearing, M., Geschwind, D. H., Ghetti, B., Gilbert, J. R., Gilman, S., Giordani, B., Glass, J. D., Growdon, J. H., Hamilton, R. L., Harrell, L. E., Head, E., Honig, L. S., Hulette, C. M., Hyman, B. T., Jicha, G. A., Jin, L. W., Johnson, N., Karlawish, J., Karydas, A., Kaye, J. A., Kim, R., Koo, E. H., Kowall, N. W., Lah, J. J., Levey, A. I., Lieberman, A. P., Lopez, O. L., Mack, W. J., Marson, D. C., Martiniuk, F., Mash, D. C., Masliah, E., Mccormick, W. C., Mccurry, S. M., Mcdavid, A. N., Mckee, A. C., Mesulam, M., Miller, B. L., et al. 2011. Common variants at MS4A4/MS4A6E, CD2AP, CD33 and EPHA1 are associated with late-onset Alzheimer's disease. *Nat Genet,* 43**,** 436-41.

Nestor, P. J., Graham, K. S., Bozeat, S., Simons, J. S. & Hodges, J. R. 2002. Memory consolidation and the hippocampus: further evidence from studies of autobiographical memory in semantic dementia and frontal variant frontotemporal dementia. *Neuropsychologia,* 40**,** 633-54.

Nilsberth, C., Westlind-Danielsson, A., Eckman, C. B., Condron, M. M., Axelman, K., Forsell, C., Stenh, C., Luthman, J., Teplow, D. B., Younkin, S. G., Naslund, J. & Lannfelt, L. 2001. The 'Arctic' APP mutation (E693G) causes Alzheimer's disease by enhanced Abeta protofibril formation. *Nat Neurosci,* 4**,** 887-93.

O'brien, R. J. & Wong, P. C. 2011. Amyloid precursor protein processing and Alzheimer's disease. *Annu Rev Neurosci,* 34**,** 185-204.

Ohno, M., Sametsky, E. A., Younkin, L. H., Oakley, H., Younkin, S. G., Citron, M., Vassar, R. & Disterhoft, J. F. 2004. BACE1 deficiency rescues memory deficits and cholinergic dysfunction in a mouse model of Alzheimer's disease. *Neuron,* 41**,** 27-33.

Okamura, N., Harada, R., Furumoto, S., Arai, H., Yanai, K. & Kudo, Y. 2014. Tau PET Imaging in Alzheimer's Disease. *Curr Neurol Neurosci Rep,* 14**,** 500.

Olsson, B., Hertze, J., Ohlsson, M., Nagga, K., Hoglund, K., Basun, H., Annas, P., Lannfelt, L., Andreasen, N., Minthon, L., Zetterberg, H., Blennow, K. & Hansson, O. 2013. Cerebrospinal fluid levels of heart fatty acid binding protein are elevated prodromally in Alzheimer's disease and vascular dementia. *J Alzheimers Dis,* 34**,** 673-9.

Olsson, B., Lautner, R., Andreasson, U., Ohrfelt, A., Portelius, E., Bjerke, M., Holtta, M., Rosen, C., Olsson, C., Strobel, G., Wu, E., Dakin, K., Petzold, M., Blennow, K. & Zetterberg, H. 2016. CSF and blood biomarkers for the diagnosis of Alzheimer's disease: a systematic review and meta-analysis. *Lancet Neurol,* 15**,** 673-84.

Ossenkoppele, R., Pijnenburg, Y. A., Perry, D. C., Cohn-Sheehy, B. I., Scheltens, N. M., Vogel, J. W., Kramer, J. H., Van Der Vlies, A. E., La Joie, R., Rosen, H. J., Van Der Flier, W. M., Grinberg, L. T., Rozemuller, A. J., Huang, E. J., Van Berckel, B. N., Miller, B. L., Barkhof, F., Jagust, W. J., Scheltens, P., Seeley, W. W. & Rabinovici, G. D. 2015. The behavioural/dysexecutive variant of Alzheimer's disease: clinical, neuroimaging and pathological features. *Brain,* 138**,** 2732-49.

Ossenkoppele, R., Schonhaut, D. R., Scholl, M., Lockhart, S. N., Ayakta, N., Baker, S. L., O'neil, J. P., Janabi, M., Lazaris, A., Cantwell, A., Vogel, J., Santos, M., Miller, Z. A., Bettcher, B. M., Vossel, K. A., Kramer, J. H., Gorno-Tempini, M. L., Miller, B. L., Jagust, W. J. & Rabinovici, G. D. 2016. Tau PET patterns mirror clinical and neuroanatomical variability in Alzheimer's disease. *Brain,* 139**,** 1551-67.

Ostrowitzki, S., Deptula, D., Thurfjell, L., Barkhof, F., Bohrmann, B., Brooks, D. J., Klunk, W. E., Ashford, E., Yoo, K., Xu, Z. X., Loetscher, H. & Santarelli, L. 2012. Mechanism of amyloid removal in patients with Alzheimer disease treated with gantenerumab. *Arch Neurol,* 69**,** 198-207.

Ownby, R. L., Crocco, E., Acevedo, A., John, V. & Loewenstein, D. 2006. Depression and risk for Alzheimer disease: systematic review, meta-analysis, and metaregression analysis. *Arch Gen Psychiatry,* 63**,** 530-8.

Palumbo, B., Siepi, D., Sabalich, I., Tranfaglia, C. & Parnetti, L. 2008. Cerebrospinal fluid neuron-specific enolase: a further marker of Alzheimer's disease? *Funct Neurol,* 23**,** 93-6.

Parks, A. L. & Curtis, D. 2007. Presenilin diversifies its portfolio. *Trends Genet,* 23**,** 140-50.

Parra, M. A., Abrahams, S., Logie, R. H., Mendez, L. G., Lopera, F. & Della Sala, S. 2010. Visual short-term memory binding deficits in familial Alzheimer's disease. *Brain,* 133**,** 2702-13.

Pedregosa, F., Varoquaux, G., Gramfort, A., Michel, V., Thirion, B., Grisel, O., Blondel, M., Prettenhofer, P., Weiss, R., Dubourg, V., Vanderplas, J., Passos, A., Cournapeau, D., Brucher, M., Perrot, M. & Duchesnay, E. 2011. Scikit-learn: Machine Learning in Python. *Journal of Machine Learning Research,* 12**,** 2825-2830.

Pegueroles, J., Vilaplana, E., Montal, V., Sampedro, F., Alcolea, D., Carmona-Iragui, M., Clarimon, J., Blesa, R., Lleo, A., Fortea, J. & Alzheimer's Disease Neuroimaging, I. 2017. Longitudinal brain structural changes in preclinical Alzheimer's disease. *Alzheimers Dement,* 13**,** 499-509.

Perrotin, A., La Joie, R., De La Sayette, V., Barre, L., Mezenge, F., Mutlu, J., Guilloteau, D., Egret, S., Eustache, F. & Chetelat, G. 2016. Subjective cognitive decline in cognitively normal elders from the community or from a memory clinic: Differential affective and imaging correlates. *Alzheimers Dement*.

Perry, D. C., Sturm, V. E., Peterson, M. J., Pieper, C. F., Bullock, T., Boeve, B. F., Miller, B. L., Guskiewicz, K. M., Berger, M. S., Kramer, J. H. & Welsh-Bohmer, K. A. 2016. Association of traumatic brain injury with subsequent neurological and psychiatric disease: a meta-analysis. *J Neurosurg,* 124**,** 511-26.

Petrie, E. C., Cross, D. J., Galasko, D., Schellenberg, G. D., Raskind, M. A., Peskind, E. R. & Minoshima, S. 2009. Preclinical evidence of Alzheimer changes: convergent cerebrospinal fluid biomarker and fluorodeoxyglucose positron emission tomography findings. *Arch Neurol,* 66**,** 632-7.

Pietrzak, R. H., Lim, Y. Y., Ames, D., Harrington, K., Restrepo, C., Martins, R. N., Rembach, A., Laws, S. M., Masters, C. L., Villemagne, V. L., Rowe, C. C., Maruff, P., Australian Imaging, B. & Lifestyle Research, G. 2015. Trajectories of memory decline in preclinical Alzheimer's disease: results from the Australian Imaging, Biomarkers and Lifestyle Flagship Study of Ageing. *Neurobiol Aging,* 36**,** 1231-8.

Pievani, M., De Haan, W., Wu, T., Seeley, W. W. & Frisoni, G. B. 2011. Functional network disruption in the degenerative dementias. *Lancet Neurol,* 10**,** 829-43.

Pike, K. E., Savage, G., Villemagne, V. L., Ng, S., Moss, S. A., Maruff, P., Mathis, C. A., Klunk, W. E., Masters, C. L. & Rowe, C. C. 2007. Beta-amyloid imaging and memory in non-

demented individuals: evidence for preclinical Alzheimer's disease. *Brain,* 130**,** 2837-44.

Pollard, H. B., Arispe, N. & Rojas, E. 1995. Ion channel hypothesis for Alzheimer amyloid peptide neurotoxicity. *Cell Mol Neurobiol,* 15**,** 513-26.

Porsteinsson, A. P., Grossberg, G. T., Mintzer, J., Olin, J. T. & Memantine, M. E. M. M. D. S. G. 2008. Memantine treatment in patients with mild to moderate Alzheimer's disease already receiving a cholinesterase inhibitor: a randomized, double-blind, placebo-controlled trial. *Curr Alzheimer Res,* 5**,** 83-9.

Proitsi, P., Kim, M., Whiley, L., Simmons, A., Sattlecker, M., Velayudhan, L., Lupton, M. K., Soininen, H., Kloszewska, I., Mecocci, P., Tsolaki, M., Vellas, B., Lovestone, S., Powell, J. F., Dobson, R. J. & Legido-Quigley, C. 2016. Association of blood lipids with Alzheimer's disease: A comprehensive lipidomics analysis. *Alzheimers Dement*.

Quiroz, Y. T., Stern, C. E., Reiman, E. M., Brickhouse, M., Ruiz, A., Sperling, R. A., Lopera, F. & Dickerson, B. C. 2013. Cortical atrophy in presymptomatic Alzheimer's disease presenilin 1 mutation carriers. *J Neurol Neurosurg Psychiatry,* 84**,** 556-61.

Raiha, I., Kaprio, J., Koskenvuo, M., Rajala, T. & Sourander, L. 1996. Alzheimer's disease in Finnish twins. *Lancet,* 347**,** 573-8.

Rasch, B. & Born, J. 2013. About sleep's role in memory. *Physiol Rev,* 93**,** 681-766.

Ray, S., Britschgi, M., Herbert, C., Takeda-Uchimura, Y., Boxer, A., Blennow, K., Friedman, L. F., Galasko, D. R., Jutel, M., Karydas, A., Kaye, J. A., Leszek, J., Miller, B. L., Minthon, L., Quinn, J. F., Rabinovici, G. D., Robinson, W. H., Sabbagh, M. N., So, Y. T., Sparks, D. L., Tabaton, M., Tinklenberg, J., Yesavage, J. A., Tibshirani, R. & Wyss-Coray, T. 2007. Classification and prediction of clinical Alzheimer's diagnosis based on plasma signaling proteins. *Nat Med,* 13**,** 1359-62.

Reiman, E. M., Langbaum, J. B., Fleisher, A. S., Caselli, R. J., Chen, K., Ayutyanont, N., Quiroz, Y. T., Kosik, K. S., Lopera, F. & Tariot, P. N. 2011. Alzheimer's Prevention Initiative: a plan to accelerate the evaluation of presymptomatic treatments. *J Alzheimers Dis,* 26 Suppl 3**,** 321-9.

Reiman, E. M., Quiroz, Y. T., Fleisher, A. S., Chen, K., Velez-Pardo, C., Jimenez-Del-Rio, M., Fagan, A. M., Shah, A. R., Alvarez, S., Arbelaez, A., Giraldo, M., Acosta-Baena, N., Sperling, R. A., Dickerson, B., Stern, C. E., Tirado, V., Munoz, C., Reiman, R. A., Huentelman, M. J., Alexander, G. E., Langbaum, J. B.

S., Kosik, K. S., Tariot, P. N. & Lopera, F. 2012. Brain imaging and fluid biomarker analysis in young adults at genetic risk for autosomal dominant Alzheimer's disease in the presenilin 1 E280A kindred: a case-control study. *The Lancet Neurology,* 11**,** 1048-1056.

Reisberg, B., Doody, R., Stoffler, A., Schmitt, F., Ferris, S., Mobius, H. J. & Memantine Study, G. 2003. Memantine in moderate-to-severe Alzheimer's disease. *N Engl J Med,* 348**,** 1333-41.

Reisberg, B., Prichep, L., Mosconi, L., John, E. R., Glodzik-Sobanska, L., Boksay, I., Monteiro, I., Torossian, C., Vedvyas, A., Ashraf, N., Jamil, I. A. & De Leon, M. J. 2008. The pre-mild cognitive impairment, subjective cognitive impairment stage of Alzheimer's disease. *Alzheimers Dement,* 4**,** S98-S108.

Rentz, D. M., Parra Rodriguez, M. A., Amariglio, R., Stern, Y., Sperling, R. & Ferris, S. 2013. Promising developments in neuropsychological approaches for the detection of preclinical Alzheimer's disease: a selective review. *Alzheimers Res Ther,* 5**,** 58.

Richardson, K., Schoen, M., French, B., Umscheid, C. A., Mitchell, M. D., Arnold, S. E., Heidenreich, P. A., Rader, D. J. & Degoma, E. M. 2013. Statins and cognitive function: a systematic review. *Ann Intern Med,* 159**,** 688-97.

Ridha, B. H., Barnes, J., Bartlett, J. W., Godbolt, A., Pepple, T., Rossor, M. N. & Fox, N. C. 2006. Tracking atrophy progression in familial Alzheimer's disease: a serial MRI study. *Lancet Neurol,* 5**,** 828-34.

Ringman, J. M., O'neill, J., Geschwind, D., Medina, L., Apostolova, L. G., Rodriguez, Y., Schaffer, B., Varpetian, A., Tseng, B., Ortiz, F., Fitten, J., Cummings, J. L. & Bartzokis, G. 2007. Diffusion tensor imaging in preclinical and presymptomatic carriers of familial Alzheimer's disease mutations. *Brain,* 130**,** 1767-76.

Rissin, D. M., Kan, C. W., Campbell, T. G., Howes, S. C., Fournier, D. R., Song, L., Piech, T., Patel, P. P., Chang, L., Rivnak, A. J., Ferrell, E. P., Randall, J. D., Provuncher, G. K., Walt, D. R. & Duffy, D. C. 2010. Single-molecule enzyme-linked immunosorbent assay detects serum proteins at subfemtomolar concentrations. *Nat Biotechnol,* 28**,** 595-9.

Ritchie, K. & Kildea, D. 1995. Is senile dementia "age-related" or "ageing-related"?--evidence from meta-analysis of dementia prevalence in the oldest old. *Lancet,* 346**,** 931-4.

Rogers, S. L., Farlow, M. R., Doody, R. S., Mohs, R. & Friedhoff, L. T. 1998. A 24-week, double-blind, placebo-controlled trial of

donepezil in patients with Alzheimer's disease. Donepezil Study Group. *Neurology,* 50**,** 136-45.

Rohrer, J. D., Woollacott, I. O., Dick, K. M., Brotherhood, E., Gordon, E., Fellows, A., Toombs, J., Druyeh, R., Cardoso, M. J., Ourselin, S., Nicholas, J. M., Norgren, N., Mead, S., Andreasson, U., Blennow, K., Schott, J. M., Fox, N. C., Warren, J. D. & Zetterberg, H. 2016. Serum neurofilament light chain protein is a measure of disease intensity in frontotemporal dementia. *Neurology*.

Rojas, J. C., Karydas, A., Bang, J., Tsai, R. M., Blennow, K., Liman, V., Kramer, J. H., Rosen, H., Miller, B. L., Zetterberg, H. & Boxer, A. L. 2016. Plasma neurofilament light chain predicts progression in progressive supranuclear palsy. *Ann Clin Transl Neurol,* 3**,** 216-25.

Rose, S. E., Janke, A. L. & Chalk, J. B. 2008. Gray and white matter changes in Alzheimer's disease: a diffusion tensor imaging study. *J Magn Reson Imaging,* 27**,** 20-6.

Rosengren, L. E., Karlsson, J. E., Karlsson, J. O., Persson, L. I. & Wikkelso, C. 1996. Patients with amyotrophic lateral sclerosis and other neurodegenerative diseases have increased levels of neurofilament protein in CSF. *J Neurochem,* 67**,** 2013-8.

Rossor, M. N. 1983. Focal changes in Alzheimer's disease and cholinergic hypothesis. *Lancet,* 2**,** 465.

Rovelet-Lecrux, A., Hannequin, D., Raux, G., Le Meur, N., Laquerriere, A., Vital, A., Dumanchin, C., Feuillette, S., Brice, A., Vercelletto, M., Dubas, F., Frebourg, T. & Campion, D. 2006. APP locus duplication causes autosomal dominant early-onset Alzheimer disease with cerebral amyloid angiopathy. *Nat Genet,* 38**,** 24-6.

Rubio-Perez, J. M. & Morillas-Ruiz, J. M. 2012. A review: inflammatory process in Alzheimer's disease, role of cytokines. *ScientificWorldJournal,* 2012**,** 756357.

Ryan, N. S., Keihaninejad, S., Shakespeare, T. J., Lehmann, M., Crutch, S. J., Malone, I. B., Thornton, J. S., Mancini, L., Hyare, H., Yousry, T., Ridgway, G. R., Zhang, H., Modat, M., Alexander, D. C., Rossor, M. N., Ourselin, S. & Fox, N. C. 2013. Magnetic resonance imaging evidence for presymptomatic change in thalamus and caudate in familial Alzheimer's disease. *Brain,* 136**,** 1399-414.

Ryan, N. S., Nicholas, J. M., Weston, P. S., Liang, Y., Lashley, T., Guerreiro, R., Adamson, G., Kenny, J., Beck, J., Chavez-Gutierrez, L., De Strooper, B., Revesz, T., Holton, J., Mead, S., Rossor, M. N. & Fox, N. C. 2016. Clinical phenotype and

genetic associations in autosomal dominant familial Alzheimer's disease: a case series. *Lancet Neurol,* 15**,** 1326-1335.

Ryan, N. S. & Rossor, M. N. 2010. Correlating familial Alzheimer's disease gene mutations with clinical phenotype. *Biomark Med,* 4**,** 99-112.

Ryman, D. C., Acosta-Baena, N., Aisen, P. S., Bird, T., Danek, A., Fox, N. C., Goate, A., Frommelt, P., Ghetti, B., Langbaum, J. B., Lopera, F., Martins, R., Masters, C. L., Mayeux, R. P., Mcdade, E., Moreno, S., Reiman, E. M., Ringman, J. M., Salloway, S., Schofield, P. R., Sperling, R., Tariot, P. N., Xiong, C., Morris, J. C., Bateman, R. J. & Dominantly Inherited Alzheimer, N. 2014. Symptom onset in autosomal dominant Alzheimer disease: a systematic review and meta-analysis. *Neurology,* 83**,** 253-60.

Sala-Llonch, R., Llado, A., Fortea, J., Bosch, B., Antonell, A., Balasa, M., Bargallo, N., Bartres-Faz, D., Molinuevo, J. L. & Sanchez-Valle, R. 2015. Evolving brain structural changes in PSEN1 mutation carriers. *Neurobiol Aging,* 36**,** 1261-70.

Salloway, S., Sperling, R., Fox, N. C., Blennow, K., Klunk, W., Raskind, M., Sabbagh, M., Honig, L. S., Porsteinsson, A. P., Ferris, S., Reichert, M., Ketter, N., Nejadnik, B., Guenzler, V., Miloslavsky, M., Wang, D., Lu, Y., Lull, J., Tudor, I. C., Liu, E., Grundman, M., Yuen, E., Black, R., Brashear, H. R., Bapineuzumab & Clinical Trial, I. 2014. Two phase 3 trials of bapineuzumab in mild-to-moderate Alzheimer's disease. *N Engl J Med,* 370**,** 322-33.

Salloway, S., Sperling, R., Gilman, S., Fox, N. C., Blennow, K., Raskind, M., Sabbagh, M., Honig, L. S., Doody, R., Van Dyck, C. H., Mulnard, R., Barakos, J., Gregg, K. M., Liu, E., Lieberburg, I., Schenk, D., Black, R., Grundman, M. & Bapineuzumab 201 Clinical Trial, I. 2009. A phase 2 multiple ascending dose trial of bapineuzumab in mild to moderate Alzheimer disease. *Neurology,* 73**,** 2061-70.

Sattlecker, M., Khondoker, M., Proitsi, P., Williams, S., Soininen, H., Kloszewska, I., Mecocci, P., Tsolaki, M., Vellas, B., Lovestone, S. & Dobson, R. J. 2016. Longitudinal Protein Changes in Blood Plasma Associated with the Rate of Cognitive Decline in Alzheimer's Disease. *J Alzheimers Dis,* 49**,** 1105-14.

Scahill, R. I., Frost, C., Jenkins, R., Whitwell, J. L., Rossor, M. N. & Fox, N. C. 2003. A longitudinal study of brain volume changes in normal aging using serial registered magnetic resonance imaging. *Arch Neurol,* 60**,** 989-94.

Scahill, R. I., Ridgway, G. R., Bartlett, J. W., Barnes, J., Ryan, N. S., Mead, S., Beck, J., Clarkson, M. J., Crutch, S. J., Schott, J. M., Ourselin, S., Warren, J. D., Hardy, J., Rossor, M. N. & Fox, N. C. 2013. Genetic influences on atrophy patterns in familial Alzheimer's Disease: a comparison of APP and PSEN1 mutations. *J Alzheimers Dis,* 35**,** 199-212.

Scheltens, P., Launer, L. J., Barkhof, F., Weinstein, H. C. & Van Gool, W. A. 1995. Visual assessment of medial temporal lobe atrophy on magnetic resonance imaging: interobserver reliability. *J Neurol,* 242**,** 557-60.

Scheltens, P., Leys, D., Barkhof, F., Huglo, D., Weinstein, H. C., Vermersch, P., Kuiper, M., Steinling, M., Wolters, E. C. & Valk, J. 1992. Atrophy of medial temporal lobes on MRI in "probable" Alzheimer's disease and normal ageing: diagnostic value and neuropsychological correlates. *J Neurol Neurosurg Psychiatry,* 55**,** 967-72.

Schenk, D., Barbour, R., Dunn, W., Gordon, G., Grajeda, H., Guido, T., Hu, K., Huang, J., Johnson-Wood, K., Khan, K., Kholodenko, D., Lee, M., Liao, Z., Lieberburg, I., Motter, R., Mutter, L., Soriano, F., Shopp, G., Vasquez, N., Vandevert, C., Walker, S., Wogulis, M., Yednock, T., Games, D. & Seubert, P. 1999. Immunization with amyloid-beta attenuates Alzheimer-disease-like pathology in the PDAPP mouse. *Nature,* 400**,** 173-7.

Scherling, C. S., Hall, T., Berisha, F., Klepac, K., Karydas, A., Coppola, G., Kramer, J. H., Rabinovici, G., Ahlijanian, M., Miller, B. L., Seeley, W., Grinberg, L. T., Rosen, H., Meredith, J., Jr. & Boxer, A. L. 2014. Cerebrospinal fluid neurofilament concentration reflects disease severity in frontotemporal degeneration. *Ann Neurol,* 75**,** 116-26.

Scheuner, D., Eckman, C., Jensen, M., Song, X., Citron, M., Suzuki, N., Bird, T. D., Hardy, J., Hutton, M., Kukull, W., Larson, E., Levy-Lahad, E., Viitanen, M., Peskind, E., Poorkaj, P., Schellenberg, G., Tanzi, R., Wasco, W., Lannfelt, L., Selkoe, D. & Younkin, S. 1996. Secreted amyloid beta-protein similar to that in the senile plaques of Alzheimer's disease is increased in vivo by the presenilin 1 and 2 and APP mutations linked to familial Alzheimer's disease. *Nat Med,* 2**,** 864-70.

Schmid, N. S., Taylor, K. I., Foldi, N. S., Berres, M. & Monsch, A. U. 2013. Neuropsychological signs of Alzheimer's disease 8 years prior to diagnosis. *J Alzheimers Dis,* 34**,** 537-46.

Schubert, D., Behl, C., Lesley, R., Brack, A., Dargusch, R., Sagara, Y. & Kimura, H. 1995. Amyloid peptides are toxic via a

common oxidative mechanism. *Proc Natl Acad Sci U S A,* 92**,** 1989-93.

Scola, E., Bozzali, M., Agosta, F., Magnani, G., Franceschi, M., Sormani, M. P., Cercignani, M., Pagani, E., Falautano, M., Filippi, M. & Falini, A. 2010. A diffusion tensor MRI study of patients with MCI and AD with a 2-year clinical follow-up. *J Neurol Neurosurg Psychiatry,* 81**,** 798-805.

Scott, L. J. & Goa, K. L. 2000. Galantamine: a review of its use in Alzheimer's disease. *Drugs,* 60**,** 1095-122.

Selkoe, D. J. 1991. The molecular pathology of Alzheimer's disease. *Neuron,* 6**,** 487-98.

Senior, K. 2002. Dosing in phase II trial of Alzheimer's vaccine suspended. *Lancet Neurol,* 1**,** 3.

Seshadri, S., Fitzpatrick, A. L., Ikram, M. A., Destefano, A. L., Gudnason, V., Boada, M., Bis, J. C., Smith, A. V., Carassquillo, M. M., Lambert, J. C., Harold, D., Schrijvers, E. M., Ramirez-Lorca, R., Debette, S., Longstreth, W. T., Jr., Janssens, A. C., Pankratz, V. S., Dartigues, J. F., Hollingworth, P., Aspelund, T., Hernandez, I., Beiser, A., Kuller, L. H., Koudstaal, P. J., Dickson, D. W., Tzourio, C., Abraham, R., Antunez, C., Du, Y., Rotter, J. I., Aulchenko, Y. S., Harris, T. B., Petersen, R. C., Berr, C., Owen, M. J., Lopez-Arrieta, J., Varadarajan, B. N., Becker, J. T., Rivadeneira, F., Nalls, M. A., Graff-Radford, N. R., Campion, D., Auerbach, S., Rice, K., Hofman, A., Jonsson, P. V., Schmidt, H., Lathrop, M., Mosley, T. H., Au, R., Psaty, B. M., Uitterlinden, A. G., Farrer, L. A., Lumley, T., Ruiz, A., Williams, J., Amouyel, P., Younkin, S. G., Wolf, P. A., Launer, L. J., Lopez, O. L., Van Duijn, C. M., Breteler, M. M., Consortium, C., Consortium, G. & Consortium, E. 2010. Genome-wide analysis of genetic loci associated with Alzheimer disease. *JAMA,* 303**,** 1832-40.

Sevigny, J., Chiao, P., Bussiere, T., Weinreb, P. H., Williams, L., Maier, M., Dunstan, R., Salloway, S., Chen, T., Ling, Y., O'gorman, J., Qian, F., Arastu, M., Li, M., Chollate, S., Brennan, M. S., Quintero-Monzon, O., Scannevin, R. H., Arnold, H. M., Engber, T., Rhodes, K., Ferrero, J., Hang, Y., Mikulskis, A., Grimm, J., Hock, C., Nitsch, R. M. & Sandrock, A. 2016. The antibody aducanumab reduces Abeta plaques in Alzheimer's disease. *Nature,* 537**,** 50-6.

Shea, Y. F., Chu, L. W., Chan, A. O., Ha, J., Li, Y. & Song, Y. Q. 2016. A systematic review of familial Alzheimer's disease: Differences in presentation of clinical features among three

mutated genes and potential ethnic differences. *J Formos Med Assoc,* 115**,** 67-75.

Sherrington, R., Rogaev, E. I., Liang, Y., Rogaeva, E. A., Levesque, G., Ikeda, M., Chi, H., Lin, C., Li, G., Holman, K., Tsuda, T., Mar, L., Foncin, J. F., Bruni, A. C., Montesi, M. P., Sorbi, S., Rainero, I., Pinessi, L., Nee, L., Chumakov, I., Pollen, D., Brookes, A., Sanseau, P., Polinsky, R. J., Wasco, W., Da Silva, H. A., Haines, J. L., Perkicak-Vance, M. A., Tanzi, R. E., Roses, A. D., Fraser, P. E., Rommens, J. M. & St George-Hyslop, P. H. 1995. Cloning of a gene bearing missense mutations in early-onset familial Alzheimer's disease. *Nature,* 375**,** 754-60.

Silverman, D. H., Small, G. W., Chang, C. Y., Lu, C. S., Kung De Aburto, M. A., Chen, W., Czernin, J., Rapoport, S. I., Pietrini, P., Alexander, G. E., Schapiro, M. B., Jagust, W. J., Hoffman, J. M., Welsh-Bohmer, K. A., Alavi, A., Clark, C. M., Salmon, E., De Leon, M. J., Mielke, R., Cummings, J. L., Kowell, A. P., Gambhir, S. S., Hoh, C. K. & Phelps, M. E. 2001. Positron emission tomography in evaluation of dementia: Regional brain metabolism and long-term outcome. *JAMA,* 286**,** 2120-7.

Simons, J. S. & Spiers, H. J. 2003. Prefrontal and medial temporal lobe interactions in long-term memory. *Nat Rev Neurosci,* 4**,** 637-48.

Sjogren, M., Blomberg, M., Jonsson, M., Wahlund, L. O., Edman, A., Lind, K., Rosengren, L., Blennow, K. & Wallin, A. 2001. Neurofilament protein in cerebrospinal fluid: a marker of white matter changes. *J Neurosci Res,* 66**,** 510-6.

Skillback, T., Farahmand, B., Bartlett, J. W., Rosen, C., Mattsson, N., Nagga, K., Kilander, L., Religa, D., Wimo, A., Winblad, B., Rosengren, L., Schott, J. M., Blennow, K., Eriksdotter, M. & Zetterberg, H. 2014. CSF neurofilament light differs in neurodegenerative diseases and predicts severity and survival. *Neurology,* 83**,** 1945-53.

Smith, M. A., Atwood, C. S., Joseph, J. A. & Perry, G. 2002. Predicting the failure of amyloid-beta vaccine. *Lancet,* 359**,** 1864-5.

Snyder, E. M., Nong, Y., Almeida, C. G., Paul, S., Moran, T., Choi, E. Y., Nairn, A. C., Salter, M. W., Lombroso, P. J., Gouras, G. K. & Greengard, P. 2005. Regulation of NMDA receptor trafficking by amyloid-beta. *Nat Neurosci,* 8**,** 1051-8.

Soares, H. D., Chen, Y., Sabbagh, M., Roher, A., Schrijvers, E. & Breteler, M. 2009. Identifying early markers of Alzheimer's

disease using quantitative multiplex proteomic immunoassay panels. *Ann N Y Acad Sci,* 1180**,** 56-67.
Society, A. S. 2014. Dementia UK update.
Sotiropoulos, S. N., Jbabdi, S., Xu, J., Andersson, J. L., Moeller, S., Auerbach, E. J., Glasser, M. F., Hernandez, M., Sapiro, G., Jenkinson, M., Feinberg, D. A., Yacoub, E., Lenglet, C., Van Essen, D. C., Ugurbil, K., Behrens, T. E. & Consortium, W. U.-M. H. 2013. Advances in diffusion MRI acquisition and processing in the Human Connectome Project. *Neuroimage,* 80**,** 125-43.
Sperling, R. A., Aisen, P. S., Beckett, L. A., Bennett, D. A., Craft, S., Fagan, A. M., Iwatsubo, T., Jack, C. R., Jr., Kaye, J., Montine, T. J., Park, D. C., Reiman, E. M., Rowe, C. C., Siemers, E., Stern, Y., Yaffe, K., Carrillo, M. C., Thies, B., Morrison-Bogorad, M., Wagster, M. V. & Phelps, C. H. 2011a. Toward defining the preclinical stages of Alzheimer's disease: recommendations from the National Institute on Aging-Alzheimer's Association workgroups on diagnostic guidelines for Alzheimer's disease. *Alzheimers Dement,* 7**,** 280-92.
Sperling, R. A., Jack, C. R., Jr. & Aisen, P. S. 2011b. Testing the right target and right drug at the right stage. *Sci Transl Med,* 3**,** 111cm33.
Sperling, R. A., Jack, C. R., Jr., Black, S. E., Frosch, M. P., Greenberg, S. M., Hyman, B. T., Scheltens, P., Carrillo, M. C., Thies, W., Bednar, M. M., Black, R. S., Brashear, H. R., Grundman, M., Siemers, E. R., Feldman, H. H. & Schindler, R. J. 2011c. Amyloid-related imaging abnormalities in amyloid-modifying therapeutic trials: recommendations from the Alzheimer's Association Research Roundtable Workgroup. *Alzheimers Dement,* 7**,** 367-85.
Sperling, R. A., Rentz, D. M., Johnson, K. A., Karlawish, J., Donohue, M., Salmon, D. P. & Aisen, P. 2014. The A4 study: stopping AD before symptoms begin? *Sci Transl Med,* 6**,** 228fs13.
Stahl, R., Dietrich, O., Teipel, S. J., Hampel, H., Reiser, M. F. & Schoenberg, S. O. 2007. White matter damage in Alzheimer disease and mild cognitive impairment: assessment with diffusion-tensor MR imaging and parallel imaging techniques. *Radiology,* 243**,** 483-92.
Stern, Y. 2012. Cognitive reserve in ageing and Alzheimer's disease. *Lancet Neurol,* 11**,** 1006-12.
Takahashi, S., Yonezawa, H., Takahashi, J., Kudo, M., Inoue, T. & Tohgi, H. 2002. Selective reduction of diffusion anisotropy in

white matter of Alzheimer disease brains measured by 3.0 Tesla magnetic resonance imaging. *Neurosci Lett,* 332**,** 45-8.

Tang, M., Ryman, D. C., Mcdade, E., Jasielec, M. S., Buckles, V. D., Cairns, N. J., Fagan, A. M., Goate, A., Marcus, D. S., Xiong, C., Allegri, R. F., Chhatwal, J. P., Danek, A., Farlow, M. R., Fox, N. C., Ghetti, B., Graff-Radford, N. R., Laske, C., Martins, R. N., Masters, C. L., Mayeux, R. P., Ringman, J. M., Rossor, M. N., Salloway, S. P., Schofield, P. R., Morris, J. C., Bateman, R. J. & Dominantly Inherited Alzheimer, N. 2016. Neurological manifestations of autosomal dominant familial Alzheimer's disease: a comparison of the published literature with the Dominantly Inherited Alzheimer Network observational study (DIAN-OBS). *Lancet Neurol,* 15**,** 1317-1325.

Tarawneh, R., D'angelo, G., Macy, E., Xiong, C., Carter, D., Cairns, N. J., Fagan, A. M., Head, D., Mintun, M. A., Ladenson, J. H., Lee, J. M., Morris, J. C. & Holtzman, D. M. 2011. Visinin-like protein-1: diagnostic and prognostic biomarker in Alzheimer disease. *Ann Neurol,* 70**,** 274-85.

Tariot, P. N., Solomon, P. R., Morris, J. C., Kershaw, P., Lilienfeld, S. & Ding, C. 2000. A 5-month, randomized, placebo-controlled trial of galantamine in AD. The Galantamine USA-10 Study Group. *Neurology,* 54**,** 2269-76.

Taylor, D. G. & Bushell, M. C. 1985. The spatial mapping of translational diffusion coefficients by the NMR imaging technique. *Phys Med Biol,* 30**,** 345-9.

Testa, C., Laakso, M. P., Sabattoli, F., Rossi, R., Beltramello, A., Soininen, H. & Frisoni, G. B. 2004. A comparison between the accuracy of voxel-based morphometry and hippocampal volumetry in Alzheimer's disease. *J Magn Reson Imaging,* 19**,** 274-82.

Teunissen, C. E., Dijkstra, C. & Polman, C. 2005. Biological markers in CSF and blood for axonal degeneration in multiple sclerosis. *Lancet Neurol,* 4**,** 32-41.

Thal, D. R., Ghebremedhin, E., Orantes, M. & Wiestler, O. D. 2003. Vascular pathology in Alzheimer disease: correlation of cerebral amyloid angiopathy and arteriosclerosis/lipohyalinosis with cognitive decline. *J Neuropathol Exp Neurol,* 62**,** 1287-301.

Thompson, P. J. & Corcoran, R. 1992. Everyday memory failures in people with epilepsy. *Epilepsia,* 33 Suppl 6**,** S18-20.

Thordardottir, S., Stahlbom, A. K., Ferreira, D., Almkvist, O., Westman, E., Zetterberg, H., Eriksdotter, M., Blennow, K. &

Graff, C. 2015. Preclinical cerebrospinal fluid and volumetric magnetic resonance imaging biomarkers in Swedish familial Alzheimer's disease. *J Alzheimers Dis,* 43**,** 1393-402.

Tomic, J. L., Pensalfini, A., Head, E. & Glabe, C. G. 2009. Soluble fibrillar oligomer levels are elevated in Alzheimer's disease brain and correlate with cognitive dysfunction. *Neurobiol Dis,* 35**,** 352-8.

Tondelli, M., Wilcock, G. K., Nichelli, P., De Jager, C. A., Jenkinson, M. & Zamboni, G. 2012. Structural MRI changes detectable up to ten years before clinical Alzheimer's disease. *Neurobiol Aging,* 33**,** 825 e25-36.

Tortelli, R., Ruggieri, M., Cortese, R., D'errico, E., Capozzo, R., Leo, A., Mastrapasqua, M., Zoccolella, S., Leante, R., Livrea, P., Logroscino, G. & Simone, I. L. 2012. Elevated cerebrospinal fluid neurofilament light levels in patients with amyotrophic lateral sclerosis: a possible marker of disease severity and progression. *Eur J Neurol,* 19**,** 1561-7.

Trzepacz, P. T., Yu, P., Sun, J., Schuh, K., Case, M., Witte, M. M., Hochstetler, H., Hake, A. & Alzheimer's Disease Neuroimaging, I. 2014. Comparison of neuroimaging modalities for the prediction of conversion from mild cognitive impairment to Alzheimer's dementia. *Neurobiol Aging,* 35**,** 143-51.

Tyas, S. L., Snowdon, D. A., Desrosiers, M. F., Riley, K. P. & Markesbery, W. R. 2007. Healthy ageing in the Nun Study: definition and neuropathologic correlates. *Age Ageing,* 36**,** 650-5.

Uchida, K., Shan, L., Suzuki, H., Tabuse, Y., Nishimura, Y., Hirokawa, Y., Mizukami, K., Akatsu, H., Meno, K. & Asada, T. 2015. Amyloid-beta sequester proteins as blood-based biomarkers of cognitive decline. *Alzheimers Dement (Amst),* 1**,** 270-80.

Ulug, A. M., Moore, D. F., Bojko, A. S. & Zimmerman, R. D. 1999. Clinical use of diffusion-tensor imaging for diseases causing neuronal and axonal damage. *AJNR Am J Neuroradiol,* 20**,** 1044-8.

Van Petten, C. 2004. Relationship between hippocampal volume and memory ability in healthy individuals across the lifespan: review and meta-analysis. *Neuropsychologia,* 42**,** 1394-413.

Vandenberghe, R., Van Laere, K., Ivanoiu, A., Salmon, E., Bastin, C., Triau, E., Hasselbalch, S., Law, I., Andersen, A., Korner, A., Minthon, L., Garraux, G., Nelissen, N., Bormans, G., Buckley, C., Owenius, R., Thurfjell, L., Farrar, G. & Brooks, D.

J. 2010. 18F-flutemetamol amyloid imaging in Alzheimer disease and mild cognitive impairment: a phase 2 trial. *Ann Neurol,* 68**,** 319-29.

Varnum-Finney, B., Purton, L. E., Yu, M., Brashem-Stein, C., Flowers, D., Staats, S., Moore, K. A., Le Roux, I., Mann, R., Gray, G., Artavanis-Tsakonas, S. & Bernstein, I. D. 1998. The Notch ligand, Jagged-1, influences the development of primitive hematopoietic precursor cells. *Blood,* 91**,** 4084-91.

Vassar, R., Bennett, B. D., Babu-Khan, S., Kahn, S., Mendiaz, E. A., Denis, P., Teplow, D. B., Ross, S., Amarante, P., Loeloff, R., Luo, Y., Fisher, S., Fuller, J., Edenson, S., Lile, J., Jarosinski, M. A., Biere, A. L., Curran, E., Burgess, T., Louis, J. C., Collins, F., Treanor, J., Rogers, G. & Citron, M. 1999. Beta-secretase cleavage of Alzheimer's amyloid precursor protein by the transmembrane aspartic protease BACE. *Science,* 286**,** 735-41.

Villemagne, V. L., Burnham, S., Bourgeat, P., Brown, B., Ellis, K. A., Salvado, O., Szoeke, C., Macaulay, S. L., Martins, R., Maruff, P., Ames, D., Rowe, C. C. & Masters, C. L. 2013. Amyloid β deposition, neurodegeneration, and cognitive decline in sporadic Alzheimer's disease: a prospective cohort study. *The Lancet Neurology,* 12**,** 357-367.

Villemagne, V. L. & Okamura, N. 2014. In vivo tau imaging: obstacles and progress. *Alzheimers Dement,* 10**,** S254-64.

Vinters, H. V. 1987. Cerebral amyloid angiopathy. A critical review. *Stroke,* 18**,** 311-24.

Vos, S. J., Xiong, C., Visser, P. J., Jasielec, M. S., Hassenstab, J., Grant, E. A., Cairns, N. J., Morris, J. C., Holtzman, D. M. & Fagan, A. M. 2013. Preclinical Alzheimer's disease and its outcome: a longitudinal cohort study. *Lancet Neurol,* 12**,** 957-65.

Walhovd, K. B., Fjell, A. M., Amlien, I., Grambaite, R., Stenset, V., Bjornerud, A., Reinvang, I., Gjerstad, L., Cappelen, T., Due-Tonnessen, P. & Fladby, T. 2009. Multimodal imaging in mild cognitive impairment: Metabolism, morphometry and diffusion of the temporal-parietal memory network. *Neuroimage,* 45**,** 215-23.

Walhovd, K. B., Fjell, A. M., Dale, A. M., Mcevoy, L. K., Brewer, J., Karow, D. S., Salmon, D. P., Fennema-Notestine, C. & Alzheimer's Disease Neuroimaging, I. 2010. Multi-modal imaging predicts memory performance in normal aging and cognitive decline. *Neurobiol Aging,* 31**,** 1107-21.

Wang, J., Tan, L., Wang, H. F., Tan, C. C., Meng, X. F., Wang, C., Tang, S. W. & Yu, J. T. 2015. Anti-inflammatory drugs and risk of Alzheimer's disease: an updated systematic review and meta-analysis. *J Alzheimers Dis,* 44**,** 385-96.

Wang, L., Goldstein, F. C., Veledar, E., Levey, A. I., Lah, J. J., Meltzer, C. C., Holder, C. A. & Mao, H. 2009. Alterations in cortical thickness and white matter integrity in mild cognitive impairment measured by whole-brain cortical thickness mapping and diffusion tensor imaging. *AJNR Am J Neuroradiol,* 30**,** 893-9.

Warren, J. D., Fletcher, P. D. & Golden, H. L. 2012. The paradox of syndromic diversity in Alzheimer disease. *Nat Rev Neurol,* 8**,** 451-64.

Warren, J. D., Rohrer, J. D., Schott, J. M., Fox, N. C., Hardy, J. & Rossor, M. N. 2013. Molecular nexopathies: a new paradigm of neurodegenerative disease. *Trends Neurosci,* 36**,** 561-9.

Warrington, E. K. 1984. *Recognition memory test,* Windsor, UK, NFER-Nelson.

Warrington, E. K. 1996. *The Camden memory tests,* Hove, Psychology Press.

Warrington, E. K., James, M. & Thames Valley Test, C. 1991. *The visual object and space perception battery,* Bury St. Edmunds, Thames Valley Test Company.

Wechsler, D. 1999. *Wechsler abbreviated scale of intelligence (WASI),* San Antonio, TX: Psychological Corporation.

West, M. J., Coleman, P. D., Flood, D. G. & Troncoso, J. C. 1994. Differences in the pattern of hippocampal neuronal loss in normal ageing and Alzheimer's disease. *Lancet,* 344**,** 769-72.

Weston, P. S., Paterson, R. W., Dickson, J., Barnes, A., Bomanji, J. B., Kayani, I., Lunn, M. P., Mummery, C. J., Warren, J. D., Rossor, M. N., Fox, N. C., Zetterberg, H. & Schott, J. M. 2016. Diagnosing Dementia in the Clinical Setting: Can Amyloid PET Provide Additional Value Over Cerebrospinal Fluid? *J Alzheimers Dis,* 54**,** 1297-1302.

Weston, P. S., Paterson, R. W., Modat, M., Burgos, N., Cardoso, M. J., Magdalinou, N., Lehmann, M., Dickson, J. C., Barnes, A., Bomanji, J. B., Kayani, I., Cash, D. M., Ourselin, S., Toombs, J., Lunn, M. P., Mummery, C. J., Warren, J. D., Rossor, M. N., Fox, N. C., Zetterberg, H. & Schott, J. M. 2015. Using florbetapir positron emission tomography to explore cerebrospinal fluid cut points and gray zones in small sample sizes. *Alzheimers Dement (Amst),* 1**,** 440-446.

Whitehouse, P. J., Price, D. L., Struble, R. G., Clark, A. W., Coyle, J. T. & Delon, M. R. 1982. Alzheimer's disease and senile dementia: loss of neurons in the basal forebrain. *Science,* 215**,** 1237-9.

Whitwell, J. L., Josephs, K. A., Murray, M. E., Kantarci, K., Przybelski, S. A., Weigand, S. D., Vemuri, P., Senjem, M. L., Parisi, J. E., Knopman, D. S., Boeve, B. F., Petersen, R. C., Dickson, D. W. & Jack, C. R., Jr. 2008. MRI correlates of neurofibrillary tangle pathology at autopsy: a voxel-based morphometry study. *Neurology,* 71**,** 743-9.

Wijsman, E. M., Daw, E. W., Yu, X., Steinbart, E. J., Nochlin, D., Bird, T. D. & Schellenberg, G. D. 2005. APOE and other loci affect age-at-onset in Alzheimer's disease families with PS2 mutation. *Am J Med Genet B Neuropsychiatr Genet,* 132B**,** 14-20.

Wilcock, G. K., Black, S. E., Hendrix, S. B., Zavitz, K. H., Swabb, E. A., Laughlin, M. A. & Tarenflurbil Phase, I. I. S. I. 2008. Efficacy and safety of tarenflurbil in mild to moderate Alzheimer's disease: a randomised phase II trial. *Lancet Neurol,* 7**,** 483-93.

Wimo, A., Winblad, B. & Jonsson, L. 2010. The worldwide societal costs of dementia: Estimates for 2009. *Alzheimers Dement,* 6**,** 98-103.

Winblad, B. & Poritis, N. 1999. Memantine in severe dementia: results of the 9M-Best Study (Benefit and efficacy in severely demented patients during treatment with memantine). *Int J Geriatr Psychiatry,* 14**,** 135-46.

Wolfson, C., Wolfson, D. B., Asgharian, M., M'lan, C. E., Ostbye, T., Rockwood, K., Hogan, D. B. & Clinical Progression of Dementia Study, G. 2001. A reevaluation of the duration of survival after the onset of dementia. *N Engl J Med,* 344**,** 1111-6.

Wood, J. G., Mirra, S. S., Pollock, N. J. & Binder, L. I. 1986. Neurofibrillary tangles of Alzheimer disease share antigenic determinants with the axonal microtubule-associated protein tau (tau). *Proc Natl Acad Sci U S A,* 83**,** 4040-3.

Yau, W. Y., Tudorascu, D. L., Mcdade, E. M., Ikonomovic, S., James, J. A., Minhas, D., Mowrey, W., Sheu, L. K., Snitz, B. E., Weissfeld, L., Gianaros, P. J., Aizenstein, H. J., Price, J. C., Mathis, C. A., Lopez, O. L. & Klunk, W. E. 2015. Longitudinal assessment of neuroimaging and clinical markers in autosomal dominant Alzheimer's disease: a prospective cohort study. *Lancet Neurol,* 14**,** 804-13.

Zerr, I., Kallenberg, K., Summers, D. M., Romero, C., Taratuto, A., Heinemann, U., Breithaupt, M., Varges, D., Meissner, B., Ladogana, A., Schuur, M., Haik, S., Collins, S. J., Jansen, G. H., Stokin, G. B., Pimentel, J., Hewer, E., Collie, D., Smith, P., Roberts, H., Brandel, J. P., Van Duijn, C., Pocchiari, M., Begue, C., Cras, P., Will, R. G. & Sanchez-Juan, P. 2009. Updated clinical diagnostic criteria for sporadic Creutzfeldt-Jakob disease. *Brain,* 132**,** 2659-68.

Zetterberg, H., Skillback, T., Mattsson, N., Trojanowski, J. Q., Portelius, E., Shaw, L. M., Weiner, M. W., Blennow, K. & Alzheimer's Disease Neuroimaging, I. 2016. Association of Cerebrospinal Fluid Neurofilament Light Concentration With Alzheimer Disease Progression. *JAMA Neurol,* 73**,** 60-7.

Zetterberg, H., Wilson, D., Andreasson, U., Minthon, L., Blennow, K., Randall, J. & Hansson, O. 2013. Plasma tau levels in Alzheimer's disease. *Alzheimers Res Ther,* 5**,** 9.

Zhang, H., Schneider, T., Wheeler-Kingshott, C. A. & Alexander, D. C. 2012. NODDI: practical in vivo neurite orientation dispersion and density imaging of the human brain. *Neuroimage,* 61**,** 1000-16.

Zhang, Y., Schuff, N., Jahng, G. H., Bayne, W., Mori, S., Schad, L., Mueller, S., Du, A. T., Kramer, J. H., Yaffe, K., Chui, H., Jagust, W. J., Miller, B. L. & Weiner, M. W. 2007. Diffusion tensor imaging of cingulum fibers in mild cognitive impairment and Alzheimer disease. *Neurology,* 68**,** 13-9.

Zhou, J., Yu, J. T., Wang, H. F., Meng, X. F., Tan, C. C., Wang, J., Wang, C. & Tan, L. 2015. Association between stroke and Alzheimer's disease: systematic review and meta-analysis. *J Alzheimers Dis,* 43**,** 479-89.

Zigmond, A. S. & Snaith, R. P. 1983. The hospital anxiety and depression scale. *Acta Psychiatr Scand,* 67**,** 361-70.

Zimmermann, J. F. & Butler, C. R. 2018. Accelerated long-term forgetting in asymptomatic APOE epsilon4 carriers. *Lancet Neurol,* 17**,** 394-395.